4-15-2021

Economic and Environmental Impacts of Drone Delivery

Juan Zhang
University of Missouri-St. Louis, jzmq3@mail.umsl.edu

Economic and Environmental Impacts of Drone Delivery

Juan Zhang

Ph.D., Business Administration, University of Missouri-St. Louis, 2021
B.S. Logistics Management, Huazhong University of Science and Technology, 2015

A Dissertation Submitted to the Graduate School at the University of Missouri-St. Louis
in Partial Fulfillment of the Requirements for the Degree
Doctor of Philosophy in Business Administration with an Emphasis in Supply Chain Management

May, 2021

Advisory Committee

James F. Campbell, Ph.D.
Chairperson

Donald C. Sweeney II, Ph.D.

Haitao Li, Ph.D.

George A. Zsidisin, Ph.D., CPSM, C.P.M.

William A. Ellegood, Ph.D.

Abstract

Economic and Environmental Impacts of Drone Delivery

Juan Zhang

Motivated by the potential huge economic and environmental benefits of drone delivery, this dissertation developed mathematical models using the continuous approximation methodology to quantify the cost and emissions savings that drone delivery can provide relative to conventional truck delivery on multi-stop routes for a range of operating characteristics, delivery environments, and carbon intensities of power generation. This research considers two types of drone delivery: drone-only delivery and truck-drone delivery. In drone-only delivery, drones travel out-and-back from a depot to make each delivery. In truck-drone delivery, a truck and drone tandem make deliveries in parallel with the drone being launched and recovered at the truck. The research suggests that the delivery cost and emissions savings relative to conventional truck delivery can be substantial, but strongly depend on drone operating cost and emissions rates and their interrelationship.

Chapters 1-2 provide the background and relevant literature. Because drone emissions depend on both the drone energy consumption rate and the electricity generation, Chapter 3 classifies five fundamental drone energy consumption models, and documents wide variability in the published drone energy consumption rates, due to different drone types, operating conditions and fundamental modeling assumptions. Chapters 4 and 5 provide continuous approximation models for the cost and the emissions with truck-only delivery and the two drone delivery services (drone-only and truck-drone), and show how

the savings with drones depend on key characteristics of the drone and the operational setting. Chapter 6 examines the cost and emissions tradeoffs with optimal use of drone-only delivery and truck-drone delivery and shows the importance of the drone operating cost and energy consumption rates, as well as the delivery density and truck capacity. Results show that replacing truck-only delivery with drones can provide both cost and environmental benefits, with drone-only delivery preferred when drone operating cost and emissions rates and/or delivery density are very low and truck-drone delivery preferred when drone operating cost and emissions rates, truck-drone capacity, and/or delivery density are not very low. Results also show there can be a large tradeoff between cost and emissions when the ratio of drone operating cost rate to drone emissions rate differs from the ratio for trucks.

Table of Contents

Acknowledgement

This dissertation would not have been possible without a lot of help and support.

I would first like to thank my advisor, Dr. James F. Campbell, whose passion for intellectual inquiry, restless endeavor to the pursuit of truth, and forward-looking insights have deeply shaped my character and the way I conduct research including this dissertation. Your optimism and unlimited imagination helped me see every problem as a potential opportunity to improve and inspired my thinking.

I would like to thank Dr. Donald C. Sweeney II for his selfless support. The tremendous time and efforts you and Dr. Campbell spent not only greatly improved the quality of this dissertation but also set very good role models for me for my future career.

I would also like to acknowledge my professors and committee members, Dr. Andrea C. Hupman, Dr. Haitao Li, Dr. George A. Zsidisin, Dr. William A. Ellegood, and Dr. L. Douglas Smith, for their valuable advice and for all of the opportunities that I was given to sharpen my research skills.

In addition, I would like to thank my grandmother who taught me to be grateful, generous and brave and whose wisdom has helped me go through many struggles in life. Big thank you to my uncle Shanqing Tang and my cousin Dr. Pei Tang. Without your support and guidance, I could not have continued my study and come to the United States for pursuing my Ph.D. Thank you mom and dad for sacrificing your life for my better life and for respecting and supporting every of my decisions.

Finally, I would like to thank my other family members and friends including aunt Binghua Tang, brother Jie Zhang, cousin Kai Tang, Yucheng Wang, Dr. Anthony G. Vatterott, Rachel Chen, and Qiujie Mei, and many others.

Chapter 1: Introduction

1.1 Background

Drone delivery, the use of drones (or unmanned aerial vehicles, UAVs) to deliver goods to customers, has been promoted and researched by a growing number of firms since 2013 when Jeff Bezos, the founder of Amazon, announced that Amazon Prime members would get their packages delivered by drones within 30 minutes in areas that are within 10 miles of an Amazon fulfillment center. Though Amazon has passed many of its deadlines for starting drone delivery due to the technical and regulatory challenges, the company has undergone various iterations of drone design and flight tests, and recently received federal approval to operate its fleet of Prime Air delivery drones in the U.S. (Palmer, 2020).

The capability of drones to make autonomous deliveries has been intensively explored by several logistics companies (e.g., DHL, UPS), e-commerce retailers (e.g., Walmart, JD.com), tech companies (e.g., Google), and startups (e.g., Matternet, Zipline). For example, DHL's Parcelcopter has made 130 trips in a mountainous region of Southern Germany in winter conditions (Edenhofer, 2018). Google's X Wing has conducted more than 100,000 test flights across three continents and is currently operating in Christiansburg, Virginia (U.S.), Helsinki (Finland), and Canberra and Logan City (both in Australia) (https://wing.com/, 2021). Though most flight tests are conducted in rural or suburban areas (or remote/hard-to-reach areas), the goal of those companies is to serve urban areas as well. For example, DHL Express and EHang formed a strategic partnership to provide last-mile drone delivery in urban areas in Guangdong, China (Rehkopf, 2019).

The design of drones for package delivery has rapidly evolved from multi-rotor drones to hybrid drones that combine vertical takeoff and landing (VTOL) capability with

aspects of fixed wing flight (to increase the efficiency and flight duration). Increasing redundancies (e.g., additional sensors, rotors, and batteries) are built into these designs to ensure safety and meet regulatory requirements. Currently, most drones envisioned for commercial package delivery are battery powered, deliver only light items (e.g., pet snacks, meals, medical supplies), make only one delivery per trip (flight), and have short flight ranges between 10-15 miles. Interestingly, the delivery system prototypes differ from company to company. For example, Amazon's Prime Air delivers items from its fulfillment center directly to a customer's doorstep (i.e., warehouse-to-customer). DHL's Parcelcopter delivers items from a delivery package locker to another delivery package locker (i.e., locker-to-locker). Google's X Wing and several startups (e.g., Postmates) collaborate with local businesses to deliver items directly to the customer's doorstep (i.e., store-to-customer). UPS and several others use a truck-drone tandem system (i.e., hybrid truck-drone delivery), where drones deliver from the truck to the customer. Some companies (e.g., Amazon, FedEx, Postmates) are testing small, wheeled ground drones (or unmanned ground vehicles, UGVs) that operate like small self-driving cars on sidewalks. In this thesis, if not otherwise specified, the term "drones" denotes aerial drones.

Last-mile or home delivery has been identified as a competitive advantage for e-commerce retailers and other firms. But the reality is that the "last mile" of shipment is most expensive and inefficient, which often exceeds 50 percent of the total cost of shipping (Capgemini, 2019). This challenge has been intensified by the continuous rise of e-commerce, the increased delivery volume, and the unquenchable customer expectations for not only fast, but also free, delivery. A recent Apex Insight report shows that global online sales were in excess of $3.3 trillion in 2019, having grown at a rate of 24% per year (Apex

Insight, 2020). Driven by these increasing online sales, the global parcel delivery industry approached $430 billion in 2019, up from just under $380 billion in 2018. COVID-19 escalated those trends. For example, Target saw a 282% increase in online sales in April 2020, compared to April 2019 (Keyes, 2020). Customers have been encouraged to expect free, faultless, and fast delivery services, thanks to companies such as Amazon and Alibaba. Studies show that 54% of shoppers abandoned their carts due to expensive shipping, 39% did so due to no free shipping, and 26% did so because the shipping was too slow (Sheffi, 2020).

The increasing volume of parcel deliveries also puts great pressure on the environment, due to the increasing truck travel and the associated energy consumption and emissions. A study published by the World Economic Forum forecasts a 36% rise in the number of delivery vehicles in the world's top 100 cities in 2030, leading to an emissions increase of over 30% (Freightwaves, 2020). Greenhouse gas (GHG) emissions are a main contributor to climate change, and a large proportion of GHG emissions comes from transportation. In the U.S., the transportation sector generates the largest share of GHG emissions, about 28% of the total GHG emissions in 2018 (USEPA, 2020). Truck transport is responsible for 24% of transportation-related GHG emissions and comprises 23% of transportation-related energy use in the U.S. (Stolaroff et al., 2018). Impacts on natural and human systems from climate change have already been observed, and climate-related risks will continue to increase if GHG emissions are not mitigated or reduced (IPCC, 2018). The Fourth National Climate Assessment stated that climate change was already having noticeable effects in the United States and predicted "more frequent and intense extreme weather and climate-related events", such as floods and hurricanes (U.S. Global Change

Research Program, 2018). The World Health Organization (2018) estimates that climate change will cause approximately 250,000 additional deaths (from malnutrition, malaria, diarrhea and heat stress) per year between 2030 and 2050, and estimates the direct damage costs to health to be between $2-4 billion per year by 2030.

Drone delivery excites many e-commerce and logistics firms because of its huge potential to transport goods in a fraction of cost, time, and energy of today's transportation. Numerous drone delivery prototypes and operation modes have been studied, including some not tested in practice yet. The technologies for drone delivery (e.g., batteries, autonomous navigation, obstacle avoidance and detection) have been improved greatly, and because drones are much smaller than trucks, drones potentially cost less and consume less energy per unit distance traveled compared with trucks. Further, since most delivery drones consume electricity (which can be generated from cleaner energy sources, such as solar, wind, etc.), they potentially emit less GHG emissions per unit energy consumed compared with traditional diesel trucks.

However, the cost efficiency and environmental friendliness of drones might be offset by the longer distances they have to travel in order to make a set of deliveries given their limited payload capacity, the additional warehouses or charging stations required to extend limited drone flight ranges, the labor required to operate drones, the carbon intensity of different power generation systems, and the competitiveness of alternative-fuel vehicles (e.g., electric and natural gas trucks). Furthermore, several studies suggest that a lack of solid scientific evidence of the benefits of drones, and large uncertainties exist about the environmental impacts of drones (Macrina et al., 2020; Kellermann et al., 2020; Shavarani et al., 2018; Park et al., 2018). Some studies show that drone-based delivery could reduce

GHG emissions and energy use in the freight sector if carefully deployed (Stolaroff et al., 2018; Goodchild and Toy, 2018), while some show that parcel delivery drones consume a similar amount of, or more, energy than trucks in many settings (Kirschstein, 2020; Gulden, 2017; Figliozzi, 2017).

Given the potential benefits and drawbacks of drones, some key questions that need greater research attention with regard to incorporating drones into small package delivery networks include:

- Is drone delivery a good alternative to truck-only delivery in terms of reducing delivery cost and life-cycle GHG emissions?
- Under what conditions is drone delivery better than truck delivery?
- How best should drones be utilized?

My focus is to address these strategic questions so as to facilitate more detailed operational drone research for particular settings.

1.2 The Framework of the Dissertation

The main purposes of this research are: (i) to examine the potential economic and environmental benefits of drone delivery, (ii) to quantify the tradeoffs between the economic and the environmental impacts of deploying drones for home delivery, (iii) to identify promising delivery system designs, and (iv) to develop managerial insights. This is achieved using continuous approximation (CA) modeling to provide a strategic analysis of a range of delivery prototypes and strategies, with a lifecycle-based analysis of operations and a sensitivity analysis for key parameters. As an illustration, Figure 1.1(a) shows conventional truck delivery where a truck travels on a multi-stop route delivering

packages to a set of customers. (For example, a typical UPS delivery route in the U.S. may include 100-150 deliveries.) The black squares denote truck stops (i.e., deliveries). Figure 1.1 (b) shows drone-only delivery to a subset of these customers (within the range of the drone) where the drone departs from the depot, visits a single customer, and returns to the depot. The red circles denote drone stops (deliveries). (The customers not served by the drone would be served in some other way (e.g., by the truck)). Figure 1.1(c) shows hybrid truck-drone delivery where the truck and drone alternate deliveries while traveling through the service region.

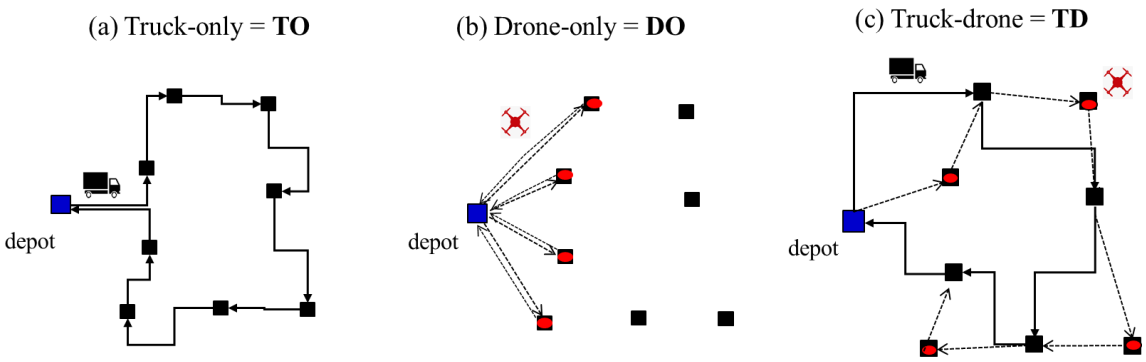

Figure 1.1. Three delivery services: truck-only, drone-only, and truck-drone

Continuous approximation models for estimating expected travel distances are formulated for each of the three delivery options, which provide the foundations for calculating the expected cost and emissions for delivery systems. In this dissertation I measure cost in $ and emissions in kg or grams of CO2e, where CO2e is the equivalent amount of CO2 for any GHG in terms of its impact on global warming (Brander, 2012).The models for cost and emissions also depend on the relevant cost rate ($/mile) and emissions rate (e.g., kilograms of CO2e/mile) associated with the operation of different vehicles. For battery powered drones, the emissions rate depends on both the energy efficiency of the

drone (Watt-hours per mile) and the emissions associated with the energy being used to charge the batteries (kg CO2e/Watt-hour). Since the use of electricity in delivery vehicles (e.g., battery powered drones) shifts the emissions from the vehicle tailpipe to upstream power plants, the emissions rate of each delivery vehicle considers the lifecycle of fuel. The cost and emissions metrics of different delivery services are then optimized analytically and compared with each other to identify the best combination of the three delivery services (as described in Fig.1.1) to serve a region. Sensitivity analyses are conducted to evaluate the impact of a wide range of operating characteristics (e.g., from inexpensive to expensive drone operating costs, small to large drone energy requirements, low to high customer service levels, etc.), delivery environments (e.g., from very rural to urban delivery regions), and carbon intensities of power generation (e.g., from very low to very high carbon intensity of generating electricity).

1.3 Contributions

This dissertation research fills gaps in the literature as follows:

1) Review and classify key drone energy consumption models in the literature by using a unified notation and framework that allows for a collective comparison of the energy consumption rates for the various drone types, payloads, operating speeds and other important operating parameters.
2) Develop an innovative strategic model to analyze truck-drone delivery, along with drone-only delivery and truck-drone delivery.
3) Provide strategic models to assess the potential economic and environmental benefits as a result of shifting from truck-only delivery to drone-only and truck-drone delivery.

4) Identify and examine the cost and emissions tradeoffs of the integrated truck and drone delivery systems that include drone-only delivery, truck-drone delivery, and truck-only delivery, and provide consistent evidence and analyses for estimating the economic and environmental benefits from drone delivery.
5) Provide a strategic analytical tool that allows the cost and emissions tradeoff to be quantified – determining not only the relative cost and/or emissions savings and the "implied carbon price", but also the set of optimal delivery services. This enables firms to better understand the consequences of deploying drones in various delivery services.

1.4 Outline

Chapter 2 is a literature review on the modeling of delivery costs and GHG emissions for trucks and drones and the methodologies developed for solving routing problems with drones. Chapter 3 provides a uniform framework designed to facilitate understanding different drone energy consumption models and the inter-relationships between key factors and performance measures to facilitate decision-making for drone delivery operations. Chapter 4 lays the theoretical foundation for modeling the expected delivery costs and GHG emissions that facilitates a strategic analysis of the design of drone delivery systems. Continuous approximation models are derived for estimating the expected delivery costs for drone-only, truck-drone and truck-only delivery. Chapter 5 extends the continuous approximation models and analyses for estimating the expected GHG emissions for drone-only, truck-drone and truck-only delivery. Numerical scenarios are presented to illustrate the magnitude of the potential savings relative to truck-only delivery. Chapter 6 examines the tradeoff between cost and emissions for drone delivery

systems, including drone-only, truck-drone and truck-only delivery. A delivery system design problem integer programming model is formulated to optimally partition the delivery region and assign delivery services to subregions, based on minimizing the delivery costs, minimizing the GHG emissions or finding Pareto efficient solutions considering both objectives. Analysis of the Pareto frontier is presented for several scenarios to quantify the cost and emission tradeoffs. Chapter 7 presents the conclusions and future research.

Chapter 2: Literature Review

This chapter reviews the relevant literature for this dissertation. Section 2.1 is a review of how cost, energy consumption and greenhouse gas (GHG) emissions are modeled in relevant literature for trucks and drones. Section 2.2 includes a review of research that uses continuous approximation modeling for freight distribution, followed by a review of the literature on routing problems with drones for last-mile delivery. Section 2.3 is a summary of the relevant literature. The literature review focuses on aerial drones for commercial delivery operations, not ground or sea drones or military drones.

2.1 Cost, Energy Consumption, and GHG Emissions

In this subsection, relevant literature on lifecycle analysis is first reviewed to determine the system scope and the functional unit of this thesis. Then, literature on the classic vehicle routing problem (VRP) and the green vehicle routing problem (GVRP) is reviewed to understand why and how environmental aspects (e.g., energy consumption and emissions) are integrated into the routing models for trucks and alternative-fuel vehicles. Finally, studies of the cost and environmental aspects of drones for last mile delivery are reviewed.

2.1.1 Life Cycle Analysis

Life cycle analysis or life cycle assessment (LCA) is a widely adopted method to measure and compare the potential environmental impacts of products through their entire life cycle, i.e., from raw material extraction, via production and use phases, to waste management (e.g., disposal, recycle, reuse) (Guinée et al., 1993, 2011; Finnveden et al., 2009). This comprehensive scope of LCA is helpful to obtain a complete picture of environmental impacts and avoid shifting impacts from one phase of the life cycle to

another, or from one region or one environmental problem to another. It is most relevant in the comparison of truck and drone deliveries because although electricity powered drones emit zero tailpipe GHG emissions, emissions are shifted to upstream power plants. In addition, trucks and drones differ in size, which may result in different magnitudes of environmental impacts.

According to ISO (2006a), there are four phases in an LCA study: (1) the goal and scope definition phase, which defines the intended application, the functional unit of the analysis and the system boundary; (2) the life cycle inventory analysis phase, which compiles the inputs (energy) from and outputs (emissions) to the environment; (3) the life cycle impact analysis phase, which quantifies and evaluates the magnitude and significance of the potential environmental impacts of the system under study; and (4) the interpretation phase, which provides conclusions and recommendations. Even though LCA has existed for decades, the methods and data used in LCA phases differ from study to study, which results in different or conflicting conclusions even when the object of the study is the same (Guinée et al., 1993, 2011; Finnveden et al., 2009). Finnveden et al. (2009) claim that LCA is very data intensive, and the lack of data may limit the conclusions that can be drawn from a study. Therefore, it is very important to clearly define the scope of the study and specify the data sources.

The applications of LCA to freight transportation have revealed that tailpipe energy use and emissions alone underestimate the total lifecycle energy use and emissions (Horvard, 2006; Lee et al., 2013). The lifecycle of a freight transportation system can be classified into three categories: (i) the fuel cycle, which includes upstream raw material extraction, processing and distribution, and tailpipe use of fuel; (ii) the vehicle cycle, which

includes upstream raw material extraction, manufacturing, tailpipe use, maintenance, and end-of-life disposal or recycle of the vehicle and battery if applicable; and (iii) the transportation infrastructure cycle, which includes the construction, operation, maintenance, and end-of-life disposal or recycle of transportation infrastructures. Horvard (2006) shows that the tailpipe emissions account for about 70% of the lifecycle emissions for the freight transportation. However, it is not uncommon to see that most LCA scopes of traditional truck delivery include only the tailpipe phase of the fuel cycle. The reasons may be that the environmental aspects of transportation are undervalued, and the availability of data is limited.

Similar phenomena are observed for drone delivery. The emissions rate differs from study to study, which is due in part to different lifecycle components being considered, different databases and functional units of analysis being adopted, and the availability of data. For example, Park et al. (2018) consider only the fuel cycle for delivering pizza using drones. Figliozzi (2017) considers both the fuel and the vehicle cycles for quadcopter drones, and the author acknowledges that there is not much data for the manufacturing of drones, thus, the analyses are done separately for the fuel cycle and the vehicle cycle. Stolaroff et al. (2018) considers the fuel cycle and the infrastructure cycle which considers the energy (i.e., electricity and natural gas) required to operate the extra warehouses required by the drones. The common functional units of analysis used are a single delivery and a unit distance traveled. In the U.S., the lifecycle emissions for diesel, natural gas, and electricity are well-documented in the GREET Model and the eGRID databases (Figliozzi, 2017; Stolaroff et al., 2018). However, there is not much data for the lifecycle emissions of drones. Studies conducted in other countries use other databases. For example, Park et

al. (2018) use data from the Korea Environmental Industry and Technology Institute for electricity and gasoline. Koiwanit (2018) uses data from multiple regions, such as the US, China, Canada, for assessing the environmental impact of drone delivery in Thailand.

In this study, the system boundary considered includes the fuel cycle and the vehicle to avoid shifting emissions from tailpipe to upstream power plants. Since the drones either depart from an existing depot or a truck, the construction of new infrastructure is not required, thus, the infrastructure cycle is not considered in the lifecycle analysis. However, the models can be easily extended to include the infrastructure cycle if additional warehouses or recharging stations are required. Two commonly utilized functional units of analysis are chosen: per unit distance traveled and per delivery.

2.1.2 Cost, Energy Use and GHG Emissions of Trucks

Medium-duty trucks are commonly used for the last-mile or home delivery (Lee et al., 2013). Those trucks generally weigh 6,350 to 11,793 kg (or 14,000 to 26,000 lbs) and are classified in the U.S. as class 4-6 trucks based on their gross vehicle weight. Since conventional truck delivery has been widely studied, there is a consensus on reasonable values for the cost and fuel consumption. For example, American Transportation Research Institute (ATRI) has continued to publish an annual update, streamlining methodologies and updating the marginal costs of trucking since 2008. According to ATRI, the operating costs of trucking (in dollar per mile) can be divided into two general categories: driver- and vehicle-based costs. The former includes driver wages and benefits (e.g., full medical, dental, vision coverages, 401(k) matching). The latter includes fuel, equipment (e.g., truck release or purchase payments), repair and maintenance, truck insurance premiums, permits and special licenses, tires and tolls. Driver and fuel costs are the dominating factors in the

overall costs (over 50%), a phenomenon that has been observed in ATRI's survey for a number of years (Williams and Murray, 2020). A shortage of qualified drivers further increases driver-based costs, and the shortage is estimated to grow to 160,000 drivers by 2028 (Costello and Karickhoff, 2019). The trend of fuel cost is closely linked with diesel prices which are affected by many factors and are highly speculative. The truck fuel consumption is commonly determined by the fuel economy. A typical Class 4 parcel delivery truck travels 11.5 miles per gallon of diesel (Stolaroff et al., 2018). Lammert (2009) reports an average of 10.2 mpg for the standard UPS signature diesel truck based on a 12-month evaluation. The fuel efficiency of diesel trucks continues to improve as logistics companies and auto manufacturers strive to reduce energy consumptions and emissions. Figliozzi (2017) uses the rated fuel efficiency of 22 mpg for a diesel cargo van. However, it is well-documented that the actual observed fuel efficiency varies with driving patterns, traffic, terrain, vehicle weight, age of the vehicles, and other parameters (Stolaroff et al., 2018; Demir et al., 2014; Bektas and Laporte, 2011).

Last-mile or home delivery by trucks is an application of the well-known vehicle routing problem (VRP) which has a rich and extensive literature since the seminal article by Dantzig and Ramser (1959). Interested readers are referred to a recent review of VRP by Braekers et al. (2016), an earlier review by Cordeau et al. (2007), and reviews of VRP solution methods (e.g., exact algorithms, heuristics and metaheuristics) by Laporte et al. (2007 and 2009). The problem involves designing delivery or pickup routes from a depot to a number of geographically distributed customers, subject to various practical constraints, such as vehicle capacity, driver working hours, time windows and the fleet mix. The objective is to minimize the total distance traveled by all vehicles or to minimize the

overall cost, usually a linear function of distance (Bektas and Laporte, 2011). The VRP is known to be NP-hard and is difficult to solve to optimality except for rather small size instances. A great number of research efforts have been devoted to the design of effective heuristics and algorithms for the VRP and its variants.

The green vehicle routing problem (GVRP) extends the classic VRP by integrating the environmental aspects (namely fuel consumption and emissions) of vehicles into routing models. Interested readers are referred to a comprehensive review of GVRP by Lin et al. (2014), a review of green logistics by Dekker et al. (2012), and a survey of sustainable logistics by Abbasi and Nilsson (2016).The GVRP includes the Green-VRP and the Pollution Routing Problem (PRP). The difference between the two is that the former utilizes alternative-fuel vehicles with the objective of minimizing fuel consumptions, while the latter aims at minimizing the pollution (especially GHG emissions) (Lin et al., 2014).

The studies of GVRP provide a rich discussion of how to incorporate environmental aspects into classical VRPs, and how to model the fuel consumption and emissions. Multiple objective functions are usually proposed that either treat energy consumption and/or the emissions independently (Bektas and Laporte, 2011) or as components of a total cost-minimization objective function (Bektas and Laporte, 2011; Cachon, 2014; Zhang et al., 2015). For example, Bektas and Laporte (2011) minimize the total cost that is composed of driver cost, fuel consumption cost and emission cost. They also establish three other objective functions, i.e., distance-minimization, energy-minimization and weighted load-minimization. The price of emissions is usually modeled as a carbon tax (e.g., $ per unit of emissions) (Bektas and Laporte, 2011; Cachon, 2014). The models of fuel consumption and emissions differ by the levels of complexity, with the simplest model

being a linear function of the distance traveled and the most sophisticated model considering various vehicle parameters, traffic, and driver behaviors (Cachon et al., 2014; Lee et al., 2013; Bektas and Laporte, 2011). A comprehensive review of these models is given by Demir et al. (2014).

Within studies that compare drone delivery with truck delivery, the modeling of truck energy consumption and emissions differs slightly from one another, resulting in different emissions factors. Figliozzi (2017) model the emissions as a product of an emission factor (11.05 kg CO2e/gallon of diesel), an average vehicle fuel economy (35.41 km per gallon), and the distance travelled. Goodchild and Toy (2018) model the emissions as a product of the distance traveled and the weighted average CO2 tailpipe emissions rate (0.61-1.06 kg CO2e/km) based on truck age and travel speed. Stolaroff et al. (2018) do not provide a fuel consumption model, but use a base fuel economy (2.17 kWh per package) and conduct a sensitivity analysis.

2.1.3 Cost, Energy Use and GHG Emissions of Drones

Though the green vehicle routing problem has been intensively studied for diesel and alternative-fuel vehicles, there is limited research on this topic for drones, mostly because drone delivery is still an emerging technology. Chiang et al. (2019) studies the cost and environmental improvements of using drones for package delivery relative to truck delivery. A mixed integer programing (MIP) model is proposed for two independent objective functions. One is to minimize CO2 emissions which are proportional to the distance traveled (based on the model of Goodchild and Toy (2018)). The drone energy consumption rate is 3.33 Wh/mile. The other is to minimize costs which include a fixed vehicle cost associated with each truck/drone tandem and a variable routing cost that is a

function of distance traveled and vehicle weight. The variable costs for the drone and the truck are $0.02/mile and $1/mile, respectively. A genetic algorithm is developed and tested on instances with up to 500 customers. The results show a positive correlation between cost reduction and CO2 emission reduction, i.e., the minimization of cost also minimizes CO2 emissions, through the integration of drones into the current truck delivery system.

Coelho et al. (2017) study the drone-only routing problem and propose an MIP model with seven weighted objective functions including total distance traveled, the maximum speed of UAVs, the number of UAVs used, the makespan of the last collected and delivered packages, the average time spent with each package, and total amount of energy for batteries. Though the authors claim it is a green vehicle routing problem, the environmental aspect and its tradeoffs with traditional objectives are not emphasized in the analysis. Troudi et al. (2018) study the capacitated drone routing problem with time windows and take into account the drone payload capacity and energy constraints. Three objective functions are proposed: minimizing distance, minimizing the number of drones used, and minimizing the number of batteries used. The distance traveled and energy consumption are correlated because the latter is proportional to the distance traveled and the payload. In their future work, the authors are interested in addressing the balance of these three different objectives in terms of cost.

Several works study the economics of drone-only delivery or hybrid truck-drone delivery (e.g., Campbell et al., 2017; Ha et al., 2018). Those studies show that drones have the potential to significantly reduce delivery costs because drones are usually associated with a much lower transportation cost rate than trucks (in $ per unit distance). However, the cost effectiveness of drone delivery depends on several factors, such as drone operating

costs and delivery density. D'Andrea (2014) performed a theoretical feasibility test of drone delivery. He claimed that batteries dominate the total drone operating costs in the long run, once drones reach a level of maturity compared to today's automobiles. The total operating costs directly associated with the drone are on the order of 10 cents for a 2 kg payload and a 10 km range. The operating costs include only battery cost (80%) and electricity cost (20%), because the analysis assumed that drones operate fully autonomously without any human intervention. ARK Invest originally suggested a price of $1 per delivery for a drone that departs from a depot and makes an average of 30 deliveries per day with each under 5 lbs and within 10 miles of the depot (Keeney, 2015). The price is determined from estimate of annual capital costs for infrastructure, drones and batteries, and annual operating costs for labor (drone operators), electricity, maintenance and insurance. Labor costs are the large majority of operating costs, even with the assumption that each operator controls 10-12 drones, which does not follow current US law. Recently, ARK Invest updated that figure to be only $0.25 per delivery for a parcel drone assuming more efficient autonomous flight and less amount of human intervention (Keeney, 2020).

Campbell et al. (2017) propose a continuous approximation model to compare the cost competitiveness of drone delivery with that of traditional truck delivery. The cost model includes a travel cost between deliveries and a stop cost for each delivery of each vehicle. The authors find that the attractiveness of using drones for home delivery strongly depends on the relative drone operating cost, the marginal drone stop cost (relative to truck delivery), and the delivery density. Ha et al. (2018) emphasize the algorithmic aspect of a traveling salesman problem with drones that minimizes operational costs including total transportation cost and the cost incurred when one vehicle has to wait for the other.

Several studies have been conducted to compare the environmental improvements of drones relative to other delivery vehicles (Kirschstein, 2020; Goodchild and Toy, 2018; Stolaroff et al., 2018; Figliozzi 2017; Gulten, 2017). The research results are mixed with regard to the energy and emissions efficiency of drone delivery. Most earlier studies show that drones have the potential to reduce energy consumption and emissions (e.g., GHG, particulates) due to their light weight, small size, and consumption of usually inexpensive and green electricity. However, how large the potential reductions are depend on several factors, such as the delivery density, drone energy requirements, which lifecycle components are considered, the carbon intensity of electricity, the number of customers served by a truck route, and the area of the service region. Considering more realistic operating environments (e.g., wind, takeoff/landing, hovering), however, some recent studies show that drone delivery often requires more energy than truck delivery, which might lead to greater emissions.

Goodchild and Toy (2018) compare the performance (i.e., vehicle miles traveled and CO2 emissions) of drone-only delivery with traditional diesel truck delivery. Tools in ArcGIS are utilized to estimate the travel distances for both the truck and the drone based on real residence addresses in Los Angeles. The CO2 emissions are modeled as a product of an emission factor (0.3773 kg CO2 per kWh), drone energy consumption rate, and total distance traveled. The emission factor includes both battery charge/discharge and power transfer efficiencies. Their results show that the vehicle miles traveled (VMT) per delivery of the drone (16.38 km/delivery) is much higher than that of the truck (0.26 km/delivery). The reason is that the drone is assumed to return to the depot after making one delivery (i.e., single stop delivery) while the truck can make multiple deliveries during its route (i.e.,

multi-stop delivery). The discrepancy becomes larger when customers are farther from the depot. The impact on CO2 emissions was evaluated by varying: (i) drone energy requirements (ranging from 10 Wh per mile to 100 Wh per mile), (ii) delivery density (ranging from 50 to 500 customers per square mile), and (iii) distance between the depot and the center of a service zone (ranging from 0 to 10 miles). Note each service zone is served by one truck route, thus the truck size changes as the delivery density changes. The results show that drones tend to emit less CO2 emissions than trucks in service zones that are either closer to the depot or have a smaller delivery density, or both. A blended system would perform the best with drones serving closer customers while trucks serve more remote ones.

Figliozzi (2017) shows that the emissions advantage of drones depends on the number of customers that can be served in a truck's route. Unlike Goodchild and Toy (2018), Figliozzi (2017) considers lifecycle greenhouse gas emissions that include emissions from both the operational vehicle phase (i.e., the fuel cycle) and the non-operational vehicle phase (i.e., the vehicle cycle). The operational vehicle phase emission is a product of an emission factor (0.56 kg CO2e per kWh) and the energy consumption. The non-operational vehicle phase emission depends on the weight of the drone body and batteries (assuming four batteries over the lifetime of the drone), with a rate of 69.2 kg CO2e per kg. However, the analysis is mainly performed for the operational vehicle phase emission. The author compares the energy consumption and CO2e emission of drone-only delivery with those of a single-stop and a multi-stop ground vehicle delivery (e.g., diesel van, electric truck and van, electric tricycle). The energy consumption per unit distance traveled and the emissions per unit energy consumed of drones are about 47 times and 22

times more efficient than those of diesel vans in the single-stop delivery scenario, respectively. However, ground vehicles outperform UAVs when a large number of customers can be served in a multi-stop delivery route. The break-even point varies from 1.5 to 1,340 customers per multi-stop route depending on the energy requirement of the drones and the size and the fuel type of ground vehicles.

In additional to Figliozzi (2017), Stolaroff et al. (2018) add one more lifecycle piece—the infrastructure cycle (e.g., emissions from operating warehouses and waystations)—into the comparison of GHG emissions of drones with that of trucks, as more warehouses may be needed in order to extend the flight range of drones. Different types of drones (i.e., quadcopter and octocopter) and ground vehicles (i.e., diesel, gasoline, natural gas and electricity vehicles) and the carbon intensity of power generation (i.e., in different regions in the United States) are studied. The emissions is modeled as a product of an emissions rate (0.645 and 1.264 kg CO2e per delivery for quadcopter and octocopter, respectively) and the number of deliveries made. The study shows that drones consume less energy per delivery per km than trucks, but the energy required for additional warehouses and the longer distances traveled by drones severely increase the lifecycle impacts. Moreover, the emissions advantage of drones also depends on the energy consumption of drones and the carbon intensity of power generation in different regions. Park et al. (2018) compare the environmental impact (e.g., GHG emission, particulates) of pizza delivery by drones with that by motorcycles. The GHG emissions rate used is of 7.1 g CO2e per mile.

Kirschstein (2020) propose a detailed energy consumption model for a drone delivery process that includes takeoff and ascent, steady level flight, descent, hovering, and

landing. It also considers the environmental conditions (e.g., wind). The energy consumed by drones is then compared to the energy consumption of diesel trucks and electric trucks serving the same set of customers from the same depot. The results indicate that switching to a solely drone-only delivery system is not worthwhile in terms of energy efficiency because drone-only delivery requires more energy than truck-only delivery, especially in urban areas where customer density is high and truck routes are relatively short. Even in rather rural areas, the energy consumption of drones is comparable to that of electric vehicles.

In summary, there are limited studies on the economic and the environmental benefits of drone delivery. Most of those studies focus on drone-only delivery, whereas only a few studies look at the truck-drone delivery which is also an important approach for using drones. Few study examines a blended delivery system that optimizes the use of drone-only delivery, truck-drone delivery, and truck-only delivery. Furthermore, there are mixed research results in regard to the energy and emissions efficiency of drone delivery due in part to a limited understanding of drone energy consumption and highly diverse drone energy consumption models and rates. Although most studies show that drones have the potential to reduce delivery costs and emissions, there is no agreement in the literature on (i) how much drones might reduce costs, and how environmentally friendly drones might be; (ii) how the magnitude of cost and emissions reductions depend on key characteristics of the drones and the operational settings; and (iii) how best drones should be used.

2.2 Methodology and Discrete Drone Delivery Models

In this subsection, studies using the continuous approximation (CA) method in the transportation field are first reviewed to demonstrate the flexibility and the validity of applying CA to the study of drone delivery. Other methods, such as discrete mathematical modeling, for modeling drone delivery are also briefly reviewed.

2.2.1 Continuous Approximation Models

The continuous approximation (CA) method formulates mathematical models of cost or other objectives as continuous functions of fundamental problem characteristics, such as the density of customers over time and space. This essentially replaces detailed discrete numerical models (e.g., MIP models) with continuous analytical models for expected costs (or other performance). Thus, analytical techniques (e.g., calculus) can be used to solve the models and find optimal or near-optimal performance measures and variable values. Key early publications on CA include the asymptotic approximation formula for the traveling salesman problem (TSP) proposed by Beardwood et al. (1959), and the strip strategy proposed by Daganzo (1984) for approximating near-optimal vehicle tour lengths. A main goal of CA is to obtain near-optimal solutions with as little information as possible, and to gain insights from a clear understanding of the relevant trade-offs. Therefore, one main use of CA method is to estimate the routing costs or other objectives within strategic or tactical problems. Interested readers are referred to recent reviews of the advancements and applications of CA models by Ansari et al. (2018) and Franceschetti et al. (2017), and an earlier review of CA models in freight distribution by Langevin et al. (1996).

The applications of CA on distribution system and network design are rich and extensive, such as distance approximations (Beardwood et al., 1956; Eilon et al., 1971; Daganzo, 1984a, b; Vaughan, 1984), various VRP variants (Campbell, 1993; Francis and Smilowitz, 2006; Figliozzi, 2007; Carlsson and Jia, 2013, 2015; Cachon, 2014;), and public transit (Szplett, 1984; Ouyang et al., 2014; Ellegood et al., 2015). Within CA, there are different ways to model the transportation cost for a single origin and multiple destinations delivery system, but a common way is to divide it into two components: travel cost and stop cost (Daganzo, 2005; Campbell et al., 2017). The travel cost is attributable to each mile traveled, which is also called the operating cost. The stop cost is attributable to each delivery (i.e., stop), regardless of the distance to reach the delivery location. For example, this includes the cost of stopping the vehicle and having it sit idle while it is being loaded and unloaded.

There are various advantages of the CA approach over discrete approaches including: the small data requirements, the ease of decomposing complex problems, and the ability to generate insights (Daganzo, 1984; Daganzo and Newell, 1986; Novaes et al., 2000; Ho and Wong, 2006; Smilowitz and Daganzo, 2007; Li et al., 2016). The CA method usually requires less data preparation than discrete methods, because the locations of customers or facilities can be represented by a continuous density function over a service area. Therefore, the exact locations of customers, which may be thousands or millions of data elements, are not required. For example, Novaes et al. (2000) compare a CA approach for designing a minimal-cost physical distribution system with a discrete modeling approach on data preparation and conclude that the former approach only needs information about ground coordination, expected delivery time and standard variance,

cargo quantities and visiting frequencies, which are easy to obtain. Thus, a CA approach can be best applied to the initial planning or design stage, since there is lack of data at that moment (Daganzo and Newell, 1986; Novaes et al., 2000; Ho and Wong, 2006).

The inherent capability of the CA method to decompose a complex problem into several solvable sub-problems makes it advantageous for studying distribution problems, such as facility location, vehicle routing, and network design, which are NP-hard. By formulating analytical models of the locally optimal design and cost as functions of the local conditions (e.g., density of deliveries), one can find a system-wide optimal solution that will vary as the underlying parameter values vary. In illustrating this focus on optimizing local behavior, Daganzo and Newell (1986) note that "the optimum operating strategy within an influence area [a local region] is not affected by decisions made outside it". Smilowitz and Daganzo (2007) reduce the total cost model for a distribution system into a series of easily solved convex sub-problems which consider one variable at a time. Another key feature of the CA method is the insights provided from the analytical formulae and solutions. Daganzo and Newell (1986) point out that a CA approach indicates near-optimal design guidelines instead of yielding a particular solution, which may also lead to improved heuristic solution methods for discrete formulations. Ho and Wong (2006) demonstrate that "as the numerical results of a continuum model can be visualized in a two-dimensional sense, the influence of different model parameters and the spatial interactions between locations can be easily detected and analyzed".

Giving the advantages of CA method, a growing number of studies have applied it for drone delivery problems. Carlsson and Song (2018) investigate the efficiency of a "horsefly delivery system" which is very similar to the truck-drone delivery in this

dissertation, except that the truck does not make any deliveries. The objective is to minimize the completion time of a route. Since the problem is a generalization of the TSP that is difficult to solve to optimality, the authors use the CA method to derive upper and lower bounds. The results show that the amount of improvement in efficiency (in terms of the completion time with the drone over the completion time without the drone) is proportional to the square root of the ratio of speeds of the drone and the truck. The original analysis is extended to also consider the impacts of the truck visiting some customers and a limited drone battery life. A similar finding is obtained. Furthermore, the authors conduct two computational experiments verifying that the CA results are valid in practice.

Chowdhury et al. (2017) study the benefits of deploying drones to serve a disaster affected region with some roads inaccessible by trucks. Both trucks and drones make direct shipments, i.e., each vehicle transports emergency goods from a distribution center (DC) to demand points and returns to the DC. The research question is modeled as a network design problem with the objective of minimizing the total distribution cost which includes the facility cost, the inventory holding cost and the transportation cost. The CA method is used to simplify the model formulation and the solution procedure. Sensitivity analysis is conducted to show the impact of key drone parameters (e.g., drone flying altitude, drone speed) on disaster relief operations. Finally, the model is tested using data from three coastal counties of Mississippi.

Campbell et al. (2017) apply the continuous approximation method to answer the question of how best to deploy drones for home delivery from a strategic perspective. The CA method employed is an extension of a strip strategy proposed by Daganzo (1984) for estimating the length of a TSP route. In this new situation, some of the deliveries are made

by drones that are carried on the roof of a truck while the truck makes the rest of the deliveries. The transportation cost includes a travel cost and a stop cost of each type of vehicle. It considers one drone per truck, multiple drones per truck, linehaul travel, and time limits on the route. The authors find that the attractiveness of using drones for home delivery strongly depends on the relative drone operating cost, drone marginal stop cost, and the delivery density.

In summary, the small data requirements, the ease of decomposing complex problems, and the ability to generate insights make the continuous approximation (CA) method appropriate for the study of drone delivery from a strategic perspective. The CA method has been applied to the study of the time and cost efficiencies of integrating drones into conventional truck delivery. Results show that drone delivery can improve delivery time efficiency and reduce delivery cost. They also indicate that the CA method is efficient and valid for solving drone delivery problems.

2.2.2 Other Drone Delivery Models

Most drone delivery research has employed mixed integer programming (MIP) formulations and solutions with various algorithms and heuristics. Interested readers are referred to the recent reviews of drone-aided routing problems in transportation by Macrina et al. (2020) and Khoufi et al. (2019), generic routing problems with drones by Rojas Viloria et al. (2020), and hybrid truck-drone optimization problems by Chung et al. (2020).

Based on Macrina et al. (2020), drone routing/delivery problems can be classified into three categories: (1) the traveling salesman problem with drone (TSP-D), (2) the vehicle routing problem with drones (VRP-D), and (3) the drone-only delivery problem (DDP). For TSP-D and VRP-D, the deliveries are made either by the truck(s) or the

drone(s). The main difference between TSP-D and VRP-D is that in VRP-D the truck capacity is restricted and more than one truck is allowed. For DDP, the deliveries are made only by the drone(s). Our proposed drone-only delivery and truck-drone delivery are in the category of DDP and VRP-D, respectively.

Murray and Chu (2015) propose MIP models for two variants of the TSP-D. One is called the flying sidekick TSP (FSTSP) where a drone is launched from, and returns to, the truck after making a single delivery, while the truck makes a delivery at the same time. The other is called the parallel drone scheduling TSP (PDSTSP). Unlike the FSTSP, the drone is separate from the truck, as both independently depart from and return to the depot. The drone is restricted by its flight endurance in both FSTSP and PDSTSP. Both objectives are to minimize the route completion time. The authors show that exact methods can only solve small-scale instances. Extensive studies have since then proposed algorithms to solve these problems and extend the work of Murray and Chu (2015) (e.g., Ponza, 2016; Ferrandez et al., 2016; Ha et al., 2018; Yurek and Ozmutlu, 2018; Bouman et al., 2018; Agatz et al., 2018; Poikonen et al., 2019; Freitas and Penna, 2020). Ponza (2016) investigates several different heuristics to solve a modified FSTSP and shows that a simulated annealing algorithm performs the best among other heuristics (e.g., ant colony optimization, naïve approach). Agatz et al. (2018) propose two route-first, cluster-second heuristics based on local search and dynamic programming to solve an extended version of FSTSP called "TSP-D" where a drone can be recovered by the truck at the node where it was launched from the truck. Only small instances with 12 customers are solved by the exact method. Freitas and Penna (2020) propose a metaheuristic to solve both the FSTSP and the "TSP-D" with instances up to 200 customers. Ha et al. (2018) propose two

heuristics for the FSTSP with a different objective which aims at minimizing operational costs.

The discrete models for drone delivery typically make many assumptions to comply with current (US) drone regulations and to make the problem more tractable. The most common assumptions are: (1) a drone can make only one delivery at a time and must return to a depot or truck after each delivery; (2) there is one drone per truck; (3) a drone can land on and depart from a truck only when the truck is parked at a customer location; (4) the pickup and delivery time by both truck and drone is negligible; (5) the recharging time of a drone is negligible; (6) the speeds of the drone and the truck are constant; (7) the truck does not need to wait for the drone because the speed of the drone is assumed to be faster than that of the truck. Many of these assumptions, such as (1)-(4), are relaxed in some studies. For example, Ferrandez et al. (2016), Wang et al. (2016), Phan et al. (2018), Salama and Srinivas (2020) investigate multiple drones per truck. Cheng et al. (2020) model a multi-trip drone routing problem with a nonlinear drone energy function that takes speed into consideration. To launch and retrieve the drone while the truck is traveling is an area of ongoing research.

Most studies compare the time efficiencies of drone delivery to that of truck delivery. Results show that total delivery time can be reduced by using drones in tandem with trucks, but how large the reduction is depends on the relative speed of drones to trucks and the number of drones per truck (Agatz et al., 2018; Ferrandez et al., 2016; Wang et al., 2016). Agatz et al. (2018) assume that the drone is faster than the truck with a factor of α, and they prove theoretically that the savings in total service time is a factor of $(1+\alpha)$ by equipping a truck with a drone compared with truck-only delivery. Ferrandez et al. (2016)

propose K-means and genetic algorithms to determine the optimal number and location of drone launch sites and the number of drones per truck.

In summary, most studies on drone delivery utilize mixed integer programming (MIP) models with the objectives of minimizing delivery time or comparing the time efficiencies with truck delivery. These studies show that drones have the potential to improve the service level. However, only small size instances ($\leq$12) can be solved to optimality within a reasonable solution time, with a significant amount of the research has been devoted to designing efficient discrete algorithms and heuristics.

2.3 Literature Review Summary

A review of relevant literature on drone delivery identifies the following trends and research gaps:

1) There is an increasing amount of academic research on the use of drones for home delivery. Although the potential economic benefits of drones are the greatest driver, much of the research focuses on the discrete modeling of routing problems using drones to minimize completion time. There is a need for strategic analyses of how best to deploy drones for home delivery in an economically sound manner.
2) Incorporating the environmental aspects into transportation planning is becoming increasingly important. However, there are only a few studies examining the environmental benefits of drone delivery (and mainly drone-only delivery). Furthermore, the research results are mixed in regard to the energy and emissions efficiency of drone delivery, which is due to a limited understanding of drone energy consumption and highly diverse drone energy consumption models and rates.

3) Although most of the studies show that drones have the potential to reduce delivery costs and emissions, there is no agreement in the literature on (i) how much drones might reduce costs, and how environmentally friendly drones might be; (ii) how the magnitude of the cost and emissions reductions depend on key characteristics of drones and the operational settings; and (iii) how best should drones be used.
4) We are not aware of any studies assessing the cost and emissions tradeoffs for an integrated truck and drone delivery system that includes drone-only delivery, truck-drone delivery, and truck-only delivery.

Chapter 3: Energy Consumption Models of Delivery Drones

An article based on this chapter has been published as "Energy consumption models for delivery drones: A comparison and assessment" in *Transportation Research Part D: Transport and Environment* (Zhang et al. 2021).

Energy consumption is a critical constraint for drone delivery operations to achieve their full potential of providing fast delivery, reducing cost, and cutting emissions. This section provides a uniform framework to facilitate understanding different drone energy consumption models and the inter-relationships between key factors and performance measures to facilitate decision making for drone delivery operations. Drone energy consumption models are classified, analyzed, and assessed. A very wide variations in the modeled energy consumption rates are documented, which are resulting from differences in: (1) the scopes and features of the models; (2) the specific designs of the drones; and (3) the details of their assumed operations and uses. The results provide useful insights for modeling energy consumption for current drones, as well as for future (not yet existing) drones.

Subsection 3.1 provides background and classification of drone energy consumption models in the literature. Subsection 3.2 discusses key drone energy consumption models using a unified notation. Subsection 3.3 documents the differences in the energy consumption rates as reported in the literature as well as in a common setting. Subsection 3.4 discusses insights and implications of the analyses, and subsection 3.5 provides concluding remarks.

3.1 Introduction

The energy requirements of drones determine the key performance metrics of range (or endurance), cost and emissions for drone delivery systems. An accurate estimation of drone energy consumption ensures feasible as well as efficient operating decisions. However, many optimization models that design drone or truck-drone routes or drone delivery systems incorporate energy consumption only indirectly as a fixed limit on drone endurance (flight time limit) or range (flight distance limit) (e.g., Murray and Chu, 2015; Chiang et al., 2019; Kithacharoenchai et al., 2020). Other drone delivery research incorporates energy directly with an energy consumption model based on the fundamental physical forces involved in flight or on field measurements (e.g., Kirschstein, 2020; Murray and Raj, 2020; Poikonen and Golden, 2020; Stolaroff et al., 2018; Figliozzi, 2017; Dorling et al., 2017). Some of these drone energy consumption models are quite simple with only a few parameters, while others are very complex comprised of multiple interdependent components that provide detailed representations of the forces of flight and drone design.

However, these various drone energy models can produce widely divergent results in terms of the energy consumed for essentially the same drone delivery operations, leading to wide differences in modeled drone ranges and emissions. These differences create the need to carefully delineate why such differences exist when modeling the same phenomena (i.e. drone flights or drone delivery) and to assess the different approaches to modeling drone energy consumption. While we limit our consideration to models of battery-powered aerial drones, such as those proposed for home delivery (Lee, 2019; Josephs, 2019) and related activities (e.g., medical deliveries over short ranges (Cohen, 2019; Drones in

HealthCare, 2020)), our analyses and insights are also applicable and important to other applications of drones with limited energy capacity.

The wide variation of energy consumption in published drone delivery research is a result of different scopes and features of the models, different designs of the drones being modeled, and different assumed operations. Thus, current research has not reached consensus on standards for drone energy consumption, nor on how to model delivery drone energy consumption – and therefore existing models may not reflect drone delivery operations well. As drone technology is evolving rapidly, our work strives to help improve understanding of drone energy consumption and to develop common standards. For conventional ground vehicles such as trucks and cars, we have good fuel consumption standards thanks to decades of rigorous research from government agencies, universities and manufacturers (Barth et al., 2005). Given that the operations of drones are more sensitive to the energy capacity than those of conventional vehicles (Cheng et al., 2020), it is critical to develop good understanding and estimation of drone energy consumption.

The key contributions of Chapter 3 are to: (1) review and classify key drone energy consumption models using a unified notation that allows a collective comparison of the energy consumption rates for the various drone types, payloads, speeds, etc.; (2) examine how the distinguishing features of different drone energy consumption models contribute to differences in the calculated energy consumption; (3) evaluate published results on energy consumption for small, medium and heavy delivery drones from both the models and field tests; and (4) compare the drone energy consumption models in a common setting for two prototypical drones to document how energy use and range vary differentially as a function of speed and payload.

3.2 Classifications of Drone Energy Consumption Models

3.2.1 Key Factors Affecting Drone Energy Consumption

Key factors affecting drone energy consumption can be classified into four categories: drone design, environment, drone dynamics, and delivery operations. Major factors in these four categories are provided in Figure 3.1 (adapted from Demir et al. (2014) for road transport). Drone design factors include the weight and size of the drone body, the number and size of rotors, the weight, size and energy capacity of the battery, power transfer efficiency, maximum speed and payload, lift-to-drag ratio, delivery mechanism and avionics. Environmental factors include air density, gravitational force, wind conditions, weather (snow, rain, etc.), ambient temperature and operating regulations. Drone dynamics factors include drone travel speed, drone motion (i.e., takeoff/landing, hover, horizontal flight), acceleration/deceleration, angle of attack and flight altitude. We also include the possibility for drones to be carried on other vehicles such as trucks or public transit, for a portion of their trip. Delivery operations factors include weight and size of the payload, "empty returns" (i.e. the return trip after delivery is without the payload, which implies a successful delivery), fleet size and mix, the number of deliveries per trip, the delivery mode, and the area of the service region. Some of these factors are determined or limited by the drone design (e.g., maximum payload, projected area of the drone, etc.), others are operational factors that can vary for a given drone design (e.g., payload, speed, etc.), and still others are external factors (e.g., weather). Further, many of these factors are interdependent and dynamic during a drone delivery trip.

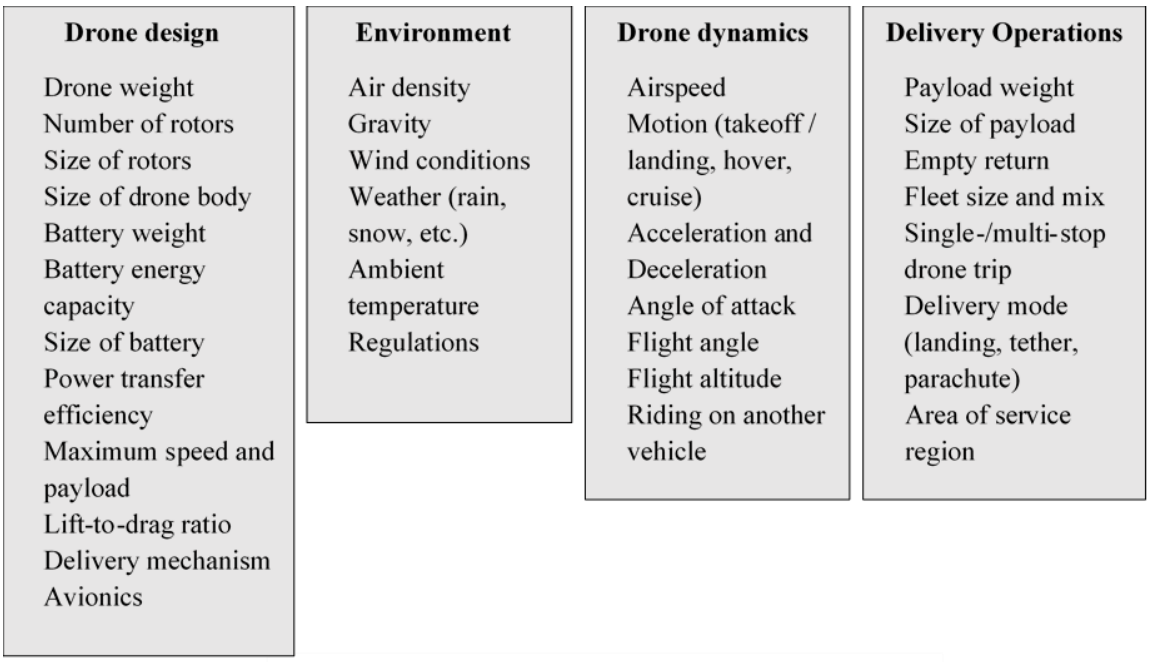

Figure 3.1. Factors affecting drone energy

Uncertainty in estimating drone energy consumption can result from all of these factors, especially drone design, drone dynamics, and delivery operations. Note that if drones are carried on other vehicles (e.g., trucks or public transit) they expend little or no energy, and that different payload delivery modes (landing, lowering via tethers, parachuting) require different levels of energy use. When drones are paired with other vehicles, or multiple drones are operating closely together (as for take-off and landing from the same site), considerable coordination and synchronization may be required, which might lead to substantial hovering by the drone(s).

A drone uses energy to fly by generating thrust and lift forces to overcome the weight and drag forces. Figure 3.2 highlights five key interrelated aspects of drone energy consumption: payload weight, battery weight, drone (airframe) weight, airspeed, and range. The airspeed, payload, drone and battery weight are important determinants of the drone

energy consumption rate. The energy consumption rate in turn, along with the battery weight (and type), determines the range. Note that the payload, drone and battery weight determine the total weight of the drone at takeoff, and involve both design decisions and operating decisions. Increasing the weight of any component increases the energy consumption rate, ceteris paribus, as indicated by the "(+)" on the three arrows from the weights to the energy consumption rate. Airspeed is an operating decision, and for drones (as well as airplanes and helicopters) the power consumed is approximately a convex function of airspeed (due to the competing forces of induced drag, parasite drag, and profile drag – see for example Rotaru and Todorov (2017)). Thus, there is a "(+/-)" on the arrow out of Airspeed. Range is determined by both the drone design and operating decisions. Note that an increase in battery weight will increase the drone energy consumption rate, ceteris paribus, which decreases the range; but the larger battery will also increase the available energy capacity, which increases the range (see Stolaroff et al. (2018) for a discussion of how battery affects drone energy use and range).

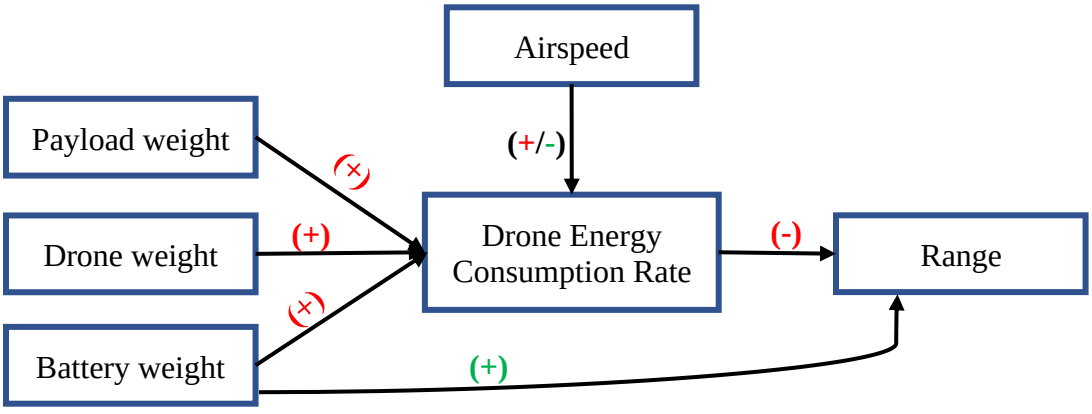

Figure 3.2. Interrelated aspects of the energy consumption rate for drone delivery

3.2.2 Distinguishing Features of Drone Energy Consumption Models

Drone travel models generally impose a fixed time or distance limit constraint to reflect the drone's limited battery capacity. Much of the research assumes a constant rate of energy consumption per unit time or unit distance, so that drone energy consumption is modeled as a linear function of time or distance traveled (e.g., Ferrandez et al., 2016; Ha et al., 2018; Moore 2019; Huang et al., 2020). Some optimization models have incorporated drone energy consumption models explicitly, with a key differentiation being the assumption regarding thrust for steady horizontal flight. The model may assume that (i) the thrust force (T) equals the drag force (D), and the weight force (W) equals the lift force (L) (therefore, $T = W/r$, where $r = L/D$ is the lift-to-drag ratio), (ii) the thrust force equals the weight force, as for a hovering helicopter, or (iii) the thrust force equals the sum of the weight, the drag and the lift forces. These different assumptions reflect different perspectives on the drone operations, e.g., whether they operate more like fixed-wing aircraft or helicopters. These three approaches give rise to three continuing streams of literature for drone energy modeling.

Table 3.1 provides a categorization of 12 key drone energy consumption models identified in the literature. Column 1 shows the reference for the model. Columns 2-4 identify the assumption regarding thrust for steady horizontal flight and show the three groupings of models as discussed earlier. Columns 5-7 reflect the scope of drone travel included in the model for the different drone flight segments (horizontal flight, hover, and vertical flight including takeoff/landing). Note that all 12 models for drone delivery include energy use for horizontal travel, but only half include energy use for hovering and vertical travel. Columns 8-10 indicate adjustments to the modeled energy consumption for wind,

avionics, and empty returns. Note that only two models do not include at least one of the three adjustments in columns 8-10, although these adjustments are often removed from the models in the reported computational results. Including avionics increases energy consumption, while modeling empty returns decreases energy consumption (the return trip has lower weight). Wind is often modeled as increasing drone energy consumption (e.g., D'Andrea (2014)), though more detailed analyses show the energy use may increase or decrease depending on wind speed and direction and drone type (e.g., headwinds may increase lift, thereby reducing the power requirements; see Kirchstein (2020) for a detailed analysis of wind effects). Columns 11-12 indicate the type of model provided (either theoretical based on modeling thrust as in columns 2-4, or regression models) and show that 10 articles provide theoretical models, while 4 papers present regression models. Column 13 indicates the five references that include field tests with a drone, often used for setting parameter values in the model.

Table 3.1. Summary of key features of the models of drone energy consumption

Reference	Thrust Assumption for Flight			Travel Components			Wind	Avionics	Empty Return	Model		Field Tests
	i T=W/r	ii T=W	iii T=W+D+L	Horizontal	Hover	Vertical				Theoretical	Regression	
D'Andrea (2014)	x			x			x	x		x		
Figliozzi (2017)	x			x					x	x		
Dorling et al. (2017)		x		x	x	x				x	x	x
Tseng et al. (2017a)				x	x	x	x	x			x	x
Tseng et al. (2017b)				x	x	x	x	x			x	x
Liu et al. (2017)			x	x	x	x	x			x		x
Lohn (2017)	x			x	x	x	x	x	x	x		
Xu (2017)	x			x	x	x	x	x	x	x		
Stolaroff et al. (2018)			x	x			x		x	x		x
Troudi et al. (2018)	x			x				x		x		
Jeong et al. (2019)		x		x						x	x	
Kirschstein (2020)			x	x	x	x	x	x	x	x		

3.3 Theoretical Models for Energy Consumption

In this section, we discuss the theoretical models for energy consumption of each of the 12 articles in Table 3.1. We first introduce in subsection 3.3.1 a unified notation to facilitate comparison of all models. We then discuss in subsection 3.3.2 the models that use an integrated approach (with the lift-to-drag ratio), followed in subsection 3.3.3 by the models that use a more complex component approach. For consistency we report all energy values in Joules (1 Joule = 1 Watt-second) and the energy consumption rate for steady level flight (Epm) in Joules/meter.

3.3.1 Unified Notation

Different authors use different notation for the same concepts, so to facilitate understanding and comparison of the models, we employ the unified notation shown in Table 3.2 (m = meter; s = seconds; J = joules). We classify the drone physical components into three categories: (i) drone body (including the airframe, propellers, motors, sensors, GPS, avionics, and a camera if used), (ii) drone battery, and (iii) payload (package). Thus, the drone body includes everything except the battery and package. Two areas that sometimes cause confusion in the literature concern the range and the battery usage. We use R to denote the drone flight range as the maximum distance that a drone can travel in one direction and still be able to return to the depot, i.e., half of the round-trip distance for an out-and-back delivery. D'Andrea (2014) and Xu (2017) use the round-trip distance to denote the maximum range, while Figliozzi (2017) does not specify how the range is defined. We define η as the power transfer efficiency, which is the energy loss from battery to the propeller. Figliozzi (2017) uses an overall power transfer efficiency, which also

includes the energy loss from charging to battery, to denote power transfer efficiency. This definition will result in a value a little smaller than η, as charging is not 100% efficient.

Table 3.2. Unified notation for drone energy models

$\rho =$ air density [kg/m^3] (e.g., 1.225 kg/m^3 at 15° C at sea level)
$g =$ acceleration of gravity [m/s^2]
$v_i =$ induced speed [m/s] (the change in the speed of the air after it flows through an object)
$v_a =$ airspeed [m/s] (speed of drone relative to the air)
$\varphi =$ ratio of headwind to airspeed [unitless]
$v =$ drone ground speed [m/s], so $v = (1 - \varphi)v_a$
$d =$ drone one-way travel distance for a single delivery trip [m]
$r =$ lift-to-drag ratio [unitless]
$\eta =$ battery and motor power transfer efficiency (from battery to propeller) [unitless]
$\eta_c =$ battery charging efficiency [unitless]
$k =$ index of the drone components: drone body=1; drone battery=2; payload (package)=3
$C_{D_k} =$ drag coefficient of drone component k [unitless]
$A_k =$ projected area of drone component k [m^2]
$m_k =$ mass of drone component k [kg]
$\gamma =$ maximum depth of discharge of the battery [unitless]
$s_{batt} =$ specific energy of the battery (energy capacity per kg) [J/kg]
$f =$ safety factor to reserve energy in the battery for unusual conditions [unitless]
$R =$ maximum one-way distance of drone travel per battery charge [m]
$P =$ power required to maintain a steady drone flight [Watt=J/s]
$P_{avio} =$ power required for all avionics on the drone (independent of drone motion) [Watt=J/s]
$n =$ number of rotors for a rotocopter drone [rotors]
$N =$ number of blades in one rotor for a rotocopter drone [blades]
$c =$ blade chord length [m]
$c_d =$ blade drag coefficient [unitless]
$\varsigma =$ area of the spinning blade disc of one rotor [m^2]
$\alpha =$ drone angle of attack [radians]
$Epm =$ energy required for steady drone flight per unit distance [J/m]

3.3.2 Energy Models Using Integrate Approaches

The seminal integrated model is provided by D'Andrea (2014) and is based on the ratio of lift-to-drag (r), which translates the fundamental flight principles of manned aircraft to a model for the much smaller scale of unmanned aerial drones. This is a simple formula for calculating the power consumption (in kJ/s) required for the drone to maintain steady flight and operate on-board electronics in terms of the drone total mass, its speed, the lift-to-drag ratio, and the battery's power transfer efficiency. The derivation of this model is given in Appendix 3.A. With no wind, D'Andrea (2014) provides the expression

$$P = \frac{\sum_{k=1}^{3} m_k v}{370 r \eta} + P_{avio}\ , \tag{1}$$

where m_k is the mass of drone component k (k =1, 2, and 3 which correspond to drone body, drone battery, and payload (package), respectively), v is the speed of the drone relative to the ground, P_{avio} is the power consumption of avionics, and the constant 370 (370 = 3600/9.8) allows velocities to be expressed in km/h rather than meters per second. In this paper, we express all speeds in m/s if not otherwise specified, so the equivalent expression is

$$P = \frac{(\sum_{k=1}^{3} m_k) g v}{r \eta} + P_{avio}. \tag{2}$$

The energy consumed for steady flight over a distance d is the power multiplied by the travel time d/v, so the energy per meter of travel (Epm) is the power divided by the speed

$$Epm = \frac{P}{v}, \tag{3}$$

So, for D'Andrea (2014) including possible headwinds as indicated via the unitless factor $\varphi = \frac{headwind\ speed}{drone\ airspeed}$, we have

$$Epm = \frac{1}{1-\varphi}\left(\frac{g \sum_{k=1}^{3} m_k}{r \eta} + \frac{P_{avio}}{v_a}\right), \tag{4}$$

where v_a is the speed of the drone relative to the air, and $v = (1 - \varphi)v_a$.

One example in D'Andrea (2014) with no headwind ($\varphi = 0$), uses $m_1 = m_2 = m_3 = 2$ kg, $v_a = 12.5$ m/s (45 km/h), $r = 3, \eta = 0.5$ and $P_{avio} = 100$ J/s. This requires total power of $P = 590$ J/s, or $Epm = 46.9$ J/m. With an 8.33 m/s headwind (30 km/h) and other values as above, the energy consumption triples to $Epm = 140.8$ J/m. In D'Andrea (2014), the avionics consume about 17% of the total power for steady flight. Without avionics, $Epm = 38.9$ J/m when there is no headwind, and $Epm = 116.8$ J/m with an $8.33\ \mathrm{m/s}$ headwind.

The D'Andrea (2014) model has been used as a basis by several other researchers with variations in the parameters, including Troudi (2018), Figliozzi (2017), Lohn (2017), Xu (2017) and Gulden (2017). Troudi et al. (2018) use the same model as D'Andrea (2014), except they state that, "the consumption of the rest of the electrical equipment in the vehicle is insignificant in our study" (p.7), so they set $P_{avio} = 0$. The authors consider an MD4-1000 drone with a battery of 1,040,400 Joules (289Wh), payload of $m_3 = 1.2$ kg, maximum takeoff weight ($m_1 + m_2 + m_3$) of 5.55 kg, and speed $v_a = 13$ m/s.

Figliozzi (2017) extends the basic model from D'Andrea (2014) for "steady flight" to consider empty returns. This model does not include power for avionics ($P_{avio} = 0$), models the lift-to-drag ratio as dependent on speed (with $r(v)$), and provides a unitless parameter for battery recharging efficiency (η_r). The overall energy consumption rate per unit distance (with no headwind) is given as

$$Epm = \frac{1}{2}\left(\frac{g\sum_{k=1}^{3} m_k}{r(v)\eta\eta_r} + \frac{g\sum_{k=1}^{2} m_k}{r(v)\eta\eta_r}\right). \quad (5)$$

The first term in parentheses is the energy consumption rate with a package, and the second term is the energy consumption rate without a package on the return trip.

The parameters used by Figliozzi (2017) are for a MicroDrones MD4-3000 and are as follows: $m_1 + m_2 = 10.1$ kg, $m_3 = 5$ kg, and the drone has a range of 36 km, though the paper suggests 70% of this, or 25 km, as the maximum range to provide a safety margin and allow for "unknown factors that can increase energy consumption such as headwinds". The lift-to-drag ratio $r(v)$ is not specified; however the article reports an Epm value of 77.8 J/m "calculated utilizing manufacturer information" and an overall power efficiency product of $\eta\eta_r = 0.9 * 0.73 = 0.66$. From these values, the lift-to-drag ratio can be calculated in reverse as $r = 2.4$. The article also assumes Epm values for a future more efficient drone at 38.9 J/m (half of the baseline value) and for a drone in "adverse conditions" (e.g., high winds) at 116.7 J/m (50% above the baseline value). This article uses a battery of 2.8 million Joules (or 777Wh).

The energy model used in the RAND Corporation studies (Lohn, 2017; Xu, 2017; Gulden, 2017) is based on D'Andrea (2014) and described in Lohn (2017). Lohn (2017) reports that for truck and drone delivery serving a city the size of Los Angeles (1500 km^2) from a centrally located drone depot, the average energy use rate is Epm =112.5 J/m (assuming uniformly distributed deliveries in a circular city). Xu (2017) models a complete drone delivery mission including ascending to 150 m of altitude, flying level at 22.2 m/s (80 km/h) into a 2.8 m/s (10 km/h) headwind and then descending to the delivery site, with 30 seconds of hovering. The return trip is similar but without the payload and also includes flying into a 2.8 m/s (or 10 km/h) headwind. Results are provided for a baseline multicopter design based on an Amazon Prime Air VTOL drone with 8 lift rotors and 2 cruise motors

and the lift-to-drag ratio $r = 3$. For this baseline hybrid drone (weighing 55 lbs with a 20 mile range), Xu (2017) provides an energy consumption of 5.4 MJ for a 2.3 kg payload flying 32.2 km, resulting in $Epm = 168$ J/m. Xu (2017) indicates for a small drone with an 8 km delivery range, the energy consumption would be 1.44 MJ for the same payload flying 16 km, resulting in $Epm = 90$ J/m. He also considers an "advanced design" drone with future improvements in drone and battery design to achieve $r = 5.6$, for which flying a 2.3-kg payload 32.2 km roundtrip provides $Epm = 29$ J/m.

3.2.3 Energy Models Using Component Approaches

A different approach for modeling drone energy consumption is based on helicopter operations, with the assumption that the power consumed during level flight, takeoff, or landing is approximately equivalent to the power consumed while hovering. This model ignores the impact of drone speed on energy consumption. Dorling et al. (2017) provides a model for drone energy consumption based on hovering only (with the assumption that this is approximately equal to the energy for drone travel). During hover, the airspeed is zero, and the thrust balances the weight force, so

$$T = g \sum_{k=1}^{3} m_k \, . \tag{6}$$

Based on helicopter theory (e.g., Leishman (2002)), the power required for the drone to hover is

$$P = \frac{T^{3/2}}{\sqrt{2n\rho\varsigma}} = \frac{\left(g \sum_{k=1}^{3} m_k\right)^{3/2}}{\sqrt{2n\rho\varsigma}} \, , \tag{7}$$

where ρ is the air density, n is the number of rotors , and ς is the area of the spinning blade disc of one rotor.

The Epm can then be calculated as

$$Epm = P/v_a = \frac{\left(g\sum_{k=1}^{3} m_k\right)^{3/2}}{v_a\sqrt{2n\rho\varsigma}}\,. \tag{8}$$

This does not include power for avionics or an adjustment for wind or power transfer efficiency η.

Field tests conducted with the Hexa-B drone with no payload showed that hovering consumed 2.3% more power than steady flight at 6 m/s, and 4.7% more power than repeated altitude changes (vertical flight) from 0 to 25 m. Field test data while hovering with small payloads of 0.5-1.5 kg provided very different, and much larger power consumption levels than the theoretical model of eq. (7) (4.5 to 5 times larger!).

The authors also approximate the hover power consumption as a linear function of the battery and payload weight for an ArduCopter Hexa-B drone with $n = 6$, $\varsigma = 0.2$ m^2, and a frame weight $m_1 = 1.5$ kg as

$$P = \beta_1(m_2 + m_3) + \beta_0\,, \tag{9}$$

where β_1 is the power consumed per kilogram of battery and package weight, and β_0 is the power required to keep the drone frame of mass m_1 in the air. Values of $\beta_1 = 46.7$ J/s-kg and $\beta_0 = 26.9$ J/s were generated from eq.(7) using linear regression with $m_2 + m_3$ ranging from 0 to 3 kg in increments of 0.001 kg. Regression parameters for eq.(9) based on the field tests with small payloads provide much larger values of β_1 and β_0,

$$Epm = P/v_a = [217(m_2 + m_3) + 185]/v_a \tag{10}$$

$$Epm = P/v_a = [171(m_2 + m_3) + 187]/v_a \tag{11}$$

for a large 14.8 V battery and a small 11.1 V battery, respectively.

Jeong et al. (2019) adopt Dorling's hovering model for a MikroKopter MK8-3500 drone. They present a linear regression equation for power based only on payload mass, and state the "proposed energy consumption model provides realistic values that are

analogous to the experiment result"; however they do not provide any parameter values for the model.

Because drones are very complicated flying vehicles subject to many different dynamic forces, detailed modeling of drone performance is not nearly as straightforward as modeling other delivery vehicles such as trucks. Stolaroff et al. (2018) provide a model based on the fundamental forces of flight, and also conduct field testing of drones. Fundamental forces opposing flight include the weight force of the aircraft (due to gravity) and the drag forces in the direction opposing the direction of travel. The two main drag forces acting on aircraft are parasite drag from the aircraft moving through the atmosphere and induced drag from redirecting the airflow to create the lift that keeps the aircraft aloft. Power is required to create the lift and thrust that overcome the weight and drag forces. For a hovering rotocopter, Stolaroff et al. (2018) provide the same power model as Dorling et al. (based on helicopters) in equation (7). But for forward flight, Stolaroff et al. (2018) present a model for thrust

$$T = W + D = g \sum_{k=1}^{3} m_k + \frac{1}{2} \rho \sum_{k=1}^{3} C_{D_k} A_k \, {v_a}^2 \,, \tag{12}$$

where the first term reflects the total drone weight and the second term is the parasite drag force, which depends on the drag coefficient C_{D_k} and the projected area perpendicular to travel A_k of each drone component (airframe, battery and payload). Note that when the drone hovers, the airspeed equals zero ($v_a = 0$) and so $T = \sum_{k=1}^{3} m_k g$, as in eq. (7).

With forward flight, or heavy wind, Stolaroff et al. (2018) use a power consumption formula adapted from Hoffman et al. (2007)

$$P = \frac{T(v_a sin\alpha + v_i)}{\eta} \,, \tag{13}$$

where α is the angle of attack (i.e., the angle of the airspeed to the drone rotor) and v_i is the induced speed, which can be found by solving (numerically)

$$v_i = \frac{g\sum_{k=1}^{3} m_k}{2n\rho\varsigma\sqrt{(v_a cos\alpha)^2+(v_a sin\alpha+v_i)^2}}\,. \tag{14}$$

The angle of attack α is given by

$$\alpha = tan^{-1}\left(\frac{\frac{1}{2}\rho\left(\sum_{k=1}^{3} C_{D_k}A_k\right){v_a}^2}{g\sum_{k=1}^{3} m_k}\right). \tag{15}$$

For large values of α the drone may become unstable, so in practice α may be limited to maintain stable flight (Ai, 2019; DJI website, 2020). The overall energy per meter is then given as

$$Epm = \frac{T(v_a sin\alpha+v_i)}{v_a\eta}\,, \tag{16}$$

with α from eq. (15) and v_i being the solution of eq. (14). Empty returns are assumed.

Stolaroff et al. (2018) consider a small quadcopter of total mass 2.57 kg, including a 0.5 kg payload (3D Robotics' Iris), and a larger octocopter of total mass 24 kg, including a 7 kg payload (Turbo Ace's Infinity 9). Field measurements consisting of 1073 flight segments with the small quadcopter in moderate winds (up to 7 m/s at random orientation to the direction of travel) are used to set some parameter values, including the power transfer efficiency $\eta = 0.7$. See Stolaroff et al. (2018) for details and all parameter values.

Stolaroff et al. (2018) also model the maximum range of a drone assuming that the drone carries the payload in one direction only (i.e., $m_3 = 0$ on the return trip). This is expressed as a function of the battery mass (m_2), battery energy capacity per kg (s_{batt}), the depth of battery discharge (γ), a battery safety factor f (assumed to be 1.2), and the energy consumption rate carrying the payload Epm_{loaded} and on the empty return $Epm_{unloaded}$

$$R = \frac{m_2 s_{batt} \gamma}{(Epm_{loaded} + Epm_{unloaded}) f} \ . \quad (17)$$

Liu et al. (2017) provide a more comprehensive and detailed energy consumption model for small quadrotor UAVs. The model has three components: (i) induced power to maintain lift, which is a function of the thrust and the vertical drone speed, (ii) parasite power as in Stolaroff et al. (2018), and (iii) profile power to overcome the rotational drag encountered by propeller blades, which is a function of the thrust and the airspeed (see Rotaru and Todorov (2017) for related details on power requirements for helicopters).

The parasitic power is the same as in Stolaroff et al. (2018) and is given by $\sum_{k=1}^{3} \frac{1}{2} \rho {v_a}^3 C_{D_k} A_k$, although the authors do not explicitly consider the drag forces for the battery and the payload. The other two power components depend on the thrust, which is given by

$$T = \sqrt{(g \sum_{k=1}^{3} m_k - c_5 (v_a cos\alpha)^2)^2 + \left(\frac{1}{2} \rho \left(\sum_{k=1}^{3} C_{D_k} A_k\right) {v_a}^2\right)^2} \ , \quad (18)$$

where the term $g \sum_{k=1}^{3} m_k$ is the weight to be lifted, the term $c_5 (v_a cos\alpha)^2$ reflects the lift generated from horizontal movements (likely to be especially important for hybrid drones with lifting surfaces), and the last term is again the parasitic drag. For a drone in steady level flight, the Epm, based on the total power from equation (14) in Liu et al. (2017), is

$$Epm = \frac{\kappa_1}{\sqrt{2n\rho\varsigma}} \frac{T^{3/2}}{v_a} + \frac{1}{2} \rho \left(\sum_{k=1}^{3} C_{D_k} A_k\right) {v_a}^2 + c_2 \frac{T^{3/2}}{v_a}, \quad (19)$$

where the first term reflects the induced power, the second term reflects the parasitic power and the last term reflects the profile power, with parameter c_2 depending on the air density and details of the rotors (including the efficiency of converting rotor angular speed to thrust, the number of blades in each propeller, the blade chord width, drag coefficient, and length). Based on field testing, Liu et al. (2017) report that with a 1.43-kg 3DR IRIS+ quadcopter,

$\kappa_1 = 0.8554$ and $c_2 = 0.3177$ (m/kg)$^{1/2}$. Note that including the profile power in the component model requires detailed information on the drone rotors and motors (for calculating c_2).

Field tests of ascending/descending flight reported in Liu et al. (2017) showed that ascending takes 9.8% more power than hovering, and descending takes 8.5% less power than hovering. Di Franco and Buttazzo (2015) found similar results from field experiments with a 1.3 kg IRIS quadcopter. The most involved field experiment in Liu et al. (2017) required the drone with no payload to ascend to 70 m, then fly a horizontal rectangular loop for about 550 m, and descend and land back at the origin. Comparing the computed power and estimated power from the proposed models, results show that the model underestimated the energy consumed in ascending by 10.7%, underestimated the energy consumed in horizontal flight by 16.3%, and overestimated the energy consumed in descending by 2.2%. For the total flight, the model underpredicted the energy consumed by 11.4%. Because the horizontal portion of flight was small (550 m), ascending and descending consumed 39% of the total energy for the flight. If the performance for horizontal flight was extended to a 10 km horizontal trip, then ascending and descending would consume only 3.4% of the total trip energy. For the rectangular loop trip (of approximate length 712 m), the reported modeled energy consumption of 1.23×10^4 J for the horizontal flight portion equates to about $Epm = 17.3$ J/m.

Kirschstein (2020) provides a component model originally from Langelaan et al. (2017) based on an idealized delivery process (like Xu (2017)) with takeoff and ascent at 45° to a cruising altitude (150 m), level flight, descent (at 45°) with hovering, then landing for delivery. The return is similar but without the payload. Like Liu et al. (2017) the model

includes energy consumed for induced power, parasite power, and profile power; but the model also includes power for climbing and avionics, and adjustments for power losses due to the electric motor, transmission and charging efficiencies. For steady flight, Kirschstein (2020) uses a thrust of

$$T = \sqrt{(g\sum_{k=1}^{3} m_k)^2 + \left(\frac{1}{2}\rho\left(\sum_{k=1}^{3} C_{D_k}A_k\right){v_a}^2\right)^2 + \rho\left(\sum_{k=1}^{3} C_{D_k}A_k\right){v_a}^2 mg\sin\theta}, \quad (20)$$

where the flight angle θ allows ascending and descending to be modeled. For hovering (i.e., $v_a = 0$), the thrust reduces to $g\sum_{k=1}^{3} m_k$. Kirschstein's general energy model is detailed in Appendix 3.B and the Epm for steady level flight (i.e., $\theta = 0$) with no wind can be written as

$$Epm = \frac{1}{\eta}\left(\frac{\kappa T w}{v_a} + \frac{1}{2}\rho\left(\sum_{k=1}^{3} C_{D_k}A_k\right){v_a}^2 + \frac{\kappa_2\left(g\sum_{k=1}^{3} m_k\right)^{1.5}}{v_a} + \kappa_3\left(g\sum_{k=1}^{3} m_k\right)^{0.5} v_a\right) + \frac{P_{avio}}{\eta_c v_a}. \quad (21)$$

The first term in the Epm is for induced power with κ being the "lifting power markup" and w the "downwash coefficient" (See Kirschstein (2020) for details). The second term in the Epm is for parasite drag (as in Liu et al. (2017) and Stolaroff et al. (2018)). The third and fourth terms are for profile power where constants κ_2 and κ_3 reflect details of the rotors and environment (as in Liu et al. (2017)). The last term in the Epm is for avionics.

Kirschstein (2020) provides analyses for delivery in an urban region (comparing drones with diesel and electric trucks) with large octocopter drones (m_1+$m_2 = 12$ kg) that carry a 2.5 kg payload ($m_3 = 2.5$ kg), travel at 22.2 m/s, have a flight radius of 9 km (and the trips include 5 minutes of hovering), power transfer efficiency $\eta = 0.73$, battery charging efficiency $\eta_c = 0.9$ and $P_{avio} = 100$ J/s (as in D'Andrea (2014)). For this drone,

the constants in eq.(20) are: $\kappa = 1.15$, $\kappa_2 = 0.502$ and $\kappa_3 = 0.118$; and the loaded $Epm = 131.5$ J/m.

Several authors have developed drone power and energy models for problems focused on drones used in wireless communication networks. These models are not for delivery drones, but rather consider drone energy consumption as it impacts the performance and endurance of drones in communication systems. See Appendix 3.C for brief discussion of these models.

3.2.4 Energy Models Using Other Approaches

Drone travel models generally impose a fixed time or distance limit constraint to reflect the drone's limited battery capacity. Much of the research assumes a constant rate of energy consumption per unit time or unit distance, so that drone energy consumption is modeled as a linear function of time or distance traveled (e.g., Ferrandez et al., 2016; ; Ha et al., 2018; Moore 2019; Huang et al., 2020). However, there is considerable variance in the assumed consumption values; for example, Ferrandez et al. (2016) use a value of 46.1 J/m (based on a 2013 Amazon delivery drone carrying 5 lbs packages at 70 km/h), while Moore (2019) uses 223.7 J/m (based on field tests with a DJI Matrice 600 Pro by the U.S. Department of Energy 2019, 2020). Rather than using a single fixed energy consumption rate, Goodchild and Toy (2018) consider energy consumption rates ranging from 22-223 J/m (10-100 Wh/mile) to assess the sensitivity of the research findings to the energy efficiency of drones. Their results show how the emissions benefits of drones relative to trucks strongly depend on the drone energy consumption rate; however, they do not suggest a particular energy consumption rate to use.

A final approach to modeling drone energy consumption is with regression based on field experiments, as in some articles previously mentioned. Tseng et al. (2017a, 2017b) present a nine-term nonlinear regression model for drone power use that includes horizontal and vertical speeds and acceleration, as well as payload mass and wind speed, and provides a good fit to the reported field data. The regression model for steady flight with no wind reduces to $P = \beta_1 v_a + \beta_7 m_2 + \beta_9$. They collected data to estimate the parameters based on test drone flights using a 3DR Solo drone (weighing 2 kg) with small payloads of 0 kg, 0.25 kg, and 0.5 kg, and a DJI Matrice 100 drone (weighing 2.8 kg) with small payloads of 0 kg, 0.3 kg, and 0.6 kg. The regression equation for Epm in Tseng et al. (2017b) and Tseng (2020) for steady flight with speeds up to 5 m/s and no wind for the larger DJI Matrice 100 drone is

$$Epm = \frac{P}{v_a} = -1.526 + \frac{0.220 m_2 + 433.9}{v_a}, \tag{22}$$

and for the smaller 3DR Solo drone it is

$$Epm = -2.595 + \frac{0.197 m_2 + 251.7}{v_a}. \tag{23}$$

Murray and Raj (2020) design truck-drone tandem delivery routes with a three-phase heuristic and is the only reference to consider multiple drone energy models, including the model of Liu et al. (2017), a simple regression model that is linear in payload, and other models with a fixed distance or time limit (essentially modeling energy consumption as a linear function of drone travel distance or time). Relevant findings for our study were that (i) the different energy models can produce very different routes, with several energy models leading to the creation of energy infeasible drone routes, and (ii) it is important to include the energy consumed outside the steady level flight portion of a

delivery trip (e.g., for launch, retrieval and delivery), especially for any hovering needed for coordination with a truck or other drones prior to landing.

3.4 Analysis and Results

In this section, we compare results for key drone energy models described in Section 3.3 to explore the interrelated aspects of payload mass, speed, energy consumption per meter and maximum drone range. The energy use and drone range are outputs determined by (i) specifics of the drone and the battery modeled, (ii) operations, specifically speed and payload mass, and (iii) energy adjustments, such as, wind, avionics, and energy loss. Table 3.3 summarizes the 11 drone energy models examined in Section 3.3, arranged in order of increasing drone weight. These are the baseline models presented in each reference (extensions to these models are presented later in Table 3.4).

Columns 1-2 provide the color and ID used in later figures. The first part of the ID (1 or 2 characters) indicates the reference and model, where DH and DR respectively indicate the theoretical hovering and the regression models in Dorling et al. (2017), and T1 and T2 indicate the two regression models from Tseng et al. (2017b). The second part of the ID is the number of rotors for the drone or the drone type. The third part of the ID indicates the drone size, with "L" for light drones (<4 kg), "M" for medium drones (4-15 kg) and "H" for heavy drones (>15 kg). Note that the majority of models are for small rotocopter drones with small payloads. Column 3 identifies the reference. Column 4 describes the model type (integrated, component or regression) as discussed in Section 3. Columns 5-8 provide information on the drone type, mass and airspeed for the baseline setting in the reference. Column 9 is the equation number in this paper for Epm. Column 10 indicates if parameters in the equation were set based on field experiments with a

particular drone. Each of these articles provides at least one data point for Epm based on a particular drone model, with the regression models based on multiple data points.

Table 3.3. Key drone energy models

Color	ID	Reference	Model Type[1]	Drone Type (index)	$m_1 + m_2$ (kg)	Payload used in results (kg)	Airspeed v_a (m/s)	Equation for Epm	Field tests to set parameters
Blue	L-4-L	Liu et al. (2017)	C	Quadcopter (4)	1.46 (L)	0	8-23	(18-19)	X
Blue	S-4-L	Stolaroff et al. (2018)	C	Quadcopter (4)	2.07 (L)	0.5	10	(12-16)	X
Blue	DH-6-L	Dorling et al. (2017)	C	Hexacopter (6)	2 (L)	1	6[2]	(8)	
Blue	DR-6-L	Dorling et al. (2017)	R	Hexacopter (6)	2 (L)	0 – 1	6	(10)	X
Blue	T1-4-L	Tseng et al. (2017b)	R	Quadcopter (4)	2 (L)	0 – 0.5	0-5	(22)	X
Blue	T2-4-L	Tseng et al. (2017b)	R	Quadcopter (4)	2.8 (L)	0 – 0.6	0-5	(23)	X
Blue	A-G-L	D'Andrea (2014)	I	General (G)	4 (L)	2	12.5	(4)	
Orange	F-4-M	Figliozzi (2017)	I	Quadcopter (4)	10.1 (M)	5	unknown	(5)	
Orange	K-8-M	Kirschstein (2020)	C	Octocopter (8)	12 (M)	2.5	22.2	(20-21)	
Red	S-8-H	Stolaroff et al. (2018)	C	Octocopter (8)	17 (H)	7	10	(12-16)	X
Red	X-H-H	Xu (2017)	I	Hybrid-current (H)	25(H)	2.3	22.2	Not available[3]	

[1]C = component model; R = regression model; I = integrated model

[2]the setting in Dorling et al. (2017) uses a drone speed of 6 m/s although the energy equation (8) does not include speed

[3]based on D'Andrea (2014)

3.4.1 Epm Results from the Literature

Figure 3.3 shows a graph of Epm versus payload mass for the models in Table 3.3 using the parameter values and setting in the reference. There are three short lines for the regression models (DR-6-L, T1-4-L, T2-4-L), and one point each for the other eight models. We emphasize that these data are for the specific drone and the setting considered in each reference (i.e., the drone size, payload and speed shown in Table 3.3) in steady level flight with no wind or avionics, with the exception of Xu (2017) which includes a complete flight profile (ascent, level flight, hovering and descent on the forward and return trip). Xu (2017) does not provide a model that allows the steady level flight portion of the trip to be extracted (although the steady level flight for the baseline model in Xu (2017) would be 98.8 J/m if steady level flight accounted for the same percentage of the total energy as in Kirschstein (2020), which uses a similar trip profile).

The purpose of Figure 3.3 is to document the wide range of energy consumption values reported in the literature for essentially the same delivery mission, albeit with payloads that range from 0-7 kg. As expected, the general trend is that larger (heavier) drones and payloads have larger Epm values; however, the range of Epm values varies substantially, both across the payloads and for similar payloads. The models for light drones with payloads ≤1 kg (and airspeeds ≤6 m/s) cluster in the lower left of Figure 3 with Epm values ranging from 16 J/m to 107 J/m. The Epm for drones with payloads of 2-5 kg (and airspeeds of 12-23 m/s) range from 39 J/m to 168 J/m, though as noted above X-H-H includes a complete delivery profile. The S-8-H model for the drone with the largest payload (7 kg) provides by far the largest Epm of 436 J/m, which is more than 5 times larger than the energy for the drone with the next largest payload (the F-4-M model with a

5 kg payload). While Figure 3.3 displays Epm values from the models or field tests for the baseline setting described in the corresponding article, these models could be used for other delivery settings, such as delivering lighter payloads. For example, using the Stolaroff et al. (2018) heavy drone S-8-H model with a small 2 kg payload would reduce the Epm to 322 J/m, which is still well above the values reported for the other models with similar payloads.

Key findings revealed by Figure 3.3 are: (i) the energy consumption rates reported in the literature for steady level flight vary substantially with the payload, from under 20 J/m to over 400 J/m for payloads up to 7 kg; and (ii) with similar payloads the energy consumption models differ by factors of several hundred percent. Other drone research that does not employ an energy model, but uses a fixed value for Epm, such as Ferrandez et al. (2016) (46.1 J/m), Moore (2019) (223 J/m) or Goodchild and Toy (2018) (23-223.1 J/m) also show a very wide range of energy consumption rates. This documents the lack of consensus in energy efficiency of drones, and has important implications when drawing conclusions from modeling drone operations.

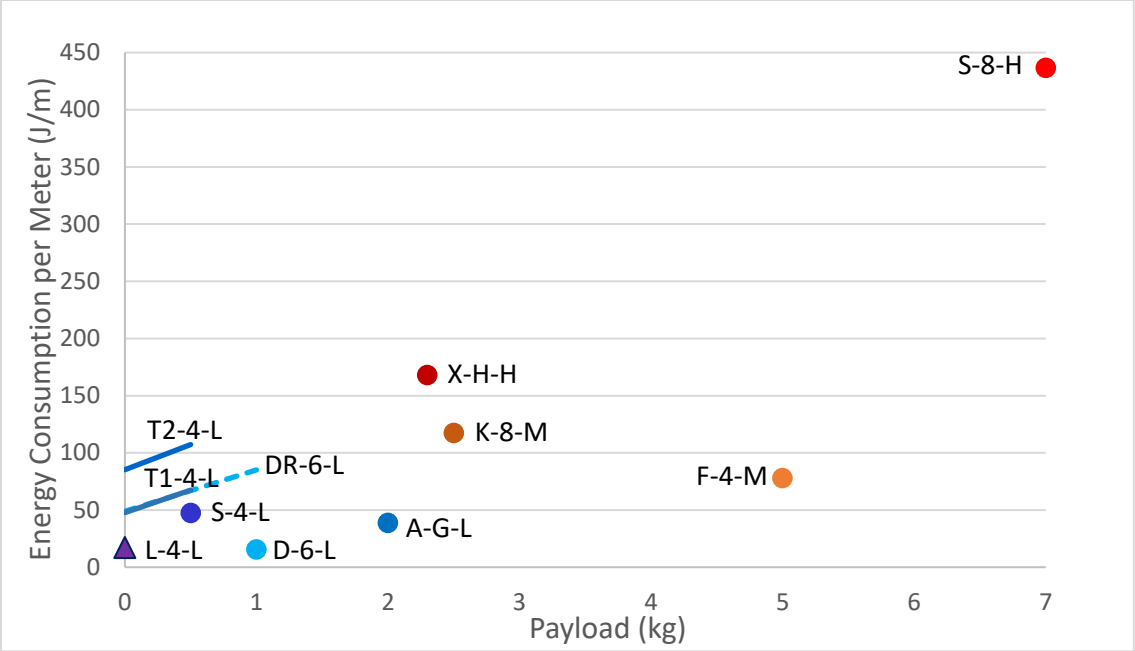

Figure 3.3. *Epm* results from baseline models in Table 3.3

Some of the references in Table 3.3 consider adjustments to the baseline energy consumption rates due to factors such as wind and weather, avionics, flight profiles and future advances in technology. Tables 3.4 summarizes the *Epm* values for these adjusted models from four of the references. The first row in each grouping for the same reference reflects the baseline setting (no avionics, or wind), with the other rows showing adjustments for various additional conditions. The format of the Table is similar to Table 3.3, but with column 3 added to show the additional considerations, column 8 reporting the *Epm* values and column 9 showing the percentage change from the baseline.

The first three rows for the D'Andrea (2014) model show the moderate increase (20%) in *Epm* due to avionics, and the very large increase (261%) from including a strong wind (30 km/h). The next three rows show the assumed 50% increase in *Epm* in Figgliozzi (2017) due to "adverse weather", and the assumed 50% reduction for a future advanced

drone. The next four rows for Kirschstein (2020) show a very small increase (3.4%) in Epm from avionics, a very large increase (129%) due to strong winds of 45 km/h, and a substantial increase (70%) by having both moderate winds (10 km/h) and modeling energy for a complete flight profile. The final three rows for Xu (2017) show the very large increase in Epm of 213% from using a larger drone with a 9.2 kg payload (and a shorter range due to using a fixed battery size), and a hypothetical large reduction in *Epm* of 83% from future advances in drones (especially in improving the lift-to-drag ratio).

Table 3.4 shows that incorporating more realistic conditions (e.g., especially high winds) and a complete delivery profile (beyond just steady level flight) increases the Epm substantially, in several cases over 100%. This suggests that using Epm values for steady level flight may significantly underestimate the total energy consumption of a drone trip. On the other hand, two researchers suggest that future developments have the potential to substantially reduce the energy requirements for drone travel. While future drone technology developments are difficult to predict, the large impact of strong winds on energy consumption is an area that needs further research, especially with field measurements in real operating environments. Some drone applications may allow flexible timing (such as inspections) to avoid wind and bad weather, while other applications (home delivery or surveillance) may have very limited time flexibility.

Table 3.4. Key drone energy models with additional conditions

ID	Reference	Additional conditions to baseline	$m_1 + m_2$ (kg)	Payload used in results (kg)	Airspeed v_a (m/s)	Range[1] (km)	Epm (J/m)	% Epm increase to baseline
A-G-L	D'Andrea (2014)	Baseline	4 (L)	2	12.5	10	39.2	-
		Avionics					47.2	20.0%
		Wind (30 km/h), avionics					141.6	261%
F-4-M	Figliozzi (2017)	Baseline	10.1 (M)	5	unknown	25	77.8	-
		Adverse weather					116.7	50.0%
		Advanced drone					38.9	-50.0%
K-8-M	Kirschstein (2020)	Baseline	12 (M)	2.5	22.2	9	127.2	-
		Avionics					131.5	3.38%
		Wind (45 km/h), avionics					300.6	129%
		A complete flight profile with wind (10 km/h) & avionics					216.4	70.1%
X-H-H	Xu (2017)	Baseline: a complete flight profile with wind (10 km/h) & avionics	25.0 (H)	2.3	22.2	16.1	168.0	-
		Large drone	70.8 (H)	9.2		12	525.0	213%
		Advanced drone	5.2 (M)	2.3		16.1	29.0	-82.7%

[1]range = half of the round-trip distance.

In summary, the published literature on drone energy consumption shows a strong lack of consensus (and standards) on the appropriate energy consumption rates, even for similar drone sizes and operations. The lack of consensus shown in Figure 3.3 is further amplified by the results in Table 3.4 from including additional practical considerations. The energy consumption estimates of drones vary substantially from under 20 J/m to over 500 J/m. Because these differences are partly due to the different drones (e.g., different sizes, motor and rotor details, etc.) and settings (speed, payload, wind, etc.) employed, and partly due to the different model structures, in the following section we compare the models in a common setting with a common set of data reflecting two prototypical drones.

3.4.2 Epm Results Using a Common Drone and Operational Setting

To assess the drone energy consumption models from the literature on a common basis, we evaluate five fundamental modeling approaches discussed in Section 3.3 using common drone design parameters and a common operational setting, where the payload and speed are allowed to vary. The modeling approaches are identified in Table 3.5, along with the key reference and the equation(s) for Epm. The first model, denoted LD, is the integrated model with a lift-to-drag ratio, based on eq.(4) from D'Andrea (2014). The second model, denoted RH, includes the energy use for rotocopter hovering only, as in eq.(8) from Dorling et al (2017). The third model, denoted R2, includes two rotocopter energy components to overcome the induced drag and parasite drag, as in Stolaroff et al. (2018). The fourth model, denoted R3, includes three rotocopter energy components, as it adds the profile drag to the induced and parasite drag, as in Kirschstein (2020). The final model, denoted LR, is the regression model from Tseng (2017b) that provides Epm as a function of payload mass and airspeed.

Table 3.5. Five fundamental models for drone energy consumption of steady level flight

Model	Key Reference	Epm
LD	D'Andrea (2014)	$\frac{\sum_{k=1}^{3} m_k g}{r\eta}$
RH	Dorling et al. (2017)	$\frac{(\sum_{k=1}^{3} m_k\, g)^{3/2}}{\eta v_a \sqrt{2n\rho\varsigma}}$
R2	Stolaroff et al. (2018)	$\frac{T(v_a sin\alpha + v_i)}{v_a \eta}$ where $T = \sum_{k=1}^{3} m_k g + \frac{1}{2}\rho \sum_{k=1}^{3} C_{D_k} A_k\, {v_a}^2$ and v_i is found from solving equations (14-15)
R3	Kirschstein (2020)	$\frac{1}{\eta}\left(\frac{\kappa T w}{v_a} + \frac{1}{2}\rho \sum_{k=1}^{3} C_{D_k} A_k\, {v_a}^2 + \frac{\kappa_2 (\sum_{k=1}^{3} m_k\, g)^{1.5}}{v_a} + \kappa_3 \left(\sum_{k=1}^{3} m_k g\right)^{0.5} v_a\right)$ where $T = \sqrt{(\sum_{k=1}^{3} m_k g)^2 + \left(\frac{1}{2}\rho \sum_{k=1}^{3} C_{D_k} A_k\, {v_a}^2\right)^2}$ and w is from solving equation (B2)
LR	Tseng (2017b)	$-2.595 + \frac{0.197 m_2 + 251.7}{v_a}$ (for small payloads and speeds less than 5 m/s)

To compare the different modeling approaches on a common basis we use the set of parameters shown in Table 3.6 (based in part on those in Stolaroff et al. 2018). Environmental parameters (e.g., gravity, air density, etc.) independent of drone design are fixed to the common values shown in Panel 1 of Table 3.6. To model small and large drones, we use the associated parameters values shown in Panel 2 of Table 3.6. The first set of parameters in column 3 of Panel 2 is associated with a small quadcopter drone capable of carrying a payload of 0.5 kg, such as might be used for medicine deliveries. The second set of parameters in column 4 of Panel 2 is associated with a larger octocopter drone capable of carrying a payload of 7 kg, such as might be used for home delivery of consumer goods. For all models, we include a common value for the power transfer efficiency of the drone,

and we also assume empty returns so the Epm values are the average of the loaded (with the payload) and unloaded (without the payload) Epm values. We consider an environmental setting with no wind, and do not include energy consumption for avionics, vertical flight or hovering. We vary either the payload mass or the airspeed to explore their effects on Epm and range. Thus, by using the same drone specification and flight conditions, we can document the Epm and flight range variabilities due to the different model structures and assumptions (not due to different input data). The performance measures of interest are Epm and flight range. Range is calculated from eq.(17) based on the Epm calculated using the equations in Table 3.5.

Table 3.6. Parameter values used in drone energy use models in a common setting.

Panel 1. Parameter values that are independent of drone type

Term	Symbol	Value
Air density [kg/m^3]	ρ	1.225
Acceleration of gravity [m/s^2]	g	9.807
Ratio of headwind to airspeed [unitless]	φ	0
Empty return (1=yes; 0=no)	ϕ	1
Specific energy of the battery [J/kg]	s_{batt}	540,000
Battery power transfer efficiency (from battery to propeller) [unitless]	η	0.7
Safety factor to reserve energy in the battery for unusual conditions [unitless]	f	1.2
Maximum depth of discharge of the battery [unitless]	γ	0.5

Panel 2. Parameter values that depend on drone type

Term	Symbol	Small Drone	Large Drone
Number of blades in one rotor [unitless]	N	4	3
Blade chord length [m]	c	0.0157	0.1
Blade lift coefficient [unitless]	c_l	0.271	0.4
Blade drag coefficient (depends on the airfoil)	c_d	0.012	0.075
Number of rotors [unitless]	n	4	8
Spinning area of one rotor [m^2]	ς	0.0507	0.027
Mass of drone body [kg]	m_1	1.07	7
Mass of battery [kg]	m_2	1	10
Mass of payload [kg]	m_3	0.5	7
Projected area of drone body [m^2]	A_1	0.0599	0.224
Projected area of battery [m^2]	A_2	0.0037	0.015
Projected area of payload [m^2]	A_3	0.0135	0.0929
Drag coefficient of drone body [unitless]	C_{D_1}	1.49	1.49
Drag coefficient of battery [unitless]	C_{D_2}	1	1
Drag coefficient of payload [unitless]	C_{D_3}	2.2	2.2
Lift-to-drag ratio [unitless]	r	3	3
Power required for avionics [Watt=J/s]	P_{avio}	0	0
Factor for induced power [unitless]	κ	1	1
Factor for profile power (m/kg)$^{1/2}$	κ_2	0.790	0.683
Factor for profile power associated with speed (m/kg)$^{-1/2}$	κ_3	0.0042	0.0868
Factor for parasite power with payload (kg/m)	κ_4	0.075	0.339
Factor for parasite power without payload (kg/m)	κ_4	0.057	0.214
Base case airspeed [m/s]	v_a	10	10

3.4.2.1 Results for Small Drones

In the small drone case, the delivery setting is a small quadcopter drone able to carry a payload up to 0.5 kg. We begin by examining the effect on Epm of changes in the payload. Figure 3.4 shows for all models an approximately linear increase in Epm with increased payload. Model LD provides the lowest Epm values of about 10 J/m, with the RH model giving values about twice as large. The R2 and LR models give similar results, about 2.5 times the LD results. The largest Epm comes from the more comprehensive R3 model, where Epm is 32-39 J/m. Note that a smaller lift-to-drag ratio in the LD model would provide very similar results to the other models, which implies that the LD model with $r = 3$ is a more efficient drone than the others. The high energy consumption for the R3 model is in part due to it including the profile drag, while using the same power transfer efficiency ($\eta = 0.7$) as the other models. So, modelers could use a lower power transfer efficiency to reflect modeling of fewer components of power (e.g., a lower η value could be used in R2 compared to R3 for not including the profile power directly in R2).

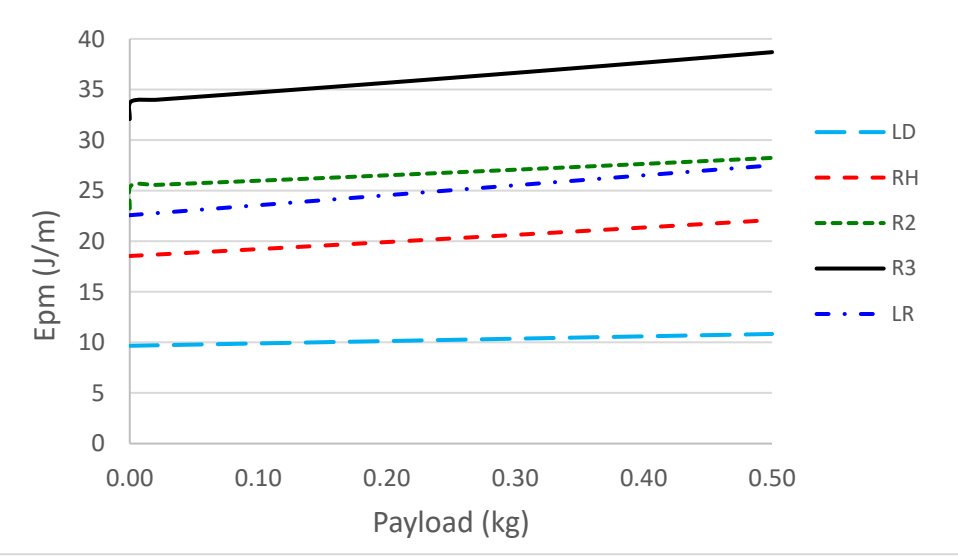

Figure 3.4. Energy consumption rate versus payload for small drones.

Overall, Figure 3.4 shows the very wide variation in Epm values for different modeling approaches (differing by a factor of 3) with the same drone operating in a common setting. These differences have strong implications for accurately modeling the energy and assessing the environmental impacts of drone delivery. These results also indicate that the selection of the lift-to-drag ratio r and the power transfer efficiency η, both of which are difficult to assess without taking measurements in flight, can be crucial in accurately estimating drone energy consumption.

Figure 3.5 shows the flight range for the five models as a function of the payload. As expected, the flight range decreases for all models as payload increases. The range decreases vary from 1.3 km (11%) for LD to 0.6 km (17%) for R3 when moving from no payload to 0.5 kg. The LD model provides the largest range of 10-12 km, and the other four models produce smaller ranges between 3-6 km, which are 28-50% of the range of the LD model. As with Epm, a smaller lift-to-drag ratio in the LD model, with r between 1.5 and 0.9 instead of 3, would produce range results between the lower limit from R3 and the upper limit from RH. As with Epm, the results show the large variability in ranges for the different models, and this has clear implications of the number of customers that could be served by drone, and the number of drone depots needed to serve a region.

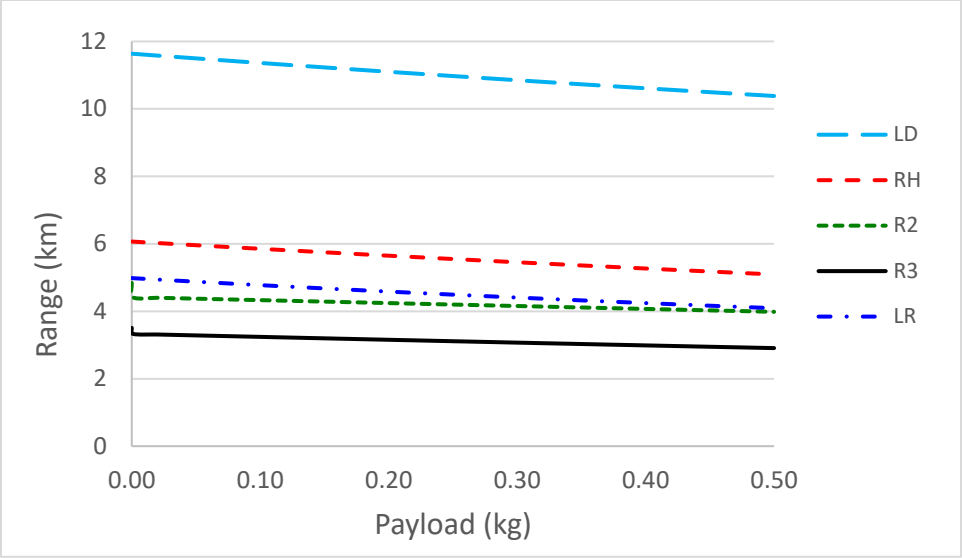

Figure 3.5. Maximum range for small drones with payload varying from 0.0-0.5 kg

Next, we fix the payload at 0.5 kg and allow the airspeed to vary from 1-25 m/s. Results for energy consumption and flight range are shown in Figures 3.6 and 3.7, respectively. The LR model is shown only for speeds up to 5 m/s as that is the relevant speed range for the regression (Tseng, 2017b). Note that Epm of the LD model does not change with speed as it assumes the lift-to-drag ratio is constant. For all other models, the Epm is a decreasing function of airspeed for low speeds, with R3 providing the highest Epm and RH and R2 providing nearly identical lowest Epm values (R2 and RH are remarkably similar for speeds up to 8 m/s). Epm is a convex function of airspeed for the component models R2 and R3, as overcoming the parasite drag at high speeds requires a large increase in energy.

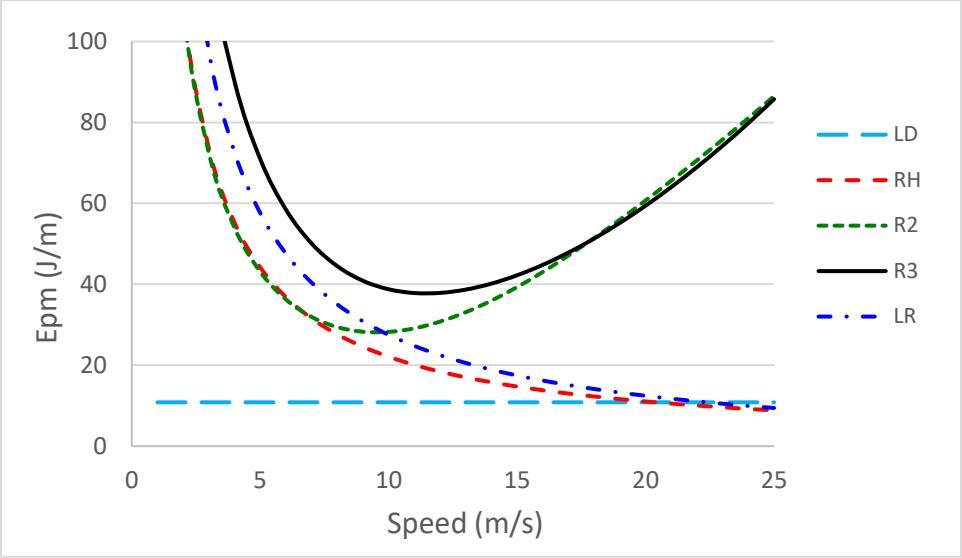

Figure 3.6. Energy consumption rate versus airspeed for small drones.

We note that the Epm is relatively flat around the energy-minimizing speed for the R2 and R3 models, which is about 10-11 m/s, though the minimum Epm value for R3 (37.8 J/m) is one-third larger than that for R2 (28.2 J/m). For models other than the LD model, the Epm is more sensitive to lower speeds than higher speeds; and while the models all have similar shapes for low speeds, they may produce very different values. For example, at 5 m/s the Epm values for the 4 models range from 43 J/m for R2 to 71 J/m for R3. The differing nature of the RH model (based on hovering) is clear as with higher speeds its Epm continues to decline as it is unable to capture the effect of increasing air resistance. As noted above, the LD model uses much less energy, though adjusting the lift-to-drag ratio r to a value 0.8-1.1 would make LD model produce results similar to the energy-minimizing values for the R2 and R3 models.

Figure 3.7 shows the drone flight range versus airspeed for the five models. As with Epm, the range for the LD model does not change with speed, and is 10.4 km. The range for the RH and LR models is linearly increasing in speed. The range for the R2 and R3

models follows a more complex pattern reflecting the convex Epm graphs. The maximum range for the R2 and R3 models (which occurs with the energy-minimizing speed) is about 4 km and 3 km, respectively, less than half the range from the LD model.

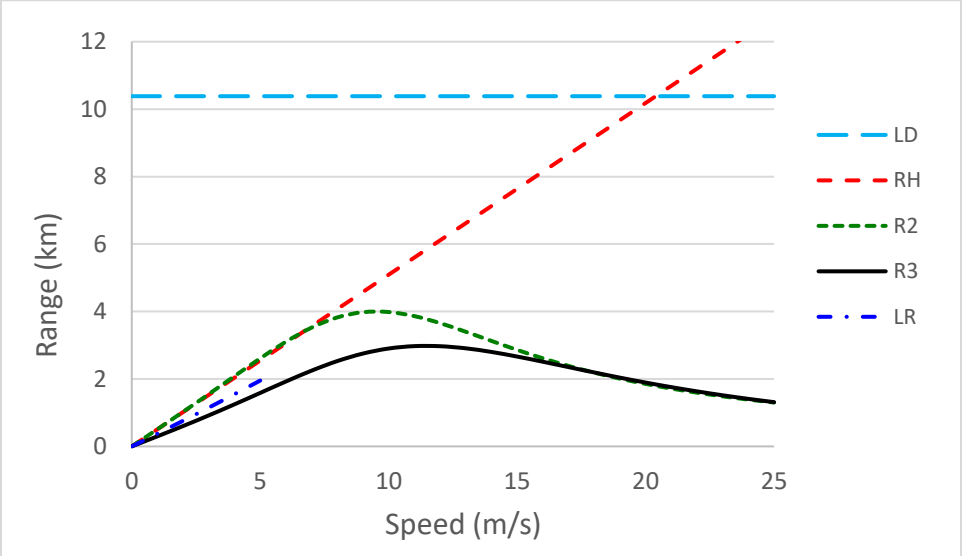

Figure 3.7. Maximum flight range versus airspeed for small drones.

We note that slower speeds quickly increase energy consumption, and the range for all models (except LD) falls quickly for slow drone speeds. For speeds below about 9 m/s, the four models other than the LD model provide similar short ranges. Note that these ranges are based on a small drone with a 1 kg battery of specific energy 540,000 J, with a 70% battery transfer efficiency, a 20% safety factor (to reserve energy for unusual conditions) and a 50% depth of battery discharge (see Panel 1). Having a larger, more efficient or more energy dense battery would increase the range. However, because the calculated range values do not include any energy for hovering, takeoff and landing or ascending and descending, the actual range would be less than that calculated based purely on steady level flight (see Kirschstein, 2020; Xu, 2017).

3.4.2.2 Results for Large Drones

This section considers the same analyses for a large drone able to carry payload up to 7 kg. For the LD model we retain the lift-to-drag ratio of $r = 3$ from D'Andrea (2014). Because the LR regression model in Tseng et al. (2017b) was developed specifically for a small drone, we do not include that model in this section. Figures 3.8-3.11 provide results for the large drone energy consumption and flight range with models LD, RH, R2 and R3, similar to Figures 3.4-3.7 for the small drone.

Figure 3.8 shows the Emp versus payload results for the large drone with payloads up to 7 kg. As for the small drone, the Epm increases linearly with payload, the LD model provides the lowest Epm (80-96 J/m); the R3 model provides the largest Epm (over 400 J/m), about 5 times larger than that from the LD model; and the RH and R2 models provide very similar performance in between, and about 2-2.5 times the LD result. The Epm increases by 22-43% for the four models as the payload rises from 0 to 7 kg. The results show that using these large drones with small payloads requires about 6 times (for R2) to 11 times (for R3) as much energy as using the corresponding model for a small drone (shown in Figure 3.4). The increased Epm is mainly due to the increased drone weight (including battery), which shows the importance of using an appropriate drone for the items (and purpose of delivery). Overall, the results for large drones behave similarly to those for small drones, although the Epm of R3 model is relatively much larger for the large drones.

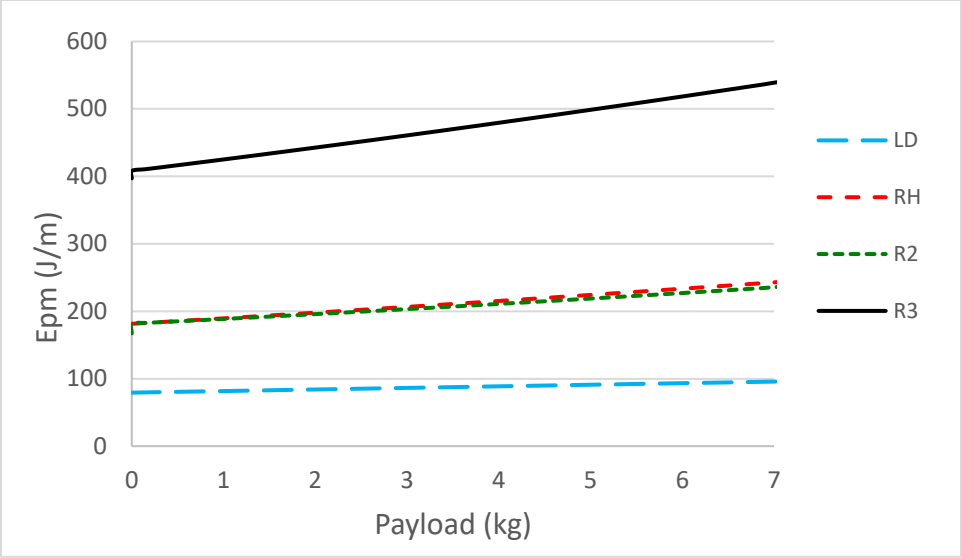

Figure 3.8. Energy consumption rate versus payload for large drones.

Figure 3.9 provides results for the flight range from the four large drone models for payloads from 0-7 kg. As expected, the drone range decreases with all models as the payload increases, with a decline of 18-30% (2.5-0.7 km) when moving from no payload to 7 kg. The LD model provides the largest range of 11.6-14.1 km, and the R3 model provides the smallest range (2.1-2.8 km). In comparison to the small drone, the large drone has a battery that is ten times larger, while the total drone weight (with battery and payload) is about 8-9 times larger (than for the small drone) depending on the payload. Results show the range values for the large drone are: (i) very similar to those for the small drone, as with the RH model; (ii) 20-40% greater than for the small drone, as with the R2 model; or (iii) 20-30% smaller than for the small drone, as with the R3 model.

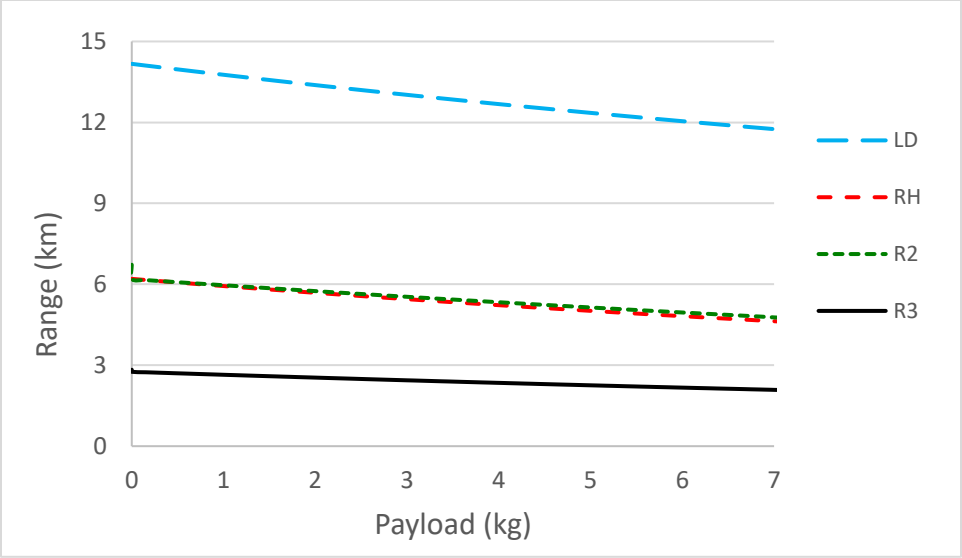

Figure 3.9. Range versus payload for large drones.

Figures 3.10-3.11 show the large drone Epm and range as a function of the airspeed, with the payload fixed at 7 kg. Most findings are similar to the small drone. The shapes of the curves for the large drone Epm are similar to those for the small drone (Figure 3.6), though the curves are less steep for large drones, and at higher speeds the Epm for model R3 remains above R2 with the large drone. As for the small drone, RH and R2 provide nearly identical lowest Epm values up to the energy-minimizing speed for R2 (about 12 m/s). The convex shapes for R2 and R3 clearly show the large parasite drag at high speeds.

Again the Epm is relatively flat around the energy-minimizing speed for the R2 and R3 models, which is about 13 m/s for R2 and 16 m/s for R3 (greater values than for the small drone). At this energy-minimizing speed, the Epm for the R3 model is about twice as large as for the R2 model (416 J/m vs 212 J/m), which is a considerably larger relative difference than with the small drone. Except for the similarity of R2 and RH (below 12 m/s), the Epm values for the different models differ dramatically. For example, at 5 m/s the Epm values range from 96 J/m for LD, 467-486 for R2 and RH, to 1090 for R3; at 10

m/s the Epm values range from 96 J/m for LD, 235-243 for R2 and RH, to 539 for R3. Again, we note that the LD model uses much less energy, though adjusting the lift-to-drag ratio r would produce results similar to the energy-minimizing values for the R2 and R3 models.

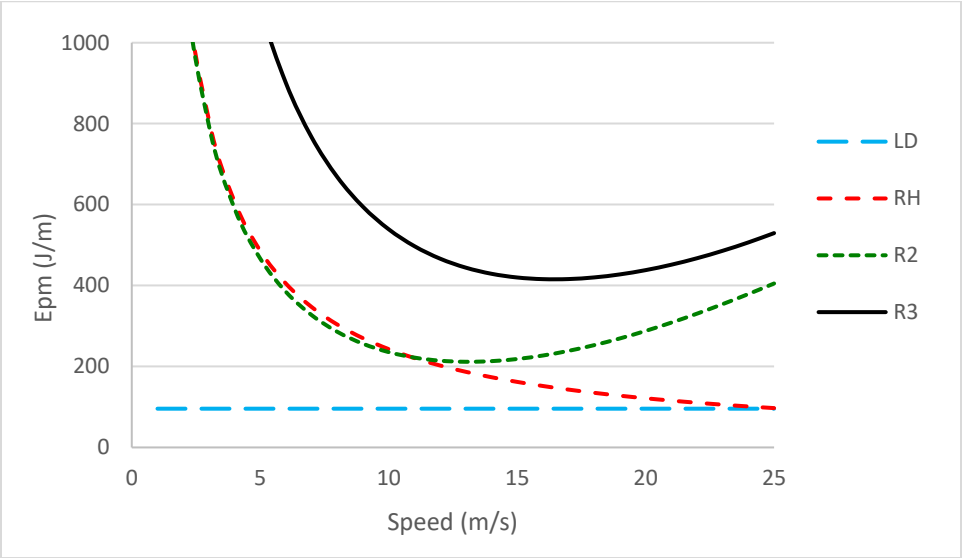

Figure 3.10. Energy consumption rate versus airspeed for large drones.

Figure 3.11 provides flight range versus speed results for the large drone with the 7 kg payload. The results are qualitatively similar to those for the small drone (Figure 7). The flight range for the LD model increases slightly to 11.8 km (vs 10.4 km for the small drone). The flight range for the R2 model increases relative to the range for the small drone, from 4 km to 5.4 km. The flight range for the R3 model slightly decreases relative to the range for the small drone, from 3 km to 2.7 km.

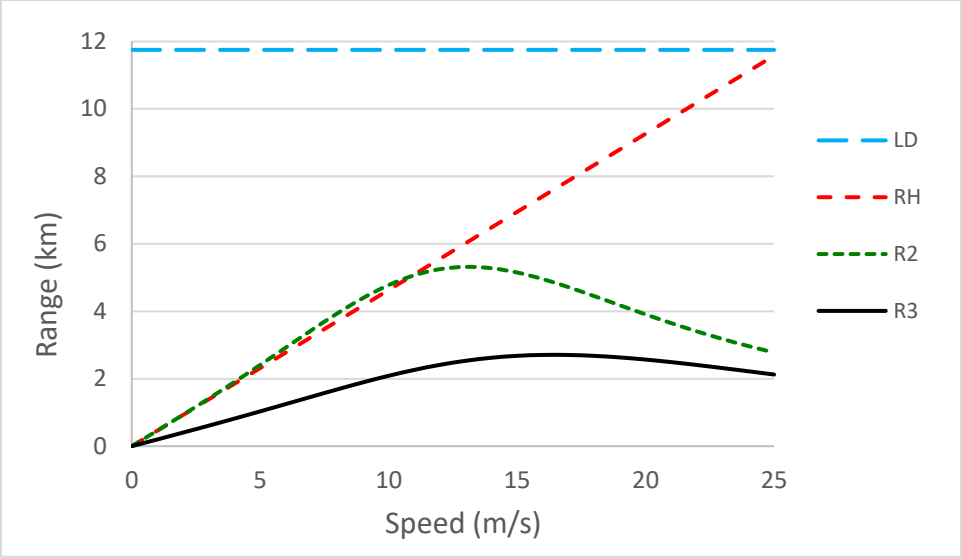

Figure 3.11. Maximum flight range versus airspeed for large drones.

3.5 Discussions and Insights

The results in this paper demonstrate very large differences in drone energy consumption rates and operating ranges derived from different models in the literature. Some of the reported results differ due to different drone types and different operating conditions. However, even with a common setting that uses the same drone design and operating parameters, the models provide Epm and range estimates for steady level flight that differ substantially. Further, we note that when a full drone delivery flight profile is included (with takeoff, ascent, hovering, descent, and landing phases), the Epm values can be substantially higher than the results for the steady level flight alone.

There are several fundamentally different approaches for modeling drone energy consumption, including integrated approaches reliant on a single lift-to-drag ratio to capture performance, component-based models developed to capture the influence of key aerodynamic forces, and regression models calibrated from field tests or from theoretical models. Integrated models (like the LD model) have the appeal of simplicity, but are very

sensitive to the choice of the lift-to-drag ratio and do not vary with airspeed. Thus, only with a properly calibrated lift-to-drag ratio (based on field experiments in the relevant setting) and operating airspeed will they provide accurate estimates of energy consumption. Models based only on energy consumption for drone hovering (like the RH model) may provide very good approximations at low airspeeds. However, at higher speeds they cannot capture the increased parasite drag that grows to dominate the energy consumption. Component models provide the most detail, but are the most difficult to develop and calibrate given the number of parameters involved. Component models capture the strong dependence of Epm and range on airspeed, and allow identification of an energy-minimizing airspeed. The two-component model (R2) and a three-component model (R3) highlighted the differences from modeling profile power directly and the importance of using a proper power transfer efficiency adjustment. All drone energy models include a power transfer adjustment to reflect losses due to a variety of sources, including battery charging efficiency, motor efficiency, drone blade performance, etc.; so it would be natural for a two component model to include a lower power transfer efficiency than a three component model to reflect power losses from the "missing" component. Our use of a common power transfer efficiency may explain in part the lower energy consumption for the R2 vs. R3 model.

For published models, the energy consumption rate (Epm) for steady level flight ranges from 16 J/m to over 400 J/m for different types of drones with different payloads. Even for small drones with payloads up to 1 kg, the literature provides Epm values that differ by a factor of six. Note that many of these Epm values reflect off-the-shelf drones (for both theoretical modeling and field experiments), not drones designed specifically for

package delivery, and thus may not reflect actual drone delivery operations. Furthermore, the large differences in Epm values cannot be reconciled by using a common set of environmental, drone design and operating parameters. Even with the common sets of parameters, the energy consumption rate (Epm) varies by a factor of 3-5 across the models (see Figures 3.4, 3.6, 3.8 and 3.10). The estimated drone flight ranges differ similarly for the models.

Notably, published results for energy consumption from drone field tests often do not agree with results from theoretical energy models. We encourage modelers to account for the energy used in the entire drone delivery/trip profile (takeoff, ascent, hovering, descent, landing, and return), as well as for avionics and wind conditions to accurately estimate total energy consumption. There is a strong need for more field experiments to establish standards for drone energy consumption, analogous to vehicle fuel efficiency standards for trucks. This could include aggregate Epm measures as well as parameter values for modeling various drone types, including new hybrid drones. Such a set of commonly accepted parameter values for effective delivery drones will be of great use in research on optimizing the design and operation of all types of drone operations, including delivery systems.

As energy consumption is important to both drone cost and emissions, an important broad research area is to better link drone energy consumption models with route optimization and strategic drone delivery systems design to assess the tradeoffs between cost, energy, and emissions in drone delivery. For drones, the role of airspeed, as well as wind conditions, has a very important influence on energy consumption, more so than for

trucks and other ground delivery vehicles, and should also be included in energy use models.

3.6 Conclusions

In this study, we provide an assessment of key energy consumption models for drone delivery. We identify the important factors that influence drone energy consumption and discuss and highlight key similarities and differences in drone energy models. We also provide an understanding of why the energy consumption models differ from each other, and identify important parameters that contribute to these differences. Our results document wide differences in drone energy consumption rates, even for models of the same drones applied in common settings. The selection of the lift-to-drag ratio r and the power transfer efficiency η, both of which are difficult to assess without taking measurements in flight, can be crucial in accurately estimating energy consumption for drones.

The energy consumption differences we document have strong implications for accurately modeling the energy and environmental implications of all drone operations, including delivery. Given that the models can provide Epm values that differ by a factor of 3-5 (or more), great care must be taken in translating results from transportation modeling (e.g., drone route modeling and optimization) to estimates and policy recommendations involving energy and emissions. The mixed research results regarding the energy and emissions efficiency of drone delivery are not surprising given the wide variability in energy consumption estimates produced from different Epm models. This underscores the need for further research to build a consensus on accurate parameter values for different types of delivery drones and different settings.

Our goal is not to identify one preferred model, but rather to document the discrepancies between models and highlight the need for accurate calibration of whatever model is adopted. All models examined in this Chapter can produce similar results with an appropriate set of parameter values. Given the lack of widespread drone delivery operations that limit direct measurements in the field, it is not surprising there is no agreement on accurate parameter values in the academic research community. Further, with the rapid rate of evolution in drone technology, those parameter values will likely change frequently as the field matures, necessitating ongoing research.

This research suggests a number of important areas for future research. Clearly, a better understanding of the accuracy of drone energy models is needed through comparing results to empirical data derived from comprehensive drone delivery field tests. These empirical tests might best be undertaken in a partnership between government agencies (e.g., the U.S. Department of Energy or EPA), academic institutions, and private sector firms. The importance of avionics and wind conditions on drone energy consumption is an area especially needing more attention, with particular care to the numbers, sizes and types of drones deployed. Future research can also help identify which type of model (complex or simple) is best in different settings, and whether or when more parsimonious models are "accurate enough" to use.

Chapter 4: Cost-Minimizing Drone Delivery Systems

In chapter 3 we showed in depth the diverse drone energy consumption rates, which is one aspect of the uncertainties in drone delivery. In this chapter, we explore under what conditions will truck and drone delivery services provide lower delivery costs and how best to utilize each type of delivery service. A brief introduction is given in section 4.1. In section 4.2, we approximate the expected travel distances for each delivery service. Section 4.3 approximates the expected delivery costs based on the expected travel distances. Section 4.4 examines the conditions that favor each type of delivery service by comparing the estimated costs of each delivery service. Selected performance measures are identified, defined and discussed in section 4.5. Section 4.6 presents the delivery system costs and modeling results for different operating settings. Conclusions are drawn in section 4.7.

4.1 Introduction

Incorporating drones into a conventional truck delivery system offers more delivery options as deliveries can be made by drone-only service, truck-only service, truck-drone service, or a combination of the three services. However, incorporating drones also complicates the optimal design of the delivery system.

Suppose that items are to be delivered from a single depot to customers distributed over a compact delivery region. Each customer is assumed to demand one item (delivery) each day and is serviced by one of the following delivery services (or modes): drone-only delivery, truck-only delivery, or truck-drone delivery. We wish to design a delivery system that minimizes the delivery costs through the best utilization of the different delivery services.

To provide a strategic analysis for this problem, we assume the delivery region is circular with radius R, the depot is centrally located, and the customers are uniformly and randomly distributed with a spatial density of δ deliveries per unit area. Drones are assumed to have a capacity of delivering one item to one customer per drone trip, regardless of being used in drone-only delivery or truck-drone delivery, due to the current drone technology. The maximum drone flight range is R_d (with $R_d \leq R$). Trucks used in truck-only delivery and truck-drone delivery are assumed to have a capacity of m_{to} and m_{td} items, respectively, which may be limited by the physical truck size, the desired service level (e.g., same-day delivery, 2-hour delivery), or regulations. We assume that the trucks are filled to full capacity and $m_{td}, m_{to} \gg 1$ (both truck-only delivery and truck-drone delivery make many deliveries per truck route) and the number of customers in the region is large compared with m_{td} and m_{to} (there are many truck-only and truck-drone routes). Thus, the delivery region can be partitioned into multiple zones where there is one truck route covering each zone with the zone size determined by the capacity of the trucks and density of customers. For zones far from the depot, there is a linehaul travel distance that the truck travels from the depot to the delivery zone and back. For zones near (or that include) the depot, there is no linehaul travel.

4.2 Modeling Expected Travel Distance

The distances traveled are estimated using the continuous approximation (CA) method as described in Campbell et al. (2017), based on earlier work in Daganzo (1984a,b). Trucks are modeled to travel via the L_1 metric for local travel and the L_2 metric for linehaul travel, and drones are modeled to travel via the L_2 metric (Murray and Chu, 2015; Carlsson

and Song, 2017). There are a few zones near the depot that would not require linehaul travel, and our models do not account for that lack of linehaul travel in those few zones.

In the following models, we use subscripts "do", "to", and "td" to denote the drone-only delivery, the truck-only delivery, and the truck-drone delivery, respectively. We use superscripts "t" and "d" to denote the truck and the drone portions of the truck-drone delivery, respectively.

4.2.1 Drone-only Travel Distance

Drone-only delivery describes a delivery service where a drone departs from a central depot, makes one delivery, and returns back to the depot. The distance traveled to a customer delivery located d units of distance from the depot is easily computed as the L2 distance of the drone flying from the depot to the customer location and returning, which gives the drone travel distance per delivery for drone-only service, $VMTD_{do}$, (Vehicle Miles Traveled per Delivery=VMTD) for a customer at distance d of

$$VMTD_{do} = 2d, \tag{4.1}$$

where d is within the flight range of the drone, i.e., $d \leq R_d$. For customers located beyond the maximum flight range of the drone, they cannot be served by the drone.

4.2.2 Truck-only Travel Distance

Truck-only delivery is the conventional delivery service where a truck departs from the depot, visits a number of customers along a route delivering one item to each customer, and then returns back to the depot. Extensive efforts have been devoted to estimating and minimizing the distance for a vehicle route that visit all customers, which is the well-known traveling salesman problem. However, we would like to estimate the distance traveled to a

customer located d units of distance from the depot. An intuitive approach is to formulate the total expected distance of a truck route and then divide it by the total number of customers visited on the route.

To estimate travel distance and also be applicable to truck-drone delivery, we adopt the expected distance approximation method using a delivery swath described in Campbell et al. (2017) and Daganzo (1984). The idea is to form a delivery zone of customers located near each other to be serviced in a single route, then have a truck travel along a swath of width *w* and visit all customers in the zone in order along the swath, like that shown in Figure 4.1. The zones are assumed to be compact and can be covered by a swath of width approximately *w* (interested readers are referred to Daganzo (1984) for details on different portioning for delivery zones). The expected horizontal distance between adjacent stops is $\frac{w}{3}$, and the expected vertical distance between adjacent stops is $\frac{1}{\delta w}$, where δ represents the delivery density (in number of deliveries per square mile). Here "horizontal" refers to the direction across the swath and "vertical" refers to the direction along the swath. Combining the expected horizontal and vertical distances between two adjacent stops gives the expected truck local travel distance per delivery for truck-only service of

$$\frac{w}{3} + \frac{1}{\delta w}. \tag{4.2}$$

The optimal swath width to minimize the expected truck-only delivery distance is

$$w_{to}^{*} = \sqrt{\frac{3}{\delta}}, \tag{4.3}$$

and the optimal expected truck local travel distance per delivery is then

$$\frac{2}{\sqrt{3\delta}}. \tag{4.4}$$

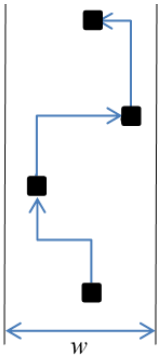

Figure 4.1. Four truck stops along a swath of width w

For zones not including the depot, there is a linehaul travel distance associated with traveling to the delivery zone from the depot which is apportioned equally to all deliveries in the zone. For a customer locating at distance d from the depot, we assume that the linehaul distance to the delivery zone of that customer is d. Since the truck makes m_{to} deliveries per route, the expected truck travel distance per delivery for truck-only service, $VMTD_{to}$, for a customer located at distance d from the depot can be approximated as

$$VMTD_{to} = \frac{2d}{m_{to}} + \frac{w}{3} + \frac{1}{\delta w}. \tag{4.5}$$

4.2.3 Truck-drone Travel Distance

In hybrid truck-drone delivery, drones are used in conjunction with trucks to make deliveries. A drone is repeatedly launched from the truck, it makes a delivery, and then returns to the truck when the delivery is completed. The truck also makes deliveries concurrently with the drone. We extend the swath strategy to account for the truck to launch and recover drones at truck delivery stops. In our truck-drone model, we consider a situation where a truck carries one drone, and the truck and drone alternate deliveries, as shown in Figure 4.2. The dashed line depicts the drone travel and the circles depict the

drone deliveries; while the solid line depicts the truck travel and the squares depict the truck deliveries.

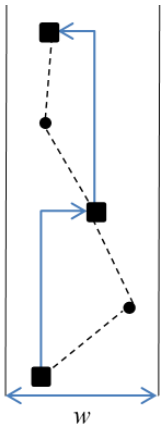

Figure 4.2. Alternating truck and drone deliveries over two cycles

Consider a delivery cycle that begins with the truck and drone together at a customer location (which is already visited by the truck in the previous delivery cycle), and contains one drone delivery and one truck delivery at the end of the cycle. A truck-drone delivery route can then be viewed as a collection of these cycles. The drone travels in a straight line and the truck and drone alternate deliveries; thus, the expected horizontal and vertical distances of one drone travel leg are $\frac{w}{3}$ and $\frac{1}{\delta w}$, respectively. The total expected drone travel distance per cycle is then $2\sqrt{\left(\frac{w}{3}\right)^2 + \left(\frac{1}{\delta w}\right)^2}$ as the drone travels two legs in one cycle. Since we have two deliveries to be made in a cycle (i.e., a truck delivery and a drone delivery), the expected drone travel distance per delivery is

$$\sqrt{\left(\frac{w}{3}\right)^2 + \left(\frac{1}{\delta w}\right)^2}. \tag{4.6}$$

The optimal swath width for the drone travel portion is

$$w_{td}^{d*} = \sqrt{\frac{3}{\delta}} = w_{to}^{*}. \tag{4.7}$$

Since the truck and drone alternate deliveries, the expected vertical distance for the truck in one cycle is doubled relative to truck-only distance as $\frac{2}{\delta w}$, while the expected horizontal distance remains the same as $\frac{w}{3}$. A simple explanation is that the expected vertical distance is calculated between two adjacent points because the points in the vertical order follow a Poisson distribution, while the expected horizontal distance is calculated between any two random points because the points in the horizontal order follow a uniform distribution. More detail can be found in Daganzo (1984a). The expected truck local travel distance per delivery in a cycle is then

$$\frac{w}{6} + \frac{1}{\delta w}. \tag{4.8}$$

The optimal swath for the truck local travel portion is

$$w_{td}^{t*} = \sqrt{\frac{6}{\delta}} = \sqrt{2} w_{to}^{*}. \tag{4.9}$$

Equation (4.9) indicates that having the drone make deliveries in parallel with the truck increases the optimal swath for the truck compared with that for truck-only delivery.

Combining the expected drone and truck local travel distances per delivery in a cycle gives the expected truck and drone local travel distance per delivery in the zone of

$$\frac{w}{6} + \frac{1}{\delta w} + \sqrt{\left(\frac{w}{3}\right)^2 + \left(\frac{1}{\delta w}\right)^2}. \tag{4.10}$$

Note that expression (4.10) models the distance when an even number of deliveries is assumed in the zone. With an odd number of deliveries, the distance is very similar as long as the number of deliveries in a zone is $\gg 1$. Details are presented in Appendix 4.A.

Similar to the truck-only delivery, there is linehaul travel required for zones not near the depot which is apportioned equally to all deliveries within the zone. The truck makes m_{td} deliveries per truck-drone route, thus, the expected truck and drone travel distance per delivery for truck-drone service, $VMTD_{td}$, for a customer located at distance d from the depot can be approximated as

$$VMTD_{td} = \frac{2d}{m_{td}} + \frac{w}{6} + \frac{1}{\delta w} + \sqrt{\left(\frac{w}{3}\right)^2 + \left(\frac{1}{\delta w}\right)^2}. \quad (4.11)$$

Since the drone is restricted for use within its maximum flight range (R_d), setting the expected drone trip distance at half the drone range or less, i.e., $2\sqrt{\left(\frac{w}{3}\right)^2 + \left(\frac{1}{\delta w}\right)^2} \leq \frac{1}{2}R_d$, helps ensure the large majority of drone trips would be within the drone range. (Detailed modeling of the distribution of drone flight distance in the swath is left for future research.) Based on equations (4.7) and (4.9), we have $\frac{\sqrt{2}}{\sqrt{3\delta}} < 2\sqrt{\left(\frac{w}{3}\right)^2 + \left(\frac{1}{\delta w}\right)^2} < \frac{\sqrt{2.5}}{\sqrt{3\delta}}$. So, to have truck-drone as an available service option, we let $\frac{\sqrt{2.5}}{\sqrt{3\delta}} \leq \frac{1}{4}R_d$, i.e., the delivery density $\delta \geq \frac{40}{3R_d^2}$.

4.3 Modeling Expected Delivery Cost

There are different types of costs incurred for delivering an item from an origin (e.g., depot, warehouse) to a customer's home. They can be usefully classified into two categories: (1) costs attributable to each incremental vehicle mile traveled, which may

include the costs of transporting the item from the origin to the destination and the return of the delivery vehicle; and (2) costs attributable to each stop of the delivery vehicle, which may include the costs of (loading) unloading, handling and delivering the item to the customer. We use c_t and c_d to denote the traveling cost per unit distance ($/mile) for the truck and the drone, respectively. We let s_t denote the stop cost per delivery ($/stop) for the truck, but let s_d denote the marginal drone stop cost, i.e., the drone stop cost relative to the truck stop cost. Thus, the drone stop cost is $s_t + s_d$. If the drone has the same stop cost as the truck, then $s_d = 0$ and if $s_d = -s_t$, then a drone delivery (stop) has zero cost.

4.3.1 Drone-only Delivery Cost

Based on equation (4.1), the delivery cost of serving a customer at distance d for drone-only delivery is

$$C_{do} = 2c_d d + s_t + s_d. \tag{4.12}$$

4.3.2 Truck-only Delivery Cost

Based on equation (4.5), the expected delivery cost of serving a customer at distance d for truck-only delivery is

$$C_{to} = c_t \left(\frac{2d}{m_{to}} + \frac{w}{3} + \frac{1}{\delta w} \right) + s_t. \tag{4.13}$$

The optimal cost (using the optimal swath width of equation (4.3)) is

$$C_{to}^* = \frac{2c_t d}{m_{to}} + \frac{2c_t}{\sqrt{3\delta}} + s_t. \tag{4.14}$$

4.3.3 Truck-drone Delivery Cost

Based on equation (4.11), the expected cost of serving a customer at distance d for truck-drone delivery is

$$C_{td} = c_t\left(\frac{2d}{m_{td}} + \frac{w}{6} + \frac{1}{\delta w}\right) + c_d\sqrt{\left(\frac{w}{3}\right)^2 + \left(\frac{1}{\delta w}\right)^2} + s_t + \frac{1}{2}s_d. \tag{4.15}$$

The delivery stop cost in a cycle of one truck delivery and one drone delivery is $s_t + s_t + s_d = 2s_t + s_d$, so the delivery stop cost per delivery is as in equation (4.15). C_{td} is a convex function of the swath width w, and the optimal swath width (w_{td}^*) is between the optimal swath widths for the drone travel portion ($w_{td}^{d*} = \sqrt{\frac{3}{\delta}}$) and the truck travel portion ($w_{td}^{t*} = \sqrt{\frac{6}{\delta}}$), i.e., $\sqrt{\frac{3}{\delta}} < w_{td}^* < \sqrt{\frac{6}{\delta}}$. We can let $w_{td}^* = k\sqrt{\frac{3}{\delta}}$, where k is a factor determined by the ratio of $\frac{c_d}{c_t}$ and $1 < k < \sqrt{2}$, see the proof in Appendix 4.B. We can then write the expected cost per delivery as

$$C_{td} = c_t\frac{2d}{m_{td}} + \frac{c_t}{\sqrt{3\delta}}\left(\frac{k}{2} + \frac{1}{k} + \frac{c_d}{c_t}\sqrt{k^2 + \frac{1}{k^2}}\right) + s_t + \frac{1}{2}s_d. \tag{4.16}$$

The optimal k is determined by taking the first derivative of $C_{td}(k)$ and setting it equal to zero, which is given by

$$C_{td}'(k) = \frac{c_t}{\sqrt{3\delta}}\left(\frac{1}{2} - \frac{1}{k^2} + \frac{1}{2}\frac{c_d}{c_t}\left(k^2 + \frac{1}{k^2}\right)^{-1/2}\left(2k - \frac{2}{k^3}\right)\right) = 0. \tag{4.17}$$

There is not a simple closed form solution for the cost-minimizing k^* though it is a function of only $\frac{c_d}{c_t}$. Equation (4.17) may then be solved for $\frac{c_d}{c_t}$ as a function of k^*, which is monotonically decreasing, see the proof in Appendix 4.B:

$$\frac{c_d}{c_t} = \frac{\left(2-(k^*)^2\right)\sqrt{(k^*)^4+1}}{2((k^*)^4-1)}. \tag{4.18}$$

Substituting the expression in equation (4.18) for $\frac{c_d}{c_t}$ into C_{td}, we obtain

$$C_{td}^* = \frac{2c_t d}{m_{td}} + \frac{c_t}{\sqrt{3\delta}}\frac{2(k^*)^3-k^*}{(k^*)^4-1} + s_t + \frac{1}{2}s_d. \tag{4.19}$$

Note that k^* is determined by $\frac{c_d}{c_t}$, via equation (4.18). The optimal swath width (determined by k^*) does not lend itself (nor does C_{td}^*) to a closed form solution, thus, we approximate the optimal cost (C_{td}^*) by using the optimal swath width for the truck travel portion (i.e., $\frac{k}{2}+\frac{1}{k}$ in equation (4.16)) where $k = \sqrt{2}$ and the optimal swath width for the drone travel portion (i.e., $\sqrt{k^2+\frac{1}{k^2}}$ in equation (4.16)) where $k = 1$. This results in a lower bound on the optimal cost $\tilde{C}_{td}^*$ which is given by

$$\tilde{C}_{td}^* = c_t\frac{2d}{m_{td}} + (c_t + c_d)\frac{\sqrt{2}}{\sqrt{3\delta}} + s_t + \frac{1}{2}s_d. \tag{4.20}$$

The cost using the approximation as described in equation (4.20) always underestimates the true optimal cost as $k^* \in (1, \sqrt{2})$. The approximation is most accurate when either $c_t \gg c_d$ or $c_d \gg c_t$ (i.e., $\frac{c_d}{c_t}$ is extremely large or small), and is least accurate when c_t and c_d are close.

The error due to the approximation can be expressed as

$$err = \frac{C_{td}^* - \tilde{C}_{td}^*}{C_{td}^*} = \frac{\frac{c_t}{\sqrt{3\delta}}\frac{2(k^*)^3-k^*}{(k^*)^4-1} - \frac{c_t}{\sqrt{3\delta}}\sqrt{2}\left(1+\frac{c_d}{c_t}\right)}{\frac{2c_t d}{m_{td}} + \frac{c_t}{\sqrt{3\delta}}\frac{2(k^*)^3-k^*}{(k^*)^4-1} + s_t + \frac{1}{2}s_d}. \tag{4.21}$$

Since both linehaul distance and stop costs are non-negative (i.e., $d, s_t + \frac{1}{2}s_d \geq 0$), the maximum error can be written as

$$err_{max} = \frac{\frac{2(k^*)^3 - k^*}{(k^*)^4 - 1} - \sqrt{2}\left(1 + \frac{c_d}{c_t}\right)}{\frac{2(k^*)^3 - k^*}{(k^*)^4 - 1}},$$

$$err_{max} = 1 - \frac{(k^*)^4 - 1}{2(k^*)^3 - k^*}\sqrt{2}\left(1 + \frac{c_d}{c_t}\right). \tag{4.22}$$

Since $k^*$is a function of only $\frac{c_d}{c_t}$, the maximum error is a function of only $\frac{c_d}{c_t}$ and can be found numerically, as shown in Figure 4.3. The maximum error in cost from using the approximation in (4.20) is about 2%, and Appendix 4.C provides more detail.

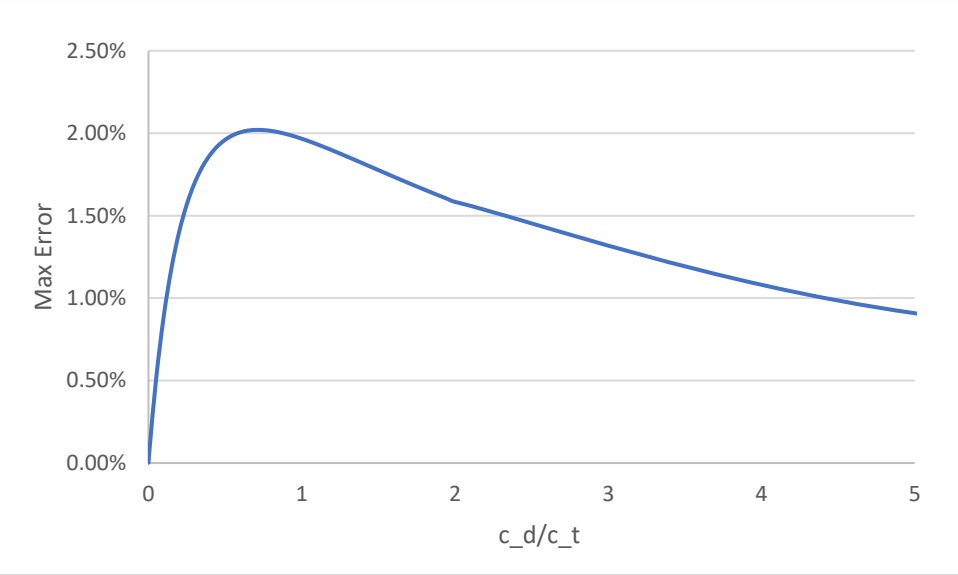

Figure 4.3. The maximum approximation error as a function of c_d/c_t

4.4 Comparing Cost of Different Delivery Services

In this section, we examine under what operating conditions will each of the three delivery services provide the lowest delivery costs in subregions of the circular delivery region of radius *R* miles. Since all delivery services have a cost that is a function of the distance to the depot, we define a critical distance d^{*c} between two delivery services as the distance (or radius) from the depot that makes the cost functions of the two delivery

services equal. Within radius d^{*c} using one service generates lower delivery costs than using the other service whereas the opposite is true beyond radius d^{*c}. Thus, the total delivery costs for the entire delivery region are minimized if we partition the circular service region at radius d^{*c} and use the cost minimizing delivery service in each subregion.

4.4.1 Drone-only Delivery vs Truck-only Delivery

We first compare drone-only delivery (DO) with truck-only delivery (TO). We require that the drone-only delivery region is within the maximum flight range of the drone. The drone-only delivery is preferred at a point when its expected delivery cost is lower than the expected optimal cost per delivery of the truck-only delivery and the point is also within the maximum flight range of the drone. To find where drone-only is preferred we set $C_{do} < C_{to}^{*}$ and solve for the critical distance:

$$2c_d d + s_t + s_d < c_t\left(\frac{2d}{m_{to}} + \frac{2}{\sqrt{3\delta}}\right) + s_t,$$

$$2(c_d - c_t/m_{to})d < c_t\frac{2}{\sqrt{3\delta}} - s_d,$$

$$d < \frac{1}{(c_d - c_t/m_{to})}\left[c_t\frac{1}{\sqrt{3\delta}} - \frac{s_d}{2}\right] \text{ for } c_d > c_t/m_{to}, \tag{4.22a}$$

$$d > \frac{1}{(c_d - c_t/m_{to})}\left[c_t\frac{1}{\sqrt{3\delta}} - \frac{s_d}{2}\right] \text{ for } c_d < c_t/m_{to}. \tag{4.22b}$$

Therefore, we can assess the utilization of drone-only and truck-only delivery in different parts of the service region based on the competitiveness of the drone operating cost per mile (c_d) compared with the truck operating cost per mile per package (c_t/m_{to}) and of the drone marginal stop cost (s_d) compared with the expected optimal truck local travel cost per delivery ($c_t\frac{2}{\sqrt{3\delta}}$), as shown in Figure 4.4(a). The horizontal axis represents

the drone marginal stop cost ($/delivery) and the vertical axis represents the drone operating cost ($/mile) (note this is also $/mile/delivery). Figure 4.4(b) shows where the delivery region is partitioned based on the cost conditions. In Figure 4.4(b), the horizontal axis measures distance from the depot d and the vertical axis is the cost per delivery. The critical distance between drone-only and truck-only delivery is at a distance d^{*c}. The black line labeled TO in Figure 4.4(b) with slope $\frac{2c_t}{m_{to}}$ represents the truck-only cost.

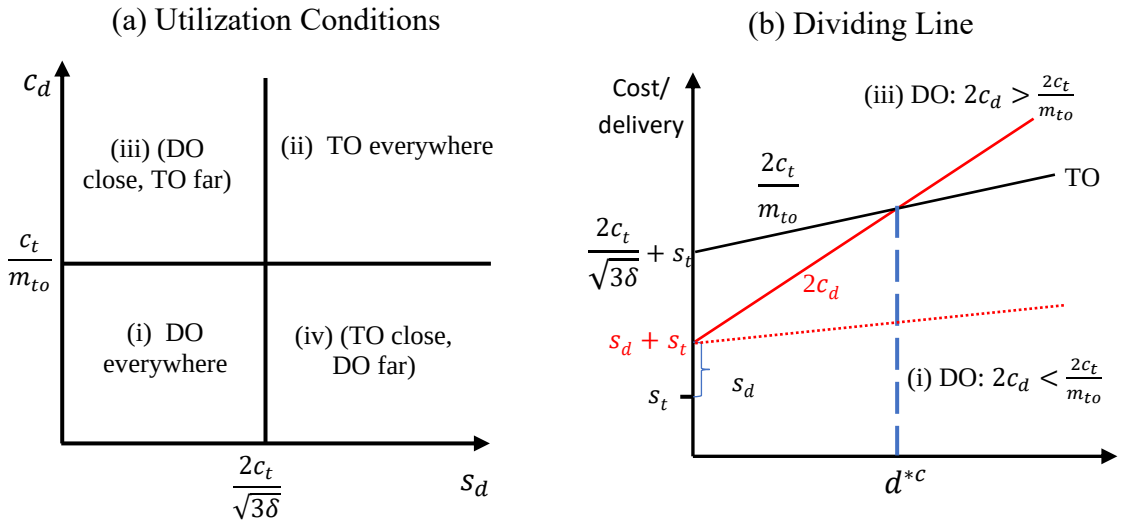

Figure 4.4. Drone-only vs Truck-only utilization conditions and delivery service dividing line

Figure 4.4(a) is divided into four quadrants by the vertical line $s_d = \frac{2c_t}{\sqrt{3\delta}}$ and the horizontal line $c_d = \frac{c_t}{m_{to}}$ to identify the four possible combinations of the two delivery services:

Quadrant (i): when $c_d < c_t/m_{to}$ and $s_d \leq c_t \frac{2}{\sqrt{3\delta}}$ (the bottom left quadrant of Figure 4.4(a)), then drone-only delivery is preferred (provides a lower cost) everywhere in the

service region. The dashed red line in Figure 4.4(b) illustrates the cost for drone only delivery in this situation. This is likely if the truck makes only a few deliveries per route (i.e., m_{to} is small) and/or the truck cost per mile is large, and the drone transport cost and marginal drone stop cost are small.

Quadrant (ii): when $c_d > c_t/m_{to}$ and $s_d > c_t \frac{2}{\sqrt{3\delta}}$ (the top right quadrant of Figure 4.4(a)), truck-only delivery is preferred (provides a lower cost) everywhere in the service region. This situation corresponds to moving the solid red line in Figure 4.4(b) for drone-only delivery (DO) above the black line for truck-only delivery (TO) (due to an increase in drone delivery cost s_d). This is likely if the truck makes many deliveries per route (i.e., m_{to} is large) and/or the truck cost per mile is small, and the drone transport cost and marginal drone stop cost are large.

Quadrant (iii): when $c_d > c_t/m_{to}$ and $s_d \leq c_t \frac{2}{\sqrt{3\delta}}$ (the top left quadrant of Figure 4.4(a)), drone-only delivery is preferred to serve customers close to the depot while truck-only delivery is preferred far from the depot, as indicated by inequality (4.22a). This situation corresponds to the solid red line in Figure 4.4(b) for DO that intersects the truck-only cost at a distance d^{*c} from the depot. In this setting, the delivery cost is optimized by using a combination of drone-only delivery near the depot and truck-only delivery farther away. The critical distance that optimizes the partitioning of the delivery region is given by

$$d^{*c} = \frac{c_t \frac{2}{\sqrt{3\delta}} - s_d}{2(c_d - c_t/m_{to})}. \tag{4.23}$$

The more competitive the drone (per delivery) operating cost per mile compared with the truck cost per mile per delivery, i.e., the smaller the difference of $(c_d - c_t/m_{to})$, the

greater the delivery range for drone-only delivery. The smaller the delivery density and/or the smaller the marginal drone stop cost, the greater the delivery range for drone-only delivery. Thus, in rural areas where the delivery density is low and the truck makes a small number of deliveries per route, drone-only delivery would have a large delivery area extending out from the depot, if not constrained by its range (e.g., due to its battery life).

Quadrant (iv): when $c_d < c_t/m_{to}$ and $s_d > c_t \frac{2}{\sqrt{3\delta}}$ (the bottom right quadrant of Figure 4.4(a)), truck-only delivery is preferred to serve customers close to the depot while drone-only delivery is preferred far from the depot, with the dividing line indicated by inequality (4.22b). This situation corresponds to moving the dashed red line in Figure 4.4(b) for DO above the black line for TO (due to an increase in drone delivery cost s_d). Again, the delivery cost is optimized by utilizing a combination of drone-only and truck-only deliveries in the service region. The dividing line for drone-only and truck-only delivery services in the delivery region is given by the same equation (4.23), except that drone-only delivery serves customers beyond distance d^{*c} from the depot and truck-only delivery serves customers closer to the depot. This makes sense because the travel cost per mile for drone delivery is lower than the travel cost per mile per delivery for truck-only delivery, while the delivery stop cost for drone-only delivery is larger than the truck-only local delivery cost $\left(\frac{2c_t}{\sqrt{3\delta}}\right)$, so truck-only delivery is more likely to be utilized in urban areas where there are many deliveries with high drone stop costs within short distances.

4.4.2 Truck-drone Delivery vs Truck-only Delivery

Comparing truck-drone delivery (TD) with truck-only delivery (TO), we use the approximate truck-drone delivery cost which is a lower bound on the actual optimal truck-

drone cost, thus, truck-only delivery is "strictly" preferred when its delivery cost is lower than that of truck-drone delivery, i.e., $C_{to}^* < \tilde{C}_{td}^*$ because $\tilde{C}_{td}^*$ slightly underestimates C_{td}^*.

$$\frac{2c_t d}{m_{to}} + c_t \frac{2}{\sqrt{3\delta}} + s_t < \frac{2c_t d}{m_{td}} + c_t \left(1 + \frac{c_d}{c_t}\right) \frac{\sqrt{2}}{\sqrt{3\delta}} + s_t + \frac{1}{2} s_d,$$

$$2c_t \left(\frac{1}{m_{to}} - \frac{1}{m_{td}}\right) d < c_t \left(1 - \sqrt{2} + \frac{c_d}{c_t}\right) \frac{\sqrt{2}}{\sqrt{3\delta}} + \frac{1}{2} s_d,$$

$$d < \frac{1}{(1/m_{to} - 1/m_{td})} \left[\left(1 - \sqrt{2} + \frac{c_d}{c_t}\right) \frac{\sqrt{2}}{2\sqrt{3\delta}} + \frac{s_d}{4c_t}\right] \text{ for } m_{td} > m_{to}, \tag{4.24a}$$

$$d > \frac{1}{(1/m_{to} - 1/m_{td})} \left[\left(1 - \sqrt{2} + \frac{c_d}{c_t}\right) \frac{\sqrt{2}}{2\sqrt{3\delta}} + \frac{s_d}{4c_t}\right] \text{ for } m_{td} < m_{to}, \tag{4.24b}$$

$$d = 0 \text{ for } m_{td} = m_{to}, c_d < \left(\sqrt{2} - 1\right) c_t - \frac{\sqrt{3\delta}}{2\sqrt{2}} s_d, \tag{4.24c}$$

$$d = \infty \text{ for } m_{td} = m_{to}, c_d > \left(\sqrt{2} - 1\right) c_t - \frac{\sqrt{3\delta}}{2\sqrt{2}} s_d. \tag{4.24d}$$

We use Figure 4.5 to illustrate the conditions that favor truck-only or truck-drone delivery, which now depend on the sizes of the trucks used in the truck-only and truck-drone routes. Here the c_d-s_d space is divided into two regions for each condition on route sizes by the line

$$c_d = \left(\sqrt{2} - 1\right) c_t - \frac{\sqrt{3\delta}}{2\sqrt{2}} s_d. \tag{4.25}$$

because this line has slope $-\frac{\sqrt{3\delta}}{2\sqrt{2}}$, the increase in the drone delivery stop cost tends to require a decrease in the drone operating cost to make using truck-drone delivery everywhere the optimal service.

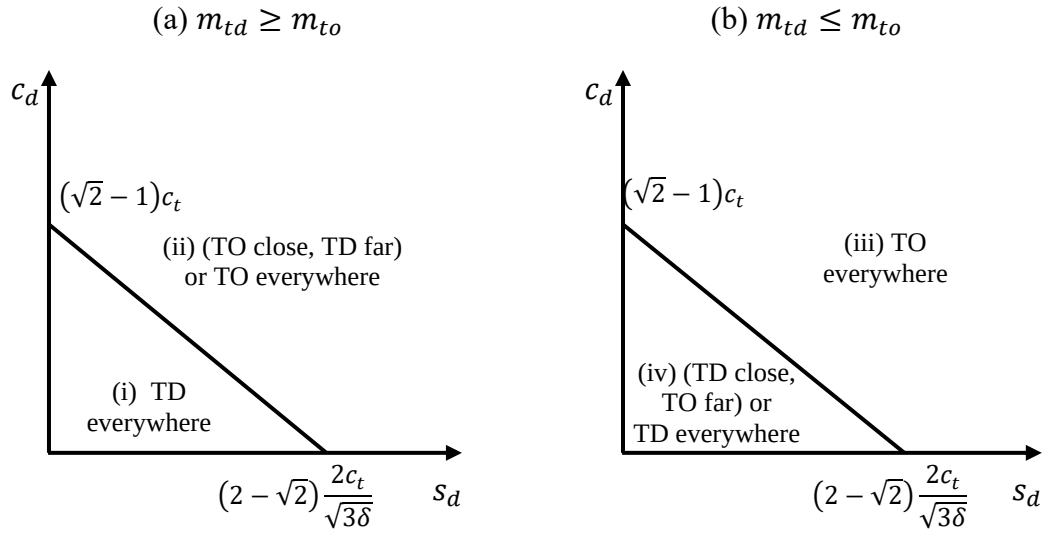

Figure 4.5. Truck-only vs Truck-drone utilization conditions and dividing line

Figure 4.5(a) illustrates the case when truck-drone routes make at least the same number of deliveries as truck-only routes, which is likely to happen through the use of drones. Figure 4.5(a) identifies two regions for two service options:

Region (i): when costs are such that $\frac{\sqrt{2}}{2}\left(c_t + c_d - \sqrt{2}c_t\right)\frac{1}{\sqrt{3\delta}} + \frac{s_d}{4} \leq 0$ and $\delta \geq \frac{40}{3R_d^2}$ (the bottom left triangle), then truck-drone delivery is preferred (provides a lower cost) everywhere in the service region.

Region (ii): when costs are such that $\frac{\sqrt{2}}{2}\left(c_t + c_d - \sqrt{2}c_t\right)\frac{1}{\sqrt{3\delta}} + \frac{s_d}{4} > 0$ (the region above the diagonal line in Figure 4.5(a)), if $m_{td} > m_{to}$ and $\delta \geq \frac{40}{3R_d^2}$, then truck-only delivery is preferred to serve customers close to the depot, as indicated by (4.24a), while truck-drone delivery is preferred far from the depot. If $m_{td} = m_{to}$, then truck-only delivery is preferred to serve customers everywhere in the service region as indicated by (4.24c).

Figure 4.5(b) illustrates the case when truck-drone routes make at most the same number of deliveries as truck-only routes, which may happen when some of the package space in truck-drone delivery is occupied by drones and associated equipment. Figure 4.5(b) also identifies two regions for two service options:

Region (iii): when costs are such that $\frac{\sqrt{2}}{2}\left(c_t + c_d - \sqrt{2}c_t\right)\frac{1}{\sqrt{3\delta}} + \frac{s_d}{4} > 0$ (the region above the diagonal line in Figure 4.5(b)), then truck-only delivery is preferred (provides a lower cost) everywhere in the service region.

Region (iv): when costs are such that $\frac{\sqrt{2}}{2}\left(c_t + c_d - \sqrt{2}c_t\right)\frac{1}{\sqrt{3\delta}} + \frac{s_d}{4} \leq 0$ and $\delta \geq \frac{40}{3R_d^2}$ (the region below the diagonal line in Figure 4.5(b)), if $m_{td} < m_{to}$, then truck-drone delivery is preferred to serve customers close to the depot while truck-drone delivery is preferred far from the depot, as indicated by (4.24b). If $m_{td} = m_{to}$, then truck-drone delivery is preferred to serve customers everywhere in the service region, as indicated by (4.24d).

In conditions (ii) and (iv) and when $m_{td} \neq m_{to}$, the delivery cost is optimized by utilizing a combination of truck-only and truck-drone deliveries in the service region. The critical distance that optimizes the partitioning of the delivery region between the two services is given by

$$d^{*c} = \frac{\left(c_t + c_d - \sqrt{2}c_t\right)\frac{2\sqrt{2}}{\sqrt{3\delta}} + s_d}{4\left(c_t/m_{to} - c_t/m_{td}\right)}. \tag{4.26}$$

4.4.3 Drone-only vs Truck-drone Deliveries

In this section we compare drone-only delivery (DO) with truck-drone delivery (TD) using the approximated truck-drone delivery cost. Drone-only delivery is only available within it maximum flight range (R_d); truck-drone delivery is only available when delivery

densities are not too small, so that the expected drone travel distance is within half of drone maximum flight range (i.e., $\delta \geq \frac{40}{3R_d^2}$). Because the approximated truck-drone cost is a lower bound on the actual optimal truck-drone cost, drone-only delivery is "strictly" preferred when its delivery cost is lower than that of the truck-drone delivery, i.e., $C_{do}^* < \tilde{C}_{td}^*$, because $\tilde{C}_{td}^*$ slightly underestimates C_{td}^*.

$$2c_d d + s_t + s_d < \frac{2c_t d}{m_{td}} + (c_t + c_d)\frac{\sqrt{2}}{\sqrt{3\delta}} + s_t + \frac{1}{2}s_d,$$

$$2(c_d - c_t/m_{td})d < (c_t + c_d)\frac{\sqrt{2}}{\sqrt{3\delta}} - \frac{1}{2}s_d,$$

$$d < \frac{1}{(c_d - c_t/m_{td})}\left[(c_t + c_d)\frac{\sqrt{2}}{2\sqrt{3\delta}} - \frac{s_d}{4}\right] \text{ for } c_d > c_t/m_{td}. \quad (4.27a)$$

$$d > \frac{1}{(c_d - c_t/m_{td})}\left[(c_t + c_d)\frac{\sqrt{2}}{2\sqrt{3\delta}} - \frac{s_d}{4}\right] \text{ for } c_d < c_t/m_{td}. \quad (4.27b)$$

Since the analyses are very similar as those described in subsection 4.4.1, we briefly describe them as follows.

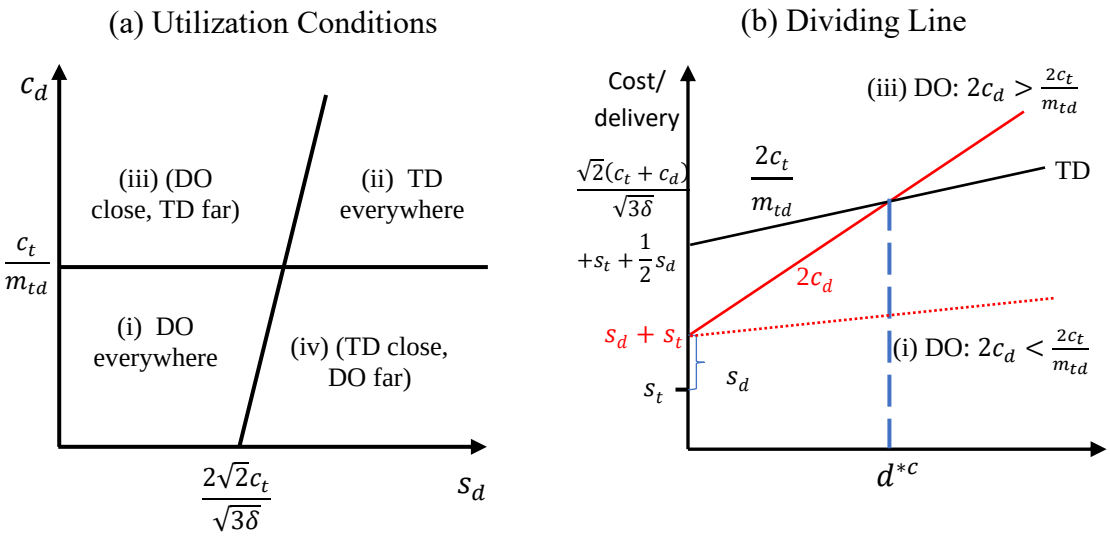

Figure 4.6. Drone-only vs Truck-drone utilization conditions and dividing line

Figures 4.6(a) and 4.6(b) are analogous to Figures 4.4(a) and 4.4(b). Figure 4.6(a) is divided into four quadrants by the positively sloped line $s_d = (c_t + c_d)\frac{2\sqrt{2}}{\sqrt{3\delta}} = (c_t + c_d)\frac{2\sqrt{2}}{\sqrt{3\delta}}$ (note this line is a function of c_d) and the horizontal line $c_d = \frac{c_t}{m_{to}}$.

Quadrant (i): when $c_d < c_t/m_{td}$ and $s_d < (c_t + c_d)\frac{2\sqrt{2}}{\sqrt{3\delta}}$ (the bottom left quadrant of Figure 4.6(a)), then drone-only delivery is preferred (provides a lower cost) everywhere in the service region.

(ii) when $c_d > c_t/m_{to}$ and $s_d \geq (c_t + c_d)\frac{2\sqrt{2}}{\sqrt{3\delta}}$ (the top right quadrant), truck-drone delivery is preferred (provides a lower cost) everywhere in the service region.

(iii) when $c_d > c_t/m_{td}$ and $s_d \leq (c_t + c_d)\frac{2\sqrt{2}}{\sqrt{3\delta}}$(the top left quadrant), drone-only delivery is preferred to serve customers close to the depot while truck-only delivery is preferred far from the depot, as indicated by equation (4.27a).

(iv) when $c_d < c_t/m_{td}$ and $s_d > (c_t + c_d)\frac{2\sqrt{2}}{\sqrt{3\delta}}$(the bottom right quadrant), truck-only delivery is preferred to serve customers close to the depot while drone-only delivery is preferred far from the depot, as indicated by equation (4.27b).

In conditions (iii) and (iv), the delivery cost is optimized by utilizing a combination of drone-only and truck-drone deliveries in the service region. The critical distance that optimizes the partitioning of the delivery region is given by

$$d^{*c} = \frac{(c_t + c_d)\frac{2\sqrt{2}}{\sqrt{3\delta}} - s_d}{4(c_d - c_t/m_{td})}. \tag{4.28}$$

4.4.4 A General Form of Comparing Two Delivery Services

Before presenting the general format for comparing the expected costs of two delivery services, we obtain a general form of the expected cost of each delivery service. We have expressions for the delivery cost as a function of the distance d for drone-only, truck-only, and truck-drone as shown in equations (4.12), (4.14), and (4.20), respectively, in Section 4.3.

$$C_{do} = 2c_d d + s_t + s_d. \tag{4.12}$$

$$C_{to}^* = \frac{2c_t}{m_{to}} d + \frac{2c_t}{\sqrt{3\delta}} + s_t. \tag{4.14}$$

$$\tilde{C}_{td}^* = \frac{2c_t}{m_{td}} d + \frac{\sqrt{2}(c_t+c_d)}{\sqrt{3\delta}} + s_t + \frac{1}{2} s_d. \tag{4.20}$$

We can provide a more general cost expression for each of the three delivery services as

$$C_s(d) = \beta_0^s + \beta_1^s d \tag{4.29}$$

where $s \in \{do, to, td\}$, $\beta_0^s \in \left\{s_t + s_d, \frac{2c_t}{\sqrt{3\delta}} + s_t, \frac{\sqrt{2}(c_t+c_d)}{\sqrt{3\delta}} + s_t + \frac{1}{2} s_d\right\}$ and $\beta_1^s \in \{2c_d, \frac{2c_t}{m_{to}}, \frac{2c_t}{m_{td}}\}$. β_0^{do} reflects the stop cost (\$/delivery) for drone-only service and β_1^{do} reflects the travel cost per mile per delivery (\$/mile/delivery) for drone-only service. β_0^{to} and β_0^{td} reflect the local delivery cost (local travel plus stop cost) per delivery (\$/delivery) for truck-only and truck-drone service, respectively. β_1^{to} and β_1^{td} reflect the linehaul travel cost per mile per delivery (\$/mile/delivery) for truck-only and truck-drone service, respectively. We observe that $\beta_0^{td} > \min\{\beta_0^{to}, \beta_0^{do}\}$ as follows:

$$\beta_0^{td} - \beta_0^{to} = \frac{1}{2}\left\{s_d - \frac{2c_t}{\sqrt{3\delta}}\left[2 - \sqrt{2}\left(1 + \frac{c_d}{c_t}\right)\right]\right\}. \tag{4.30}$$

$$\beta_0^{td} - \beta_0^{do} = \frac{1}{2}\left\{\frac{2c_t}{\sqrt{3\delta}}\sqrt{2}\left(1 + \frac{c_d}{c_t}\right) - s_d\right\}. \quad (4.31)$$

$$\beta_0^{to} - \beta_0^{do} = \frac{1}{2}\left\{\frac{2c_t}{\sqrt{3\delta}} - s_d\right\}. \quad (4.32)$$

If $\beta_0^{to} \geq \beta_0^{do}$ i.e., $s_d \leq \frac{2c_t}{\sqrt{3\delta}}$, then $\frac{2c_t}{\sqrt{3\delta}}\sqrt{2}\left(1 + \frac{c_d}{c_t}\right) - s_d > 0$ always holds, i.e., $\beta_0^{td} > \beta_0^{do}$. If $\beta_0^{to} < \beta_0^{do}$ i.e., $s_d > \frac{2c_t}{\sqrt{3\delta}}$, then $s_d - \frac{2c_t}{\sqrt{3\delta}}\left[2 - \sqrt{2}\left(1 + \frac{c_d}{c_t}\right)\right] > 0$ always holds, i.e., $\beta_0^{td} > \beta_0^{to}$. Thus, $\beta_0^{td} > \min\{\beta_0^{to}, \beta_0^{do}\}$. The relationship also holds using C_{td}^*. When choosing the low cost delivery service from the three services (i.e., truck-only, drone-only, and truck-drone), truck-drone delivery cannot serve customers very close to the depot.

The cost difference between delivery services i and j at distance d from the depot can be written as:

$$\Delta C_{ij}(d) = C_i(d) - C_j(d) = \beta_0^i + \beta_1^i d - \left(\beta_0^j + \beta_1^j d\right),$$

$$\Delta C_{ij}(d) = \left(\beta_1^i - \beta_1^j\right)d + \left(\beta_0^i - \beta_0^j\right). \quad (4.33)$$

Let $\Delta\beta_1^{ij} = \beta_1^i - \beta_1^j$ and $\Delta\beta_0^{ij} = \beta_0^i - \beta_0^j$, we can rewrite equation (4.33) as

$$\Delta C_{ij}(d) = \Delta\beta_1^{ij} d + \Delta\beta_0^{ij}, \quad (4.34)$$

where $\Delta\beta_1^{ij}$ reflects the difference of the linehaul travel cost per mile per delivery between services i and j, and $\Delta\beta_0^{ij}$ reflects the difference of the local delivery costs per delivery between services i and j. A critical distance where the delivery costs of the two services are equal is determined by setting $\Delta C_{ij} = 0$, which exists only when a higher linehaul travel cost per mile per delivery of service i (i.e., $\Delta\beta_1^{ij} > 0$) is compensated by a lower local delivery cost per delivery of that service (i.e., $\Delta\beta_0^{ij} < 0$) compared with service j, and vice

versa. In Figure 4.7, we show the cost difference as a function of the critical distance. Note that service i and service j are symmetric because we assume the vehicles are not restricted by their travel range.

In Figure 4.7, we clearly see how the utilization of a delivery service is determined by the cost rates and the size (radius) of the delivery region. If both linehaul travel and local delivery cost rates of service i are no greater than those of service j, i.e., $\Delta\beta_1^{ij} \leq 0$, $\Delta\beta_0^{ij} \leq 0$, then service i is preferred everywhere in the delivery region (e.g., graphs (f) and (i)), and vice versa. Another case when one service is preferred everywhere is when the dividing line between the two services is beyond the delivery region (e.g., graphs (a) and (d)). In other situations, the delivery costs are optimized by utilizing a combination of services i and j in the region.

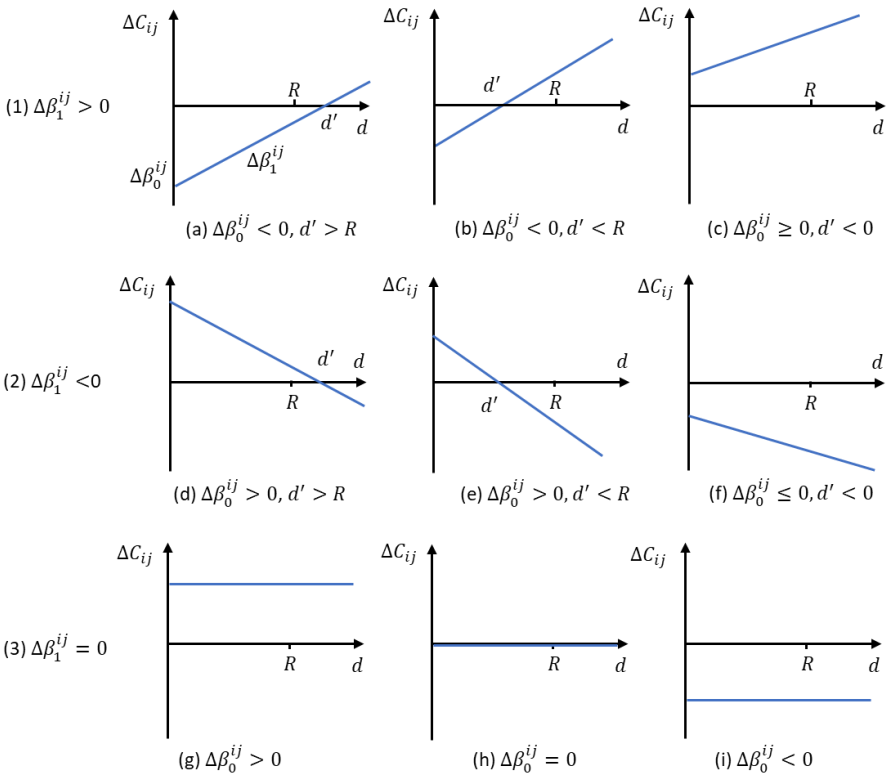

Figure 4.7. Cost dividing line between two delivery services

4.5 Performance Measures

We are interested in the following five performance measures associated with delivery service combinations: the expected total delivery cost (ETC), the expected cost per delivery (EC), the expected number of truck routes (NR), the expected truck route length (RL) and the expected truck route time (RT). Based on our observations that a combination of at most two services can provide an expected delivery cost within 1% of the optimal expected delivery cost of combining all three delivery services, thus we generate performance measures for comparing two services. We develop the performance measures in absolute values first, and then in percentage values compared with the identical measure of the performance of the truck-only delivery service.

4.5.1 Performance Measures in Absolute Values

To obtain the absolute performance measures, we define the following variables:

m_s: the truck capacity of delivery service s, for $s \in \{do, to, td\}$ and $m_{do} = \infty$. (Although there is no trucks used within drone-only delivery, defining an infinite truck capacity for drone-only allows a unified model to be developed for all three services.)

p_s: the proportion of drone deliveries to total deliveries of service s. $p_{to} = 0$, $p_{td} = 0.5$, $p_{do} = 1$.

ELD_s: the expected local truck distance per truck route of service s. $ELD_{to} = \frac{2m_{to}}{\sqrt{3\delta}}$, $ELD_{td} = \frac{\sqrt{2}m_{td}}{\sqrt{3\delta}}$, $ELD_{do} = 0$.

ELH_s: the expected linehaul truck distance per truck route of service s. $ELH_{do} = 0$. $ELH_{to} = ELH_{td} = \frac{4}{3}d$ if the truck-only delivery or truck-drone delivery serves customers

up to d distance from the depot. $ELH_{to} = ELH_{td} = \left(\frac{4}{3}\right)\frac{R^3-d^3}{R^2-d^2}$ if the truck-only delivery or truck-drone delivery serves customers beyond distance d of the delivery region of radius R. (Note that the expected round trip distance is 4/3 times the radius.)

τ_t: the truck stop time.

v_t: the truck local travel speed.

v_{tl}: the truck linehaul travel speed.

4.5.1.1 Service i Everywhere, Service j Nowhere

When the entire region is served by delivery service i, such as in Figures 4.7(a), 4.7(f) and 4.7(i) in subsection 4.4.4, the expected total delivery cost (ETC) over the region is given by

$$\int_0^R C_i(r)(2\pi r\delta)dr = \int_0^R \left(\beta_0^i + \beta_1^i r\right)(2\pi r\delta)dr,$$

$$ETC_i = \left[\beta_0^i + \beta_1^i\left(\frac{2}{3}R\right)\right](\pi R^2\delta). \tag{4.35}$$

The expected cost per delivery (EC) over the region is thus

$$EC_i = \frac{\left[\beta_0^i+\beta_1^i\left(\frac{2}{3}R\right)\right](\pi R^2\delta)}{\pi R^2\delta} = \beta_0^i + \beta_1^i\left(\frac{2}{3}R\right). \tag{4.36}$$

The expected number of truck routes (NR) is given by

$$NR_i = \frac{\pi R^2\delta}{m_i}. \tag{4.37}$$

The expected truck route length (RL) is given by

$$RL_i = ELH_i + ELD_i, \tag{4.38}$$

where $ELH_{to} = ELH_{td} = \frac{4}{3}R$.

The expected truck route time (RT) is given by

$$RT_i = \frac{ELH_i}{v_{tl}} + \frac{ELD_i}{v_t} + (1 - p_i)m_i\tau_t. \tag{4.39}$$

4.5.1.2 Service i Nowhere, Service j Everywhere

When the entire region is served by service j, which corresponds to Figures 4.7(c), 4.7(d) and 4.7(g) in subsection 4.4.4, then the performance measures have the same form as in equations (4.35) through (4.39), except that index i is replaced with index j.

4.5.1.3 Service i Close, Service j Far

When the entire region is served by a combination of service i and service j, where service i delivers close to the depot (within distance d of the depot) while service j serves the rest of the region, which corresponds to Figure 4.7(b) in subsection 4.4.4, then the expected total delivery cost over the region is given by

$$\int_0^d C_i(r)(2\pi r\delta)dr + \int_d^R C_j(r)(2\pi r\delta)dr = \int_0^d \left(\beta_0^i + \beta_1^i r\right)(2\pi r\delta)dr + \int_d^R \left(\beta_0^j + \beta_1^j r\right)(2\pi r\delta)dr,$$

$$ETC_{ij} = \left[\Delta\beta_0^{ij} + \Delta\beta_1^{ij}\left(\frac{2}{3}d\right)\right](\pi d^2\delta) + \left[\beta_0^j + \beta_1^j\left(\frac{2}{3}R\right)\right](\pi R^2\delta). \tag{4.40}$$

Since ETC_{ij} is a function of the distance d where delivery service i is replaced by delivery service j, taking the first derivative of $ETC_{ij}(d)$ with respect to d, we have

$$ETC_{ij}'(d) = 2\pi\delta d\left(\Delta\beta_0^{ij} + \Delta\beta_1^{ij}d\right) = 0,$$

$$d = 0 \text{ or } d = d^{*c} = -\Delta\beta_0^{ij}/\Delta\beta_1^{ij}.$$

Since $\Delta\beta_1^{ij} > 0, d > 0$, thus, $ETC_{ij}(d) \geq ETC_{ij}(d')$, i.e., the minimum total delivery cost is achieved when $d = d^{*c}$. Thus, we have

$$ETC_{ij}^* = \left[\Delta\beta_0^{ij} + \Delta\beta_1^{ij}\left(\frac{2}{3}d^{*c}\right)\right](\pi d^{*c2}\delta) + \left[\beta_0^j + \beta_1^j\left(\frac{2}{3}R\right)\right](\pi R^2\delta). \quad (4.41)$$

The optimal expected cost per delivery over the region is thus

$$EC_{ij}^* = \frac{\left[\Delta\beta_0^{ij}+\Delta\beta_1^{ij}\left(\frac{2}{3}d^{*c}\right)\right](\pi d^{*c2}\delta)+\left[\beta_0^j+\beta_1^j\left(\frac{2}{3}R\right)\right](\pi R^2\delta)}{\pi R^2\delta},$$

$$EC_{ij}^* = \left[\Delta\beta_0^{ij} + \Delta\beta_1^{ij}\left(\frac{2}{3}d^{*c}\right)\right]\left(\frac{d^{*c}}{R}\right)^2 + \beta_0^j + \beta_1^j\left(\frac{2}{3}R\right). \quad (4.42)$$

The expected number of truck routes (NR) is given by

$$NR_{ij} = \frac{\pi d^{*c2}\delta}{m_i} + \frac{\pi\left(R^2 - d^{*c2}\right)\delta}{m_j}. \quad (4.43)$$

The expected truck route length (RL) is given by

$$RL_{ij} = \frac{\pi\delta}{NR_{ij}}\left[\frac{d^{*c2}}{m_i}(ELH_i + ELD_i) + \frac{R^2 - d^{*c2}}{m_j}\left(ELH_j + ELD_j\right)\right], \quad (4.44)$$

where $ELH_i = \frac{4}{3}d^{*c}$ and $ELH_j = \left(\frac{4}{3}\right)\frac{R^3 - d^{*c3}}{R^2 - d^{*c2}}$ when $i, j \in \{to, td\}$.

The expected truck route time (RT) is given by

$$RT_{ij} = \frac{\pi\delta}{NR_{ij}}\left[\frac{d^{*c2}}{m_i}\left(\frac{ELH_i}{v_{tl}} + \frac{ELD_i}{v_t} + (1 - p_i)m_i\tau_t\right) + \frac{R^2 - d^{*c2}}{m_j}\left(\frac{ELH_j}{v_{tl}} + \frac{ELD_j}{v_t} + \left(1 - p_j\right)m_j\tau_t\right)\right]. \quad (4.45)$$

4.5.1.4 Service i Far, Service j Close

When the entire region is served by a combination of service i and service j, where service i serves far from the depot while service j serves close to the depot, corresponding

to Figure 4.7(e) in subsection 4.4.4, the expected total delivery cost and cost per delivery over the region are given by

$$ETC_{ji}^{*} = \left[\Delta\beta_0^{ji} + \Delta\beta_1^{ji}\left(\frac{2}{3}d^{*c}\right)\right](\pi d^{*c^2}\delta) + \left[\beta_0^{i} + \beta_1^{i}\left(\frac{2}{3}R\right)\right](\pi R^2\delta). \tag{4.46}$$

$$EC_{ji}^{*} = \left[\Delta\beta_0^{ji} + \Delta\beta_1^{ji}\left(\frac{2}{3}d^{*c}\right)\right]\left(\frac{d^{*c}}{R}\right)^2 + \beta_0^{i} + \beta_1^{i}\left(\frac{2}{3}R\right). \tag{4.47}$$

The expected number of truck routes (NR) is given by

$$NR_{ji} = \frac{\pi\left(R^2 - d^{*c^2}\right)\delta}{m_i} + \frac{\pi d^{*c^2}\delta}{m_j}. \tag{4.48}$$

The expected truck route length (RL) is given by

$$RL_{ji} = \frac{\pi\delta}{NR_{ji}}\left[\frac{R^2 - d^{*c^2}}{m_i}(ELH_i + ELD_i) + \frac{d^{*c^2}}{m_j}\left(ELH_j + ELD_j\right)\right], \tag{4.49}$$

where $ELH_i = \left(\frac{4}{3}\right)\frac{R^3 - d^{*c^3}}{R^2 - d^{*c^2}}$ and $ELH_j = \frac{4}{3}d^{*c}$ when $i, j \in \{to, td\}$.

The expected truck route time (RT) is given by

$$RT_{ji} = \frac{\pi\delta}{NR_{ji}}\left[\frac{R^2 - d^{*c^2}}{m_i}\left(\frac{ELH_i}{v_{tl}} + \frac{ELD_i}{v_t} + (1 - p_i)m_i\tau_t\right) + \frac{d^{*c^2}}{m_j}\left(\frac{ELH_j}{v_{tl}} + \frac{ELD_j}{v_t} + \left(1 - p_j\right)m_j\tau_t\right)\right]. \tag{4.50}$$

4.5.2 Performance Measures in Percentage Values

The performance measures in percentage values are measured relative to the truck-only delivery service which we designate as service i. To provide a general form for the relative performance measures, we define the following variables:

u: the utilization of delivery service j in the delivery region, which is defined as the proportion of area serviced by service j over the area of the entire delivery region (this is also equal to the proportion of the deliveries as well).

σ: the ratio of the critical distance d^{*c} to the radius of the entire delivery region, i.e., $\sigma = \frac{d^{*c}}{R}$, where d^{*c} is the distance where the cost of delivery service j equals that of delivery service i, or vice versa.

λ: the ratio of the truck capacity of service j to the truck capacity of the truck-only service (i.e., service i), i.e., $\lambda = \frac{m_j}{m_i}$.

α: the ratio of drone operating cost to truck operating cost per unit of distance, i.e., $\alpha = \frac{c_d}{c_t}$.

4.5.2.1 Service i Everywhere, Service j Nowhere

Since service i is designated as the truck-only service, the percentage differences between the performance measures of service i and itself are thus zero. The utilization of service j is therefore $u = 0$.

4.5.2.2 Service i Nowhere, Service j Everywhere

When the delivery service j is used everywhere, the utilization of service j is $u = 1$. The percentage performance measures are as follows:

The percentage savings in the expected cost per delivery ($PSAV_{EC}$) of service j relative to service i is given by

$$PSAV_{EC} = 1 - \frac{EC_j}{EC_i},$$

$$PSAV_{EC} = 1 - \frac{\beta_0^j + \beta_1^j\left(\frac{2}{3}R\right)}{\beta_0^i + \beta_1^i\left(\frac{2}{3}R\right)}. \quad (4.51)$$

The percentage savings in the expected number of truck routes ($PSAV_{NR}$) relative to service i is given by

$$PSAV_{NR} = 1 - \frac{NR_j}{NR_i},$$

$$PSAV_{NR} = 1 - \frac{1}{\lambda}. \quad (4.52)$$

The percentage savings in the expected truck route length ($PSAV_{RL}$) relative to service i is given by

$$PSAV_{RL} = 1 - \frac{RL_j}{RL_i},$$

$$PSAV_{RL} = 1 - \frac{ELH_j + ELD_j}{ELH_i + ELD_i}. \quad (4.53)$$

The percentage savings in the expected truck route time ($PSAV_{RT}$) relative to service i is given by

$$PSAV_{RT} = 1 - \frac{RT_j}{RT_i},$$

$$PSAV_{RT} = 1 - \frac{\frac{ELH_j}{v_{tl}} + \frac{ELD_j}{v_t} + (1-p_j)m_j\tau_t}{\frac{ELH_i}{v_{tl}} + \frac{ELD_i}{v_t} + (1-p_i)m_i\tau_t}. \quad (4.54)$$

4.5.2.3 Service i Close, Service j Far

In this service combination, service j is utilized beyond the critical distance d^{*c} to the edge of the delivery region, thus, the utilization of service j is $u = \frac{\pi R^2 - \pi d^{*c^2}}{\pi R^2} = 1 - \sigma^2$. The percentage performance measures are as follows:

The percentage savings in the expected cost per delivery ($PSAV_{EC}$) of service $i+j$ relative to delivery by service i only is given by

$$PSAV_{EC} = 1 - \frac{EC_{ij}}{EC_i},$$

$$PSAV_{EC} = 1 - \frac{\beta_0^j + \beta_1^j\left(\frac{2}{3}R\right)}{\beta_0^i + \beta_1^i\left(\frac{2}{3}R\right)} - \frac{\Delta\beta_0^{ij} + \Delta\beta_1^{ij}\left(\frac{2}{3}d^{*c}\right)}{\beta_0^i + \beta_1^i\left(\frac{2}{3}R\right)}(1-u). \tag{4.55}$$

The percentage savings in the expected number of truck routes ($PSAV_{NR}$) relative to service i is given by

$$PSAV_{NR} = 1 - \frac{NR_{ij}}{NR_i},$$

where $NR_{ij} = (1-u)NR_i + uNR_j$ as described in equation (4.43), thus, we have

$$PSAV_{NR} = \left(1 - \frac{1}{\lambda}\right)u. \tag{4.56}$$

The percentage savings in the expected truck route length ($PSAV_{RL}$) relative to service i is given by

$$PSAV_{RL} = 1 - \frac{RL_{ij}}{RL_i},$$

where $RL_{ij} = \frac{1}{1-\left(1-\frac{1}{\lambda}\right)u}\left[(1-u)(ELH_i + ELD_i) + \frac{u}{\lambda}\left(ELH_j + ELD_j\right)\right]$ as described in equation (4.44); thus, we have

$$PSAV_{RL} = 1 - \frac{u}{(1-u)\lambda + u}\frac{ELH_j + ELD_j}{ELH_i + ELD_i} - \frac{(1-u)\lambda}{(1-u)\lambda + u}. \tag{4.57}$$

The percentage savings in the expected truck route time ($PSAV_{RT}$) relative to service i is given by

$$PSAV_{RT} = 1 - \frac{RT_{ij}}{RT_i},$$

where $RT_{ij} = \frac{1}{1-\left(1-\frac{1}{\lambda}\right)u}\left[(1-u)\left(\frac{ELH_i}{v_{tl}} + \frac{ELD_i}{v_t} + (1-p_i)m_i\tau_t\right) + \frac{u}{\lambda}\left(\frac{ELH_j}{v_{tl}} + \frac{ELD_j}{v_t} + (1-p_j)m_j\tau_t\right)\right]$; thus, we have

$$PSAV_{RT} = 1 - \frac{u}{(1-u)\lambda+u}\frac{\frac{ELH_j}{v_{tl}}+\frac{ELD_j}{v_t}+(1-p_j)m_j\tau_t}{\frac{ELH_i}{v_{tl}}+\frac{ELD_i}{v_t}+(1-p_i)m_i\tau_t} - \frac{(1-u)\lambda}{(1-u)\lambda+u}. \quad (4.58)$$

4.5.2.4 Service i Far, Service j Close

In this situation, service j is utilized from the depot to the critical distance d^{*c}, thus, the utilization of service j is $u = \frac{\pi d^{*c2}}{\pi R^2} = \sigma^2$. The percentage performance measures are as follows:

The percentage savings in the expected cost per delivery ($PSAV_{EC}$) of delivery service $i + j$ relative to only delivery service i is given by

$$PSAV_{EC} = 1 - \frac{EC_{ij}}{EC_i},$$

$$PSAV_{EC} = \frac{\Delta\beta_0^{ij} + \Delta\beta_1^{ij}\left(\frac{2}{3}d^{*c}\right)}{\beta_0^i + \beta_1^i\left(\frac{2}{3}R\right)}u. \quad (4.59)$$

The percentage savings in the expected number of truck routes ($PSAV_{NR}$) relative to service i is given by

$$PSAV_{NR} = 1 - \frac{NR_{ji}}{NR_i},$$

where $NR_{ij} = (1-u)NR_i + uNR_j$ as described in equation (4.48), thus, we have

$$PSAV_{NR} = \left(1 - \frac{1}{\lambda}\right)u. \quad (4.60)$$

The percentage savings in the expected truck route length ($PSAV_{RL}$) relative to service i is given by

$$PSAV_{RL} = 1 - \frac{RL_{ji}}{RL_i},$$

where $RL_{ji} = \frac{1}{1-\left(1-\frac{1}{\lambda}\right)u}\left[(1-u)(ELH_i + ELD_i) + \frac{u}{\lambda}\left(ELH_j + ELD_j\right)\right]$ as described in equation (4.44); thus, we have

$$PSAV_{RL} = 1 - \frac{u}{(1-u)\lambda+u}\frac{ELH_j+ELD_j}{ELH_i+ELD_i} - \frac{(1-u)\lambda}{(1-u)\lambda+u}. \quad (4.61)$$

The percentage savings in the expected truck route time ($PSAV_{RT}$) relative to service i is given by

$$PSAV_{RT} = 1 - \frac{RT_{ji}}{RT_i},$$

where $RT_{ji} = \frac{1}{1-\left(1-\frac{1}{\lambda}\right)u}\left[(1-u)\left(\frac{ELH_i}{v_{tl}} + \frac{ELD_i}{v_t} + (1-p_i)m_i\tau_t\right) + \frac{u}{\lambda}\left(\frac{ELH_j}{v_{tl}} + \frac{ELD_j}{v_t} + (1-p_j)m_j\tau_t\right)\right]$; thus, we have

$$PSAV_{RT} = 1 - \frac{u}{(1-u)\lambda+u}\frac{\frac{ELH_j}{v_{tl}}+\frac{ELD_j}{v_t}+(1-p_j)m_j\tau_t}{\frac{ELH_i}{v_{tl}}+\frac{ELD_i}{v_t}+(1-p_i)m_i\tau_t} - \frac{(1-u)\lambda}{(1-u)\lambda+u}. \quad (4.62)$$

4.5.2.5 A General Form

Based on the observations of the previous four subsections that describe the percentage performance measures for four different service combinations; we provide a general form of all the relative performance measures with the exception of the percentage saving in the expected cost per delivery ($PSAV_{EC}$). For service i close and

service j far, the percentage savings in the expected cost per delivery ($PSAV_{EC}$) relative to service i is given by

$$PSAV_{EC} = 1 - \frac{\beta_0^j + \beta_1^j\left(\frac{2}{3}R\right)}{\beta_0^i + \beta_1^i\left(\frac{2}{3}R\right)} - \frac{\Delta\beta_0^{ij} + \Delta\beta_1^{ij}\left(\frac{2}{3}d^{*c}\right)}{\beta_0^i + \beta_1^i\left(\frac{2}{3}R\right)}(1-u), \tag{4.63}$$

For service i far and service j close, the percentage savings in the expected cost per delivery ($PSAV_{EC}$) relative to service i is given by

$$PSAV_{EC} = \frac{\Delta\beta_0^{ij} + \Delta\beta_1^{ij}\left(\frac{2}{3}d^{*c}\right)}{\beta_0^i + \beta_1^i\left(\frac{2}{3}R\right)}u. \tag{4.64}$$

Both equations (4.63) and (4.64) include situations when only one service is used.

The percentage savings in the expected number of truck routes ($PSAV_{NR}$) relative to service i is given by

$$PSAV_{NR} = \left(1 - \frac{1}{\lambda}\right)u. \tag{4.65}$$

The percentage savings in the expected truck route length ($PSAV_{RL}$) relative to service i is given by

$$PSAV_{RL} = 1 - \frac{u}{(1-u)\lambda + u}\frac{ELH_j + ELD_j}{ELH_i + ELD_i} - \frac{(1-u)\lambda}{(1-u)\lambda + u}. \tag{4.66}$$

The percentage savings in the expected truck route time ($PSAV_{RT}$) relative to service i is given by

$$PSAV_{RT} = 1 - \frac{u}{(1-u)\lambda + u}\frac{\frac{ELH_j}{v_{tl}} + \frac{ELD_j}{v_t} + (1-p_j)m_j\tau_t}{\frac{ELH_i}{v_{tl}} + \frac{ELD_i}{v_t} + (1-p_i)m_i\tau_t} - \frac{(1-u)\lambda}{(1-u)\lambda + u}. \tag{4.67}$$

4.6 Illustrations of Minimum-Cost Delivery Systems

The purpose of this section is to determine (i) the optimal use of drone delivery (including truck-drone and drone-only services) as a complement to traditional truck-only delivery to minimize the expected total delivery costs and (ii) to assess the effect of drone delivery on other associated performance metrics (e.g., reductions in vehicle miles traveled, number of vehicles required, driver-hours worked, energy consumption, and emissions). Table 4.1 shows the operating environment assumed in the base case, derived from data in Gulden (2017) who modeled a circular delivery region with a 10-mile radius and a central depot for drone-only delivery in Minneapolis, Minnesota. The Minneapolis delivery area has a total of 7,740 delivery locations, yielding a delivery density of 23.8 stops per square mile, which is similar to the 25 stops per square mile in our base case. This delivery density is representative of a typical suburban environment that features single family (or standalone) homes that often have yards or porches that are convenient and efficient for a package to be delivered (USPS report, 2020). The USPS report further shows that 76% of the US population lives in suburban areas which accounts for 14% of the US land area and has delivery densities ranging from about 1-725 packages per square mile.

Table 4.2 shows the vehicle characteristics data for the truck and the drone we employ in the base case. Data is obtained from Campbell et al. (2017). The truck consumes diesel fuel and the drone consumes electricity. We differentiate the truck types in truck-only delivery (Truck-1) and truck-drone delivery (Truck-2) by the truck carrying capacities m_{to} and m_{td} (measured in packages, where each delivery is one package). A typical UPS driver makes about 100-150 stops (including both deliveries and pickups) in a typical 8 to 9 hour truck route (Holland et al., 2017; Stolaroff et al., 2018; Perez, 2018). However, the

actual number of stops in a route depends on the time of week, month, and season as well as the delivery area. For example, UPS drivers disclosed that the number of stops can surge to 300-800 during holiday seasons (with several helpers assisting the driver to make the deliveries). In contrast, rural routes can have as low as 20-30 stops (deliveries) while routes in New York City can have over 120 stops without the delivery vehicle moving a mile(Quora, 2020). Note that some of these deliveries are likely to include the delivery of multiple packages to a single stop. However, we treat one stop as one package or one delivery in this dissertation.

Driver working hours in the United States transportation industry are limited by Department of Transportation regulations. One requirement is that drivers can work no more than 60 hours in 7 days, another requirement is that drivers work no more than 70 hours in 8 days (Freightwaves, 2019). Thus, the number of stops a driver can make is limited by his (her) allowable work hours rather than the capacity of the truck. In the base case we use a truck capacity of m_{to} =100 deliveries for Truck-1, and m_{td} = 150 deliveries for truck-drone delivery (Truck-2), as more deliveries can be made with the parallel use of drones to complete deliveries. Although the main analyses focus on cost-related metrics, we also explore associated energy consumption and emissions metrics. The data for lifecycle carbon intensity of fuels, energy consumption rates and emissions are from Stolaroff et al. (2018).

Table 4.1. Base case parameter values for the operating environment

Specification	**Value**
Delivery radius (miles)	10
Delivery density (# stops/ square mile)	25
Total number of deliveries	7,854

Table 4.2. Base case parameter values for the drone and the truck

Specification	**Drone**	**Truck-1**	**Truck-2**
Fuel type	electricity	diesel	diesel
Travel cost rate ($/mile)	0.1	1.25	1.25
Stop cost rate ($/stop)	0.4	0.4	0.4
Travel range (miles)	10	unlimited	unlimited
Linehaul speed (mph)	40	40	40
Local speed (mph)	40	20	20
Stop time (minute)	1	1	1
Work duration (hours)	8	8	8
Capacity (# of packages)	1	100	150
Lifecycle carbon intensity of fuel (kg CO2e/kWh)	0.654	0.335	0.335
Energy consumption rate (kWh/mile)	0.018[1]	3.27[2]	3.27[2]
Travel emissions rate (kg CO2e/mile)	0.012	1.09	1.09
Stop emissions rate (kg CO2e/stop)	0	0	0

[1]Drone energy consumption rate = 40 Joules/meter; [2]Truck energy consumption rate = 11.5 MPG.

To make the cost illustrations clear, we define and distinguish two terms “delivery service” and “delivery service combination”. We model three delivery services: truck-only (TO), drone-only (DO), and truck-drone (TD). These delivery services can be combined, using different services in different subregions, to create a delivery service combination. We require each geographic subregion of the service region to be served by a single delivery service, but allow different parts of the service region to be served with different services. Thus, we have seven delivery service combinations: TO, DO, TD, TO+DO, TO+TD, DO+TD, and TO+DO+TD. Note that for a service option consisting of two or more delivery services, there is an infinite collection of realizations of the delivery services, depending on where each service is used. Even with a fixed fraction of the region served by each delivery service (e.g., 20% by TO and 80% by TD), the region can be geographically partitioned into 20% and 80% subregions in an infinite number of ways. However, in most cases, we care more about the realization that optimizes delivery costs,

or possibly other performance measures of interest. In the following analyses, we define "drone delivery" to refer to a service combination that includes drones for some part of the service region.

4.6.1. Base Case

4.6.1.1 Minimum-cost Division of Delivery Region by Different Delivery Services

In the base case, the minimum-cost delivery system has drone-only (DO) serve deliveries up to 1.2 miles from the depot, and truck-drone (TD) serve the rest of the delivery region (from 1.2 miles to 10 miles away from the depot). Figure 4.8(a) illustrates the delivery cost of each of the three delivery services as a linear function of distance from the depot. The vertical axis is the delivery cost and the horizontal axis shows the distance from the depot. Truck-only (TO) is represented by the blue solid line, drone-only (DO) by the orange dashed line, and truck-drone (TD) by the green long-dash line. The red triangles indicate the delivery service that provides the lowest cost at each distance from the depot. Drone-only delivery (i.e., the orange dashed line) provides the lowest delivery cost for all deliveries within 1.2 miles of the depot, where the number of DO deliveries is 115 (about 1.5% of total deliveries) and the delivery cost is $64 (about 1.1% of total costs), on an average of about 56 cents per delivery. Beyond 1.2 miles, truck-drone delivery (i.e., the green long-dash line) provides the lowest delivery cost, and drone-only delivery becomes much more expensive than truck-drone and truck-only deliveries, as the orange dashed line is far above the green long-dash line and the solid blue line. However, we note that the green long-dash line is only slightly below the solid blue line and becomes a little farther below as deliveries are farther from the depot, which indicates that the savings from using

truck-drone relative to truck-only delivery is not very large when the serving area is not too large.

Figure 4.8(b) demonstrates how the delivery region is partitioned by the optimal services described in Figure 4.8(a). We use one quarter of the circular region to illustrate the optimal partition. The area shaded in orange shows that drone-only delivery serves customers within 1.2 miles of the depot, and the rest of the area (shaded in green) is served by truck-drone.

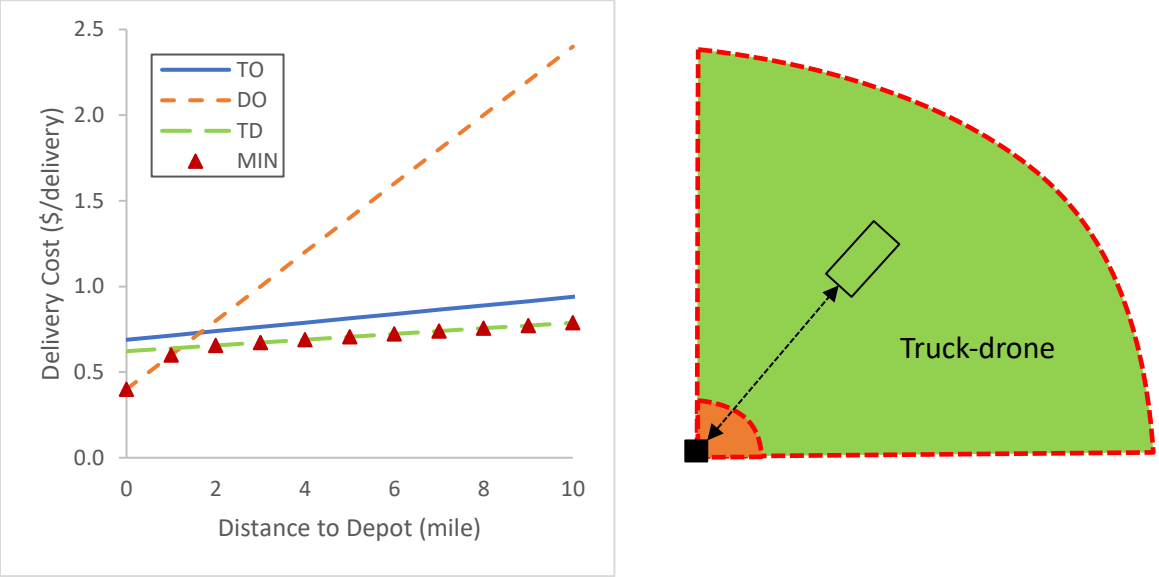

Figure 4.8: (a) Delivery cost of each delivery service as a function of distance from the depot (left); (b) Partition of delivery region by optimal delivery services (right)

4.6.1.2 Cost Savings of Drone Delivery to Truck-only Delivery

Figure 4.9(a) shows the minimum expected total delivery cost of five different service combinations. The first three bars show the cost for using a single delivery service throughout the service region (i.e., truck-only, drone-only, truck-drone), and the other two bars show the cost for the optimal (cost minimizing) combinations of truck-only and drone-

only, and of truck-drone and drone-only. From Figure 4.8 we observed that the combination of drone-only service (up to 1.2 miles) and truck-drone service (beyond 1.2 miles) gives the lowest expected total delivery cost among all service combinations. However, we see that using truck-drone for the entire delivery region is almost as good (in terms of total expected delivery cost) as using the optimal combination of delivery services. This is because drone-only accounts for just 1.1% of the total delivery cost (due to there being very few, low cost DO deliveries all near the depot). Likewise, using TO alone is nearly as good as using DO+TO. It might be economical to use a smaller number of services whenever possible if there are incremental costs associated with managing additional delivery services.

Figure 4.9(b) shows the percentage expected cost savings of the four other service combinations relative to truck-only delivery. Positive cost savings indicate that this other service combination provides lower delivery cost than truck-only delivery. The largest expected cost savings are over 14% and are provided by using truck-drone alone or the optimal combination of drone-only and truck-drone. Using a combination of truck-only and drone only services provides very little expected cost savings (only 0.3%). Using drone-only alone is much more expensive than truck-only in the base case, over 100% more expensive.

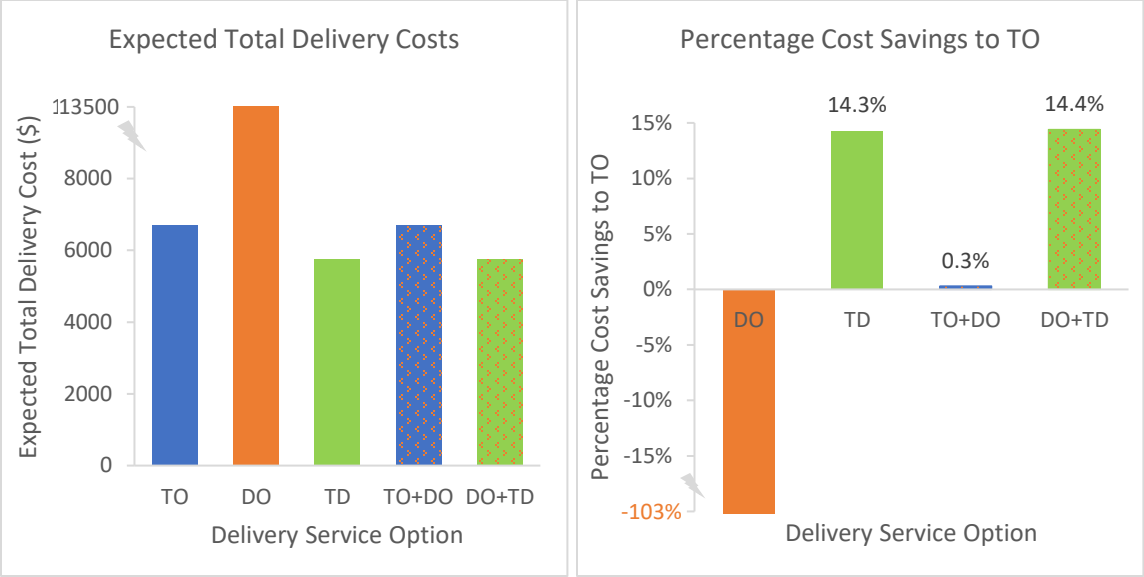

Figure 4.9: (a) Expected total delivery cost of different delivery service combinations (left); (b) Percentage cost savings of different delivery service combinations relative to truck-only delivery (right)

4.6.1.3 Other Benefits of Drone Delivery in addition to Cost Savings

Table 4.3 shows selected other relevant performance measures, in addition to delivery cost for truck-only and the optimal service combination (i.e., DO+TD) in the base case. Columns 4 and 5 indicate the absolute and the percentage changes in performance for the selected measures, respectively.

Table 4.3. Performance comparisons for truck-only and the optimal delivery service combination in the base case

Performance (Expected value)	**TO**	**DO+TD**	**Change**	**%Change**
% Area (customers) Served by TO	100.0%	0.0%	-100.0%	-100%
% Area (customers) Served by DO	0.0%	1.5%	1.5%	-
% Area (customers) Served by TD	0.0%	98.5%	98.5%	-
Total Delivery Cost ($)	**6717.8**	**5750.3**	**-967.5**	**-14%**
Truck Delivery Cost	6717.8	4000.2	-2717.6	-40%
Drone Delivery Cost	-	1750.1	1750.1	-
Total GHG Emissions (kg CO2e)	**3132.2**	**2166.4**	**-965.8**	**-31%**
Truck Emissions	3132.2	2148.0	-984.2	-31%
Drone Emissions	-	18.4	18.4	-
Truck Miles Traveled (mile)	2861.0	1962.0	-899.0	-31%
Drone Miles Traveled (mile)	-	1562.1	1562.1	-
Driver Hours Worked (hour)	247.8	145.2	-102.6	-41%
Drone Hours Operated (hour)	-	105.5	105.5	-
#Trucks Required (SL[1] = 8 hrs)	31.0	18.1	-12.8	-41%
#Drones Required (SL[1] = 8 hrs)	-	19.0	19.0	-
Number of Truck Routes	78.5	51.6	-26.9	-34%
Truck Route Length (mile)	36.4	38.0	1.6	4%
Truck Route Time (hour)	3.2	2.8	-0.3	-11%
Drone Stops	-	3984.6	3984.6	-

[1]SL= Service Level, which is one day in the base case

Rows 2-4 indicate the percentage of the total delivery area (or customers) served by TO, DO, and TD in each service combination, respectively. Row 5 indicates the expected total delivery costs (including both truck and drone delivery costs) of the two service options. Expected total delivery costs are reduced from $6,718 (for TO) to $5,750 (for DO+TD), with truck delivery cost reduced by $2,718 (about a 40% reduction) afforded by drone operating costs of $1,750. The associated emissions (produced from the minimum-cost routes), in row 6, are reduced from 3,132 kg CO2e (for TO) to 2,166 kg CO2e (for DO+TD), with truck emissions reduced by 984 kg CO2e and drone emissions increased by only 18 kg CO2e, which indicates that the emissions-efficiency of drones

relative to trucks is much greater than the operating cost efficiency of drones relative to trucks. The expected truck travel miles (in row 11) are reduced by 899 miles (about a 31% reduction). However, the expected drone travel miles (in row 12) are increased by 1,562 miles. In row 13, the expected number of hours that drivers work is reduced by 103 hours to only 145 hours using DO+TD rather than TO, which is about a 41% reduction. In row 14, we also show the number of hours that drones operate (not including hours that the drones ride on the trucks). We compute the number of trucks and drones required (in rows 15-16) based on the driver hours required and a work day of 8 hours. Thus, the expected number of trucks required to serve the delivery region is 31 for TO and 18.1 for DO+TD. The expected number of drones required is 18.1 for those that make deliveries from the truck and 0.8 for those that make deliveries from the depot. The number of truck routes (in row 17) is reduced from 79 (for TO) to 52 (for DO+TD), about a 34% reduction. The truck route length increases slightly (about 1.6 miles) for DO+TD relative to TO. This is because having one half of the TD deliveries made by the drone increases the swath width of the truck-drone route so much that it offsets the miles reduced by having the truck make fewer deliveries in one route. However, we could also view it as although the truck-drone route makes 50% more deliveries than the truck-only route, the truck travel miles is increased only 4.4% for DO+TD. The truck route time decreases by 21 minutes as the drone works in parallel with the truck to make one half of the TD deliveries.

4.6.1.4 Allocation of Selected Performance Measures to Each Component

Figure 4.10 shows the allocation of the expected total delivery cost to each component (i.e., truck linehaul and local travel cost, truck and drone stop cost, and drone travel cost) of TO (solid blue bars) versus DO+TD (mixed dotted orange and green bars).

We also include TD (hatched green bars) to demonstrate that the near-optimal service option, TD, is about as good as the optimal service option, TO+TD. The expected total delivery cost of TO includes costs for truck linehaul travel (about 19%), truck local travel (about 34%) and truck delivery stops (about 47%) – the largest cost proportion comes from delivery stops, i.e., making the deliveries. For DO+TD and TD, two additional cost components, i.e., drone travel and drone stop, are incurred. Comparing DO+TD with TO, the delivery costs for truck linehaul travel, truck local travel, and truck stop are reduced by 33%, 30%, and 51%, respectively. Although the largest cost reduction comes from the reduction of truck delivery stops, the same amount of cost ($1,594) is now added by the drone delivery stops as the total number of deliveries does not change and the truck and the drone have the same unit stop cost in the base case (i.e., $0.4/stop). In Figure 4.10, we see that the expected cost of each component of TD is about the same as that of DO+TD. Using TD alone might be more appealing as it reduces the possible complexity of managing multiple delivery services.

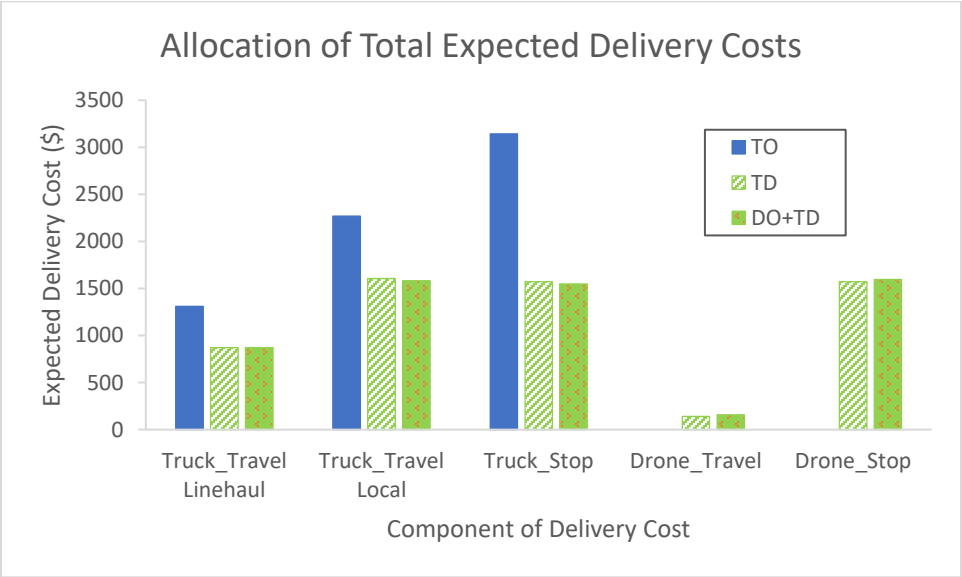

Figure 4.10. The allocation of expected cost to each component in TO, DO+TD, and TD

Although not the main focus in the cost analysis, Figure 4.11 shows how environmentally friendly drone travel is in the base case compared with truck travel. Delivery stop emissions are zero for both drone and truck delivery so they are not shown in the graph. For TO, the expected emissions include truck linehaul travel (about 34%) and truck local travel (about 66%). Replacing TO with DO+TD (or TD) has a similar impact on total emissions as on delivery costs, except that drone emissions account for only 0.85% of emissions vs drone delivery costs accounting for 30% in DO+TD (or TD), due to the high drone stop cost

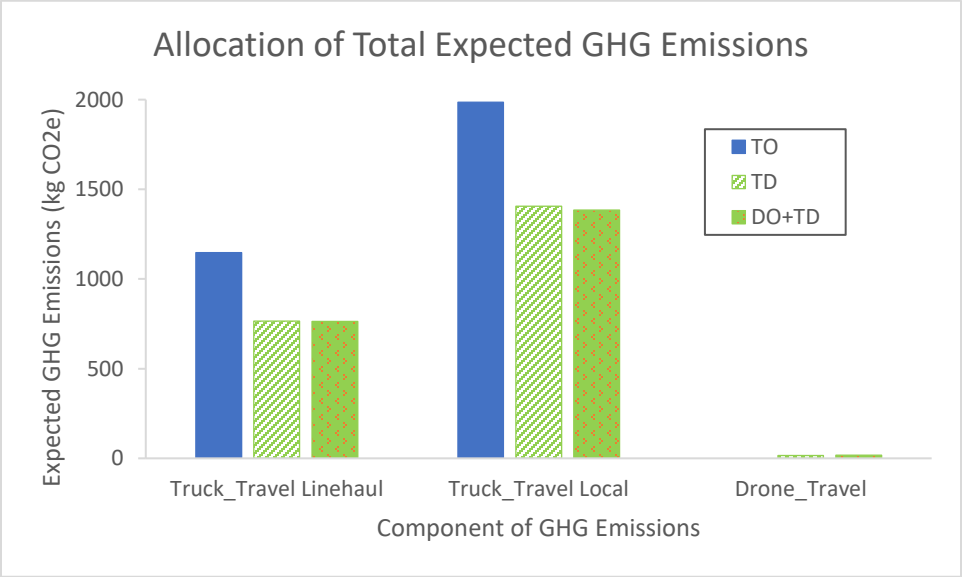

Figure 4.11. The allocation of emissions to each component in TO, DO+TD, and TD

One of the benefits of using drones (i.e., in truck-drone and drone-only delivery) is the reduction in truck travel miles, especially truck linehaul travel miles afforded by reducing the number of truck routes, which in turn then reduces truck travel costs (and emissions). This is because truck travel is much (about 12.5 times) more expensive and much (about 182 times) more polluting than drone travel. Thus, reducing truck travel miles has a large impact on reducing total cost and emissions. However, we note that although

slightly more than half of the deliveries are replaced by drones with DO+TD (vs TO), this does not reduce truck local travel miles by 50% for DO+TD or TD compared with TO, as shown in Figure 4.12. Comparing TD with DO+TD, we see truck local travel miles are slightly higher while drone travel miles are significantly lower. Together, these changes may indicate that having truck and drone alternate deliveries as in our TD model may not be the most efficient way of using drones with trucks. When drone travel is much lower cost than truck travel, it might be more beneficial to have drones make more deliveries, such as by allowing more than one drone per truck or having drones make multiple deliveries per truck delivery.

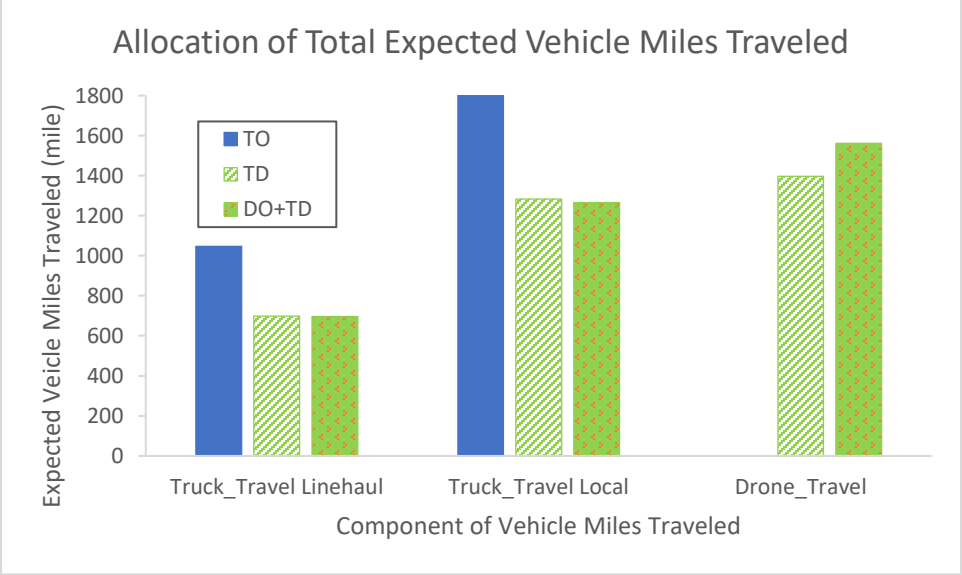

Figure 4.12. The allocation of expected vehicle miles traveled to each component in TO, DO+TD, and TD

Figure 4.13 shows the allocation of total expected driver hours worked to each component of TO (solid blue bars) versus DO+TD (mixed dotted orange and green bars) versus TD (hatched green bars). The components of driver hours worked in TO include hours spent in truck linehaul travel (26 hours or 11%), truck local travel (91 hours or

37%), and truck delivery stops (131 hours or 53%). Compared with TO, DO+TD significantly reduces the truck stop time by 66 hours (or 51%) thanks to the parallel operation of drone delivery from the truck. It also reduces driver hours spent in truck linehaul and local travel by 33% and 30%, respectively.

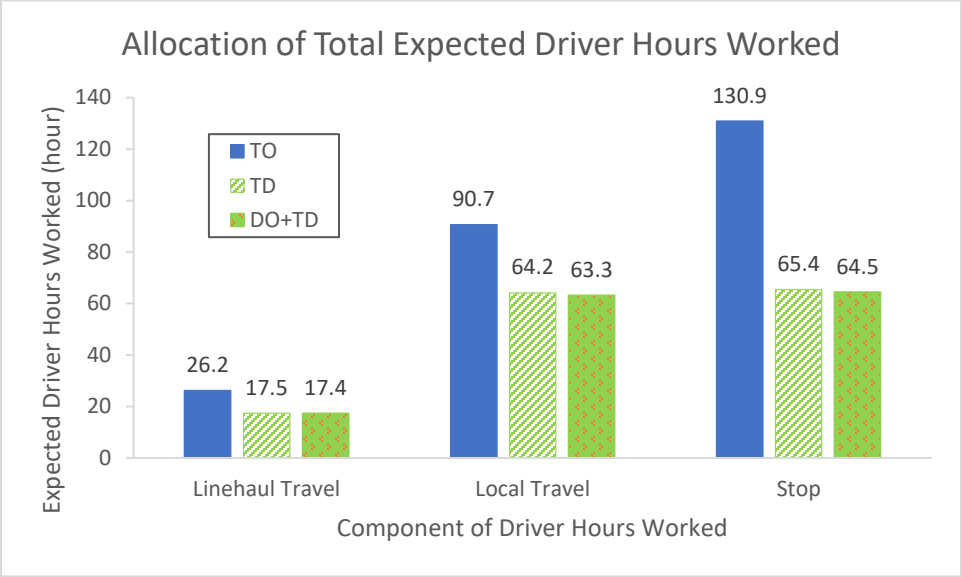

Figure 4.13. The allocation of expected driver hours worked to each component in TO, DO+TD, and TD

4.6.2. Expensive vs Inexpensive Unit Drone Travel Cost (c_d)

To assess the impact of drone travel cost on the performance metrics, we consider two other unit drone travel costs: $c_d = \$0.625$/mile and $c_d = \$0.01$/mile in addition to the base case of $c_d = \$0.10$. The relatively expensive c_d case may represent near-future drone operations due to high equipment purchase prices and strict operating regulations (e.g., an operator is required for a limited number of drones in delivery; night delivery is restricted, etc.). The relatively inexpensive c_d case may represent long-term future drone operations

with equipment purchase prices greatly reduced and operating technologies improved that allow regulation to be loosened for efficiency purposes.

4.6.2.1 Performance Effects of Drone Delivery

Table 4.4 shows the performance measures of interest for TO, TD, and the optimal service option for three different levels of c_d, i.e., DO+TO+TD ($c_d = \$0.625$/mile), DO+TD (base case c_d =\$0.1/mile), and DO ($c_d = \$0.01$/mile), showing in columns 4,6,8, respectively.

Table 4.4 provides several interesting observations:

(1) in the optimal service combination, the lower the drone travel cost (c_d), the higher the percentage of customers served by DO (in row 5) and the lower the percentage of customers served by TD (row6). We note that TD use decreases with decreasing drone travel cost (c_d) for intermediate values of c_d not displayed in Table 4.4. For example, TD use is reduced from 98.5% to 49.6% (~50% reduction) when c_d is reduced from 0.1 to 0.023 \$/mile (~77% reduction); and reduced from 49.6% to 0% (~50% reduction) when c_d is reduced from 0.023 to 0.018 \$/mile (~22% reduction).

(2) when $c_d = \$0.625$/mile, the optimal service combination has DO serve only those customers who are within 0.24 miles of the depot, which account for less than 0.1% of total customers; TO serves customers who are between 0.24 and 2.84 miles of the depot accounting for 8% of total customers; and TD serves the rest of the delivery area (about 92% of the customers). The cost savings compared to truck-only service is only 3.8%. However, the emissions savings is 28%. Compared with the base case optimal service combination DO+TD, there are only slight changes in other performance measures,

especially measures associated with truck use (e.g., truck route length and time, number of trucks required).

(3) with low-cost drone travel, $c_d = \$0.01$/mile, the optimal service combination has DO delivery serve all customers, which provides the largest cost savings of 37.6% relative to TO. The emissions are reduced even more by 60.6%. However, drone travel miles are increased from 0 to 104,720 miles. The total system time is 2,749 hours for the drone to complete all the deliveries. If we assume the service level is one day and the drone can work 8 hours, the number of drones required is 344. If in the future the drones are allowed to work 24 hours per day, the number of drones required is reduced to 115. If the service level is increased to 2-hour delivery (vs 8-hour in the base case) (e.g., for on-demand grocery delivery), and we assume the orders are evenly distributed throughout the day (e.g., from 8AM to 8 PM), then the number of drones required is reduced to 230.

(4) In both the expensive c_d case and the base case, TD performs very similarly to the optimal service combination. This is because all these service combinations consist of a large proportion of TD use (more than 92%), which indicates that TD may be an important type of service when the drone travel cost is not at very low level. However, when drone travel cost becomes extremely low ($c_d = \$0.01$/mile), then TD provides about 50% smaller cost savings and emissions reductions than using the optimal service combination (i.e., just DO). However, comparing TD with DO for other performance measures shows: the total travel miles are 97% less (3,263.2 vs 104,719.8), total system time is 94% less (147 vs 2,618), the number of drones required is 95% less (15 vs 344) given the same service level.

(5) By changing drone travel cost alone, we cannot obtain a case where all three services (i.e., TO, DO, TD) serve approximately the same number of customers. However, by changing other parameters at the same time, we can find such cases.

Table 4.4. Performance for TO, TD, and the optimal delivery service combinations for three levels of c_d

Performance Measure	**Status Quo**	**Expensive c_d Case**		**Base Case**		**Inexpensive c_d Case**	
c_d ($/mile)	∞	0.625		0.1		0.01	
Service Option	TO	TD	DO+TO+TD*	TD	DO+TD*	TD	DO*
% Area (customers) Served by TO	100.0%	-	8.0%	-	0.0%	-	-
% Area (customers) Served by DO	-	-	0.1%	-	1.5%	-	100.0%
% Area (customers) Served by TD	-	100.0%	92.0%	100.0%	98.5%	100.0%	-
Total Delivery Cost (TDC) ($)	**6717.8**	**6467.1**	**6461.7**	**5758.8**	**5750.3**	**5631.8**	**4188.8**
% TDC Change to TO	-	-3.7%	-3.8%	-14.3%	-14.4%	-16.2%	-37.6%
Truck Delivery Cost	6717.8	4070.4	4255.2	4048.4	4000.2	4046.7	-
Drone Delivery Cost	-	2396.7	2206.5	1710.4	1750.1	1585.1	4188.8
Total GHG Emissions (kg CO2e)	**3132.2**	**2204.8**	**2256.3**	**2186.4**	**2166.4**	**2185.3**	**1232.8**
% Emissions Change to TO	-	-29.6%	-28.0%	-30.2%	-30.8%	-30.2%	-60.6%
Truck Emissions	3132.2	2189.3	2242.0	2170.0	2148.0	2168.5	-
Drone Emissions	-	15.6	14.3	16.4	18.4	16.8	1232.8
Truck Miles Traveled (mile)	**2861.0**	**1999.7**	**2047.8**	**1982.1**	**1962.0**	**1980.7**	**-**
Drone Miles Traveled (mile)	-	1321.4	1216.5	1396.3	1562.1	1429.4	104719.8
Driver Hours Worked (hour)	**247.8**	**148.0**	**155.4**	**147.1**	**145.2**	**147.0**	**-**
Drone Hours Operated (hour)	-	98.5	90.7	100.4	105.5	101.2	2748.9
#Trucks Required (SL = 8 hrs)	31.0	18.5	19.4	18.4	18.1	18.4	-
#Drones Required (SL = 8 hrs)	-	18.5	19.4	18.4	19.0	18.4	343.6
Number of Truck Routes	**78.5**	**52.4**	**54.4**	**52.4**	**51.6**	**52.4**	**-**
Truck Route Length (mile)	36.4	38.2	37.6	37.9	38.0	37.8	-
Truck Route Time (hour)	3.2	2.8	2.9	2.8	2.8	2.8	-
Drone Stops	**-**	**3927.0**	**3615.5**	**3927.0**	**3984.6**	**3927.0**	**7854.0**

*The optimal service combination that minimizes total delivery cost.

4.6.2.2 Allocation of Selected Performance Measures to Each Component

To understand the mechanisms by which drones improve delivery performance, we show the components of delivery cost (Figure 4.14), travel miles (Figure 4.15), and system time (Figure 4.16) of the optimal service combination with the three different levels of c_d. In each figure, colors light blue, blue, and dark blue represent the expensive c_d case, the base case, and the inexpensive c_d case, respectively. TO is represented by solid bars, TD by dotted bars, and the optimal service option by hatched bars. We include TD to demonstrate that this single delivery service is a near-optimal service alternative.

Figure 4.14 shows the allocation of the total expected cost in truck linehaul travel, truck local travel and drone travel of the different service combinations with the three levels of c_d. We do not include stop costs in the figure as the total delivery stop costs are the same for all alternatives. For each level of c_d, the same pattern appears as evident in the base case. The delivery costs for truck linehaul and local travel are reduced by increasing the cost for drone travel. Comparing the optimal delivery service combination of expensive drones ($c_d = \$0.625$/mile), i.e., DO+TO+TD, with the optimal service combination of the base case, i.e., DO+TD, the linehaul truck travel cost stays almost the same (about 1.3% increase), the local truck travel cost increases slightly by 6.1%, while the drone travel cost increases most noticeably from \$156 to \$760, which is more than a 387% increase. Comparing the optimal delivery service combination of inexpensive drones ($c_d = \$0.01$/mile), i.e., DO, with the optimal delivery service combination of the base case, i.e., DO+TD, the cost components associated with truck travel are reduced to zero and drone travel cost is increased by \$1,047, which provides a 60% reduction in the total travel cost (including truck linehaul, truck local and drone travel). However, the inexpensive drones

provide only a 27% reduction in overall costs (including stop costs). The high stop cost per delivery reduces the percentage decrease in operating costs. Similarly, the noticeable differences in drone travel cost of TD for different c_d levels make TD a very good alternative to the optimal delivery service combination consisting of more than one service when c_d is high, and not as good an alternative as the optimal delivery service combination when c_d is extremely low.

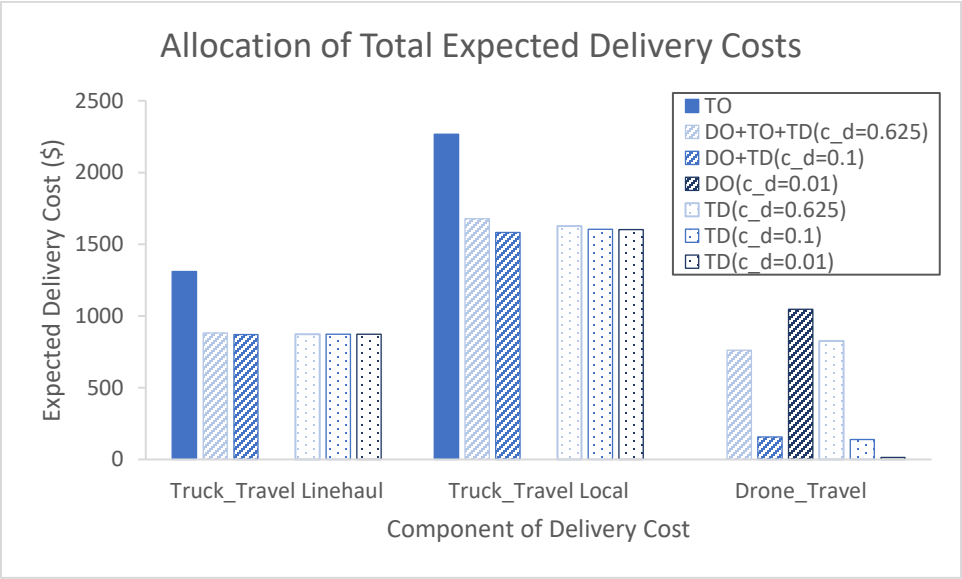

Figure 4.14. Cost allocation in TO, TD, and the optimal delivery service combination for three levels of c_d

Figure 4.15 shows the allocation of vehicle miles traveled, which is very similar to Figure 14.14 if we just look at truck travel. However, the drone travel miles increase as drone travel cost becomes lower because more customers are served by drones (for the optimal delivery service combinations) and/or the swath width is increased to reduce truck travel (for delivery service combinations that include TD). The drone travel miles are increased from 1,562 miles (in the base case) to 104,720 miles (for DO when $c_d = 0.01$),

about a 6,600% increase. The drone travel miles are decreased by 22% when c_d is increased from 0.1 to 0.625. For TD, we see the truck linehaul travel miles stay the same, and there are slight decreases in truck local travel miles and some increases in drone travel miles when c_d decreases from 0.625 to 0.1 to 0.01, which is due to the swath width change in truck-drone routes. However, the swath width change is not enough to make TD used for low c_d.

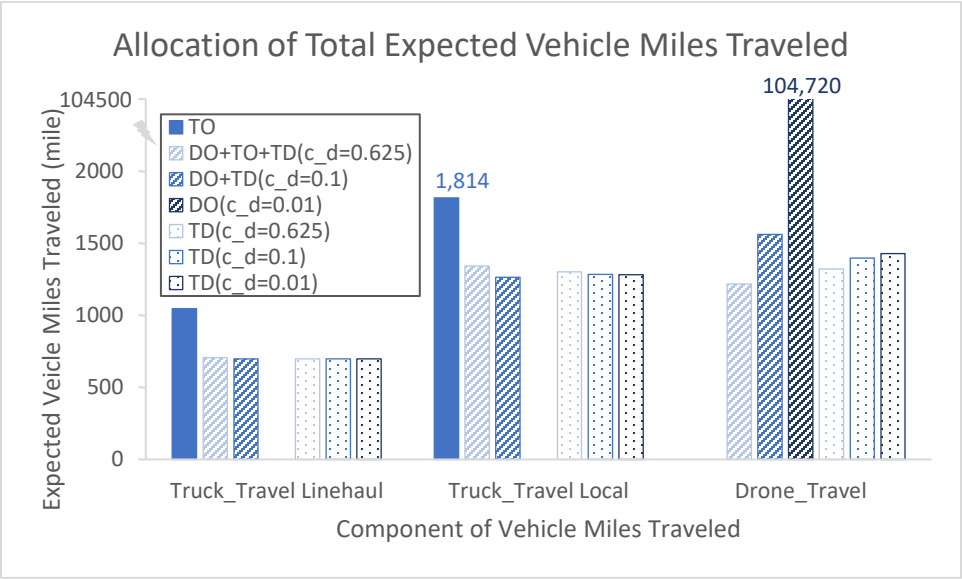

Figure 4.15. Allocation of vehicle miles traveled in TO, TD, and the optimal delivery service combinations for three levels of c_d

The large amount of travel miles of DO also leads to the high travel hours as shown in Figure 4.16. We have discussed before that the number of drone travel hours affects the number of drones required. For delivery service options that consist of truck, the system delivery time is usually determined by the truck hours operated, and drones help reduce that time by making deliveries in parallel with the truck. We observe that the reduction in

truck hours operated does not change much when c_d increases from 0.1 to 0.625 compared with the optimal delivery service combinations.

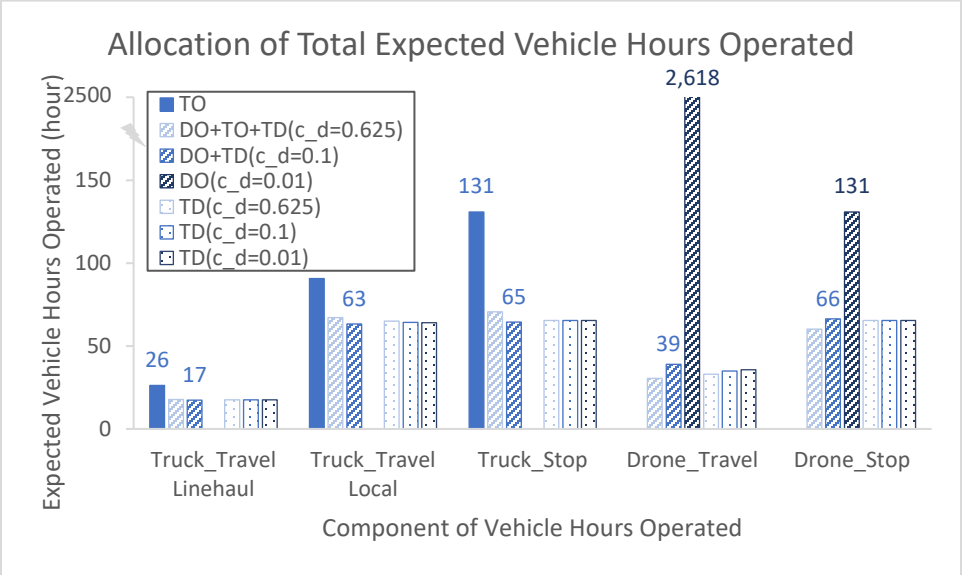

Figure 4.16. Allocation of vehicle hours operated in TO, TD, and the optimal delivery service combination for three levels of c_d

4.6.3. Expensive vs Inexpensive Marginal Drone Stop Cost (s_d)

In this section we consider two other levels of marginal drone stop cost in addition to the base case ($s_d = \$0$/stop): a relatively expensive marginal drone stop cost ($s_d = \$0.2$/stop) and a relatively inexpensive marginal drone stop cost ($s_d = -\$0.2$/stop). The expensive s_d case may represent near-future drone operations that face landing challenges (e.g., drones require a large amount of hover time per delivery as mentioned in current literature, e.g., Kirchstein, 2020), thus, the marginal drone stop cost may be greater than zero, indicating that drone stop cost is higher than that of the truck. The inexpensive s_d case may represent long-term future drone operations where the landing challenges have been resolved or drones are used in areas where truck stop time or cost is longer (e.g.,

wealthier neighborhoods, very rural areas), and thus the marginal drone stop cost is negative, indicating that drone stop cost is lower than that of the truck. Because the drone stop time τ_d and the marginal drone stop cost s_d may be correlated, we change drone stop time accordingly with the costs and increase drone stop time by 50% to 90 seconds per stop under the expensive s_d case; and decrease the drone stop time by 50% to 30 seconds per stop under the inexpensive s_d case.

4.6.3.1 Performance Effects of Drone Delivery

Table 4.5 shows the performance measures of interest for TO, TD, and the optimal delivery service combination for three different levels of s_d and associated τ_d, i.e., DO+TO+TD ($s_d = \$0.2$/stop, $\tau_d = 90$ seconds/stop), DO+TD (base case $s_d = \$0$/stop, $\tau_d = 60$ seconds/stop), and DO+TD ($s_d = -\$0.2$/stop, $\tau_d = 30$ seconds/stop), in columns 4,6,8, respectively.

Like the impact of different drone travel costs (c_d), the lower the marginal drone stop cost (s_d), the higher the percentage of customers served by DO (0.3%, 1.5%, and 3.1% when $s_d = 0.2$, 0, and -0.2 \$/stop, respectively) and the larger the number of drone deliveries (3314, 3985, and 4048 when $s_d = 0.2$, 0, and -0.2 \$/stop, respectively) in the optimal delivery service combinations. It is interesting that when s_d is high, the utilization of each service in the optimal delivery service combination responds similarly to when c_d is high. In both cases, three delivery services are used, with similar DO utilization (less than 0.3%) but different TO and TD utilizations. TO is used for about 16% of deliveries for the expensive s_d case, and for about 8% of deliveries for the expensive c_d case. Accordingly, TD is used for about 84% of deliveries for the expensive s_d case, and for about 92% of deliveries for the expensive c_d case. Like the base case, DO+TD is the

optimal service combination when $s_d = -\$0.2$/stop, with the service provided by DO increased from 1.2 to 1.8 miles.

Although the total operating hours of drones are less than those of trucks, in some cases (e.g., TD when $s_d = 0.2$ \$/stop), the total time for drones in the system, which includes the time drones ride on trucks during linehaul travel, may exceed the total time for trucks in the system, thus, the use of drones for such cases does not improve the overall service level. In all cases, the cost savings of TD and the optimal delivery service combination relative to TO are very similar, which indicates that TD is a good alternative to the optimal delivery service combination for a wide range of marginal drone stop costs.

Table 4.5. Performance for TO, TD, and the optimal delivery service combinations under three levels of s_d and associated τ_d

Performance Measure	**Status Quo**	**Expensive s_d Case**		**Base Case**		**Inexpensive s_d Case**	
Drone cost ($/) & time (sec) per stop	∞	$s_d = 0.2, \tau_d = 90$		$s_d = 0, \tau_d = 60$		$s_d = -0.2, \tau_d = 30$	
Service Option	TO	TD	DO+TO+TD*	TD	DO+TD*	TD	DO+TD*
% Area (customers) Served by TO	100.0%	-	15.9%	-	0.0%	-	0.0%
% Area (customers) Served by DO	-	-	0.3%	-	1.5%	-	3.1%
% Area (customers) Served by TD	-	100.0%	83.9%	100.0%	98.5%	100.0%	96.9%
Total Delivery Cost (TDC) ($)	**6717.8**	**6544.2**	**6529.5**	**5758.8**	**5750.3**	**4973.4**	**4947.4**
% TDC Change to TO	-	-2.6%	-2.8%	-14.3%	-14.4%	-26.0%	-26.4%
Truck Delivery Cost	6717.8	4048.4	4422.4	4048.4	4000.2	4048.4	3945.6
Drone Delivery Cost	-	2495.8	2107.1	1710.4	1750.1	925.0	1001.8
Total GHG Emissions (kg CO2e)	**3132.2**	**2186.4**	**2296.9**	**2186.4**	**2166.4**	**2186.4**	**2145.1**
% Emissions Change to TO	-	-30.2%	-26.7%	-30.2%	-30.8%	-30.2%	-31.5%
Truck Emissions	3132.2	2170.0	2282.9	2170.0	2148.0	2170.0	2122.4
Drone Emissions	-	16.4	13.9	16.4	18.4	16.4	22.6
Truck Miles Traveled (mile)	**2861.0**	**1982.1**	**2085.2**	**1982.1**	**1962.0**	**1982.1**	**1938.7**
Drone Miles Traveled (mile)	-	1396.3	1185.0	1396.3	1562.1	1396.3	1921.2
Driver Hours Worked (hour)	**247.8**	**147.1**	**161.9**	**147.1**	**145.2**	**147.1**	**143.0**
Drone Hours Operated (hour)	-	133.1	112.5	100.4	105.5	67.6	81.8
Drone Total Time in System (hour)	-	**150.5**	130.5	117.8	122.9	85.1	99.1
#Trucks Required (SL = 8 hrs)	31.0	18.4	20.2	18.4	18.1	18.4	17.9
#Drones Required (SL = 8 hrs)	-	18.4	20.3	18.4	19.0	18.4	19.9
Number of Truck Routes	78.5	52.4	56.4	52.4	51.6	52.4	50.7
Truck Route Length (mile)	36.4	37.9	37.0	37.9	38.0	37.9	38.2
Truck Route Time (hour)	3.2	2.8	2.9	2.8	2.8	2.8	2.8
Drone Stops	-	3927.0	3314.4	3927.0	3984.6	3927.0	4048.2

*The optimal delivery service combination that minimizes total delivery cost.

4.6.3.2 Allocation of Selected Performance Measures to Each Component

Figure 4.17 shows the cost per delivery of each delivery service combination for the three levels of s_d. Again, colors dark blue, blue, and light blue represent the inexpensive s_d case, the base case, and the expensive s_d case, respectively. The figure shows that TD is nearly as good as the optimal delivery service combination in terms of cost per delivery in all cases. The lower the marginal drone stop cost s_d, the lower the cost per delivery for all service combinations. It is interesting to see that the cost per delivery decreases by \$0.2 for DO (as the marginal drone delivery cost s_d decreases by \$0.2), while it decreases by only \$0.1for TD when s_d decreases by \$0.2. This is because only half of the deliveries on TD routes are made by drones.

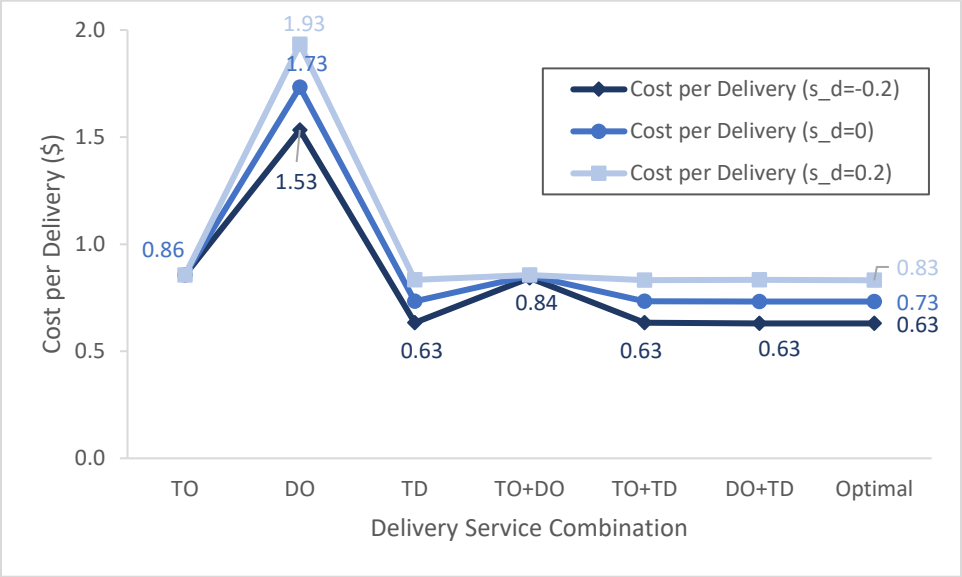

Figure 4.17. Cost per delivery of all delivery service combinations for three levels of s_d

Figure 4.18 shows the allocation of vehicle hours operated. For the optimal delivery service combinations (bars 2-4 in each set), the hours spent on truck linehaul travel, local travel and delivery stops decrease as the marginal drone stop cost (s_d) decreases, with

reductions (3% in truck linehaul travel, 7% in truck local travel, and 15% in truck delivery stops) from the expensive s_d case to the base case being greater than those (0.4% in truck linehaul travel, 1.6% in truck local travel, and 1.6% in truck stop) from the base case to the inexpensive s_d case. This is because TO serves more customers when s_d is expensive, thus truck linehaul and local travel increase; and the truck stop time increases because drone stop time increases as s_d increases. Hours spent on drone travel increase while drone stop time decreases as s_d decreases. However, the decrease in drone travel and stop time may indicate that it is beneficial in terms of both cost and time to have more customers served by drones. For TD under these three cases (the last 3 bars in each set), the only change is in drone stop time, which naturally decreases as s_d decreases (due to the assumed correlation of drone stop time and marginal drone stop cost).

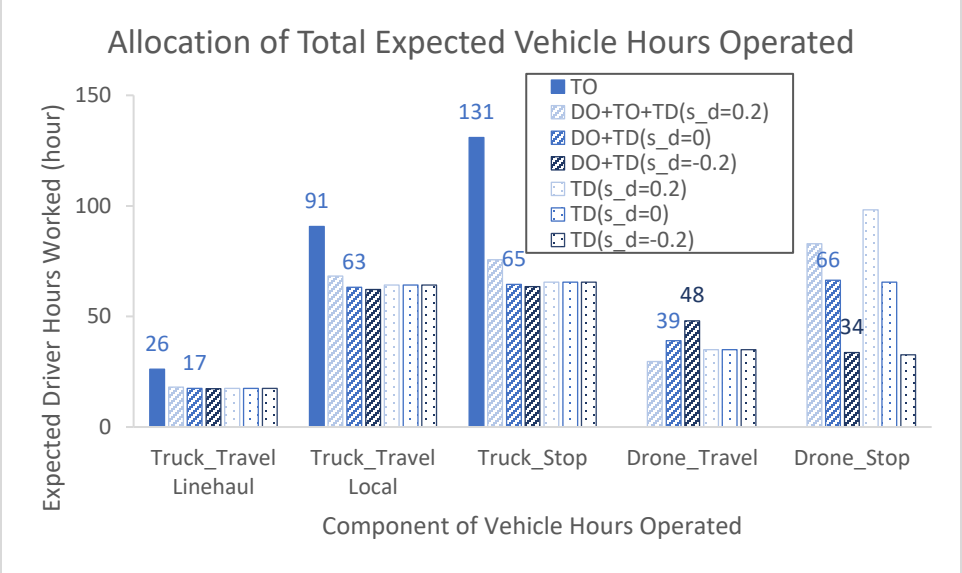

Figure 4.18. Allocation of vehicle hours operated in TO, TD, and the optimal delivery service combinations for three levels of s_d and associated τ_d

Figure 4.19 shows the allocation of vehicle miles traveled. It is interesting to see that all components of TD remain the same across the three cases (last 3 bars in each set). This is because s_d has no impact on the swath width of truck-drone route. However, we see the vehicle miles change in the optimal services, which is because s_d has an impact on the optimal sub-delivery partitioning distance, i.e., the utilization of each service when more than one service is used.

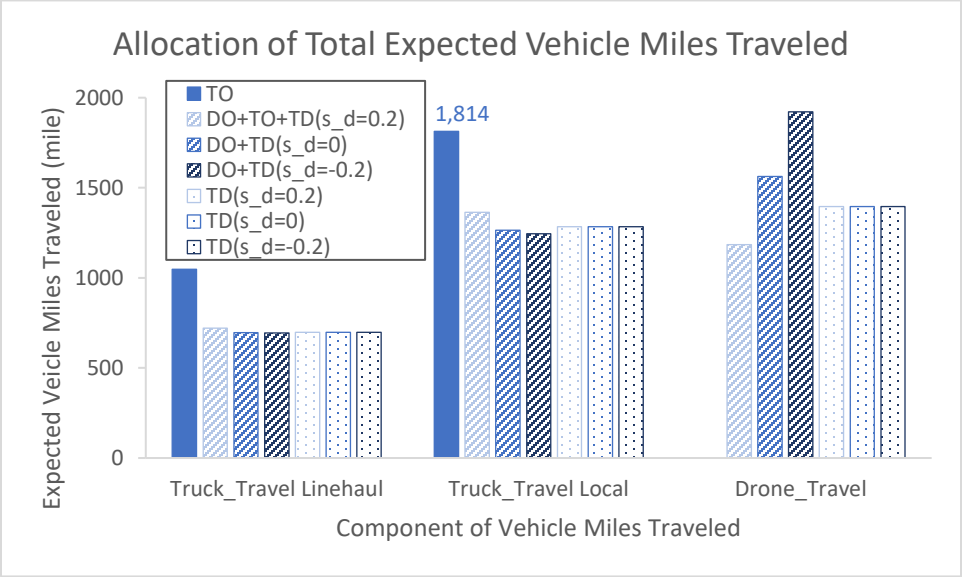

Figure 4.19. Allocation of vehicle miles traveled in TO, TD, and the optimal delivery service combination for three levels of s_d and associated τ_d

In summary, s_d has no impact on the swath width but has an impact on the performance of the optimal set of services. If the drone stop time τ_d and the marginal drone stop cost s_d change in the same direction, then the cost and time benefits of drone delivery will go hand by hand, with cost savings being more straightforward than time reductions.

4.6.4. Large vs Small Truck Capacity for Truck-drone Delivery (m_{td})

In this section we consider two other levels of truck capacity for truck-drone delivery in addition to the base case level where $m_{td} = 150$ deliveries per route: a large truck capacity with $m_{td} = 300$ deliveries per route and a small truck capacity with $m_{td} = 75$ deliveries per route. The truck capacity has an impact on delivery economies of scale for the multi-stop routes through altering the truck linehaul travel cost per delivery. The larger the capacity, the smaller the amount of linehaul cost associated with each delivery.

4.6.4.1 Performance Effects of Drone Delivery

Table 4.6 shows the performance measures of interest for TO, TD, and the optimal delivery service combination for three different levels of m_{td}, i.e., DO+TD+TO ($m_{td} = 75$), DO+TD (base case $m_{td} = 150$), and DO+TD ($m_{td} = 300$), in columns 4,6, and 8, respectively.

There are several interesting observations from Table 4.6:

(1) for the optimal delivery service combination for the three levels of m_{td}, the larger the truck capacity for truck-drone delivery, the lower the percentage of customers served by DO (in row 5) and the higher the percentage of customers served by TD (in row 6). We note that the impact of m_{td} on the increasing utilization of TD is marginally diminishing. For example, when m_{td} increases from 75 to 150, TD utilization (i.e., the percentage number of customers served by TD) increases from 62% to 98.5% (a 36.5% increase); when m_{td} is further doubled (from 150 to 300), TD utilization increases only 0.2% (from 98.5% to 98.7%).

Table 4.6. Performance for TO, TD, and the optimal delivery service combinations for three levels of m_{td}

Performance Measure	**Status Quo**	**Small TD Capacity**		**Base Case**		**Large TD Capacity**	
Truck-drone capacity m_{td}	$m_{td} = 0$	$m_{td} = 75$		$m_{td} = 150$		$m_{td} = 300$	
Service Option	TO	TD	DO+TD+TO*	TD	DO+TD*	TD	DO+TD*
% Area (customers) Served by TO	100.0%	-	36.2%	-	-	-	-
% Area (customers) Served by DO	-	-	1.8%	-	1.5%	-	1.3%
% Area (customers) Served by TD	-	100.0%	62.0%	100.0%	98.5%	100.0%	98.7%
Total Delivery Cost (TDC) ($)	**6717.8**	**6631.5**	**6596.4**	**5758.8**	**5750.3**	**5322.5**	**5314.7**
% TDC Change to TO	-	-1.3%	-1.8%	-14.3%	-14.4%	-20.8%	-20.9%
Truck Delivery Cost	6717.8	4921.1	5455.3	4048.4	4000.2	3612.1	3568.7
Drone Delivery Cost	-	1710.4	1141.0	1710.4	1750.1	1710.4	1745.9
Total GHG Emissions (kg CO2e)	**3132.2**	**2950.7**	**2941.4**	**2186.4**	**2166.4**	**1804.3**	**1786.5**
% Emissions Change to TO	-	-5.8%	-6.1%	-30.2%	-30.8%	-42.4%	-43.0%
Truck Emissions	3132.2	2934.3	2928.3	2170.0	2148.0	1787.8	1768.3
Drone Emissions	-	16.4	13.1	16.4	18.4	16.4	18.1
Truck Miles Traveled (mile)	**2861.0**	**2680.2**	**2674.8**	**1982.1**	**1962.0**	**1633.0**	**1615.2**
Drone Miles Traveled (mile)	-	1396.3	1113.6	1396.3	1562.1	1396.3	1540.6
Driver Hours Worked (hour)	**247.8**	**164.6**	**191.2**	**147.1**	**145.2**	**138.4**	**136.6**
Drone Hours Operated (hour)	-	100.4	70.7	100.4	105.5	100.4	104.8
#Trucks Required (SL = 8 hrs)	31.0	20.6	23.9	18.4	18.1	17.3	17.1
#Drones Required (SL = 8 hrs)	-	20.6	25.0	18.4	19.0	17.3	17.8
Number of Truck Routes (NTR)	**78.5**	**104.7**	**93.4**	**52.4**	**51.6**	**26.2**	**25.8**
% NTR Change to TO	-	33.3%	18.9%	-33.3%	-34.3%	-66.7%	-67.1%
Truck Route Length (mile)	36.4	25.6	28.6	37.9	38.0	62.4	62.5
Truck Route Time (hour)	3.2	1.6	2.0	2.8	2.8	5.3	5.3
Drone Stops	-	3927.0	2574.2	3927.0	3984.6	3927.0	3979.7

*The optimal delivery service combination that minimizes total delivery cost.

(2) when $m_{td} = 75$, the optimal service combination has DO serve those deliveries that are within 1.3 miles of the depot, which account for about 1.8% of total customers; TD serves customers who are between 1.3 and 8.0 miles of the depot and account for 62% of total customers; and TO serve the rest of the delivery area (about 36.2% of customers). The cost and emissions savings compared to truck-only delivery are both small, about 1.8% and 6.1%, respectively. When we extend the radius of the delivery region (to 20 or 30 miles), since the regions where DO and TD are used will not change, these cost and emissions savings from drone delivery will be even lower, as more deliveries further from the depot are made by TO. However, the service level might be improved by using a smaller truck-drone capacity, as the truck route time is 2 hours, which is about 35% less than that of TO.

(3) with large truck capacity for truck-drone delivery, $m_{td} = 300$, the optimal service combination has DO serve customers who are within 1.2 miles of the depot and TD serve the rest of the customers. Although the set and the utilization of services are almost identical to those in the base case ($m_{td} = 150$), the optimal delivery service combination for $m_{td} = 300$ provides a larger cost savings of about 21% (vs 14.4% in the base case) and emissions savings of 43% (vs ~31% in the base case) relative to truck-only. This is because the truck linehaul travel is greatly reduced due to a larger truck capacity. However, the route time is 5.3 hours, which is about a 68% increase compared with TO and a 88% increase compared with the optimal delivery service combination of the base case.

(4) in both the large truck capacity case ($m_{td} = 300$) and the base case ($m_{td} = 150$), TD performs very similarly to the optimal delivery service combination. This is because all these service combinations consist of a large proportion of TD (more than 98%). But even in the small truck capacity case ($m_{td} = 75$), TD does not perform too differently than the

optimal delivery service combination. This may indicate that TD is an important delivery service when the number of deliveries it makes is not too small.

(5) to assess how smaller number of deliveries that each truck-drone route can make affects the performance of TD, we select and evaluate two other smaller levels of m_{td} (not shown in Table 4.6): $m_{td} = 50$ and $m_{td} = 35$. When $m_{td} = 50$, the optimal delivery service combination has TD serve customers between 1.5-2.7 miles of the depot (about 5% of total customers). The cost and emissions savings relative to truck-only delivery is small (0.4% and 1.7%, respectively). For TD alone, the cost and emissions savings compared to truck-only delivery are 12% and 19% greater, respectively. However, the truck route time is only 1.2 hours (vs 3.8 hours for TO). When $m_{td} = 35$, the optimal delivery service combination does not include TD. For TD alone, the cost and emissions savings compared to truck-only delivery are 28.4% and 50% greater, respectively. However, the truck route time is less than one hour, which is a 71% reduction compared to TO.

4.6.4.2 Allocation of Select Performance Measures to Each Component

Figure 4.20 shows the cost per delivery of each delivery service combination for the three levels of m_{td}. Colors darker blue, blue, and lighter blue represent the large m_{td} case, the base case, and the small m_{td} case, respectively. The figure shows that TD is nearly as good as the optimal delivery service combination in terms of cost per delivery in all different truck size cases. The larger the m_{td}, the lower the cost per delivery for service combinations consisting of TD, but that impact is marginally diminishing as evidenced by the smaller difference between the blue and darker blue lines than the difference between the lighter blue and blue lines given the same scale of m_{td} change. In addition, m_{td} has no impact on other service combinations that do not include TD.

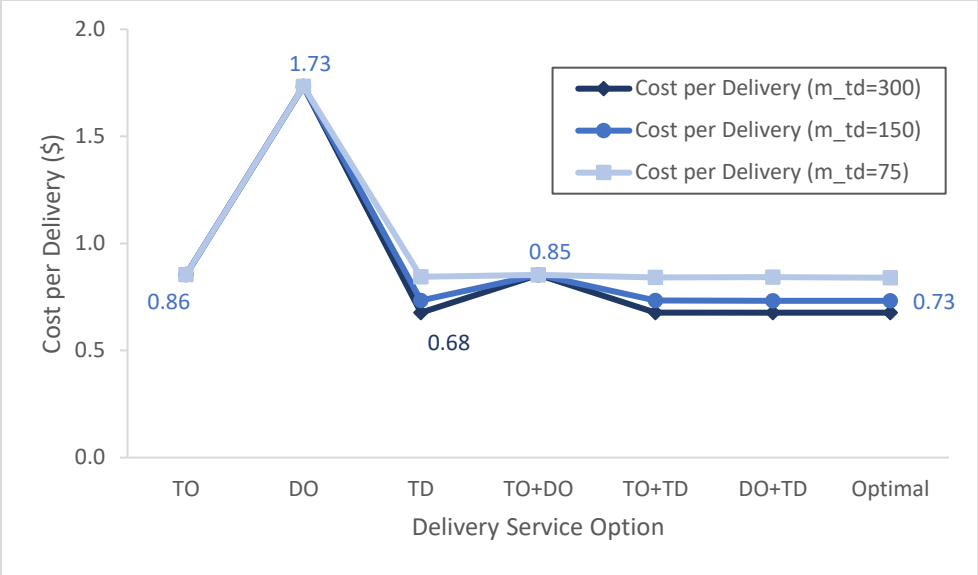

Figure 4.20. Cost per delivery of all delivery service combinations for three levels of m_{td}

Figure 4.21 shows the allocation of vehicle hours operated for TO, TD, and the optimal delivery service combination for the three levels of m_{td}. For the optimal delivery service combinations, the hours allocated on truck linehaul travel decrease noticeably as the truck capacity for truck-drone delivery (m_{td}) increases. Truck linehaul travel hours are reduced by 43% when m_{td} is doubled from 75 to 150, and are further reduced by 50% when m_{td} is doubled again from 150 to 300. However, compared to truck-only delivery (the blue bar), truck hours allocated on the linehaul travel increase (about 17%) for $m_{td} = 75$ (which is ¾ of the truck capacity for truck-only) and decrease for the other two cases. Compared to truck-only delivery, the hours spent on truck local travel and delivery stops decrease as m_{td} increases, with reductions (about 20% in truck local travel, and 33% in truck delivery stops) for the small m_{td} case being less than those for the other two cases which have very similar reductions (30% in truck local travel, and 51% in truck delivery stops) due to the similar utilization of DO and TD services. For TD under these three cases

(the last 3 bars in each set), the only change is in truck linehaul travel, which naturally decreases as m_{td} increases (due to the reduced truck routes).

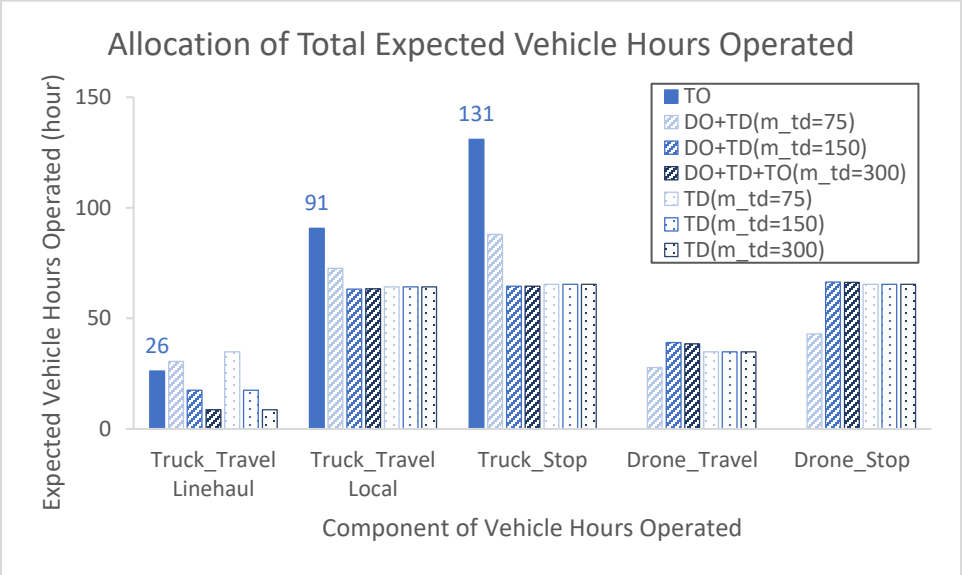

Figure 4.21. Allocation of vehicle hours operated in TO, TD, and the optimal delivery service combinations for three levels of m_{td}

The impact of m_{td} on each component of the vehicle miles traveled is very similar to that on vehicle hours operated, thus, we do not describe them further. In summary, the truck capacity for truck-drone delivery m_{td} has a large impact on reducing truck linehaul travel but increase the truck route time, and has a marginal impact on increasing the utilization of TD as m_{td} increases.

4.6.5. Low vs High Delivery Density (δ)

In this section, we explore the impact of delivery density on the performance measures of using drones. We consider two levels of delivery density in addition to the base case level with $\delta = 25$ deliveries per square mile: a low delivery density where $\delta = 1$ and a high delivery density where $\delta = 625$. According to one report by USPS, these

three delivery densities represent suburban areas that feature standalone houses with yards or porches that are convenient and efficient for a package to be dropped (USPS, 2020). Moreover, the majority of the US population (76%) lives in suburban areas. In addition to geographic areas, we note that the delivery density also varies by time of the day/week/season/year. Thus, our low delivery density may represent areas where houses are far apart from each other and/or deliveries for off-season periods. Our high delivery density may represent dense areas where houses are located very near to each other and/or peak delivery periods.

4.6.5.1 Performance Effects of Drone Delivery

Table 4.7 shows the performance measures of interest for TO, TD, and the optimal delivery service combination for three different levels of δ. Since the number of deliveries linearly increases as δ increases (e.g., the number of deliveries are 314, 7854, and 196,350 for $\delta = 1$, 25, and 625 in the circular region, respectively), we normalize some of the performance measures by the number of deliveries.

There are several interesting observations from Table 4.7:

(1) In all three density cases, DO+TD is the optimal service combination and DO serves customers who are close to the depot. However, the utilization of DO and TD differs in each case. The lower the delivery density, the larger the percentage of customers served by DO (36.7%, 1.5%, and 0.1% for $\delta = 1$, 25, and 625 deliveries per square mile, respectively). The higher the delivery density, the higher percentage of customers served by TD (63.3%, 98.5%, and 99.9% for $\delta = 1$, 25, and 625 deliveries per square mile, respectively).

Table 4.7. Performance for TO, TD, and the optimal service combination for three levels of δ

Performance Measure	**Low Density ($\delta = 1$)**			**Medium Density ($\delta = 25$)**			**High Density ($\delta = 625$)**		
Service option	TO	TD	DO+TD*	TO	TD	DO+TD*	TO	TD	DO+TD*
% Area (customers) Served by TO	100.0%	-	0.0%	100.0%	-	0.0%	100.0%	-	0.0%
% Area (customers) Served by DO	-	-	36.7%	-	-	1.5%	-	-	0.1%
% Area (customers) Served by TD	-	100.0%	63.3%	-	100.0%	98.5%	-	100.0%	99.9%
% Deliveries by Drone	0.0%	50.0%	68.3%	0.0%	50.0%	50.7%	0.0%	50.0%	50.0%
Cost per Delivery ($/delivery)	**2.01**	**1.62**	**1.49**	**0.86**	**0.73**	**0.73**	**0.62**	**0.56**	**0.56**
Total Delivery Cost ($)	**631.5**	**509.5**	**466.8**	**6717.8**	**5758.8**	**5750.3**	**122601.0**	**109079.3**	**109077.6**
Truck Portion	1.00	0.82	0.58	1.00	0.70	0.70	1.00	0.63	0.63
Drone Portion	-	0.18	0.42	-	0.30	0.30	-	0.37	0.37
Absolute Cost Change to TO ($)		-122.0	-164.7		-959.0	-967.5	-	-13521.7	-13523.4
% Cost Change to TO	-	-19.3%	-26.1%	-	-14.3%	-14.4%	-	-11.0%	-11.0%
Emissions per Delivery (kg CO2e/delivery)	**1.41**	**1.00**	**0.68**	**0.40**	**0.28**	**0.28**	**0.20**	**0.13**	**0.13**
Total Emissions (kg CO2e)	**443.0**	**315.0**	**214.8**	**3132.2**	**2186.4**	**2166.4**	**38590.4**	**26218.3**	**26214.3**
Truck Portion	1.00	0.99	0.94	1.00	0.99	0.99	1.00	1.00	1.00
Drone Portion	-	0.01	0.06	-	0.01	0.01	-	0.00	0.00
Absolute Emissions Change to TO (kg CO2e)		-128.0	-228.2	-	-945.8	-965.8	-	-12372.1	-12376.1
% Emissions Change to TO	-	-28.9%	-51.5%	-	-30.2%	-30.8%	-	-32.1%	-32.1%
#Truck Deliveries/Truck Mile	0.78	0.55	0.54	2.75	1.98	1.97	5.57	4.11	4.11
#Truck Deliveries/Driver Hour	12.86	9.72	9.63	31.70	26.70	26.65	44.82	41.02	41.01
#Trucks Required (SL = 8 hrs)	3.1	2.0	1.3	31.0	18.4	18.1	547.6	299.2	299.1
#Drones Required (SL = 8 hrs)	-	2.0	4.4	-	18.4	19.0	-	299.2	299.4
Number of Truck Routes	**3.1**	**2.1**	**1.3**	**78.5**	**52.4**	**51.6**	**1963.5**	**1309.0**	**1308.2**
Truck Route Length (mile)	128.8	135.9	139.0	36.4	37.9	38.0	18.0	18.2	18.2
Truck Route Time (hour)	7.8	7.7	7.8	3.2	2.8	2.8	2.2	1.8	1.8

*The optimal delivery service combination that minimizes total delivery cost.

(2) The cost per delivery for TO decreases as the delivery density increases (in row 7). This is because the denser the deliveries, the shorter the distance per delivery. In other words, the denser the deliveries, the higher the number of deliveries being made per mile. The costs per delivery are \$2.01, \$0.86, and \$0.62 for $\delta = 1$, 25, and 625, respectively. The costs increase by 135% for low density ($\delta = 1$) and decrease by 35% for high density ($\delta = 625$) compared with the base density ($\delta = 25$). The number of deliveries per mile are 0.78, 2.75, and 5.57 for $\delta = 1$, 25, and 625, respectively. The deliveries per mile decrease by 72% for low density ($\delta = 1$) and increase by 103% for high density ($\delta = 625$) compared with the base density ($\delta = 25$).

It costs less per delivery for the optimal delivery service combination than for TO for all three density levels, and the absolute per delivery cost differences (between the optimal delivery service combination and TO) become smaller as the delivery density increases. For example, it costs \$0.52, \$0.12, and \$0.07 less per delivery with the optimal service combination than for TO for $\delta = 1$, 25, and 625, respectively. In row 12, the percentage cost savings of the optimal service combination relative to TO also decreases as delivery density increases, 26.1%, 14.4%, 11.0% for $\delta = 1$, 25, and 625, respectively. However, row 11 shows that the absolute total cost differences (between the optimal delivery service combination and TO) become larger as the delivery density increases, which is due to the increased number of deliveries. For example, although the optimal service combination saves only \$0.07 per delivery for $\delta = 625$, which is about 44% less than that for the base density $\delta = 25$, the total cost savings is \$13,526, which is about 14 times greater than that for the base density $\delta = 25$.

(3) We observe similar patterns for emissions performance as for delivery costs. Emissions per delivery decrease as delivery density increases for all service combinations. Like the pattern observed for costs, the absolute total emissions savings of optimal service combination relative to TO increase as delivery density increases, 228, 966, and 12,376 kg CO2e for $\delta = 1$, 25, and 625, respectively. But we no longer observe a decreasing trend for percentage emissions savings relative to TO as delivery density increases, 51.5%, 30.8%, and 32.1% for $\delta = 1$, 25, and 625, respectively. We also observe that drone operations constitute a much larger portion of delivery costs than their contributions to emissions for all three density cases. For example, drone operations constitute 42% (about \$0.63) of the \$1.49 per delivery cost, whereas they constitute only 6% (about 0.04 kg CO2e) of the 0.68 kg CO2e emissions per delivery for the low density case ($\delta = 1$). We observe the drone portion of emissions decreases as density increases, but we do not observe such a trend for that of cost.

(4) Rows 7 and 6 show the number of truck deliveries per truck mile and per driver hour for TO increase as delivery density increases, which again shows that the higher the delivery density, the more mileage and time efficient TO is. Compared with TO, the number of truck deliveries per truck mile for the optimal service combination decreases for all three density cases (0.54 vs 0.78, 1.97 vs 2.75, 4.11 vs 5.57 for $\delta = 1$, 25, and 625, respectively). The largest percentage decrease is 30.5% for low density $\delta = 1$. The same patterns are observed for the number of truck deliveries per truck mile for the optimal service combination compared with TO. The reason why these two measures decrease for the optimal service combination is that although some of the truck deliveries are replaced

by drone deliveries, some of these drones are launched by the truck, thus it still requires the driver to drive the truck.

(5) The final two rows show the truck route length and truck route time for TO decreases as the delivery density increases. Note that the number of deliveries for truck-only routes is fixed at 100 deliveries. Again, these two measures show that the denser the deliveries, the shorter and faster the truck route. Compared with TO, the truck route is slightly longer but quite a bit faster for the optimal service combination for the medium and high-density cases. Not shown in Table 4.7 but evident in the data, the percentage truck route length increase relative to TO are 7.9%, 4.4%, and 1.6%, and the percentage truck route time reduction relative to TO are -0.2%, 10.8%, and 18% for $\delta = 1$, 25, and 625, respectively.

(6) For the optimal delivery service combination for the three levels of delivery density, the lower the delivery density, the higher the percentage of deliveries made by drone (in row 6). For example, for $\delta = 1$, 25, and 625 deliveries per square mile, the percentages of deliveries made by drone are 63.3%, 50.7%, and 50.0%, respectively.

4.6.5.2 Allocation of Selected Performance Measures to Each Component

To understand the impact of delivery density on the performance of drone delivery, we show how the vehicle miles (Figure 4.22) and vehicle time (Figure 4.23) are allocated for three different levels of δ. Please note all those measures are converted to per delivery. In all the figures, lighter blue, blue and darker blue colors represent the base case ($\delta = 25$), the low density case ($\delta = 1$), and the high density case ($\delta = 625$), respectively. TO is represented by solid bars, TD by dotted bars, and the optimal service option by hatched bars. We include TD to demonstrate that this single delivery service is near-optimal for some density levels.

Figure 4.22 shows the allocation of the expected vehicle miles per delivery to truck linehaul travel, truck local travel and drone travel for the three density levels. The patterns are very noticeable. As density increases, truck local travel and drone travel miles per delivery are greatly reduced whereas truck linehaul travel miles (though a little difficult to see) remain roughly the same for all corresponding service combinations. For example, compared with TO of the base case ($\delta = 25$), truck local travel miles are 5 times greater for TO of the low density case ($\delta = 1$) and is 1/5 times less for TO of the high density case ($\delta = 625$). The same trend is observed for the optimal service combination (and TD only) for the three density levels. Truck local travel is more than 3 times greater for DO+TD of the low-density case ($\delta = 1$) and is over 1/5 for DO+TD of the high-density case ($\delta = 625$) than for the base case. Compared with TO, the optimal service combination reduces both truck linehaul and local travel miles and increases drone travel miles for all three delivery density levels. By replacing truck deliveries with drone deliveries, the truck linehaul travel miles are reduced by 48%, 33%, and 33% for $\delta = 1$, 25, and 625, respectively; and the truck local travel miles are reduced by 55%, 30%, and 29% for $\delta = 1$, 25, and 625, respectively. One truck mile is replaced by 5, 1.7, and 0.6 drone miles for $\delta = 1, 25, \text{and } 625, \text{respectively}$. TD only performs very similarly to the optimal service combination when density is not very low.

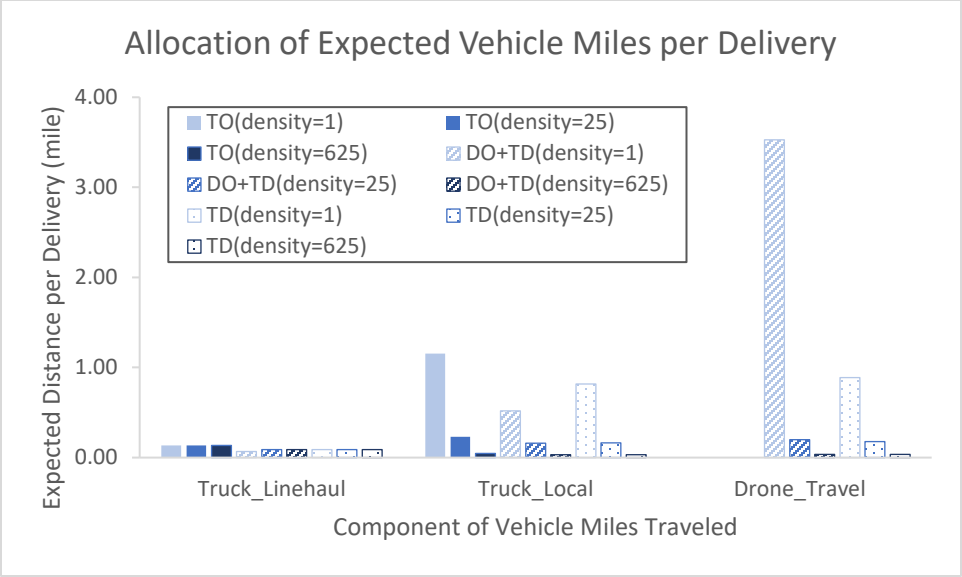

Figure 4.22. Allocation of vehicle miles traveled per delivery in the optimal service combinations for three levels of delivery density δ

Figure 4.23 shows the allocation of the expected vehicle time spent per delivery in truck linehaul travel, truck local travel, truck delivery stops, drone travel, and drone delivery stops for the three levels of δ. Like vehicle travel miles, noticeable changes occur in truck local travel and drone travel time. As density increases, the time spent on truck local travel and drone travel per delivery are greatly reduced whereas the time spent on truck linehaul travel does not change much for all corresponding service combinations. For example, compared with TO of the base case ($\delta = 25$), truck local travel time is 5 times greater for TO of the low density case ($\delta = 1$) and is 1/5 times less for TO of the high density case ($\delta = 625$). The same trend is observed for the optimal service combination and TD only for the three density levels. Compared with TO, the optimal service combination reduces both truck linehaul and local travel time and increases drone travel time for all three delivery density levels. TD only performs very similarly to the optimal service combination when density is not very low.

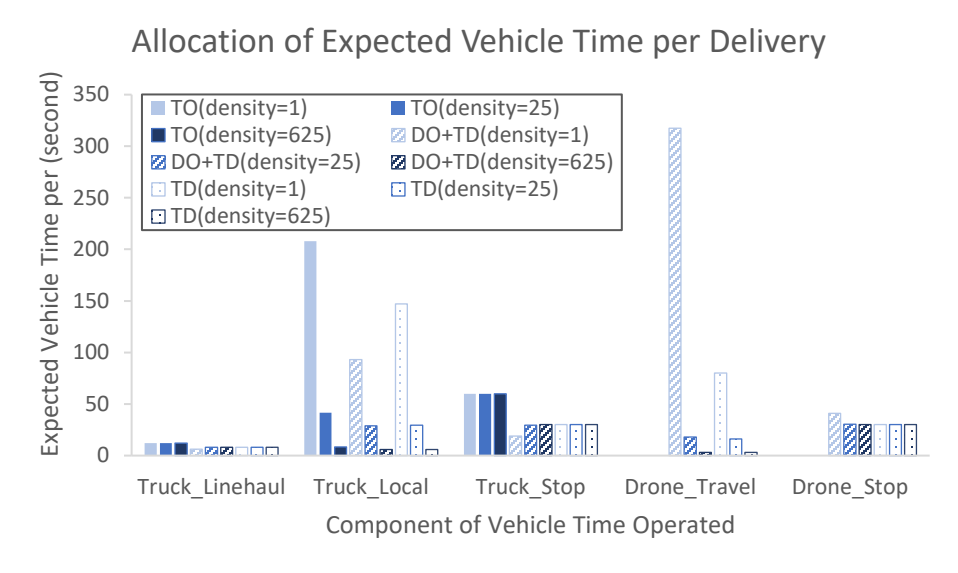

Figure 4.23. Allocation of vehicle time per delivery in the optimal service combinations for three levels of delivery density δ

Figure 4.24(a) shows that the delivery density δ has an impact on the "cost per delivery" measure for service combinations that include truck deliveries, i.e., the higher the delivery density, the lower the cost per delivery for service combinations that include truck deliveries. Comparing the same service combinations for each density level, we observe that the difference between the lighter blue line (i.e., $\delta = 1$) and the base blue line (i.e., $\delta = 25$) is much (more than 3 times) greater than the difference between the base blue line (i.e., $\delta = 25$) and the darker blue line (i.e., $\delta = 625$). This shows that delivery density δ has a marginally diminishing effect on reducing cost per delivery as δ increases. Interestingly, the cost per delivery for DO remain the same ($1.73 per delivery) for all three cases, which might indicate that delivery method DO does not have economies of scale as delivery volumes increase. When delivery density becomes high, using DO alone becomes much more expensive than just using TO.

Figures 4.24(a) and 4.24(b) indicate that cost per delivery in the low-density case is high, although the percentage cost savings to truck-only delivery is also high. Positive percentage cost savings indicate that the delivery cost of the other service combinations is lower than that of TO and vice versa. We note that some service combinations provide the same cost per delivery or percentage cost savings, for example, TD and TO+TD in all three cases, which is because TO is not used. We also observe that using TD is almost as good as the optimal service combination for the medium and high delivery density cases (i.e., δ =25 and 625) in terms of cost per delivery and percentage cost savings relative to TO.

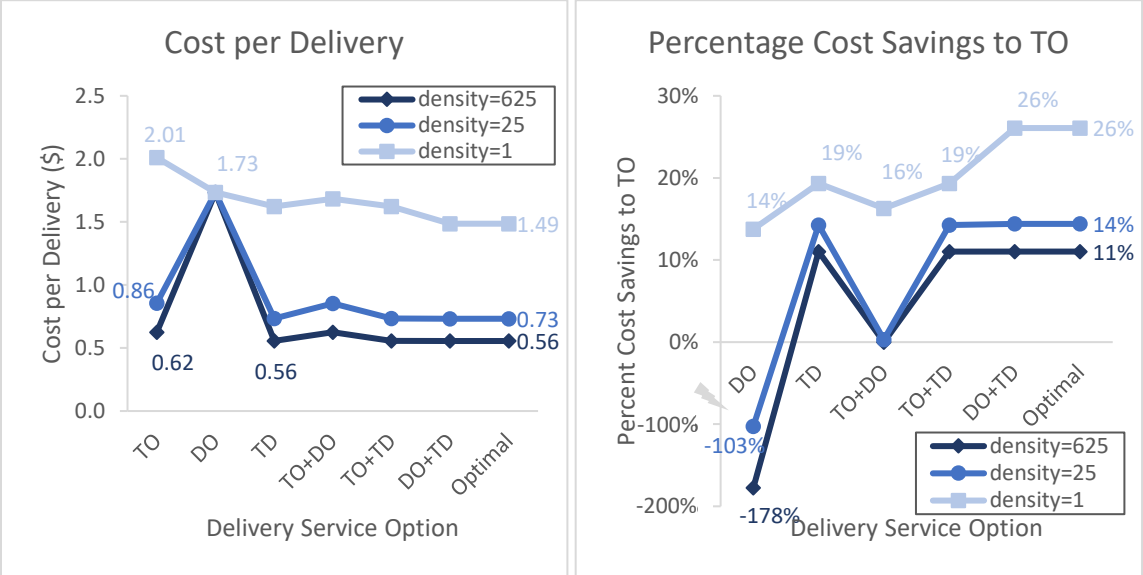

Figure 4.24: (a) Cost per delivery of each service combination (left); (b) Percentage cost savings of each service combination relative to TO for three levels of delivery density δ

4.6.6. Large vs Medium Delivery Region Size (R)

To assess the performance impacts of the size of the delivery region, we consider two other delivery region sizes in addition to the base case size where $R = 10$ miles: a medium delivery region size with $R = 20$ miles and a large delivery region size with $R =$

30 miles. The base level $R = 10$ miles was chosen based on the common assumption in the literature that delivery drones have a limited flight range of 10-15 miles and are at first envisioned for the point-to-point delivery of small packages from a fixed depot to customer homes (e.g., Amazon). Xu (2017) indicates that the radii of the vast majority of U.S. cities (i.e., all cities with more than 100,000 people) is in a 2 to 6 mile range (by assuming the areas of these cities are circles), thus, a central depot of 10-mile radius is often sufficient to cover a city and suburbs. Having a small depot in each city is ideal but depots are not constructed and operated without cost. This is the reality of many logistics and e-commerce firms who usually operate larger depots (to achieve economies of scale in inventory, space, and maintenance) that can cover larger areas than that a 10-mile radius. For example, UPS has about 1,000 package operating centers for the pick-up and delivery of packages in the U.S. (UPS, 2020). To cover the entire US land area (3.797 million square mile), the average radii of the package operating centers is about 35 miles. However, we understand that those centers are usually not evenly spatially distributed. Many small depots may be positioned in urban areas while a few large depots may be positioned in rural areas. So, we choose $R = 20$ miles and $R = 30$ miles to represent different types of depots. We also test $R = 5$ miles as Lyon-Hill et al. (2020) assume that drones have a flight range of up to 5 miles and a 5-mile radius might meet also customer's demand for faster delivery.

4.6.6.1 Performance Effects of Drone Delivery

Since the number of deliveries quadratically increases as the delivery region size increases, we normalize the performance measures by the base region size. For example, the region of $R = 30$ miles is equivalent in area to having 9 regions of $R = 10$ miles, so we divide the total costs (and other performance measures) by 9 to obtain a common

measure that is comparable to the base case. Table 4.8 shows the normalized performance measures of interest for TO, TD, and the optimal delivery service combination for three different levels of R.

There are several interesting observations based on Table 4.8:

(1) For all three deliver region size cases, DO+TD is the optimal combination of delivery services and DO serves the same number of customers up to 1.2 miles from the depot with TD serving the rest of the delivery region (rows 3-5). Because the number of deliveries (or customers) increases as the delivery region size increases, the utilization of DO decreases from 1.5% to 0.4% to 0.2% for $R = 10$, 20, and 30 miles, respectively.

(2) In row 6 as the delivery region size R increases, the total delivery cost (of the base region size) for TO increases. This is because the truck has to travel longer distances to get to more remote areas (e.g., for $R = 30$ compared to $R = 10$, i.e., the average linehaul distance is longer for $R = 30$ than $R = 10$). The delivery costs are increased by 19% and 39% for the medium ($R = 20$) and large ($R = 30$) region size, respectively, compared with the base region size ($R = 10$). In addition, the truck route length (last row 3) and the truck route time (last row 2) are 73% and 19% longer, respectively, for $R = 30$ than for $R = 10$, and are 37% and 9% longer for $R = 20$ than for $R = 10$, respectively. Considering only delivery cost, there is clearly evident an incentive to have many small depots rather than a few large ones as the former can reduce both delivery time and delivery cost.

Table 4.8. Normalized performance (by base region size) for TO, TD, and the optimal delivery service combination for three levels of *R*

Performance Measure	**Small Region (R= 10)**			**Medium Region (R= 20)**			**Large Region (R= 30)**		
Service option	TO	TD	DO+TD*	TO	TD	DO+TD*	TO	TD	DO+TD*
% Area (customers) Served by TO	100.0%	-	0.0%	100.0%	-	0.0%	100.0%	-	0.0%
% Area (customers) Served by DO	-	-	1.5%	-	-	0.4%	-	-	0.2%
% Area (customers) Served by TD	-	100.0%	98.5%	-	100.0%	99.6%	-	100.0%	99.8%
Total Delivery Cost ($)	**6717.8**	**5758.8**	**5750.3**	**8026.8**	**6631.5**	**6629.4**	**9335.8**	**7504.2**	**7503.2**
Truck Portion	1.00	0.70	0.70	1.00	0.74	0.74	1.00	0.77	0.77
Drone Portion	-	0.30	0.30	-	0.26	0.26	-	0.23	0.23
TDC Change to TO	-	-959.0	-967.5	-	-1395.3	-1397.5	-	-1831.7	-1832.6
% TDC Change to TO	-	-14.3%	-14.4%	-	-17.4%	-17.4%	-	-19.6%	-19.6%
Total GHG Emissions (kg CO2e)	**3132.2**	**2186.4**	**2166.4**	**4278.7**	**2950.7**	**2945.7**	**5425.1**	**3715.0**	**3712.8**
Truck Portion	1.00	0.99	0.99	1.00	0.99	0.99	1.00	1.00	1.00
Drone Portion	-	0.01	0.01	-	0.01	0.01	-	0.00	0.00
% Emissions Change to TO	-	-30.2%	-30.8%		-31.0%	-31.2%	-	-31.5%	-31.6%
Truck Miles Traveled (mile)	**2861.0**	**1982.1**	**1962.0**	**3908.2**	**2680.2**	**2675.2**	**4955.4**	**3378.3**	**3376.1**
Drone Miles Traveled (mile)	-	1396.3	1562.1	-	1396.3	1437.7	-	1396.3	1414.7
Driver Hours Worked (hour)	**247.8**	**147.1**	**145.2**	**273.9**	**164.6**	**164.1**	**300.1**	**182.0**	**181.8**
Drone Hours Operated (hour)	-	100.4	105.5	-	100.4	101.6	-	100.4	100.9
#Trucks Required (SL = 8 hrs)	31.0	18.4	18.1	34.2	20.6	20.5	37.5	22.8	22.7
#Drones Required (SL = 8 hrs)	-	18.4	19.0	-	20.6	20.7	-	22.8	22.8
Number of Truck Routes (NTR)	**78.5**	**52.4**	**51.6**	**78.5**	**52.4**	**52.2**	**78.5**	**52.4**	**52.3**
%NTR to TO	-	-33%	-34%	-	-33%	-34%	-	-33%	-33%
Truck Route Length (mile)	36.4	37.9	38.0	49.8	51.2	51.3	63.1	64.5	64.6
Truck Route Time (hour)	3.2	2.8	2.8	3.5	3.1	3.1	3.8	3.5	3.5
Drone Stops	-	3927.0	3984.6	-	3927.0	3941.4	-	3927.0	3933.4

*The optimal delivery service combination that minimizes total delivery cost.

(3) Compared with TO, the optimal service combination provides lower delivery costs for all three region sizes. Unlike the impact of density, both the absolute and the percentage cost savings relative to TO increase as the delivery region size increases. For example, the absolute cost savings relative to TO are \$968, \$1,398, and \$1,833, and the percentage cost savings relative to TO are 14.4%, 17.4%, and 19.6% for $R = 10$, 20, and 30 miles, respectively. As the delivery region size increases, we observe that the contribution of the drone to the total delivery cost decreases in the optimal service combination. For example, the cost contributions of the drone (row 8) are 30%, 26%, and 23% for $R = 10$, 20, and 30 miles, respectively. Although the optimal service combination slightly increases truck route length, it reduces the truck time by about 8%-12%.

(4) We observe exactly the same patterns for emissions as for delivery cost. Emissions increase as the delivery region size increases for all service combinations. For the optimal service combination, the absolute and the percentage emissions savings relative to TO increase and the emissions reduction contributions of the drone decrease as the delivery region size increases.

(5) In all cases, TD performs very similarly to the optimal service combination. This is because all these service options consist of a large proportion of TD use (more than 98%), which may indicate that TD is an important type of service when the delivery region size is not extremely small (e.g., 1.2 miles where DO is preferred everywhere).

(6) Not shown in Table 4.8, we also examined a case with $R = 5$ miles, and we observed consistent behaviors compared with the base case: DO+TO is the optimal service combination and DO serves the same number of customers but its relative utilization

increases as the total number of customers decreases; the total delivery costs, emissions, and truck route time and length all decrease as well.

4.6.6.2 Allocation of Selected Performance Measures to Each Component

To understand the impact of delivery region size on the performance of drone delivery, we show how the vehicle miles (Figure 4.25) and vehicle time (Figure 4.26) are allocated for the three different levels of R. Please note all those measures are converted to a region size of the base case $R = 10$. In all figures, colors blue, darker and darkest blue represent the base case ($R = 10$), the medium region size ($R = 20$), and the large region size ($R = 30$). TO is represented by solid bars, TD by dotted bars, and the optimal service option by hatched bars. We include TD to demonstrate that this single service is near-optimal for most delivery region sizes.

Figure 4.25 shows the allocation of the expected vehicle miles (per base region size) in truck linehaul travel, truck local travel and drone travel for the three levels of R. The patterns are very noticeable. As delivery region size increases, truck linehaul miles increase significantly whereas truck local and drone travel miles remain roughly the same for all corresponding delivery service combinations. For example, compared with the base case ($R = 10$) TO, the linehaul travel miles are doubled and tripled for the medium region case ($R = 20$) TO and the large region case ($R = 30$) TO, respectively. A similar relationship applies to the optimal service combination and TD service. Compared with TO, the optimal service combination reduces both truck linehaul and local travel miles and increases drone travel miles for all three delivery region sizes. The truck linehaul and local travel miles are reduced by 33% and 30%, respectively, through replacing TO with the optimal service combination (i.e., DO+TD) for all three delivery region sizes; and one truck mile is

replaced by 1.7, 1.2, and 0.9 drone miles for $R = 10$, 20, and 30 miles, respectively. In all cases, TD performs very similarly to the optimal service combination.

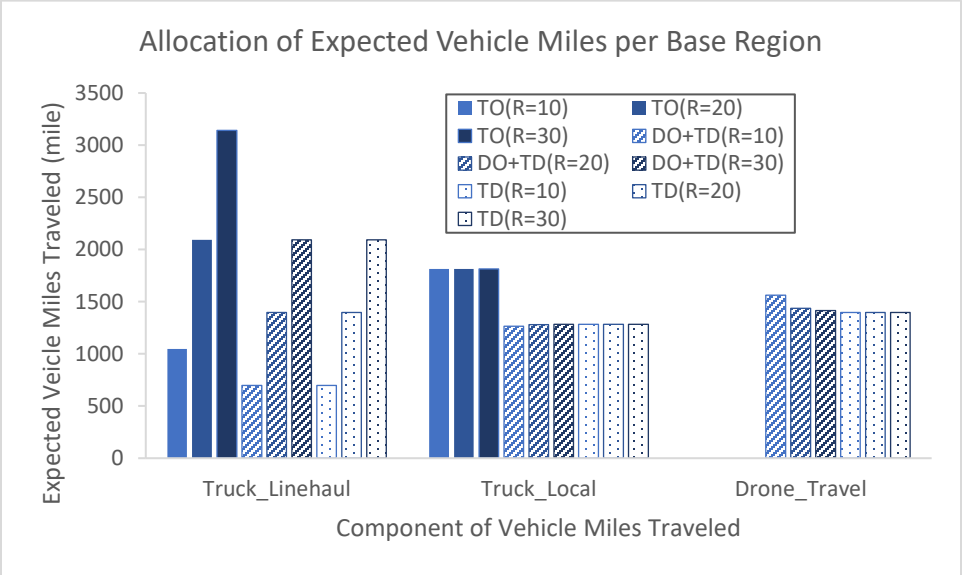

Figure 4.25. Allocation of vehicle miles traveled (per base region size) for TO, TD and the optimal service combination for three levels of delivery region R

Figure 4.26 shows the allocation of the expected vehicle time spent (per base region size) in truck linehaul travel, truck local travel, truck delivery stops, drone travel, and drone delivery stops for the three different radii of R. Like vehicle miles, truck time spent on linehaul is doubled (and tripled) when the delivery region size is doubled (and tripled) for all corresponding service combinations. However, delivery region size has little to no impact on the time spent on other components when comparing the same service combination. Compared with TO, DO+TD significantly reduces the truck delivery stop time by about 51%, truck linehaul travel time by about 33%, and truck local travel time by about 30% for all three delivery region sizes. Unlike vehicle miles, the increased drone

travel and drone delivery stop time often does not increase the total system time due to the parallel operation of truck and drone deliveries in TD service.

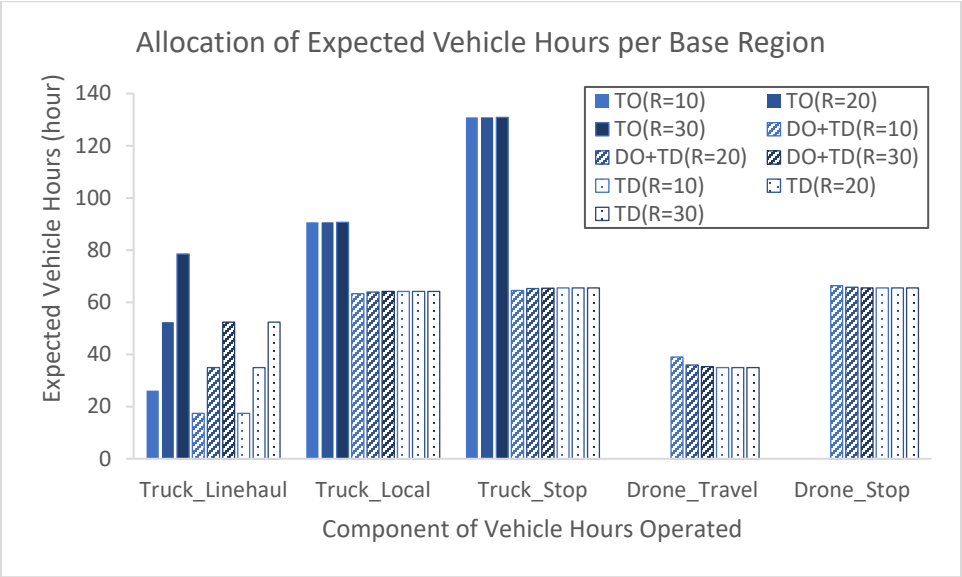

Figure 4.26. Allocation of vehicle operating hours (per base region size) for TO, TD and the optimal service combination for three levels of delivery region R

Figures 4.27(a) and 4.27(b) show the larger the delivery region size, the higher the cost per delivery for each service combination and the higher the percentage cost savings of other service combinations relative to TO. We do not include DO in the figures because when $R > 10$, it is beyond the flight range of drones, thus, DO is not used in the $R = 20$ and $R = 30$ cases. We observe a linear relationship between cost per delivery and the delivery region size and between percentage cost savings relative to TO and the delivery region size.

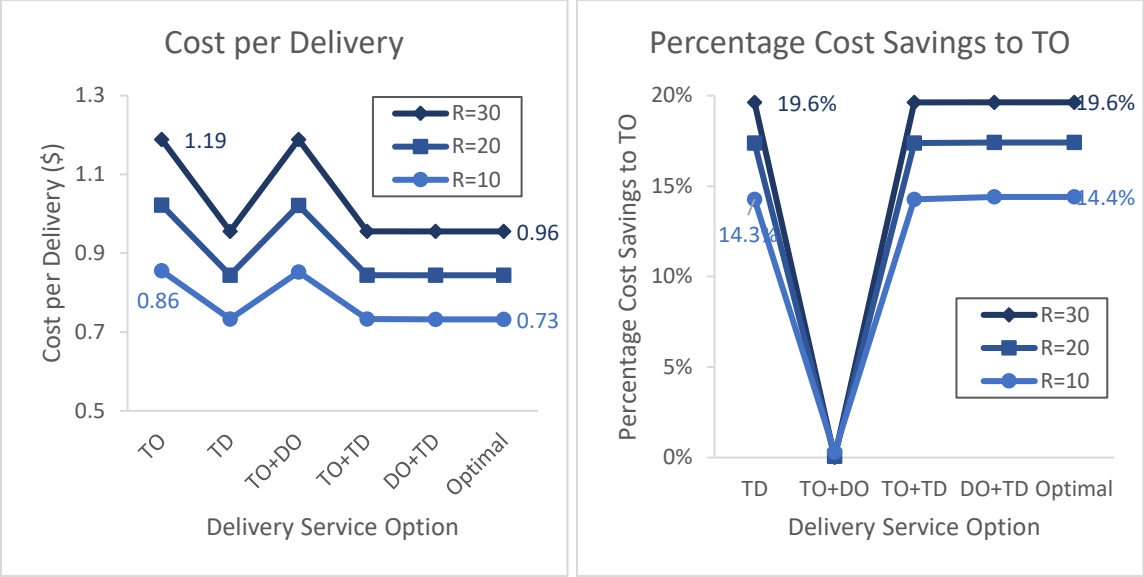

Figure 4.27: (a) Cost per delivery of each service combination (left); (b) Percentage cost savings of each service combination relative to TO for three levels of delivery region radius R

4.6.7 Summary of Impacts of Key Parameters on Selected Performance Measures

We explored the impacts of unit drone operating cost (c_d), marginal drone stop cost (s_d), truck capacity for truck-drone delivery (m_{td}), delivery density (δ), and the size (radius) of the delivery region (R) on a number of performance measures (e.g., utilization of delivery service, delivery costs, delivery emissions, vehicle miles traveled, vehicle hours operated, number of vehicles required). The key findings are summarized in Table 4.9. Column 1 indicates the cases. Column 2-3 show the utilization of DO and TD, respectively. Columns 4-5, 6-7, 8-9, 10-11, and 12-11 show the absolute and percentage reductions (relative to truck-only) in delivery costs, GHG emissions, truck travel distances, driver work hours, and the number of trucks required, respectively. Columns 13-14 show the absolute increase in drone travel distances and the number of drones required, respectively.

Table 4.9. Summary of the performance of the optimal service combination relative to truck-only delivery for different parameter values

Case	DO Use	TD Use	Cost Savings		Emissions Savings		Truck Miles Reduced		Driver Hours Reduced		#Truck Reduced	Drone Miles Increased	#Drones Increased
	(%)	(%)	($)	(%)	(kg CO2e)	(%)	(mile)	(%)	(hour)	(%)	-	(mile)	-
Base case	1.5	98.5	968	14.4	967	30.8	899	31	103	41	12.8	1,562	19.0
$6.25c_d$	0.1	92.0	256	3.8	876	28.0	813	28	91	37	11.5	1,217	19.4
$0.1c_d$	100.0	0.0	2,529	37.6	1,899	60.6	2,861	100	248	100	31.0	104,720	343.6
$s_d + 0.2$	0.3	83.9	188	2.8	835	26.7	776	27	86	35	10.7	1,185	20.3
$s_d - 0.2$	3.1	96.9	1,770	26.4	987	31.5	922	32	105	42	13.1	1,921	19.9
$2m_{td}$	1.3	98.7	1,403	20.9	1,346	43.0	1,246	44	111	45	13.9	1,541	17.8
$m_{td}/2$	1.8	62.0	121	1.8	191	6.1	186	7	57	23	7.1	1,114	25
25δ	0.1	99.9	13,523	11.0	12,376	32.1	11,380	32	1,988	45	248.5	7,015	299.4
$\delta/25$	36.7	63.3	165	26.1	228	51.5	220	56	24	58	1.8	1,108	4.4
$2R$	0.4	99.6	5,590	17.4	5,332	31.2	4,932	32	407	40	54.9	5,751	82.9
$3R$	0.2	99.8	16,494	19.6	15,411	31.6	14,214	32	1,065	39	133.1	12,733	205.3
$R/2$	5.9	94.1	194	12.8	209	32.6	196	34	30	44	3.3	515	4.9

In most cases, truck-drone delivery (TD) is the dominant delivery service which serves at least 62% of the deliveries in the entire delivery region, whereas drone-only delivery (DO) serves very small percentages of customers (0.1-6%) who are located close to the depot. Only when drone travel cost is very inexpensive and/or the delivery density is very low is DO used extensively. Only when drone operating cost per mile is very high, drone stop cost is high, and/or truck-drone capacity is low is truck-only delivery (TO) used to some extent.

The percentage cost savings in Table 4.9 range from about 2% (or $0.02/delivery) to 38% (or $0.32/delivery), and the percentage associated emissions savings range from about 6% (or 0.02 kg CO2e) to 61% (or 0.24 kg CO2e), with both of the lowest savings results for the low truck-drone capacity case (50% of the base case), and both of the highest savings results for the very inexpensive drone case (10% of the base case). The potential savings are huge even for the worst case we considered, which would represent for UPS about $96 million and 96,000 metric tonnes CO2e savings per year in the U.S. (assuming the daily package volume of 16 million (Holland et al., 2017) and 300 days in a year). Using the same assumption for the best case, the savings would increase to $1.5 billion and 1.2 million metric tonnes CO2e per year for UPS in the U.S.

The drone operating cost per mile, marginal drone stop cost, and truck-drone capacity seem to have much greater impact on the percentage cost and emissions savings than do delivery density and delivery region size. For example, the cost savings decrease from 14% to only 2% when the truck capacity decreases to 50% of the base case, whereas it decreases from 14% to about 13% when the radius of delivery region decreases to 50% of the base case. However, both absolute savings are less than $200 because a smaller

region size covers a much smaller number of deliveries although the savings per delivery is high. So, it is important to have both percentage and absolute performance measures.

Even in circumstances when drone delivery does not provide substantial cost savings but is use extensively, it can considerably reduce GHG emissions, truck miles traveled, driver work hours, and the number of trucks required. In all cases with the exception of the small truck-drone capacity case, the percentage emissions savings can be at least 26%, the percentage reduction in truck miles traveled can be at least 27%, and percentage reduction in driver hours worked as well as the number of trucks required can be at least 35%. This re-emphasizes the importance and large potential benefits from drone delivery in addition to cost savings.

4.7 Conclusions

In this chapter, we developed rigorous strategic delivery models to analyze the cost and other performance of truck-drone delivery (TD), along with truck-only delivery (TO) and drone-only delivery (DO). We partitioned the delivery region based on the best use of different delivery services (i.e., DO, TD, and TO) that minimize delivery costs. We provided both theoretical analyses and numerical scenarios to illustrate the circumstances in which drone delivery (i.e., DO and TD) provides large and small cost savings relative to truck-only delivery and quantified the scale of the savings. The potential cost savings from DO and TD can be huge, but depend strongly on the drone operating parameters (i.e., drone operating cost per mile, marginal drone stop cost, and truck drone capacity) and the operating environment (i.e., the delivery region size and the delivery density). Under most circumstances, TD is a very important delivery method.

Chapter 5: Emissions-Minimizing Drone Delivery Systems

In this chapter, we explore the impacts of the parameters of interest on greenhouse gas (GHG) emissions by integrating drones into the delivery system. In section 5.1, we introduce the importance of minimizing GHG emissions. In section 5.2, we develop emissions-optimizing models for truck-only, drone-only, and truck-drone delivery. Section 5.3 presents the illustrations of delivery system emissions and modeling results for different operating settings. Conclusions are presented in section 5.4.

5.1 Introduction

In Chapter 4, we have explored the optimal delivery system designs that minimize merely the delivery costs, which roughly represents the status quo in the transportation industry. However, we see strong trends toward green transportation that focuses on minimizing GHG emissions (or carbon footprint) and other pollutants to the environment. Cachon (2014) argues that failing to account for GHG emissions may lead to a poor delivery system design as it affects the climate and poses a serious challenge to the environment and ultimately the global economy. In their annual sustainability report, UPS state that their "main economic risk currently related to climate change is a regulatory risk – the possibility that countries or regions of the world will increase regulation of GHG emissions to include significant new taxes, fees, or other costs for transportation and logistics companies" (UPS, 2019).

The policy pressure is increasing. Countries and regions of the world are not only imposing new carbon taxes or fees but also announcing plans to phase out internal combustion vehicles (Bloomberg, 2020). For example, California announced that gas-

powered vehicles would be banned after 2035 to drastically reduce demand for fossil fuel in California's fight to slow climate change as more than 50% of GHG emissions are generated by transportation in California (Office of Governor, 2020). The key for the transportation industry to reduce GHG emission is to shift from petroleum to cleaner alternative fuels with advanced vehicle technology that makes economic sense. Findings in Chapter 3 (on energy consumption models for delivery drones) reveal that the energy consumption rates used in research studies for drone operations vary widely by a factor of 20 or more. Thus, it is important to design a drone delivery system with GHG emissions in mind.

5.2 Modeling Expected GHG Emissions

Like the cost expressions formulated in Chapter 4, we classify the lifecycle greenhouse gas (GHG) emissions into two categories: (1) GHG emissions attributable to each incremental vehicle mile, which may include the emissions that occur when transporting items from the origin to the destination and the ultimate return of the vehicle back to the origin; and (2) GHG emissions attributable to each delivery stop of the vehicle, which may include the emissions for stopping, idling, and restarting the vehicle. We use e_t and e_d to denote the traveling GHG emissions per unit distance (kg CO2e/mile) for the truck and the drone, respectively; ξ_t to denote the stop emissions per delivery (kg CO2e/stop) for the truck, and ξ_d to denote the marginal drone stop emissions per delivery (kg CO2e/stop) relative to a truck stop.

Since battery powered drones have no tailpipe emissions but instead shift those emissions to the upstream power plant where the electricity is generated, we consider the lifecycle GHG emissions for both generating electricity (used by drones) and burning

diesel fuel (used by trucks). This helps provide a more complete picture of the environmental impacts and avoids shifting impacts from one phase of the life cycle to another, or from one region or one environmental problem to another. We use CI_e and CI_f to denote the lifecycle carbon intensity, i.e., the GHG emissions per unit energy (kg CO2e/ kWh), of electricity and diesel fuel, respectively. We use Epm_t and Epm_d to denote the energy consumption per unit distance (kWh/mile) for the truck and the drone, respectively. Thus, the truck operating emissions per mile $e_t = CI_f \times Epm_t$, and the drone operating emissions per mile $e_d = CI_e \times Epm_d$. Thus the emissions rates incorporate both the carbon intensity of the vehicle fuel/electricity and the energy efficiency of the vehicles.

5.2.1 Drone-only Delivery Emissions

Based on the expected distance equation (4.1), the expected GHG emissions of serving a customer at distance d for drone-only delivery is

$$E_{do} = 2e_d d + \xi_d + \xi_t. \tag{5.1}$$

5.2.2 Truck-only Delivery Emissions

Based on the expected distance equation (4.5), the expected GHG emissions of serving a customer at distance d for truck-only delivery is

$$E_{to} = e_t \left(\frac{2d}{m_{to}} + \frac{w}{3} + \frac{1}{\delta w}\right) + \xi_t. \tag{5.2}$$

The expected emissions when the swath width is optimal (using the optimal swath width of equation (4.3)) is

$$E_{to}^* = \frac{2e_t}{m_{to}} d + \frac{2e_t}{\sqrt{3\delta}} + \xi_t. \tag{5.3}$$

5.2.3 Truck-drone Delivery Emissions

Based on the expected distance equation (4.11), the expected GHG emissions of serving a customer at distance d for truck-drone delivery is

$$E_{td} = e_t\left(\frac{2d}{m_{td}} + \frac{w}{6} + \frac{1}{\delta w}\right) + e_d\sqrt{\left(\frac{w}{3}\right)^2 + \left(\frac{1}{\delta w}\right)^2} + \frac{\xi_d}{2} + \xi_t. \tag{5.4}$$

Like the delivery cost C_{td}, expression, E_{td} is also a convex function of the swath width w, and we let the optimal swath width of the truck-drone route $w_{td}^* = \kappa\sqrt{\frac{3}{\delta}}$, where κ is a factor determined by the ratio of $\frac{e_d}{e_t}$ and $1 < \kappa < \sqrt{2}$. The expected emissions when the swath width is optimal is

$$E_{td}^* = \frac{2e_t}{m_{td}}d + \frac{e_t}{\sqrt{3\delta}}\frac{2(\kappa^*)^3 - \kappa^*}{(\kappa^*)^4 - 1} + \frac{\xi_d}{2} + \xi_t, \tag{5.5}$$

where κ^* is given by the solution of $\frac{e_d}{e_t} = \frac{\left(2-(\kappa^*)^2\right)\sqrt{(\kappa^*)^4+1}}{2((\kappa^*)^4-1)}$.

5.2.3 A General Delivery Emissions Model

A general expected GHG emissions model for all delivery services to a customer located at d unit distances from the depot can be expressed as

$$E_s = a_s d + b_s, \tag{5.6}$$

where $s \in \{do, to, td\}$, $a_s \in \left\{2e_d, \frac{2e_t}{m_{to}}, \frac{2e_t}{m_{td}}\right\}$, and $b_s \in \left\{\xi_d + \xi_t, \frac{2e_t}{\sqrt{3\delta}} + \xi_t, \frac{e_t}{\sqrt{3\delta}}\left(\frac{k}{2} + \frac{1}{k} + \frac{e_d}{e_t}\sqrt{k^2 + \frac{1}{k^2}}\right) + \frac{\xi_d}{2} + \xi_t\right\}$.

5.3 Illustration of Emissions-Minimizing Delivery Systems

Similar to the delivery cost illustrations presented in Chapter 4, the purpose of this section is to determine and illustrate the optimal, use of drone delivery (including truck-drone and drone-only) as a possible substitute for some or all traditional truck deliveries to minimize the expected total lifecycle greenhouse gas (GHG) emissions for a delivery region. The base case data remains the same as described in Chapter 4 and is displayed again for convenience in Table 5.1.

To make the expected emissions illustrations clear, we again define and distinguish the terms "delivery service" and "delivery service combination". We model three different delivery services: truck-only delivery (TO), drone-only delivery (DO), and truck-drone delivery (TD). These delivery services can be combined, using different services in different subregions, to create a delivery service combination. We require each geographic subregion of the service region to be served by a single delivery service, but allow different areas of the entire service region to be served with different services. We denote the combination of two or more delivery services with a "+" (e.g., TO+DO), where the combination generates lower GHG emissions than any of its component services. For example, if services TO and DO are to be combined as TO+DO, the GHG emissions generated from using TO+DO must be lower than those generated from using TO and DO alone. Note that for a service combination consisting of two or more delivery services, there is an infinite collection of possible realizations of the delivery services, depending on where each service is used. However, in most cases, we are interested in the allocation that optimizes GHG emissions. In the following analyses, we define "drone delivery" to refer to a service combination that includes drones for some part of the service region.

Table 5.1. Parameters definition and parameter values for the base case

Parameter	Unit	Definition	Baseline	Reference
R	mile	The radius of the circular delivery region	10	Xu (2017)
δ	#deliveries/mile^2	The number of deliveries per square mile	25	Gulden (2017)
CI_e	kg CO2e/kWh	Carbon intensity of electricity, i.e., the quantity of lifecycle* CO2e emissions produced by consuming 1 kWh of electricity	0.654	Stolaroff et al. (2018)
CI_f	kg CO2e/kWh	Carbon intensity of diesel fuel, i.e., the quantity of lifecycle* CO2e emissions produced by consuming (1/37.6) gallon of diesel	0.335	Stolaroff et al. (2018)
c_t	$/mile	The cost to move a truck one mile	1.25	Campbell et al. (2017)
s_t	$/stop	The cost to make a truck delivery	0.4	Campbell et al. (2017)
f_t	miles per gallon	Truck fuel economy	11.5	Stolaroff et al. (2018)
Epm_t	kWh/mile	$Epm_t = 37.6/f_t$, 1 gallon of diesel = 37.6 kWh (the conversion factor is from Stolaroff et al. (2018))	3.26	Stolaroff et al. (2018)
e_t	kg CO2e/mile	Truck operating emissions per mile $e_t = CI_d \times 37.6/f_t = CI_d \times Epm_t$	1.09	Stolaroff et al. (2018)
ξ_t	kg CO2e/stop	Truck emissions per stop	0	Figliozzi (2017), Stolaroff et al. (2018), Goodchild and Toy (2018)
m_{to}	#deliveries/route	Number of total deliveries per truck-only route	100	Assumed based on Holland et al. (2017), Stolaroff et al. (2018)
c_d	$/mile	Drone operating cost per mile	0.1	Campbell et al. (2017)
s_d	$/stop	Marginal drone stop cost relative to truck stop cost	0	Campbell et al. (2017)
Epm_d	kWh/mile	The amount of electricity consumed by drones flying one mile	0.018	Stolaroff et al. (2018)
e_d	kg CO2e/mile	The amount of CO2e emitted by drones flying one mile $e_d = CI_e \times Epm_d$	0.01	Stolaroff et al. (2018)
ξ_d	kg CO2e/stop	Marginal stop emissions of drone relative to truck	0	Figliozzi (2017), Stolaroff et al. (2018), Goodchild and Toy (2018)
R_d	mile	Maximum drone flight range per full battery charge	10	Xu (2017)
m_{td}	#deliveries/route	Number of total deliveries per truck-drone route	150	Assumed

*Lifecycle CO2e emissions includes emissions from the resource extraction, transportation of the resource to the production facility, the creation of the fuel or electricity from various raw materials, the transportation of the fuel or electricity to a fuel or charging station, and then its use to power the vehicle

5.3.1 Base Case

5.3.1.1 Minimum-emissions Portioning of the Delivery Region

In the base case, the minimum expected emissions delivery system has drone-only delivery (DO) serve all the customers in the entire 10-mile radium delivery region. Figure 5.1(a) illustrates the expected GHG emissions of each of the three delivery services as a function of distance from the depot. The vertical axis is the expected GHG emissions per delivery and the horizontal axis shows the distance from the depot. Truck-only delivery (TO) is represented by the blue solid line, drone-only delivery (DO) by the green dashed line, and truck-drone delivery (TD) by the orange long-dash line. Note that each delivery service's expected GHG emissions increases linearly with distance from the depot. The red triangles indicate the delivery service that produces the lowest emissions at any distance from the depot.

DO (i.e., the green dashed line) produces the lowest expected GHG emissions for all deliveries within 10 miles of the depot, therefore the number of DO deliveries is 7,854 and the expected total GHG emissions is 1,233 kg CO2e, which is an average of about 0.16 kg CO2e per delivery. We observe that the orange long-dash line is moving closer to the green dashed line with increasing distance, which indicates that eventually TD will produce lower GHG emissions than DO for customers located very far (beyond 20 miles) from the depot. The slope of the blue solid line is slightly lower than that of the green dashed line and much higher than that of the orange long-dash line, which indicates that TO is never a good choice in terms of reducing emissions and that the emissions savings relative to truck-only from drone delivery will be even greater if the delivery region size is extended.

Figure 5.1(b) shows that the entire delivery region is served by DO to minimize emissions in the base case. We use the upper right quadrant composed of one quarter of the circular region to illustrate the emissions-minimizing service(s).

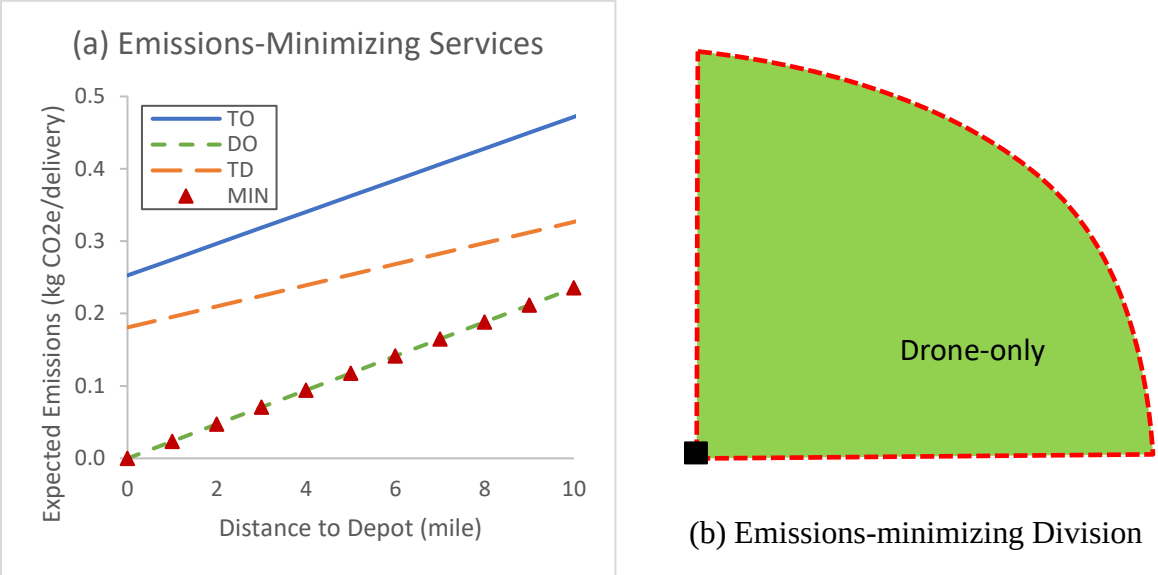

(b) Emissions-minimizing Division

Figure 5.1: (a) Expected GHG emissions of each delivery service as a function of distance from the depot; (b) Emissions-minimizing service(s) in the delivery region

5.3.1.2 Emissions Savings of Drone Delivery to Truck-only Delivery

Figure 5.2(a) shows the expected total GHG emissions of the different services. We note that drone-only delivery (DO) generates lower GHG emissions than truck-drone delivery (TD), and TD generates lower GHG emissions than truck-only delivery (TO), across the entire delivery region. Figure 5.2(b) shows the percentage GHG emissions savings of drone-only and truck-drone delivery relative to truck-only delivery. The largest expected GHG emissions savings is about 61%, provided by using drone-only everywhere in the delivery region. Although using truck-drone significantly reduces GHG emissions by 30% compared with truck-only, it produces less than half of the emissions savings from drone-only delivery for the entire region.

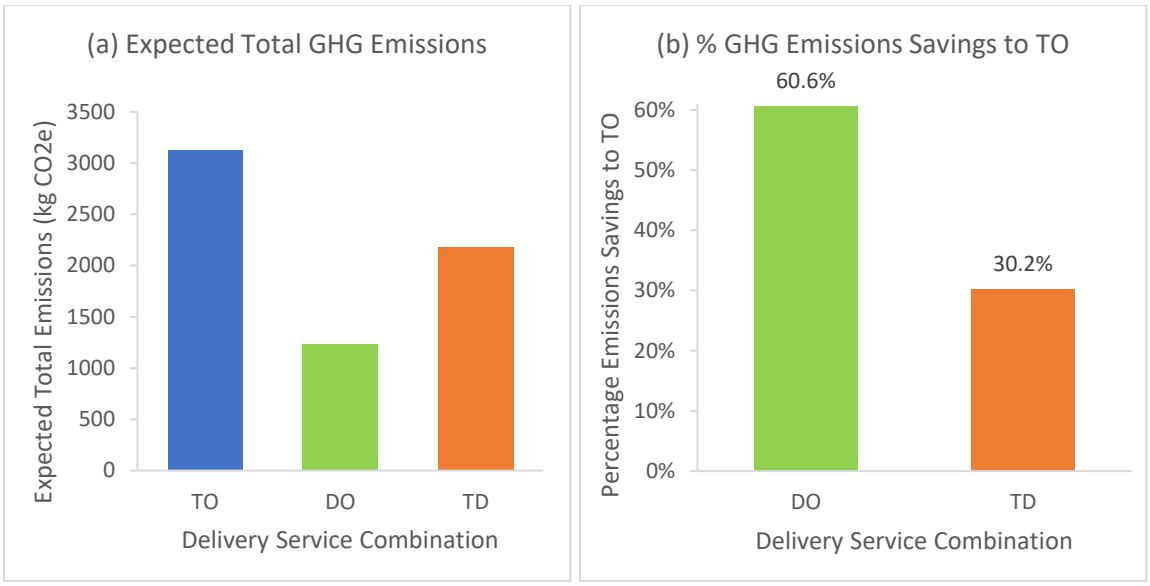

Figure 5.2: (a) Expected total GHG emissions of different delivery services; (b) Percentage GHG emissions savings of different services relative to truck-only delivery

5.3.1.3 Other Benefits of Drone Delivery in addition to Emissions Savings

Table 5.2 shows other selected performance measures in addition to the expected GHG emissions for truck-only delivery (column 2), the cost-minimizing delivery services combination identified in Chapter 4 (column 3), and the emissions-minimizing service "combination" (DO only) (column 4) for the base case. Columns 5 and 6 indicate the absolute and the relative changes in performance of the emissions-minimizing service (DO) relative to truck-only. We show column 3 as a reference, but defer discussion of the comparison of cost-minimizing and emissions-minimizing services to the Chapter 6. Please note that all the performance measures are expressed in expected values.

Table 5.2. Performance comparisons for truck-only delivery and the optimal service combination in the base case

Performance Measures	TO	DO+TD[*c]	DO[*e]	Change (DO[*e] vs TO)	%Change
% Area (customers) Served by TO	100.0%	0.0%	0.0%	-100.0%	-100%
% Area (customers) Served by DO	0.0%	1.5%	100.0%	100.0%	-
% Area (customers) Served by TD	0.0%	98.5%	0.0%	0.0%	-
Total Delivery Cost ($)	**6717.8**	**5750.3**	**13613.6**	**6895.7**	**103%**
Truck Delivery Cost	6717.8	4000.2	0.0	-6717.8	-100%
Drone Delivery Cost	-	1750.1	13613.6	13613.6	-
Total GHG Emissions (kg CO2e)	**3132.2**	**2166.4**	**1232.8**	**-1899.0**	**-61%**
Truck Emissions	3132.2	2148.0	0.0	-3131.8	-100%
Drone Emissions	-	18.4	1232.8	1232.8	-
Truck Miles Traveled (mile)	2861.0	1962.0	0.0	-2861.0	-100%
Drone Miles Traveled (mile)	-	1562.1	104719.8	104719.8	-
Driver Hours Worked (hour)	247.8	145.2	0.0	-247.8	-100%
Drone Hours Operated (hour)	-	105.5	2748.9	2748.9	-
#Trucks Required (SL[1] = 8 hrs)	31.0	18.1	0.0	-31.0	-100%
#Drones Required (SL[1] = 8 hrs)	-	19.0	343.6	343.6	-
Number of Truck Routes	78.5	51.6	0.0	-78.5	-100%
Truck Route Length (mile)	36.4	38.0	0.0	-36.4	-100%
Truck Route Time (hour)	3.2	2.8	0.0	-3.2	-100%
Drone Stops	-	3984.6	7854.0	7854.0	-

[1]SL= Service Level, which is one day in the base case; [*c] indicates the optimal service combination that minimize delivery costs; [*e] indicates the optimal service combination that minimizes GHG emissions

Rows 2-4 show the percentage of the delivery area (or customers) served by TO, DO, and TD in each service combination, respectively. When GHG emissions are minimized, DO is used in 100% of the delivery region. Row 5 indicates that the associated expected total delivery costs effectively double from $6,718 for TO to $13,614 for DO[*e] when GHG emissions are minimized. The total expected GHG emissions (row 6) are reduced by 61% from 3,132 kg CO2e for TO to 1,233 kg CO2e for DO[*e], with truck emissions reduced by 3,132 kg CO2e (a 100% reduction) and drone emissions increased by 1,233 kg CO2e (about one third of the reduction in truck emissions). The incremental

delivery costs of $6,896 incurred to reduce 1,899 kg CO2e in emissions imply an implicit "carbon price" of $3,600/tCO2e. As a reference, "the United Nations Global Compact has called for businesses to adopt an internal carbon price of at least $100/tCO$_2$e by 2020, which will be needed to keep GHG emissions consistent with a 1.5-2°C pathway" (The World Bank). Thus, for the base case, a carbon price of $100/tCO2e might be too low to incentivize businesses to adopt the emissions minimizing but much more expensive delivery method (DO^{*e} vs. TO).

The expected truck travel miles (row 11) are reduced by 2,861 miles (a 100% reduction). However, the expected drone travel miles (row 12) are increased by 104,720 miles. This indicates that on average one truck mile is replaced by about 37 drone miles. The relative cost and emissions efficiencies of drone travel to truck travel are 12.5 (i.e., $\frac{c_t}{c_d}$) and 93 (i.e., $\frac{e_t}{e_d}$), respectively. So, if we can replace one truck mile with less than 12.5 drone miles, we can reduce emissions and cost at the same time (which we have observed for the base case in Chapter 4). This suggests that when all truck deliveries are replaced by drone deliveries, if we can find ways to replace one truck mile with fewer drone miles, both emissions and cost savings relative to truck-only will increase. On the other hand, when not all truck deliveries are replaced by drone deliveries, and one truck mile is replaced with less than $min\left\{\frac{e_t}{e_d}, \frac{c_t}{c_d}\right\}$ drone miles, the more we increase the use of drones, the more emissions and cost savings we can obtain.

Row 13 shows that the expected number of driver work hours is reduced from 248 to zero because drivers are all replaced by drones in this emissions-minimizing base case. Row 14 shows the number of hours that drones operate is increased from zero to 2,749.

One nice thing about drones is that they are much smaller and less expensive than trucks; thus, it may be more affordable to have a large number of drones work in parallel to replace a large number of trucks. We compute the number of trucks and drones required (in rows 15-16) based on total driver hours and a work-day of 8 hours for both truck (driver) and drone. The expected number of trucks required to serve the delivery region is reduced from 31 to zero; and the expected number of drones required is increased from zero to 344 when switching from TO to DO^{*e}. We anticipate the number of drones required to be smaller if drones are allowed to work longer than the 8 hours assumed in the base case. The number of truck routes (row 17), truck route length (row 18) and truck route time (row 19) are all reduced to zero when switching from TO to DO^{*e}.

5.3.1.4 Allocation of Selected Performance to Each Component

Figure 5.3 shows the allocation of the expected total GHG emissions to each component of travel (i.e., truck linehaul travel, truck local travel, and drone travel) for TO (blue bars), DO^{*e} (hatched green bars) and TD (hatched orange bars). It shows that TD is significantly more environmentally friendly than TO, but much less environmentally friendly than DO. Consequently, in the emissions-minimizing base case, we do not have a near-optimal solution using TD delivery alone, as we did for the nearly cost minimizing solution in the base case (see Figure 4.10). Note that in the base case there are no emissions per delivery stop ($\xi_t = \xi_d = 0$) as in prior research, which differs from the cost model in Chapter 4 where there is a non-zero delivery stop cost for trucks and drone. Thus, the expected GHG emissions of TO include emissions for truck linehaul travel (about 37%) and truck local travel (about 63%). For DO^{*e}, both truck linehaul and local travel are completely replaced by drone travel. Comparing TD with TO, the emissions for truck

linehaul travel and truck local travel are reduced by 33% and 29%, respectively, and the emissions from drone travel are increased by only 16.8 kg CO2e.

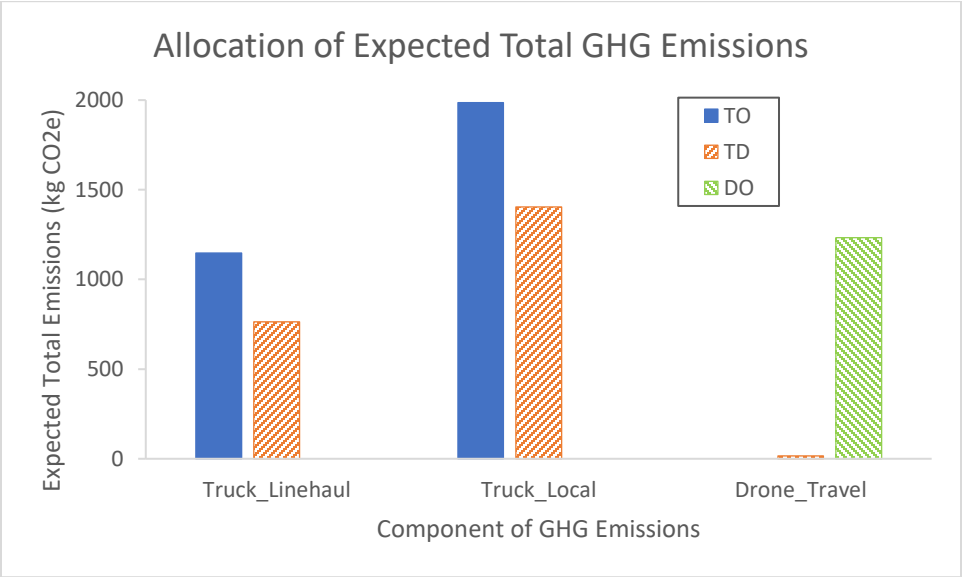

Figure 5.3. Expected total GHG emissions of travel components in TO, DO^{*e}, and TD

Figure 5.4 highlights that although DO^{*e} is the most environmentally friendly delivery service, it is also by far the most expensive service. The delivery costs of DO^{*e} include costs for drone travel (about 77% of the total) and drone delivery stops (about 23% of the total). Compared with TO, the increased cost for drone delivery stops is the same as the reduced cost for truck delivery stops due to truck and drone have the same stop cost per delivery. However, the increased cost for the drone travel is much greater than the cost reduction for truck linehaul and local travel. Comparing TD with TO, delivery costs are reduced and the GHG emissions are reduced by replacing some truck travel with drones.

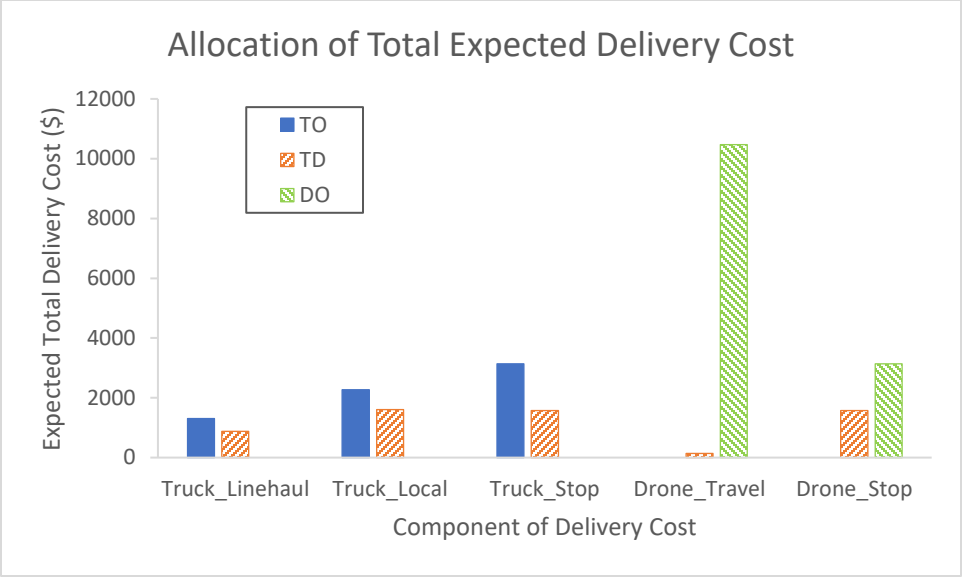

Figure 5.4. The expected total costs of each travel component in TO, DO^{*e}, and TD

Figure 5.5 shows the allocation of the expected total travel miles to each component of travel (i.e., truck linehaul, truck local travel and drone travel) for TO (blue bars), DO^{*e} (hatched green bars) and TD (hatched orange bars). One of the benefits of using drones (i.e., truck-drone and drone-only) is the reduction in truck travel miles. This is because on a per mile basis truck travel generates much more GHG emissions (about 93 times) and is also much more expensive (about 12.5 times) than drone travel. Thus, reducing truck travel miles has a large impact on reducing total emissions and costs. However, there is a threshold on how much the drone miles can be increased and still have a net emissions or cost benefit. Assuming equal stop costs and emissions per delivery, if the ratio of the increased drone travel miles and the reduced truck travel miles (i.e., the "mile-replace ratio") is less than $min\left\{\frac{e_t}{e_d}, \frac{c_t}{c_d}\right\}$, both emissions and delivery costs will be reduced. However, if the mile-replace ratio is between $min\left\{\frac{e_t}{e_d}, \frac{c_t}{c_d}\right\}$ and $max\left\{\frac{e_t}{e_d}, \frac{c_t}{c_d}\right\}$, reducing emissions will increase delivery costs and decreasing delivery costs will increase emissions.

The mile-replace ratio should always be less than $max\left\{\frac{e_t}{e_d}, \frac{c_t}{c_d}\right\}$, otherwise, drones should not be used at all or not used very much. In the base case, $min\left\{\frac{e_t}{e_d}, \frac{c_t}{c_d}\right\} = 12.5$, $max\left\{\frac{e_t}{e_d}, \frac{c_t}{c_d}\right\} = 93$, and the mile-replace ratio of DO^{*e} is 37, which is between 12.5 and 93, whereas the mile-replace ratio of TD is 1.6, which is lower than 12.5. This explains why DO^{*e} reduces emissions but increases delivery costs a large amount, whereas TD reduces emissions and delivery costs simultaneously. Furthermore, there is a huge room for improvement for TD because drones are used for only 50% of deliveries, and the mile-replace ratio is fairly low.

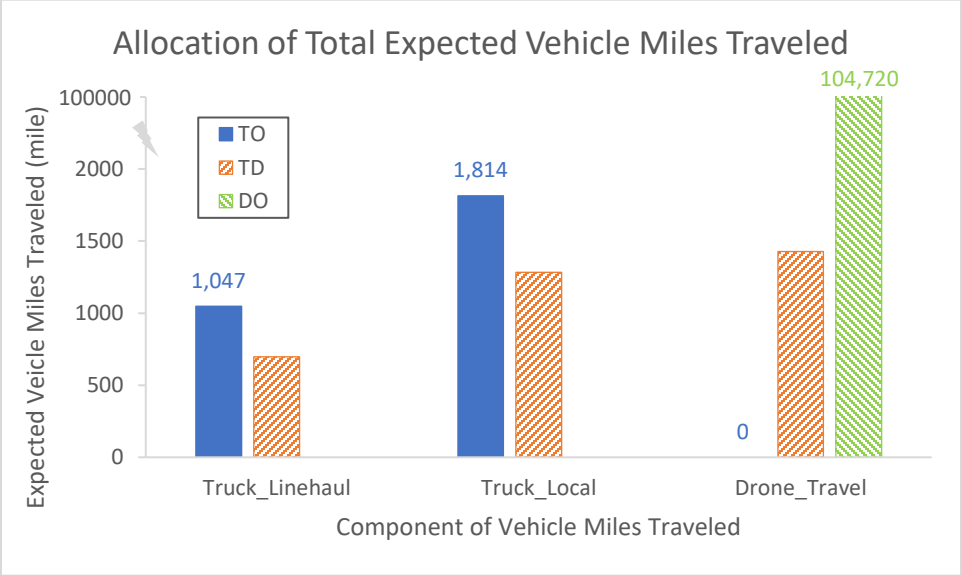

Figure 5.5. The expected miles traveled of each travel component in TO, DO^{*e}, and TD

5.3.2. Relatively Inefficient vs Efficient Drone Energy Consumption Rates (Epm_d)

To assess the impact of the drone energy consumption rate on the performance measures of drone delivery, we consider two other drone energy consumption rates in addition to the base case rate of $Epm_d = 18$ Wh/mile: $Epm_d = 36$ Wh/mile (inefficient

EPM case) and $Epm_d = 9$ Wh/mile (efficient EPM case). Please note that even 36 Wh/mile might be a very efficient drone energy consumption rate. We use the terms efficient and inefficient to distinguish the two cases. In subsection 5.3.2.3, we show the impact of a much wider Epm range on the performance metrics, especially emissions savings, of drone delivery relative to truck-only delivery.

5.3.2.1 Performance Effects of Drone Delivery

Table 5.3 shows selected performance measures of interest for TO, TD, and the emissions-minimizing service combination for three different levels of Epm_d, i.e., DO+TD^{*e} minimizes GHG emissions for $Epm_d = 36$ Wh/mile, DO^{*e} minimizes GHG emissions for the base case $Epm_d = 18$ Wh/mile, and DO^{*e} minimizes GHG emissions for $Epm_d = 9$ Wh/mile. The optimal combinations are in columns 4, 6, and 8, respectively.

Table 5.3 provides several interesting observations:

(1) in the emissions-minimizing service combinations, the lower the drone energy consumption rate (Epm_d), the higher the percentage of customers served by DO (row 5) and the lower the percentage of customers served by TD (row 6). Not shown in Table 5.3 but evident in an exploration of a wider range of drone energy consumption rates on the percentage of customers served by DO versus TD, when $Epm_d < 25$ Wh/mile, DO is used everywhere in the delivery region to minimize emissions. However, when $630 \geq Epm_d \geq 25$ Wh/mile, as Epm_d increases the utilization of DO decreases at a diminishing rate. For example, at $Epm_d = 27$ Wh/mile, DO utilization is 77%; at $Epm_d = 36$ Wh/mile, DO utilization is under 32%; and at $Epm_d = 72$ Wh/mile, DO utilization is only about 4%. For all these cases, DO makes deliveries close to the depot, and TD serves the rest of the delivery region.

Table 5.3. Performance for TO, TD, and the emissions-minimizing delivery service combinations for three levels of Epm_d

Performance Measure	**Status Quo**	**Inefficient Epm_d Case**		**Base Case**		**Efficient Epm_d Case**	
Epm_d (Wh/mile)	–	36		18		9	
Service Option	TO	TD	DO+TD[*e]	TD	DO[*e]	TD	DO[*e]
% Area (customers) Served by TO	100.0%	-	0.0%	-	0.0%	-	0.0%
% Area (customers) Served by DO	-	-	31.7%	-	100.0%	-	100.0%
% Area (customers) Served by TD	-	100.0%	68.3%	100.0%	0.0%	100.0%	0.0%
Total Delivery Cost (TDC) ($)	**6717.8**	**5759.8**	**6921.8**	**5760.3**	**13613.6**	**5760.5**	**13613.6**
Truck Proportion	1.00	0.70	0.42	0.70	0.00	0.70	0.00
Drone Proportion	0.00	0.30	0.58	0.30	1.00	0.30	1.00
Cost per Delivery ($/delivery)	0.86	0.73	0.88	0.73	1.73	0.73	1.73
% Cost Change to TO	-	-14.3%	3.0%	-14.3%	102.6%	-14.3%	102.6%
Total GHG Emissions (kg CO2e)	**3131.8**	**2201.8**	**2049.7**	**2185.0**	**1232.8**	**2176.6**	**616.4**
Truck Proportion	1.00	0.98	0.77	0.99	0.00	1.00	0.00
Drone Proportion	0.00	0.02	0.23	0.01	1.00	0.00	1.00
Emissions per Delivery (kg CO2e/delivery)	0.40	0.28	0.26	0.28	0.16	0.28	0.08
% Emissions Change to TO	-	-29.7%	-34.6%	-30.2%	-60.6%	-30.5%	-80.3%
Truck Miles Traveled (mile)	**2861.0**	**1980.8**	**1449.0**	**1980.7**	**0.0**	**1980.7**	**0.0**
Drone Miles Traveled (mile)	-	1422.2	19690.0	1427.9	104719.8	1430.9	104719.8
Mile-replace Ratio	**-**	**1.6**	**13.9**	**1.6**	**36.6**	**1.6**	**36.6**
Driver Hours Worked (hour)	**247.8**	**147.0**	**102.8**	**147.0**	**0.0**	**147.0**	**0.0**
Drone Hours Operated (hour)	-	101.0	578.5	101.1	2748.9	101.2	2748.9
#Trucks Required (SL = 8 hrs)	31.0	18.4	12.8	18.4	0.0	18.4	0.0
#Drones Required (SL = 8 hrs)	-	18.4	76.5	18.4	343.6	18.4	343.6
Number of Truck Routes	**78.5**	**52.4**	**35.7**	**52.4**	**0.0**	**52.4**	**0.0**
Truck Route Length (mile)	36.4	37.8	40.5	37.8	0.0	37.8	0.0
Truck Route Time (hour)	3.2	2.8	2.9	2.8	0.0	2.8	0.0
Drone Stops	**-**	3927.0	5173.1	3927.0	7854.0	3927.0	7854.0

[*e] The optimal service combination that minimizes total GHG emissions.

(2) Comparing the emissions-minimizing service combinations with TO, as Epm_d decreases, the total GHG emissions (row 12) decrease at a diminishing rate. However, the total delivery costs (row 7) increase as Epm_d decreases, because drone-only is an environmentally friendly, but not cost-efficient, delivery method for the entire delivery region. The mile-replace ratios of the emissions-minimizing service combination are 13.9, 36.6, and 36.6 for $Epm_d = 36$, 18, and 9 Wh/mile, respectively, which all exceed the corresponding truck to drone cost ratio (i.e., $\frac{c_t}{c_d} = 12.5$). The more the mile-replace ratio exceeds the truck to drone cost ratio, the greater the delivery costs of the emissions-minimizing service combination. For example, compared with TO, the delivery costs of the emissions-minimizing service combination increase by about 3%, 103%, and 103% for $Epm_d = 36$, 18, and 9 Wh/mile, respectively. The truck to drone emissions ratios (i.e., $\frac{e_t}{e_d}$) of the emissions-minimizing service combination are 46, 93, and 186 for $Epm_d = 36$, 18, and 9 Wh/mile, respectively, which are well above their corresponding mile-replace ratio. The greater the difference, the greater the emissions savings. For example, the percentage emissions savings of the emissions-minimizing service combination relative to TO are 35%, 61%, and 80% for $Epm_d = 36$, 18, and 9 Wh/mile, respectively. The difference between the mile-replace ratio and the truck-to-drone emissions ratio suggests there is room for further reducing emissions. For service combinations with less than 100% drone deliveries, finding ways to replace more truck deliveries with drone deliveries would further reduce emissions. For service combinations with 100% drone deliveries, finding ways to reduce the drone travel distance without decreasing drone utilization would reduce emissions.

(3) When Epm_d is fairly low (e.g., <25 Wh/mile), the emissions-minimizing service combination is the same as that in the base case, and emissions are reduced as Epm_d decreases.

(4) In all Epm_d cases, TD performs very similarly, with about 14.3% cost reductions and about 30% emissions reductions compared with TO. The truck travel miles decrease very slightly and the drone travel miles increase slightly as Epm_d decreases, which is due to the fact that the truck-drone swath width is designed more toward minimizing truck travel when Epm_d gets smaller. However, the impact of the swath width through Epm_d on the truck-drone travel is small and can be ignored. When $Epm_d = 36$ Wh/mile, the delivery costs of TD are about 17% less and the emissions of TD are only about 7% greater than that of DO+TD^{*e}. This might indicate that TD is a well-balanced delivery service when Epm_d is not relatively low.

(5) Decreasing Epm_d affects emissions savings and other performance measures in two ways: a) by reducing emissions through changing the optimal set and utilization of individual delivery services, which also has an impact on other performance measures; and b) by directly reducing emissions without changing the optimal set and utilization of delivery services, which does not have an impact on other performance measures.

5.3.2.2 Allocation of Selected Performance to Each Component

Similar to the analyses above for the base case, to further understand the mechanism through which drones improve delivery performance, we identify the contributing components of expected total GHG emissions (Figure 5.6), the vehicle miles traveled (Figure 5.7), and the vehicle travel times (Figure 5.8) of the optimal service combination for the three different levels of Epm_d. In each figure, colors light blue, blue, and dark blue

represent the inefficient Epm_d case, the base case, and the efficient Epm_d case, respectively. TO delivery is represented by solid bars, TD delivery by dotted bars, and the optimal service combination by hatched bars. We include TD to demonstrate how this single delivery service compares with the emissions-minimizing service combinations.

Figure 5.6 shows the allocation of the expected total GHG emissions to truck linehaul travel, truck local travel and drone travel of TO, TD, and the emissions-minimizing service combination for the three selected levels of Epm_d. As in the base case, both the linehaul and local travel of trucks in TO are completely replaced with drone travel of DO^{*e} for $Epm_d = 9$ Wh/mile (see bars 1 and 4 in each grouping in Fig. 5.6). However, the emissions increase with DO^{*e} is only 20% (vs. 39% in the base case) of the emissions reductions in truck travel, due to drones being more energy efficient than in the base case. Unlike the complete replacement of truck delivery in the base case, for $Epm_d = 36$ Wh/mile, the combination of DO+TD^{*e} deliveries minimizes emissions with the emissions from the truck linehaul and local travel reduced by 45% and 52%, respectively, compared to TO. For $Epm_d = 36$ Wh/mile the emissions increase from drone travel is 464 kg CO2e (about 30% of the emissions reduction in truck travel). Consequently, DO+TD^{*e} reduces overall emissions by 34% compared with TO when $Epm_d = 36$ Wh/mile. This indicates that an energy consumption rate of 36 Wh/mile still makes drones more energy- and emissions- efficient than trucks.

In all three Epm_d levels, TD service performs very similarly in terms of reducing emissions, with the emissions contribution from drone travel very small and decreasing as Epm_d increases (but it might be difficult to observe due to the scale of Figure 5.6). The drone travel emissions are only 34, 17, and 8 kg CO2e for $Epm_d = 36$, 18, and 9 Wh/mile,

respectively. In terms of total GHG emissions, TD performs similarly to DO+TD[*e] for $Epm_d = 36$ Wh/mile, creating only 7% more emissions. However, TD creates much higher emissions than the emissions minimizing service (DO[*e]) for $Epm_d = 18$ and 9 Wh/mile. This shows how emissions are reduced by increasing drone utilization when Epm_d is low; but that truck-drone delivery can be a better way to use drones than drone-only when Epm_d is not as low.

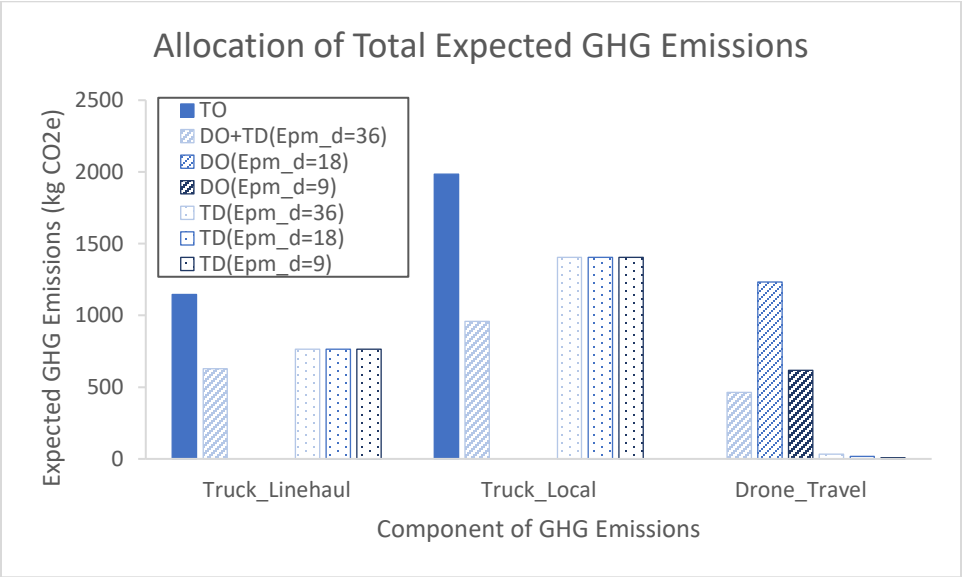

Figure 5.6. Emission allocation in TO delivery, TD delivery and the emissions-minimizing service combination for three selected levels of Epm_d

Figure 5.7 shows the allocation of vehicle miles traveled for the same three drone energy consumption rates as in Fig. 5.6. The trends of truck travel miles are very similar to those shown in Figure 5.6, but due to the scale are difficult to discern as clearly in Figure 5.7. We observe that as the drone energy consumption rate decreases, DO becomes the dominant delivery service, and the drone travel miles increase dramatically, exactly like what we observed in the base case. For both $Epm_d = 18$ and 9 Wh/mile, drone travel miles

remain the same at 104,720 miles for DO^{*e}, which is about 37 times the mileage reduction for truck travel of TO. For Epm_d =36 Wh/mile, the drone travel mileage is still relatively high, about 14 times the mileage reduction for truck linehaul and local travel when comparing DO+TD^{*e} with TO. Comparing TD with DO+TD^{*e} for Epm_d =36 Wh/mile, the drone travel mileage is 1,431 miles for TD, which is about only 7% of the 19,690 miles for DO+TD^{*e}; and the truck linehaul and local travel mileage for TD are just about 1.2 and 1.5 times as great as those for DO+TD^{*e}.

This again shows how the use of very efficient drones can lead to a very large increase in drone travel mileage, much greater than the reduction in truck travel mileage. It also suggests that truck-drone delivery is a better way of using drones than drone-only delivery when the relative energy efficiency of drones to trucks decreases.

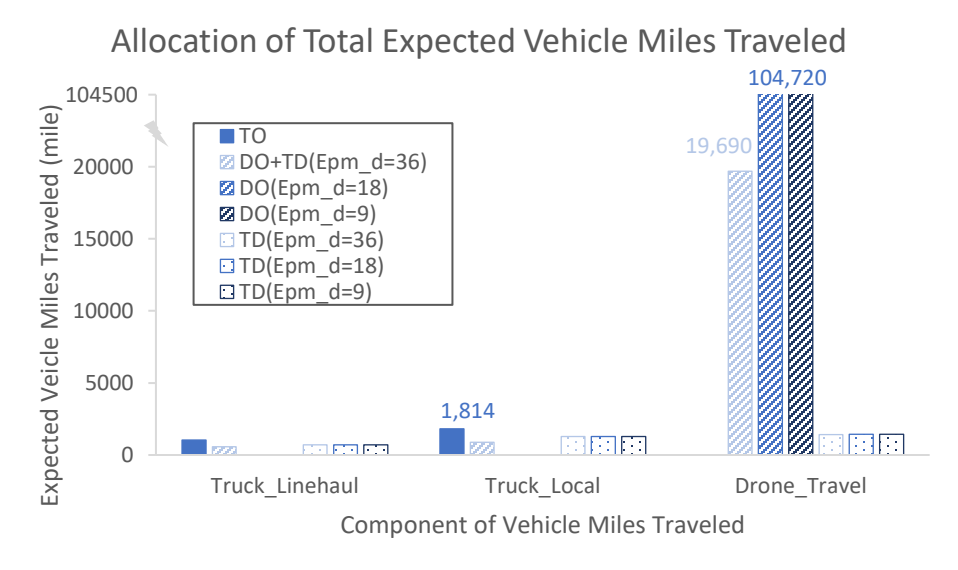

Figure 5.7. Allocation of vehicle miles traveled in TO, TD, and the emissions-minimizing service combination for three selected levels of Epm_d

The large amount of travel miles of DO^{*e} shown in Fig 5.7 lead to the large amount of travel hours of DO^{*e} as shown in Figure 5.8. This is important because the number of drone travel hours affects the number of drones required. For a work day of 8 hours, the number of drones required is 344. If we double the work day to 16 hours for drones, then the number of drones required is halved to 172. For service combinations that include both truck and drone deliveries, the total delivery time is usually determined by the truck hours operated, and drones help reduce that time by making deliveries in parallel with the truck. For example, comparing DO+TD^{*e} with TO for Epm_d =36 Wh/mile, the hours spent on truck linehaul travel, truck local travel and truck delivery stops are reduced by 45% (or 12 hours), 52% (or 47 hours) and 66% (82 hours), respectively. Drone operating hours spent on drone travel and drone delivery stops are increased by 492 and 86 hours, respectively. The expected number of drones required is 76.5 including 12.8 drones that make deliveries from the truck and 63.7 drones that make deliveries from the depot.

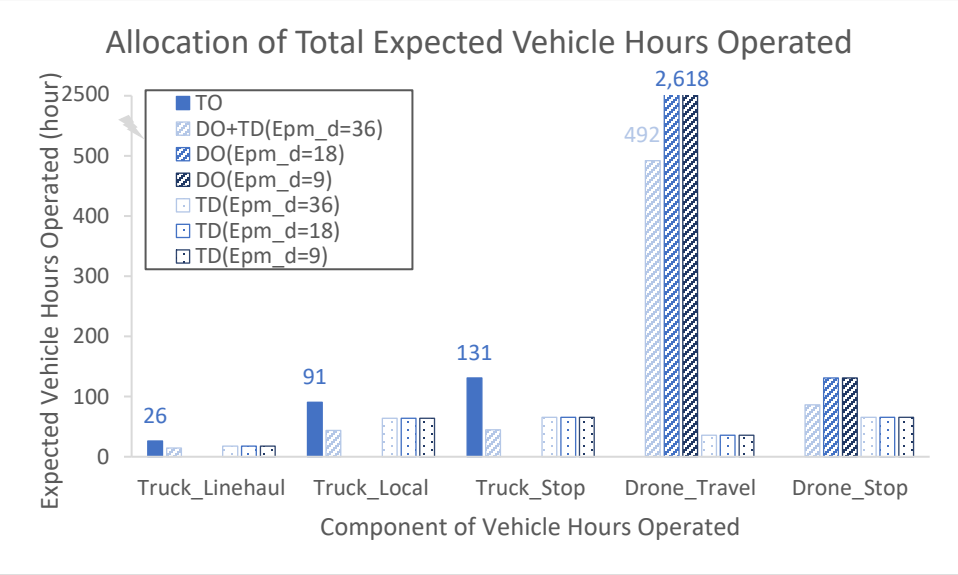

Figure 5.8. Allocation of vehicle hours operated in TO, TD, and the emissions-minimizing service combination for three selected levels of Epm_d

5.3.2.3 The Impact of Epm_d and c_d on Emissions and Costs

The energy consumption rates of drones (i.e., Epm_d) evident in the drone delivery literature have a very large range, from under 9 Wh/mile (or 20 J/m) to over 225 Wh/mile (or 500 J/m) (Zhang et al. 2021). Large Epm_d values might indicate the drones are large (heavy), able to carry large (heavy) payloads and can fly long distances with a single battery charge. These drones might also be expensive to purchase and operate. Small Epm_d values might indicate the drones are small (light), able to carry only small (light) payloads and have very limited flight range. These drones might be relatively inexpensive to purchase and operate. To further explore the impact of Epm_d and drone type, we vary the Epm_d value from the base case (Epm_d =18 Wh/mile) by multiplying it by the factors 20, 10, 7.5, 5, 3, 2, and 0.5 to assess how the wide range of Epm_d affects the emissions reduction from using drones. We first explore results with Epm_d ranging from 9 Wh/mile to 360 Wh/mile with the drone operating cost held constant at \$0.1/mile.

Figures 5.9 (a) and (b) show the percentage emissions and cost savings of drone delivery relative to truck-only delivery as a function of the drone energy consumption rate, respectively. This is for the emissions minimizing service combination TO+DO+TD^{*e} (which might include only one service). DO is represented by a light green solid line with circles, TD is represented by an orange solid line with triangles, and the optimal service combination TO+DO+TD^{*e} is represented by a dark green dashed line with diamonds. The enlarged circle, triangle, and diamond for the corresponding lines indicate the baseline value (to provide a reference). Figure 5.10 (a) and (b) are truncated versions of Figure 5.9 (a) and (b) and included for the purpose of seeing the effects of a smaller variation in Epm_d more clearly.

In Figures 5.9(a) and 5.10(a), we observe that the larger the Epm_d, the smaller the percentage emissions savings. However, the decreasing rate of that savings depends on both Epm_d and the service combination. For the single delivery services DO and TD, the decreasing rates of the percentage emissions savings are constant across all Epm_d values, with the slope of DO being much steeper than that of TD. If the Epm_d value increases by 100 Wh/mile, the percentage emissions savings decreases by 219% and 3% for DO and TD, respectively. The emissions-minimizing service combination TO+DO+TD^{*e} coincides with DO for low Epm_d ($\leq$25 Wh/mile) as TD and TO are not used; and it nearly coincides with TD for high Epm_d ($\geq$54 Wh/mile) as DO is very lightly used. Figure 5.9(a) suggests that DO delivery is a good way to use drones to reduce emissions for low Epm_d ($\leq$25 Wh/mile). But for larger Epm_d values, DO alone is not enough and using drones through TD is very helpful to reduce emissions. Even for $Epm_d = 360$ Wh/mile (20 times greater than the base level), TD reduces emissions by about 20% whereas DO increases emissions by 687% compared with TO.

Comparing Figure 5.9 (a) and (b) (or Figure 5.10 (a) and (b)), we observe the percentage cost savings of DO and TD remain the same across all Epm_d values, with DO being about 103% more and TD being about 14.3% less expensive than TO. The percentage cost savings of the emissions-minimizing service combination TO+DO+TD^{*e} ranges between the values for DO and TD, and thus TO+DO+TD^{*e} can be very expensive (relative to TO) for small values of Epm_d. As Epm_d increases, TO+DO+TD^{*e} becomes similar to TD, and using drones in TD is very helpful to reduce both cost and emissions.

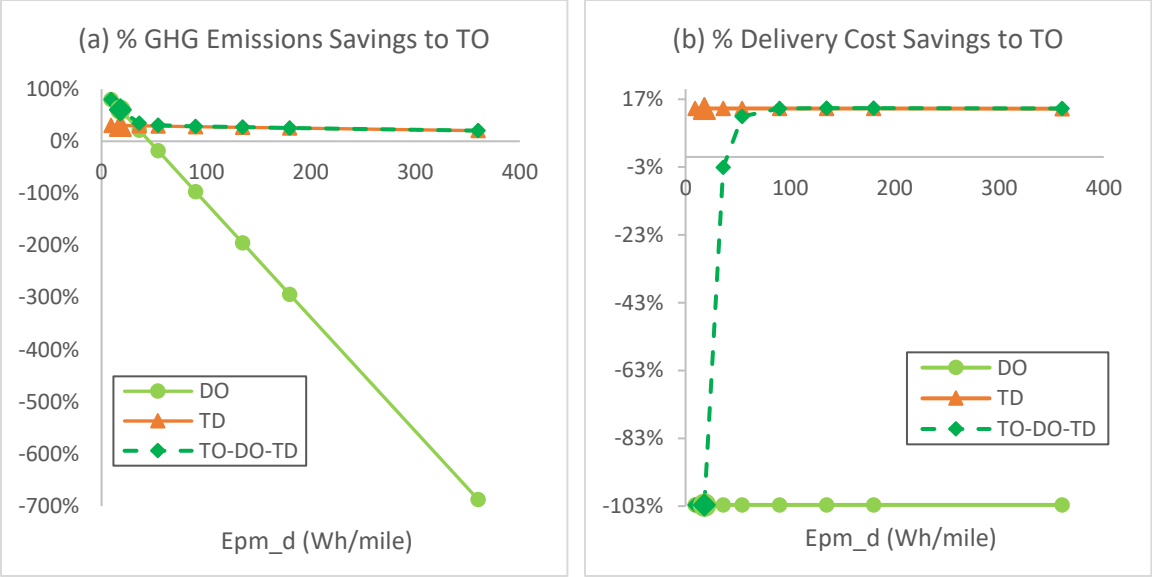

Figure 5.9. Percentage GHG emissions and delivery cost savings relative to truck-only as a function of drone energy consumption rate with c_d = \$0.1/mile (as in the base case)

Figure 5.10. Zoom-in figures of Figure 5.9

Finally, in Table 5.4 we report results where the values of c_d and Epm_d are correlated so that larger values of Epm_d are associated with a larger value of c_d. Thus, each row moving down through the table reflects a more expensive and less energy efficient (e.g., larger) drone. Table 5.4 shows the percentage emissions (columns 3, 6, and

9) and cost (columns 4,7, and10) savings of DO, TD, and TO+DO+TD^{*e} relative to truck-only delivery for each Epm_d and c_d pair in columns 1 and 2. The percentage emissions savings remain the same as described in Figure 5.8 for all service combinations. However, the percentage cost savings of DO and TD decrease now as the c_d increases along with the increasing Epm_d. When both c_d and Epm_d are very low (i.e., c_d =\$0.01/mile, $Epm_d = 9$ Wh/mile), DO provides the largest percentage emissions reductions of 80.3% and the largest percentage cost savings of 37.6%. However, DO provides the worst percentage emissions and cost savings when both c_d and Epm_d increase. Another possibility to note is that TD and the emissions-minimizing service combination may increase delivery costs when Epm_d gets large if c_d increases with Epm_d. Table 5.4 also shows the implied "Carbon Price" (the cost to reduce one metric ton of CO2e) of DO, TD, and TO+DO+TD^{*e} whenever there is a savings in emissions (a reduction in "carbon") and an increase in costs. These are reported in columns 5, 8, and 11. The implied carbon prices for TD are much lower than that of DO, which indicates that TD might be a more cost efficient way of reducing emissions than DO. The magnitude of the implied carbon price relative to current global standards (e.g., \$100/tCO2e) suggests that the implied carbon prices for TD and TO+DO+TD are not far from the global standards. However, the implied carbon prices for DO might be much higher than these standards, and thus, might not provide enough incentive for companies to adopt a cleaner but more expensive delivery method. We will further discuss the impact of carbon prices in Chapter 6.

Table 5.4. Percentage emissions and cost savings of DO, TD, and TO+DO+TD[*e] relative to truck-only with Epm_d and c_d varying in the same direction.

Epm_d	c_d	DO			TD			TO+DO+TD[*e]		
		Emissions Savings	Cost Savings	Carbon Price	Emissions Savings	Cost Savings	Carbon Price	Emissions Savings	Cost Savings	Carbon Price
(Wh/mile)	($/mile)	(%)	(%)	($/tCO2e)	(%)	(%)	($/tCO2e)	(%)	(%)	($/tCO2e)
9	0.01	80.3	37.6	-	30.5	16.2	-	80.3	37.6	-
18	0.1	60.6	-102.6	3,630	30.2	14.3	-	60.6	-102.6	3,630
36	0.1	21.3	-102.6	1,030	29.7	14.3	-	34.6	-3.0	190
54	0.15	-18.1	-180.6	-	29.2	13.2	-	30.9	8.2	-
90	0.25	-97.8	-336.5	-	28.1	11.1	-	28.6	9.8	-
135	0.375	-195.2	-531.3	-	26.8	8.6	-	27.0	8.0	-
180	0.5	-293.6	-726.2	-	25.5	6.0	-	25.6	5.7	-
360	1	-687.2	-1,505.6	-	20.3	-4.0	420	20.4	-4.0	420

5.3.3. High vs Low Carbon Intensity of Electricity (CI_e)

A change in the carbon intensity of electricity (e.g., from different electricity generation methods) has the same effect as changing the drone energy consumption rate, since e_t and e_d are proportional to the carbon intensity (see Table 5.1). Doubling or halving CI_e is equivalent to doubling or halving Epm_d. Because of the variation in the carbon intensity of electricity, both over geography and over time (especially in the future), we follow Stolaroff et al. (2018) who use four carbon intensity values from "the U.S. Environmental Protection Agency's estimate of regional, non-baseload GHG emissions in the United States", reflecting California (a low-carbon region), the U.S. average (the base case), Missouri (a region with the current highest value), and "a low-GHG case about half as carbon intensive as California." We show the results in Table 5.8 in the summary section.

5.3.4. Large vs Jumbo Truck Capacity for Truck-drone Delivery (m_{td})

In the base case, since drone-only is the dominant emissions reducing delivery service, decreasing the truck-capacity for truck-drone deliveries will not change the emissions-minimizing service, thus, we increase the truck-drone capacity to two higher levels than the base case level of $m_{td} = 150$ deliveries per route: large truck capacity with $m_{td} = 300$ deliveries per route and jumbo truck capacity with $m_{td} = 750$ deliveries per route. Increasing the capacity of truck-drone service distributes the emissions and costs of truck travel over greater numbers of deliveries.

5.3.4.1 Performance Effects of Drone Delivery

Table 5.5 shows the performance measures of interest for TO (column 2), TD (columns 3, 5 and 7), and the optimal delivery service combinations (DO^{*e} in column 4,

DO^{*e} in column 6 , and DO+TD^{*e} in column 8) for the three different levels of m_{td}, i.e., (the base level $m_{td} = 150$), $m_{td} = 300$ and $m_{td} = 750$).

There are several interesting observations from Table 5.5:

(1) for TD to be used as part of the emissions-minimizing service combination (e.g., TD is used 23% with the jumbo truck capacity), the truck capacity for truck-drone delivery needs to be very large (e.g., 750). Moreover, the impact of m_{td} on increasing TD utilization appears to be marginally diminishing. For example, when m_{td} is increased from 300 to 750, TD utilization (i.e., the percentage of customers served by TD) increases from 0 to 23% (a 23% increase) as shown in the Table 5.5; when m_{td} is further doubled (from 750 to 1,500, which is not shown in Table 5.5), TD utilization increases by only 10% (from 23% to 33%).

(2) When $m_{td} \leq 300$ the emissions-minimizing service combination has DO serve all the customers in the delivery region of 10-mile radius. In fact, the truck capacity for truck-drone delivery (m_{td}) has no impact on the performance of the emissions-minimizing service combination when $m_{td} \leq 400$.

(3) With the jumbo truck capacity in Table 5.5 ($m_{td} = 750$), the emissions-minimizing service combination has DO serve customers who are within 8.8 miles of the depot (77% of the deliveries) with TD serving the remaining more distant customers (23%). The emissions-minimizing service combination for $m_{td} = 750$ provides a slightly larger emissions savings (61.4% vs 60.6%) and a much smaller cost increase (59% vs 103%) than using DO^{*e} for the base case (with $m_{td} = 150$).

Table 5.5. Performance for TO, TD, and the emissions-minimizing delivery service combinations for three levels of m_{td}

Performance Measure	**TO**	**Base Case**		**Large m_{td} Case**		**Jumbo m_{td} Case**	
m_{td} (#deliveries/truck route)	0	150		300		750	
Service Option	TO	TD	DO[*e]	TD	DO[*e]	TD	DO+TD[*e]
% Area (customers) Served by TO	100.0%	-	0.0%	-	0.0%	-	0.0%
% Area (customers) Served by DO	-	-	100.0%	-	100.0%	-	76.9%
% Area (customers) Served by TD	-	100.0%	0.0%	100.0%	0.0%	100.0%	23.1%
Total Delivery Cost (TDC) ($)	**6717.8**	**5760.3**	**13613.6**	**5323.9**	**13613.6**	**5062.1**	**10667.1**
Truck Portion	1.00	0.70	0.00	0.68	0.00	0.66	0.07
Drone Portion	0.00	0.30	1.00	0.32	1.00	0.34	0.93
Cost per Delivery ($/delivery)	0.86	0.73	1.73	0.68	1.73	0.64	1.36
% Cost Change to TO	-	-14.3%	102.6%	-20.7%	102.6%	-24.6%	58.8%
Total GHG Emissions (kg CO2e)	**3131.8**	**2185.0**	**1232.8**	**1802.9**	**1232.8**	**1573.6**	**1209.3**
Truck Portion	1.00	0.99	0.00	0.99	0.00	0.99	0.31
Drone Portion	0.00	0.01	1.00	0.01	1.00	0.01	0.69
Emissions per Delivery (kg CO2e/delivery)	0.40	0.28	0.16	0.23	0.16	0.20	0.15
% Emissions Change to TO	-	-30.2%	-60.6%	-42.4%	-60.6%	-49.8%	-61.4%
Truck Miles Traveled (mile)	**2861.0**	**1980.7**	**0.0**	**1631.6**	**0.0**	**1422.2**	**341.3**
Drone Miles Traveled (mile)	-	1427.9	104719.8	1427.9	104719.8	1427.9	70988.7
Mile-replace Ratio	**-**	**1.6**	**36.6**	**1.2**	**36.6**	**1.0**	**28.2**
Driver Hours Worked (hour)	**247.8**	**147.0**	**0.0**	**138.3**	**0.0**	**133.1**	**31.0**
Drone Hours Operated (hour)	-	101.1	2748.9	101.1	2748.9	101.1	1890.5
#Trucks Required (SL = 8 hrs)	31.0	18.4	0.0	17.3	0.0	16.6	3.9
#Drones Required (SL = 8 hrs)	-	18.4	343.6	17.3	343.6	16.6	237.3
Number of Truck Routes	**78.5**	**52.4**	**0.0**	**26.2**	**0.0**	**10.5**	**2.4**
Truck Route Length (mile)	36.4	37.8	0.0	62.3	0.0	135.8	141.3
Truck Route Time (hour)	3.2	2.8	0.0	5.3	0.0	12.7	12.8
Drone Stops	**-**	3927.0	7854.0	3927.0	7854.0	3927.0	6948.0

[*e] The optimal service combination that minimizes total GHG emissions.

(4) Unlike the emissions-minimizing service combination, TD reduces both emissions and delivery costs for all three levels of m_{td}, and the emissions and cost savings increase as m_{td} increases. The percentage emissions savings relative to TO are 30%, 42%, and 50% for $m_{td} = 150$, 300, and 750, respectively. The percentage cost savings relative to TO are about 14%, 21%, and 25% for $m_{td} = 150$, 300, and 750, respectively. Many other performance measures (e.g., truck travel miles, driver hours, number of trucks and drones) improve as m_{td} increases, and again the improvement is marginally diminishing. However, the truck routes become longer as m_{td} increases. Larger trucks reduce both cost and emissions, but provide worse service in terms of truck route time. For example, the jumbo trucks ($m_{td} = 750$) have over 12-hour truck routes.

5.3.5. Low vs High Delivery Density (δ)

In this section, we explore the impact of delivery density on the emissions for delivery with drones. We consider two levels of delivery density in addition to the base case level of $\delta = 25$: a low delivery density with $\delta = 1$ and a high delivery density with $\delta = 625$. According to USPS (2020), all three of these delivery density values can represent "suburban areas that feature standalone houses with yards or porches that are convenient and efficient for leaving a package". Because delivery density varies by time of the day/week/season/year (as well as over geographic regions), the low delivery density may represent areas where houses are far from each other and/or off-peak periods, and the high delivery density may represent dense areas where houses are next to each other and/or peak periods.

5.3.5.1 Performance Effects of Drone Delivery

Table 5.6 shows the performance measures of interest for TO (columns 2, 5 and 8), TD (columns 3, 6 and 9), and the optimal delivery service combination for three different levels of δ, i.e., DO^{*e} for $\delta = 1$, DO^{*e} for the base level $\delta = 25$, and DO+TD^{*e} for $\delta = 625$, in columns 4, 7, and 10, respectively.

There are several interesting observations from Table 5.6:

(1) when delivery density is low, with $\delta \leq 25$ deliveries per square mile, the emissions-minimizing service combination is for DO to serve all the customers in the delivery region of 10-mile radius. In fact, but not shown in the table, DO is optimal to minimize emissions in the base case for $\delta \leq 100$ deliveries per square mile. If we measure the performance on the per delivery level (rows 10 and 15), the delivery density has no impact on the performance of DO; however, the relative performance of DO to TO deteriorates as delivery density increases, which is due to the fact that the per delivery performance of TO improves as delivery density increases. The denser the deliveries, the shorter the distance per delivery for truck deliveries (including TO and TD), and thus the greater the number of deliveries per truck mile. Therefore, TO and TD become more attractive than DO as delivery density increases.

Table 5.6. Performance for TO, TD, and the emissions-minimizing delivery service combinations for three levels of δ

Performance Measure	**Low Density**			**Base Case**			**High Density**		
δ (#deliveries/square mile)	1			25			625		
Service Option	TO	TD	DO[*e]	TO	TD	DO[*e]	TO	TD	DO+TD[*e]
% Area (customers) Served by TO	100.0%	-	0.0%	100.0%	-	0.0%	100.0%	-	0.0%
% Area (customers) Served by DO	-	-	100.0%	-	-	100.0%	-	-	16.3%
% Area (customers) Served by TD	-	100.0%	0.0%	-	100.0%	0.0%	-	100.0%	83.7%
Total Delivery Cost (TDC) ($)	**631.5**	**509.8**	**544.5**	**6717.8**	**5760.3**	**13613.6**	**122601.0**	**109086.5**	**123519.9**
Truck Portion	1.00	0.82	0.00	1.00	0.70	0.00	1.00	0.63	0.49
Drone Portion	0.00	0.18	1.00	0.00	0.30	1.00	0.00	0.37	0.51
Cost per Delivery ($/delivery)	2.01	1.62	1.73	0.86	0.73	1.73	0.62	0.56	0.63
% Cost Change to TO	-	-19.3%	-13.8%	-	-14.3%	102.6%	-	-11.0%	0.7%
Total GHG Emissions (kg CO2e)	**442.9**	**314.7**	**49.3**	**3131.8**	**2185.0**	**1232.8**	**38585.3**	**26209.2**	**25822.1**
Truck Portion	1.00	0.99	0.00	1.00	0.99	0.00	1.00	1.00	0.92
Drone Portion	0.00	0.01	1.00	0.00	0.01	1.00	0.00	0.00	0.08
Emissions per Delivery (kg CO2e/delivery)	1.41	1.00	0.16	0.40	0.28	0.16	0.20	0.13	0.13
% Emissions Change to TO	-	-28.9%	-88.9%	-	-30.2%	-60.6%	-	-32.1%	-33.1%
Truck Miles Traveled (mile)	**404.6**	**284.4**	**0.0**	**2861.0**	**1980.7**	**0.0**	**35248.9**	**23866.2**	**21664.4**
Drone Miles Traveled (mile)	0.0	285.6	4188.8	-	1427.9	104719.8	0.0	7139.5	178995.1
Mile-replace Ratio	**-**	**2.4**	**10.4**	**-**	**1.6**	**36.6**	**-**	**0.6**	**13.2**
Driver Hours Worked (hour)	**24.4**	**16.1**	**0.0**	**247.8**	**147.0**	**0.0**	**4380.4**	**2393.2**	**2044.5**
Drone Hours Operated (hour)	0.0	9.8	110.0	-	101.1	2748.9	0.0	1814.7	6378.6
#Trucks Required (SL = 8 hrs)	3.1	2.0	0.0	31.0	18.4	0.0	547.6	299.2	255.6
#Drones Required (SL = 8 hrs)	0.0	2.0	13.7	-	18.4	343.6	0.0	299.2	863.1
Number of Truck Routes	**3.1**	**2.1**	**0.0**	**78.5**	**52.4**	**0.0**	**1963.5**	**1309.0**	**1095.0**
Truck Route Length (mile)	128.8	135.8	0.0	36.4	37.8	0.0	18.0	18.2	19.8
Truck Route Time (hour)	7.8	7.7	0.0	3.2	2.8	0.0	2.2	1.8	1.9
Drone Stops	**-**	**157**	**314**	**-**	**3927**	**7854**	**-**	**98175**	**114223**

[*e] The optimal service combination that minimizes total GHG emissions.

(2) When delivery density $\delta > 100$, TD utilization increases as delivery density increases. For example, TD utilization increases from 0 to 84% when the density increases from 100 to 625 deliveries per square mile. DO always serves customers who are close to the depot although the number of customers becomes smaller as delivery density becomes greater. This might imply that truck-drone and/or truck-only might be a better delivery method (in terms of minimizing emissions) for dense suburban and urban areas whereas drone-only delivery is better for the majority of sparse suburban and rural areas and a small proportion of urban areas that are within walking distance from the depot (or retail store) because drone-only provides lower emissions than TD and TO serving customers that are very close the depot.

(3) The emissions per delivery of TO (row 15) decreases as delivery density increases, and so does the cost per delivery of TO (row 10). The expected emissions per delivery is 1.41, 0.4, and 0.2 kg CO2e for $\delta = 1$, 25, and 625, respectively. It is increased by 253% for low density ($\delta = 1$) and decreased by 50% for high density ($\delta = 625$) compared with the base density ($\delta = 25$). The expected cost per delivery is \$2.01, \$0.86, and \$0.62 for $\delta = 1$, 25, and 625, respectively. It is increased by 135% for low density ($\delta = 1$) and decreased by 35% for high density ($\delta = 625$) compared with the base density ($\delta = 25$). The truck route length and time decrease as delivery density increases given that each truck makes 100 deliveries per route. The truck route time is increased by more than 4 hours for low density ($\delta = 1$) and decreased by 36 minutes for high density ($\delta = 625$) compared with the base density ($\delta = 25$).

(4) The emissions-minimizing service combination produces less GHG emissions per delivery than TO for all three density levels, and the absolute per delivery emissions

differences (between the emissions-minimizing service combination and TO) become smaller as the delivery density increases. For example, the emissions-minimizing service combination produces 1.25, 0.24, and 0.07 less kg CO2e per delivery than TO for $\delta = 1$, 25, and 625, respectively. Row 16 shows that the percentage emissions savings relative to TO also decreases as delivery density increases, which are 89%, 61%, and 33% for $\delta = 1$, 25, and 625, respectively. However, the absolute total GHG emissions differences (between the emissions-minimizing service combination and TO) become greater as delivery density increases, which is due to the increased number of deliveries. For example, although DO+TD^{*e} reduces only 0.07 kg CO2e per delivery (relative to TO) for $\delta = 625$, which is just 29% of the reduction for the base density $\delta = 25$, the total GHG emissions reduction is 12,763 kg CO2e, which is about 7 times greater than that for the base density $\delta = 25$.

(5) The emissions-minimizing service combination also reduces delivery costs for low density but increases delivery costs for medium and high delivery density areas. For low and medium density levels, the cost and the emissions per delivery for DO remain the same, however, the cost and the emissions per delivery for TD decrease as delivery density increases. Therefore, the percentage cost and emissions savings of DO relative to TO increase as delivery density decreases. For medium and high density delivery levels, we see a tradeoff between cost and emissions due to the different use of delivery services that minimize cost and that minimize emissions. More details regarding cost and emissions tradeoffs are provided in Chapter 6.

5.3.6. Large vs Medium Delivery Region Size (R)

To assess the impact of the delivery region size, we consider two other delivery region sizes in addition to the base case level where $R = 10$ miles: a medium delivery region with $R = 20$ miles and a large delivery region with $R = 30$ miles. The base level $R = 10$ miles was chosen based on the assumption that delivery drones have a limited roundtrip flight range of 10-15 miles first envisioned for the point-to-point delivery of small packages from a fixed depot to customer homes (e.g., Amazon). Having a small depot near the center of each city may be ideal, but finding feasible locations (including the cost for central locations) is likely to be a challenge in many cities. It is not surprising that many logistics and e-commerce firms operate larger depots (to achieve economies of scale in inventory, space, and maintenance) that can cover larger areas than a 10-mile radius, and that are located around the periphery of urban areas. We use $R = 20$ miles and $R = 30$ miles to represent different types of depots.

5.3.6.1 Performance Effects of drone delivery

Since the number of deliveries for a fixed density (and area served) increases quadratically as the delivery region size increases, we normalize the performance measures to the number of deliveries in the base region. For example, the region of $R = 30$ miles is equivalent in area and deliveries to 9 regions of $R = 10$ miles, so we divide the total costs (and other performance measures) by 9 to obtain a measure that is comparable to the base case. Table 5.7 shows the normalized performance measures of interest for TO, TD, and the optimal delivery service combination for three different levels of R.

Table 5.7. Normalized performance (by base region size) for TO, TD, and the optimal service combination for three levels of *R*

Performance Measure	**Base Case**			**Medium Region Size**			**Large Region Size**		
R (mile)	10			20			30		
Service Option	TO	TD	DO[*e]	TO	TD	DO+TD[*e]	TO	TD	DO+TD[*e]
% Area (customers) Served by TO	100.0%	-	0.0%	100.0%	-	0.0%	100.0%	-	0.0%
% Area (customers) Served by DO	-	-	100.0%	-	-	25.0%	-	-	11.1%
% Area (customers) Served by TD	-	100.0%	0.0%	-	100.0%	75.0%	-	100.0%	88.9%
Total Delivery Cost (TDC) ($)	**6717.8**	**5760.3**	**13613.6**	**8026.8**	**6632.9**	**8596.3**	**9335.8**	**7505.6**	**8378.2**
Truck Portion	1.00	0.70	0.00	1.00	0.74	0.45	1.00	0.77	0.64
Drone Portion	0.00	0.30	1.00	0.00	0.26	0.55	0.00	0.23	0.36
Cost per Delivery ($/delivery)	0.86	0.73	1.73	1.02	0.84	1.09	1.19	0.96	1.07
% Cost Change to TO	-	-14.3%	102.6%	-	-17.4%	7.1%	-	-19.6%	-10.3%
Total GHG Emissions (kg CO2e)	**3131.8**	**2185.0**	**1232.8**	**4278.1**	**2949.2**	**2711.1**	**5424.4**	**3713.4**	**3607.6**
Truck Portion	1.00	0.99	0.00	1.00	0.99	0.88	1.00	1.00	0.96
Drone Portion	0.00	0.01	1.00	0.00	0.01	0.12	0.00	0.00	0.04
Emissions per Delivery (kg CO2e/delivery)	0.40	0.28	0.16	0.54	0.38	0.35	0.69	0.47	0.46
% Emissions Change to TO	-	-30.2%	-60.6%	-	-31.1%	-36.6%	-	-31.5%	-33.5%
Truck Miles Traveled (mile)	**2861.0**	**1980.7**	**0.0**	**3908.2**	**2678.8**	**2183.7**	**4955.4**	**3377.0**	**3156.9**
Drone Miles Traveled (mile)	-	1427.9	104719.8	-	1427.9	27250.9	0.0	1427.9	12904.8
Mile-replace Ratio	**-**	**1.6**	**36.6**	**-**	**1.2**	**15.8**	**-**	**0.9**	**7.2**
Driver Hours Worked (hour)	**247.8**	**147.0**	**0.0**	**273.9**	**164.5**	**127.7**	**300.1**	**181.9**	**165.6**
Drone Hours Operated (hour)	-	101.1	2748.9	0.0	101.1	763.1	0.0	101.1	395.3
#Trucks Required (SL = 8 hrs)	31.0	18.4	0.0	34.2	20.6	16.0	37.5	22.7	20.7
#Drones Required (SL = 8 hrs)	-	18.4	343.6	0.0	20.6	101.9	0.0	22.7	58.9
Number of Truck Routes	**78.5**	**52.4**	**0.0**	**78.5**	**52.4**	**39.3**	**78.5**	**52.4**	**46.5**
Truck Route Length (mile)	36.4	37.8	0.0	49.8	51.2	55.6	63.1	64.5	67.8
Truck Route Time (hour)	3.2	2.8	0.0	3.5	3.1	3.3	3.8	3.5	3.6
Drone Stops	**-**	**3927**	**7854**	**0**	**3927**	**4909**	**0**	**3927**	**4363**

[*e] The optimal service combination that minimizes total GHG emissions.

There are several interesting observations from Table 5.7:

(1) for all three cases, the emissions-minimizing service combination has DO serve all customers who are within 10 miles from the depot, and TD serve the rest of the delivery region (rows 4-6). The utilization of DO decreases from 100% to 25% to 11% for $R = 10$, 20, and 30 miles, respectively. This is because the number of deliveries (or customers) increases as the delivery region size increases. In all cases, the flight range of drones is 10 miles. If drone flight range can be increased to 20 miles, the emissions-minimizing service combination will have DO serve all customers who are within 20 miles from depot. If we can further increase drone flight range, it will not affect the emissions-minimizing service combination, because TD produces lower GHG emissions per delivery than DO beyond 20 miles, thus, TD is the dominant delivery service beyond 20 miles.

(2) Rows 7 and 12 show that the total delivery costs and GHG emissions (of the base region size) for TO increase as the delivery region size R increases, respectively. This is because the trucks travel longer distances to get to more remote areas with the larger values of R, i.e., the average linehaul distance is longer for $R = 30$ than for $R = 10$. The delivery costs are increased by 19% and 39% for the medium ($R = 20$) and large ($R = 30$) region sizes, respectively; and the GHG emissions are increased by 37% and 73% for the medium ($R = 20$) and large ($R = 30$) region sizes, respectively, compared with the base region size ($R = 10$). Furthermore, the truck route length (row 25) and the truck route time (row 26) are 73% and 19% longer, respectively, for $R = 30$ than for $R = 10$, and are 37% and 9% longer for $R = 20$ than for $R = 10$, respectively. Considering only delivery costs and GHG emissions, there is an incentive for companies to have many small depots rather than a few large ones as the former can reduce both delivery costs, GHG emissions, and delivery times.

On the other hand, the costs of operating 9 small depots (e.g., fixed facility costs, operating costs, etc.) may be larger than the costs of operating one large depot serving the same number of customers.

(3) Comparing with TO, the emissions-minimizing service combination reduces GHG emissions for all three region sizes. Like the impact of density, the percentage emissions reductions relative to TO decrease as the region size increases. For example, the percentage emissions reductions relative to TO are 61%, 37%, and 34% for $R = 10$, 20, and 30 miles, respectively. This is due to the fact that DO is much more emissions-efficient than any other services for a delivery region of a 10-mile radius, so, the larger the DO utilization, the larger the percentage emissions reductions relative to TO. Unlike the impact of density, the absolute emissions reductions relative to TO first decrease and then increase as the regional size increases. For example, the absolute emissions reduction relative to TO are 1899, 1567, and 1817 kg CO2e for $R = 10$, 20, and 30 miles, respectively.

(4) Although not shown in Table 5.7, it is interesting to look at the number of drone launches per depot per minute as the delivery region size increases. With a drone flight range equal to 10 miles, there are 7,854 drone launches for the DO portion in all optimal solutions, which equates to about 16.3 drone launches per minute or one every 3.7 seconds. Therefore, three launchers per depot are needed if we assume a drone can be launched every 10 seconds. For a delivery region size of $R = 30$ miles, 27 drone launchers or launch stations are required if 9 small depots covering a delivery region size of 10 miles are employed. In contrast, with one large depot serving the entire delivery region of $R = 30$ miles would require only three drone launchers or launch stations. Thus, using small depots

requires 9 times as many staff (e.g., drone personnel) and facilities (e.g., drone launch station) as using one large depot.

5.3.7. Summary of Impacts of Key Parameters on Selected Performance Measures

We have explored the impacts of drone energy consumption rates (Epm_d), the correlation between Epm_d and the unit drone operating cost (c_d), the carbon intensity of electricity (CI_e), the truck capacity for truck-drone delivery (m_{td}), the delivery density (δ), and the size (radius) of the delivery region (R) on a number of performance measures (e.g., utilization of delivery service, delivery costs, delivery emissions, vehicle miles traveled, vehicle hours operated, number of vehicles required). Some of the key findings are summarized in Table 5.8. Column 1 indicates the selected 14 cases (the changes of the parameters relative to the base case level). Column 2-3 show the utilization of DO and TD, respectively. Columns 4-5, 6-7, 8-9, 10-11, and 12-11 show the absolute and percentage reductions (relative to truck-only) in delivery costs, GHG emissions, truck travel distances, driver work hours, and the number of trucks required, respectively. Columns 13-14 show the absolute increase in drone travel distances and the number of drones required, respectively.

Table 5.8. Summary of the performance of the optimal service combination relative to truck-only delivery for different parameter values

Case	DO Use	TD Use	Cost Savings		Emissions Savings		Truck Miles Reduced		Driver Hours Reduced		#Truck Reduced	Drone Miles Increased	#Drones Increased
	(%)	(%)	($)	(%)	(kg CO2e)	(%)	(mile)	(%)	(hour)	(%)	-	(mile)	-
Base case	100.0	0.0	-6,896	-102.6	1,899	60.6	2,861	100.0	248	100.0	31.0	104,720	343.6
$Epm_d/2$	100.0	0.0	-6,896	-102.6	2,515	80.3	2,861	100.0	248	100.0	31.0	104,720	343.6
$10Epm_d$	0.8	99.2	966	14.4	802	25.6	889	31.1	102	41.0	12.7	1,453	18.6
$Epm_d/2$, $0.1c_d$	100.0	0.0	2,529	37.6	2,515	80.3	2,861	100.0	248	100.0	31.0	104,720	343.6
$10Epm_d$, $5c_d$	0.8	99.2	385	5.7	802	25.6	889	31.1	102	41.0	12.7	1,453	18.6
$CI_e/2$	100.0	0.0	-6,896	-102.6	2,515	80.3	2,861	100.0	248	100.0	31.0	104,720	343.6
$1.5CI_e$	77.1	22.9	-4,197	-62.5	1,306	41.7	2,342	81.9	212	85.8	26.6	71,253	238.7
$2m_{td}$	100.0	0.0	-6,896	-102.6	1,899	60.6	2,861	100.0	248	100.0	31.0	104,720	343.6
$5m_{td}$	76.9	23.1	-3,949	-58.8	1,922	61.4	2,520	88.1	217	87.5	27.1	70,989	237.3
$\delta/5$	100.0	0.0	87	13.8	394	88.9	405	100.0	24	100.0	3.1	4,189	13.7
25δ	16.3	83.7	-919	-0.7	12,763	33.1	13,584	38.5	2336	53.3	292.0	178,995	863.1
$2R$	25.0	75.0	-2,278	-7.1	6,268	36.6	6,898	44.1	585	53.4	73.1	109,003	407.5
$3R$	11.1	88.9	8,619	10.3	16,351	33.5	16,186	36.3	1211	44.8	151.3	116,143	529.9
$R/2$	100.0	0.0	-579	-38.2	486	75.9	584	100.0	59	100.0	7.3	13,090	45.0

The partitioning of the delivery region that minimizes GHG emissions can be very different from that that minimizes delivery costs presented in Chapter 4. In many cases, drone-only delivery (DO) is the dominant delivery service and it serves at least 77% of the deliveries in the entire delivery region, whereas truck-drone delivery (TD) serves small percentages of customers (0-23%) who are located far from the depot. However, TD is used extensively when the drone energy consumption rate, the delivery density, and/or the delivery region size are large. In all cases, truck-only delivery (TO) is not used at all.

The percentage emissions savings relative to truck-only delivery in Table 5.8 range from about 26% (or 0.1 kg CO2e/delivery) to 89% (or 1.25 kg CO2e/delivery), with the lowest savings from the high drone energy consumption rate case (10 times the base case) and the highest savings from the very low density case (1/25 of the base case). To put a 26% savings in perspective, it would represent for UPS about 480,000 metric tonnes CO2e savings per year in the U.S. (assuming the daily package volume of 16 million (Holland et al., 2017) and 300 days for a year), which is equivalent to removing more than 100,000 cars from the road for one year (USEPA, 2020).

However, high percentage emissions savings might be achieved by considerably increasing or decreasing the delivery costs, depending on the drone energy consumption rate, the carbon intensity of electricity, the unit drone operating cost, the delivery density, and the delivery region size. The percentage emission and cost savings are both high when drone energy consumption and the unit drone operating cost are both low, and/or the delivery density is low. However, the delivery costs are substantially increased when the drone energy consumption rate and/or the carbon intensity of electricity are low while the unit drone operating cost is as high as the base case level. For example, the 61% emissions

savings (or 0.24 kg CO2e) in the base case is achieved by increasing the delivery costs by about 103% (or $0.88/delivery). Using the same assumption, it would represent for UPS reducing more than one million metric tonnes CO2e per year but at the expense of $5 billion. This suggests a clear tension between the environmental and the financial performance.

If TD is used exclusively for the 14 selected cases, the cost savings relative to TO range from about 11% to 25%, and the emissions savings relative to TO range from about 26% to 50%. This might indicate that the cost and the emissions savings are more balanced by using TD than the emission-minimizing service combination (which largely uses DO) under most circumstances.

5.4 Conclusions

In this chapter, we used a partition of the delivery region based on the best use of different delivery services (i.e., DO, TD, and TO) to minimize GHG emissions. We provided numerical scenarios to illustrate the circumstances in which drone delivery (i.e., DO and TD) provides large and small emissions savings relative to truck-only delivery and quantified the scale of the savings. The potential emissions savings from DO and TD can be huge but depend strongly on the drone energy consumption rate and the carbon intensity of electricity, the delivery density, and the size of the delivery region. The high emissions savings might come at the expense of the delivery costs, which suggests the need to examine the cost and emissions tradeoffs when designing a delivery system.

Chapter 6: Emissions and Cost Tradeoffs of Drone Delivery Systems

In Chapters 4 and 5 we have shown how delivery costs and greenhouse gas (GHG) emissions depend on the use of different delivery services and the key parameters that determine the relative cost and emissions of each delivery service. In this chapter, we explore the tradeoff between the delivery costs and emissions for delivery systems with drones. In section 6.1, we discuss the possible tradeoffs and define the Pareto frontier. In section 6.2, to obtain the Pareto frontier we present an integer programming (IP) model using the cost and emissions expressions derived earlier. In section 6.3, we provide several illustrations of the tradeoff through varying key parameters. Section 6.4 presents the conclusions.

6.1 Definition of Tradeoff and Pareto Frontier

A tradeoff is a balance or compromise achieved between two desirable but incompatible objectives, where one objective improves and the other degrades. The Pareto frontier (or Pareto front, Pareto set) is the set of all Pareto efficient solutions in which no objective can be better off without making another objective worse off. We use the Pareto frontier to graphically evaluate the cost and emissions tradeoff.

The cost and emissions tradeoff is largely driven by the extent of use of drones in drone-only and truck-drone delivery, which is primarily determined by the relative cost- and emissions-efficiencies of drones to trucks. Drone-only delivery is especially important in determining the tradeoff, because it has a larger travel distance per delivery compared

with truck-only and truck-drone delivery due to the drones being assumed to make only one delivery per flight.

6.2 An Integer Programming Model for Computing Cost-Emissions Tradeoffs

In order to construct the Pareto frontier to elucidate the tradeoff between the delivery costs and the GHG emissions, we develop an integer programming model with two objectives, i.e., minimizing the expected total delivery costs (or delivery costs for short) and minimizing the expected total GHG emissions (or GHG emissions for short). This bi-objective optimization model can have an infinite number of Pareto efficient solutions. The Pareto frontier (i.e., a set of all Pareto efficient solutions) can be obtained by the ε-constraint method, i.e., by bounding one of the objectives and adding it as a constraint (Turkensteen and Heuvel, 2019).

6.2.1 Assumptions

To develop the IP model, we consider a circular delivery region of radius R, and discretize this by dividing it into a set of non-overlapping rings of the same width. Each ring is served by one type of delivery service so as to minimize the expected total delivery costs or the expected total GHG emissions. Therefore, the delivery region is partitioned into several subregions with each served by one type of delivery service. The IP model solution provides the optimal partitioning of the service region, and the associated delivery cost and emissions.

With the IP model, we need to ensure the service partitioning is such that (near) optimal swath widths can be used for truck-only and truck-drone delivery. Thus, we require enough consecutive rings to be assigned to define the truck-only and truck-drone subregions, termed a "service region ring", so that the collective width of the service region

ring exceeds the (near) optimal swath width. Suppose the (near) optimal swath for truck-only delivery is w (=0.22 mile), and the width of a single ring is Δ (=0.05 mile), thus, a minimum number of $\left\lceil \frac{w}{\Delta} \right\rceil$ (=5) consecutive rings must be assigned to truck-only. A "service region ring" for truck-only is the number of consecutive rings that is no less than $\left\lceil \frac{w}{\Delta} \right\rceil$ (=5). Figure 6.1 shows a "service region ring" in green comprised of five adjacent rings of width Δ each, where the collective width of the 5 rings (equal to 5Δ) is equal or greater than the swath width. This service region ring would be served with the same delivery service (e.g., TO). For truck-only and truck-drone delivery we use the same truck capacities throughout the service region. We also need to ensure that each service region ring is large enough to include at least as many deliveries as the truck capacity. However, we note that in some cases a lower cost and/or emissions level may be achieved with swath widths and the service region ring width less than the optimal swath widths.

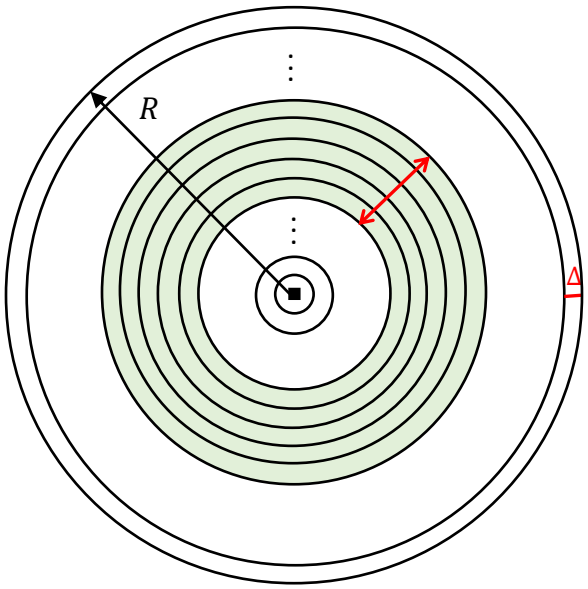

Figure 6.1 An illustration of a service region ring (in green) of radial width 5Δ

The drone is restricted for use within its maximum flight range R_d which is generally less than the radius of the service region ($R_d \leq R$), and we require the expected drone trip distance to be at most half the drone range for truck-drone delivery. This provides the constraint $\delta \geq \frac{40}{3R_d^2}$ (details see subsection 4.2.3 in Chapter 4) and helps ensure that the drone delivery trip length with truck-drone delivery is not too long.

6.2.2 Notation and Mathematical Formulation

The following parameter notations are used in the integer programming (IP) formulation . Let R represents the radius of the circular service region which is divided into a set of rings of small radial width Δ. Each ring is indexed by its sequence when counting from the "ring" that includes the depot. Note the "ring" that includes the depot is actually a small circle with radius of Δ, but for notation convenience we call it ring 0 or the 0th ring. We use $N = \{0, 1, \dots, n, \dots\}$ to represent the set of all rings. Therefore, the distance from the depot to the far-edge of the n^{th} ring can be computed as $d_n = (n+1)\Delta$. Since customers (deliveries) are assumed to be randomly and uniformly distributed over the service region with density δ, the number of deliveries in the n^{th} ring can be computed as $M_n = \delta\pi\left({d_n}^2 - {d_{n-1}}^2\right)$, thus, $M_n = \delta\pi(2n+1)\Delta^2$.

Let $S = \{do, to, td\}$ represent the set of the delivery services, where do, to, and td indicate drone-only delivery, truck-only delivery, and truck-drone delivery, respectively. Let $P = \{c, e\}$ represent the set of objectives, where c indicates the delivery costs, and e indicates the GHG emissions. The truck capacity of service $s \in \{to, td\}$ is denoted by m_s. The near-optimal swath width of service $s \in \{to, td\}$ for objective $p \in \{c, e\}$ is denoted by w_{ps}. Since the radial width of a "service region ring" is at least w_{ps} to ensure the near-

optimal swath width, the minimum number of rings of a "service region ring" is then $L_{ps} = \left\lceil \frac{w_{ps}}{\Delta} \right\rceil$ and $\lceil X \rceil$ is the ceiling function that maps X to the least integer greater than or equal to X. The minimum number of truck routes of service $s \in \{to, td\}$ is denoted by N_s.

Based on equations (4.29) and (5.6) in Chapters 4 and 5, the cost and the emissions per delivery of delivery service $s \in \{do, to, td\}$ at distance d_n can be modeled as $C_{sn} = a_{cs} + b_{cs} d_n$ and $E_{sn} = a_{es} + b_{es} d_n$, respectively. Note we assume the linehaul distance is d_n for customers in the nth ring instead of the expected linehaul distance described in subsection 4.5. Detailed formulations of a_{cs}, a_{es}, b_{cs} and b_{es} are given in Table 6.1. U_c and U_e represent the constants that set the upper bounds of the expected total delivery costs and GHG emissions, respectively.

With the defined parameters , we now define the decision variables and objective functions. Let $x_{sn} \in \{0,1\}$ equal one if delivery service s is assigned to the customers in ring$n$; and 0 otherwise. The expected delivery cost for ring n with delivery service s is modeled as $M_n C_{sn} x_{sn}$, the cost at the far edge of the ring. Thus. the expected total delivery cost for the service region is $z_c = \sum_{s \in S} \sum_{n \in N} M_n C_{sn} x_{sn}$, and the expected total GHG emissions of the service region is $z_e = \sum_{s \in S} \sum_{n \in N} M_n E_{sn} x_{sn}$. The IP model for the delivery system design problem, denoted DSDP, is defined as follows:

Minimize z_c or z_e (6.1)

$s.t.$ $z_e = \sum_{s \in S} \sum_{n \in N} M_n E_{sn} x_{sn} \leq U_e$, or

$z_c = \sum_{s \in S} \sum_{n \in N} M_n C_{sn} x_{sn} \leq U_c$ (6.2)

$\sum_{s \in S} x_{sn} = 1, \quad \forall n \in N$ (6.3)

$$\sum_{i=n}^{n+L_{ps}-1} x_{si} \geq L_{ps}\left(x_{sn} - x_{s(n-1)}\right),\ \forall s \in \{to, td\}, 1 \leq n \leq |N| - L_{ps} + 1 \quad (6.4)$$

$$\sum_{i=|N|-L_{ps}+1}^{|N|} x_{si} \geq L_{ps}\left(x_{s(n+1)} - x_{sn}\right),$$

$$\forall s \in \{to, td\},\ |N| - L_{ps} + 1 < n \leq |N| - 1 \quad (6.5)$$

$$\sum_{i=n-L_{ps}+1}^{n} x_{si} \geq L_{ps}\left(x_{sn} - x_{s(n+1)}\right),$$

$$\forall s \in \{to, td\}, L_{ps} - 1 \leq n \leq |N| - 1 \quad (6.6)$$

$$\sum_{i=0}^{L_{ps}-1} x_{si} \geq L_{ps}\left(x_{s(n-1)} - x_{sn}\right),\ \forall s \in \{to, td\}, 1 \leq n < L_{ps} - 1 \quad (6.7)$$

$$\sum_{i=n}^{|N|} M_n x_{si} \geq N_s m_s x_{sn},\ \forall s \in \{to, td\}, \forall n \in N \quad (6.8)$$

$$x_{sn} \in \{0,1\},\ \forall s \in S, \forall n \in N \quad (6.9)$$

The objective function (6.1) minimizes the expected total delivery costs (z_c) or the expected total GHG emissions (z_e). The GHG emissions or the delivery costs is bounded by constraint (6.2). Constraint (6.3) ensures that each delivery ring is assigned to exactly one delivery service. Constraints (6.4)-(6.7) ensure that the collection of service region rings can fit the (near) optimal swath width for truck-only or truck-drone delivery. Specifically, constraint (6.4) ensures that if ring n is served by service to or service td, while the preceding ring $n-1$ is not served by the same service, then the succeeding adjacent L_{ps} rings are served by the same service as ring n. Constraint (6.5) ensures that the last L_{ps} adjacent rings are the same to or td delivery service if any of them are that service type. Similarly, constraint (6.6) ensures that if ring n is served by service to or service td, while the succeeding ring $n+1$ is not served by the same service, then the preceding adjacent L_{ps} rings are served by the same service as ring n. Constraint (6.7)

ensures that the first L_{ps} adjacent rings are served by the same to or td delivery service if any of them are that service type. Constraints (6.8) ensure that there are adequate number of deliveries in a service region ring for the truck routes. Constraint (6.9) specifies the domain of the decision variables.

Table 6.1. The sets and parameters for the IP model

Notation	Definition	Range/Expression
S	The set of delivery services.	$s \in S = \{do, to, td\}$
P	The set of performance measures.	$p \in P = \{c, e\}$
N	The set of number of rings of width Δ.	$N = \{0, 1, \dots, n\}$
R	The radius of the delivery region.	
R_d	The flight range of the drone.	$R_d \leq R$
Δ	The width of each ring.	
δ	Delivery density.	
d_n	The distance between the far edge of the nth ring and the depot.	$d_n = (n+1)\Delta$
M_n	The number of deliveries within the nth ring.	$M_n = \delta\pi\left[{d_n}^2 - {d_{n-1}}^2\right]$, and $M_n = \delta\pi(2n+1)\Delta^2$
m_s	The truck capacity of delivery service s.	$m_s,\ s \in \{to, td\}$
N_s	The minimum number of truck routes of delivery service s.	$s \in \{to, td\}$, $p \in \{c, e\}$
w_{ps}	The optimal swath width of the truck route of delivery service s.	$s \in \{to, td\}$, $p \in \{c, e\}$
L_{ps}	The minimum number of adjacent rings for service s that uses truck to optimize objective p.	$L_{ps} = \left[\frac{w_{ps}}{\Delta}\right]^+$, $s \in \{to, td\}$, where $[X]^+$takes the integer of $X+1$. We define a collection of these rings as the service region ring.
b_{ps}	The slope of the linear line of objective p using service s.	$b_{cs} \in \{2c_d, \frac{2c_t}{m_{to}}, \frac{2c_t}{m_{td}}\}$, $b_{es} \in \{2e_d, \frac{2e_t}{m_{to}}, \frac{2e_t}{m_{td}}\}$.
a_{ps}	The intercept of the linear line of objective p using service s.	$a_{cs} \in \left\{s_t + s_d, \frac{2c_t}{\sqrt{3\delta}} + s_t, s_t\left(\frac{w_{cs}}{6} + \frac{1}{\delta w_{cs}}\right) + s_d\sqrt{\left(\frac{w_{cs}}{3}\right)^2 + \left(\frac{1}{\delta w_{cs}}\right)^2} + \xi_t + \frac{\xi_d}{2}\right\}$, $a_{es} \in \left\{\xi_t + \xi_d, \frac{2e_t}{\sqrt{3\delta}} + \xi_t, e_t\left(\frac{w_{es}}{6} + \frac{1}{\delta w_{es}}\right) + e_d\sqrt{\left(\frac{w_{es}}{3}\right)^2 + \left(\frac{1}{\delta w_{es}}\right)^2} + \xi_t + \frac{\xi_d}{2}\right\}$.
C_{sn}	The cost per delivery of service s at the nth ring.	$C_{sn} = a_{cs} + b_{cs}d_n$
E_{sn}	The emission per delivery of service s at the nth ring.	$E_{sn} = a_{es} + b_{es}d_n$
U_c	Upper bound of total delivery costs.	
U_e	Upper bound of total GHG emissions.	

6.2.3 The Pareto Frontier and Its Characteristics

The Pareto frontier is a set of all Pareto efficient solutions, and to find the Pareto frontier we solve the DSDP with the following procedure:

Steps 1 and 2 find the two extreme points along the Pareto frontier.

1. Solve DSDP to minimize costs (z_c) without bounding the emissions z_e (i.e., without constraint (6.2)) to obtain the cost-minimizing solution s_c^* and the optimal costs z_c^*. Then solve DSDP to minimize emissions (z_e) with cost constraint (6.2) where $U_c = z_c^*$ to obtain the solution that minimizes emissions with the minimum cost level $z_e(s_c^*)$. The point $(z_e(s_c^*), z_c^*)$ is a Pareto efficient solution.
2. Similarly, solve DSDP to minimize emissions (z_e) without bounding the costs z_c, (i.e., without constraint (6.2)) to obtain the emissions-minimizing solution s_e^* and the optimal emissions z_e^*. Then solve DSDP to minimize costs (z_c) with emissions constraint (6.2) where $U_e = z_e^*$ to obtain the solution that minimizes cost with the minimum emissions level $z_c(s_e^*)$. The point $(z_e^*, z_c(s_e^*))$ is another Pareto efficient solution.

Steps 3 finds intermediate points along the Pareto frontier.

3. To calculate n points spaced along the Pareto frontier, first calculate the step size $\Delta z_c = \frac{z_c(s_e^*) - z_c^*}{n+1}$ (the difference between the optimal cost z_c^* and the cost at the emissions-minimizing point $z_c(s_e^*)$ divided by $n+1$). For $k = 1$ to n, we first solve DSDP to minimize emissions (z_e) with the cost constraint where $U_c = z_c(s_e^*) - k\Delta z_c$. This provides the minimum emissions, denoted z_{ek}^* for a constrained level of cost. Then we solve DSDP to minimize cost with the added

emissions constraint (6.2), where $U_e = z_{ek}^*$. This provides the minimum cost solution, denoted z_{ck}^*, that is constrained by the emissions level z_{ek}^*. (This ensures there is no lower cost solution achievable for that level of emissions, nor a lower emissions solution for that level of cost.) The point found with cost z_{ck}^* is then on the Pareto frontier. Repeating this n times (for $k = 1$ to n) provides n points along the Pareto frontier (some of which may coincide).

Figure 6.2 gives an example of a Pareto frontier (in red) and a set of Pareto efficient solutions. The boxed points show a set of selected feasible solutions (i.e., combinations of delivery services in the service region), and smaller values of costs and emissions are preferred to larger ones. Each feasible solution reflects a certain utilization of truck-only, drone-only, and truck-drone delivery services. The Pareto frontier is constructed by those feasible solutions that are not strictly dominated by any other. For example, point A (the cost-minimizing solution $(z_e(s_c^*), z_c^*)$) and point B (the emissions-minimizing solution $(z_e^*, z_c(s_e^*))$ represent the extreme points for the Pareto frontier. The feasible solutions that form the Pareto frontier are called the Pareto efficient solutions (or Pareto optimal solutions, non-dominated solutions) which reflect the best utilization of all delivery services. Point C is a feasible solution but not a Pareto efficient solution because it is dominated by both point C_1 and point C_2. Therefore, the Pareto frontier shows the best options a decision maker can choose from based on his/her preference for costs and emissions, and provides opportunities for improving current non-efficient solutions.

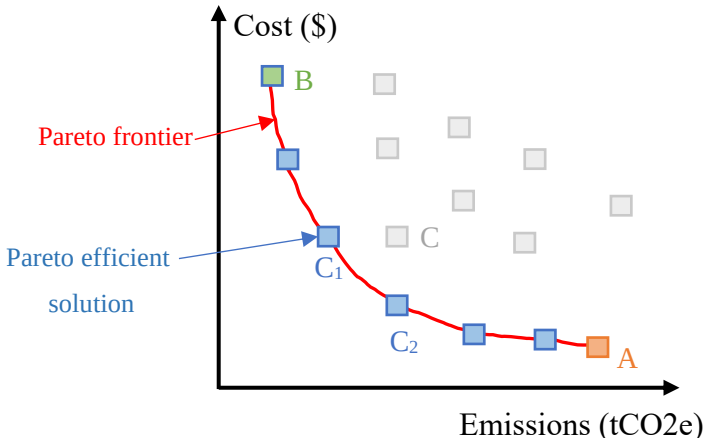

Figure 6.2 An example of a Pareto frontier and a set of Pareto efficient solutions

Solutions along the Pareto frontier can help businesses select the most appropriate delivery services based on their internal assessment of the cost and emissions tradeoffs. It may also be useful to help an agency design regulations or markets to incentivize businesses to move to systems with lower emissions. Since the Pareto frontier in Figure 6.2 is convex, the marginal delivery costs of reducing one extra unit of GHG emissions is non-decreasing (i.e., it is more and more expensive to reduce one more unit of GHG emissions) when moving up the frontier from right to left. This implies a dynamic cost of reducing a given amount of emissions depending on where the initial solution lies on the Pareto frontier. We define this dynamic cost as the marginal emission reduction cost (MERC).

6.3 Illustrations of the Cost and Emissions Tradeoff

A number of feasible scenarios are examined in this section to illustrate the cost and emissions tradeoff by solving the DSDP model with different parameter settings. We consider a delivery region with a radius of 10 miles divided into 200 rings of width 0.05 miles. All computational work was conducted on an Lenovo ThinkPad X1 Carbon 5th

laptop PC with a dual-core Intel i7-7600 CPU and 16 GB RAM running Microsoft Windows 10 Pro in 64-bit mode. The DSDP model was coded using Python version 3.6.3 and solved via GUROBI version 9.0.3 on Spyder IDE. The solution times are all less than 0.1 seconds for 600 decision variables (i.e., with 200 rings for a delivery region with a radius of 10 miles).

The base case results are described in subsection 6.3.1. In subsection 6.3.2, we examine an inexpensive to operate, but energy-intensive drone, and in subsection 6.3.3 we assess the impact of the drone energy consumption rate on the cost and emissions tradeoff. In subsection 6.3.4, we examine the impact of the delivery density on the cost and emissions tradeoff for the inexpensive, but energy-intensive drone. The impact of truck-drone capacity is presented in subsection 6.3.5.

6.3.1 The Base Case

The data for the base case is the same as described in Chapters 4 and 5, and is displayed again for convenience in Table 6.2.

Table 6.2. Definitions and values of parameters for the base case

Parameter	Unit	Definition	Baseline	Reference
R	mile	The radius of the circular delivery region	10	Xu (2017)
δ	#deliveries/mile^2	The number of deliveries per square mile	25	Gulden (2017)
CI_e	kg CO2e/kWh	Carbon intensity of electricity, i.e., the quantity of lifecycle* CO2e emissions produced by consuming 1 kWh of electricity	0.654	Stolaroff et al. (2018)
CI_f	kg CO2e/kWh	Carbon intensity of diesel fuel, i.e., the quantity of lifecycle* CO2e emissions produced by consuming (1/37.6) gallon of diesel	0.335	Stolaroff et al. (2018)
c_t	$/mile	The cost to move a truck one mile	1.25	Campbell et al. (2017)
s_t	$/stop	The cost to make a truck delivery	0.4	Campbell et al. (2017)
f_t	miles per gallon	Truck fuel economy	11.5	Stolaroff et al. (2018)
Epm_t	kWh/mile	$Epm_t = 37.6/f_t$, 1 gallon of diesel = 37.6 kWh (the conversion factor is from Stolaroff et al. (2018))	3.26	Stolaroff et al. (2018)
e_t	kg CO2e/mile	Truck operating emissions per mile $e_t = CI_d \times 37.6/f_t = CI_d \times Epm_t$	1.09	Stolaroff et al. (2018)
ξ_t	kg CO2e/stop	Truck emissions per stop	0	Figliozzi (2017), Stolaroff et al. (2018), Goodchild and Toy (2018)…
m_{to}	#deliveries/route	Number of total deliveries per truck-only route	100	Assumed based on Holland et al. (2017), Stolaroff et al. (2018), Quora
c_d	$/mile	Drone operating cost per mile	0.1	Campbell et al. (2017)
s_d	$/stop	Marginal drone stop cost relative to truck stop cost	0	Campbell et al. (2017)
Epm_d	kWh/mile	The electricity consumption of drones flying one mile	0.018	Stolaroff et al. (2018)
e_d	kg CO2e/mile	The quantity of CO2e emitted by drones flying one mile $e_d = CI_e \times Epm_d$	0.01	Stolaroff et al. (2018)
ξ_d	kg CO2e/stop	Marginal stop emissions of drone relative to truck	0	Figliozzi (2017), Stolaroff et al. (2018), Goodchild and Toy (2018)
R_d	mile	Maximum drone flight range per full battery charge	10	Xu (2017)
m_{td}	#deliveries/route	Number of total deliveries per truck-drone route	150	Assumed

*Lifecycle CO2e emissions includes emissions from the resource extraction, transportation of the resource to the production facility, the creation of the fuel or electricity from various raw materials, the transportation of the fuel or electricity to a fuel or charging station, and then its use to power the vehicle.

Table 6.3 reports 12 Pareto efficient solutions found by solving the DSDP model with the procedure described earlier. Columns 1 and 2 show the utilization of DO and TD in the system designs. Column 3 shows the GHG emissions and column 4 shows the delivery costs. Column 5 shows the marginal emission reduction cost (MERC) for adjacent solutions along the Pareto frontier. The final two rows of Table 6.3 show the cost and emissions pairs for using only TO or TD. Figure 6.3 shows the Pareto frontier (the blue line) created by joining the Pareto efficient solutions (the blue circles). The vertical axis is the expected total delivery cost ($) and the horizontal axis is the expected total GHG emissions (kg CO2e). Table 6.3 shows the MERC changes over the Pareto frontier and that it tends to be increasingly expensive per unit reduction of emissions when moving up Table 6.3 (or moving left in Figure 6.3) from the cost-minimizing solution towards the emissions-minimizing solution. However, rows 6 and 8 in Table 6.3 show two (small) exceptions.

Table 6.3 Pareto efficient solutions for the base case

u(DO)	u(TD)	Emissions	Cost	Marginal Emission Reduction Cost
(%)	(%)	(kg CO2e)	($)	($/tCO2e)
100.0	0.0	1,237	13,653	
91.2	8.8	1,302	12,565	16,738
86.7	13.3	1,337	12,060	14,429
80.1	19.9	1,387	11,275	15,700
72.6	27.5	1,450	10,492	12,429
65.0	35.0	1,513	9,702	12,540
56.6	43.5	1,587	8,911	10,689
47.7	52.3	1,666	8,123	9,975
37.4	62.6	1,766	7,332	7,910
28.1	71.9	1,860	6,720	6,511
25.1	74.9	1,892	6,544	5,500
1.4	98.6	2,170	5,754	2,842
0.0	100.0	2,186	5,759	
0.0	0.0	3,132	6,718	

The Pareto frontier in Figure 6.3 appears to be convex and nearly linear for lower levels of expected GHG emissions (high values of expected cost). The absolute value of the slope of the Pareto frontier could be interpreted as the marginal cost of reducing emissions which indicates the incremental change in delivery costs per unit change in GHG emissions (i.e., MERC), which is generally non-decreasing as also evidenced in Column 5 of Table 6.3. This indicates that it is lowest cost per unit to reduce GHG emissions when emissions are at the highest level on the Pareto frontier.

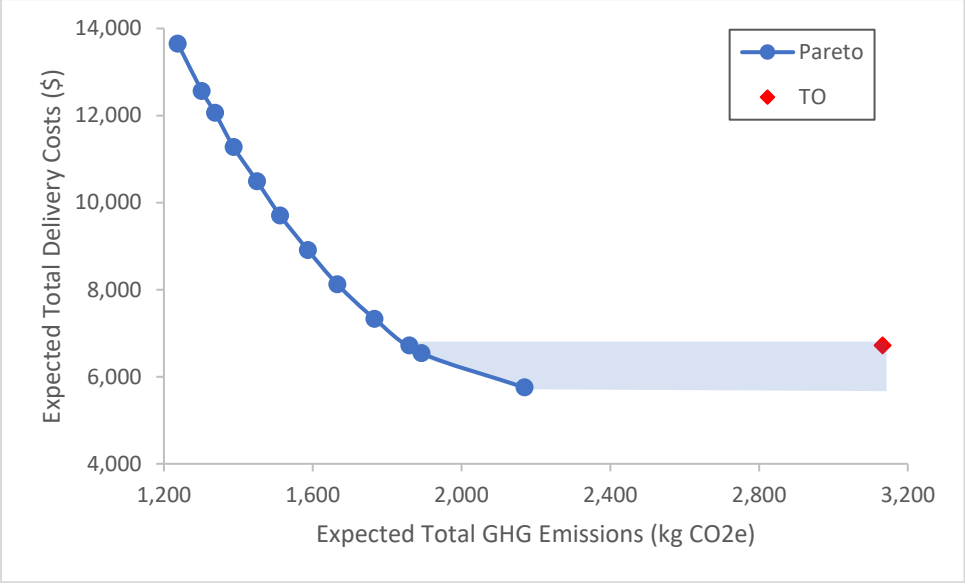

Figure 6.3. An illustration of the Pareto frontier for the base case drone (i.e., $c_d =$ \$0.1/mile, $Epm_d =$18 Wh/mile)

Figure 6.3 also shows the current operation (red diamond) that reflects the baseline delivery service (i.e., truck-only delivery), which is far to the right of the Pareto frontier (i.e., it has much higher emissions). The blue shaded area highlights Pareto superior improvements from moving from truck-only delivery toward the Pareto frontier. Any solution in the shaded area dominates the truck-only solution, i.e., both the GHG emissions

and the delivery costs can be reduced compared with truck-only. The maximum amount of costless emission reduction (i.e., the amount of GHG emissions that can be reduced with no increase in the delivery costs) relative to truck-only delivery is about 1,272 kg CO2e (i.e., a 41% reduction). The maximum amount of cost reduction in the shaded region is $964 (i.e. a 14.3% reduction) which can be achieved by reducing GHG emissions simultaneously by 962 kg CO2e (or 31%). Moving away from the existing truck-only delivery solution to other Pareto efficient solutions outside of the shaded area on the Pareto frontier involves an increase in delivery costs to reduce GHG emissions. For example, moving to the emissions-minimizing solution (upper left point of Figure 6.3) increases the expected total delivery costs by $6,935 (or 103%) and reduces the expected total GHG emissions by 1,895 kg CO2e (or 61%).

Figure 6.4 shows exactly how much DO and TD services are used for each Pareto efficient solution on the Pareto frontier in Figure 6.3. The secondary vertical axis on the right shows the utilization of DO and TD as percentages of total deliveries. The green shaded area represents the percent utilization of DO, and the hatched orange striped area represents the percent utilization of TD. As the Pareto efficient solution moves from left to right (i.e., from the emission-minimizing solution to the cost-minimizing solution), the utilization of drone-only delivery decreases from 100% to 1.5%, whereas the utilization of truck-drone delivery increases from 0% to 98.5%.

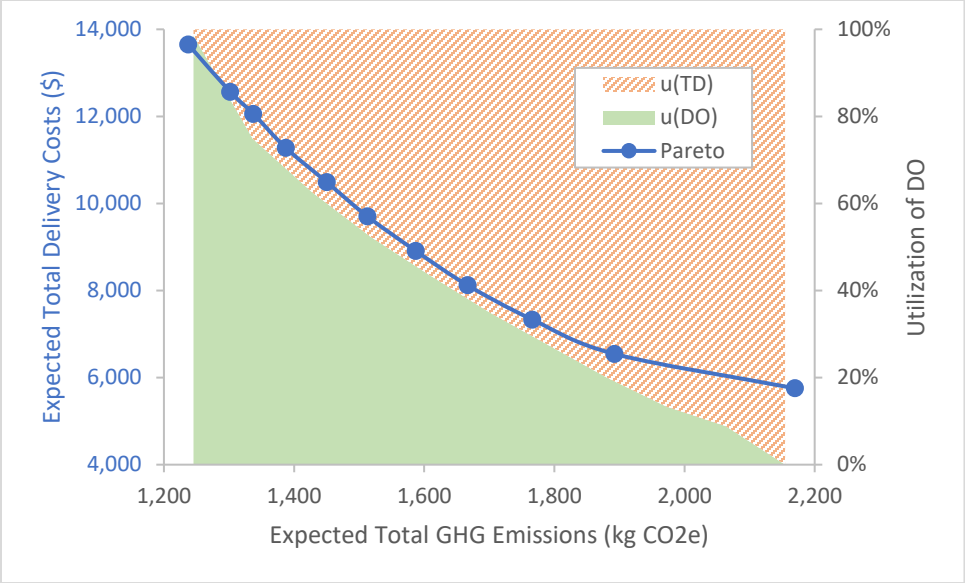

Figure 6.4 The Pareto frontier with the utilization of truck-drone and drone-only for the base case drone (i.e., c_d = \$0.1/mile, Epm_d =18 Wh/mile)

Figures 6.5 (a) and (b) provide more detail on the two extreme Pareto efficient solutions, i.e., the cost- and the emissions-minimizing solutions. These figures show the expected delivery cost and the expected GHG emissions of each of the three delivery services as a linear function of distance from the depot. Truck-only (TO) delivery is represented by the blue solid line, drone-only (DO) delivery by the green dashed line, and truck-drone (TD) delivery by the orange long-dash line. The red triangles indicate the optimal services that make up the cost- and the emission- minimizing delivery systems. This shows for the base case how TD delivery is more cost-efficient than TO delivery except near the depot (within 1.7 miles) and how TD delivery is much more environmentally-friendly than TO delivery at any distance from the depot. Note that TO is the most expensive service beyond about 2 miles for the depot (Figure 6.5(a)), but it is by far the most environmentally-friendly delivery service at all distances (Figure 6.5(b)). Thus the heavy use of DO to minimize emissions, leads to a very high level of cost.

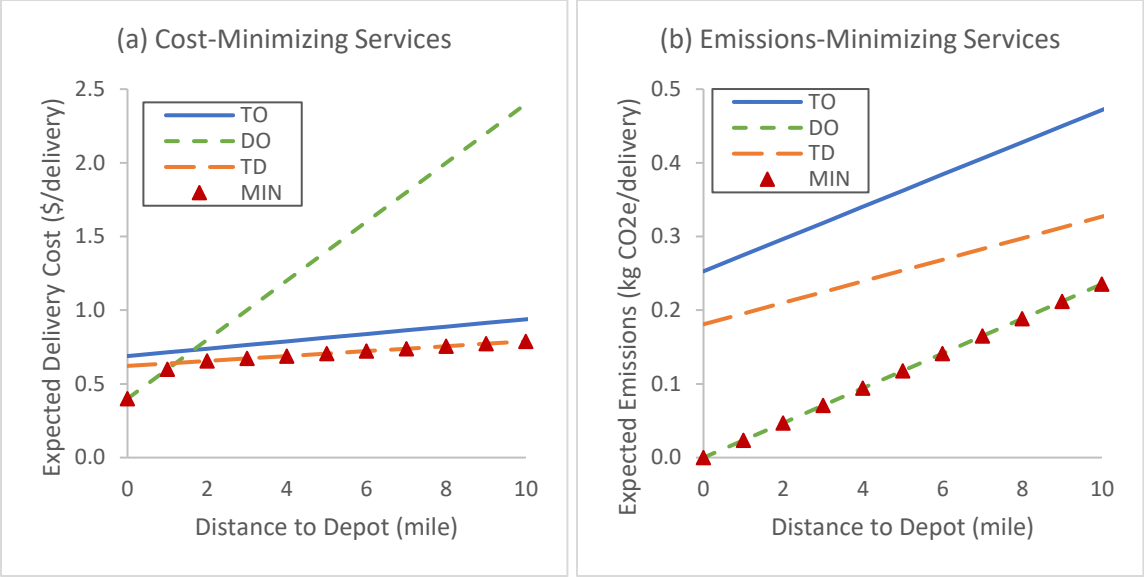

Figure 6.5: (a) Expected delivery costs and (b) expected GHG emissions of each delivery service as a function of distance from the depot

Some other findings from the analysis of the base case are:

(1) Comparing the emissions minimizing system (100% drone-only) with the cost minimizing system (98.6% truck-drone and 1.4% drone-only) shows that the expected total delivery costs are increased by $7,854 from $5,760 to $13,614 (a 136% increase), whereas the expected total GHG emissions are reduced by 933 kg CO2e from 2,166 to 1,233 kg CO2e (a 43% reduction). This indicates that the emissions are very expensive to reduce in the base case, an emissions reduction cost per ton of $8,418 between the two extreme points of the Pareto frontier.

(2) Compared with truck-only delivery (the baseline service), moving to the cost-minimizing services (98.6% truck-drone and 1.4% drone-only) reduces both the expected total delivery costs and GHG emissions, by $968 (or 14.4%) and 966 kg CO2e (or 30.8%), respectively;

(3) Compared with truck-only delivery (the baseline service), moving to the emissions-minimizing service (100% DO) increases the expected total delivery costs by $6,896 (or 102.6%) and reduces the expected total GHG emissions by 1,899 kg CO2e (or 60.6%), an emissions reduction cost per ton of $3,631/tCO2e.

(4) Shifting from TO to a greater use of DO and TD reduces the number of deliveries by truck, and the work hours for truck drivers, and the number of trucks required. For example, the number of trucks required is reduced from 31 for 100% TO to 19 for the cost-minimizing services (98.6% truck-drone and 1.4% drone-only) and to zero for the emissions-minimizing service (100% DO). This shift increases the number of drones required from zero for 100% TO, to 19 for the cost-minimizing services (98.6% truck-drone and 1.4% drone-only) and to 344 for the emissions-minimizing service (100% DO), assuming drones work for 8-hours per day.

6.3.2 An Inexpensive, but Energy-intensive Drone

In this section, we consider a drone that is very inexpensive to operate, but energy-intensive. The drone operating cost is only 20% of the base case, i.e., $c_d = \$0.02$/mile, whereas the drone energy consumption rate is 10 times the base case, i.e., $Epm_d = 180$ Wh/mile. This setting might reflect drone deliveries operated fully autonomously at scale, where the drones might be large in size with sophisticated functionalities, and/or powered by electricity from "dirty" generation, and/or operated at high speeds (to meet the ever increasing demand for fast delivery). All other parameter values remain the same as for the base case.

Similar to Table 6.3, Table 6.4 reports the Pareto efficient solutions from solving the DSDP model. Columns 1 and 2 shows the utilization of DO and TD, respectively.

Column 3 shows the GHG emissions and column 4 shows the delivery costs. Column 5 shows the marginal emission reduction cost (MERC). The final two rows show the cost and emissions pairs for TO and TD. Figure 6.6 shows the estimated Pareto frontier created by joining the Pareto efficient solutions presented in Table 6.4. As the Pareto efficient solution moves closer to the cost-minimizing solution (moving down in Table 6.4 and moving towards the right in Fig. 6.6), the MERC decreases. This again shows how the MERC changes and that it is less expensive per unit reduction in GHG emissions when the emissions level is relatively high than when the level is relatively low. However, the magnitudes of the MERC presented in Table 6.4 ($12 - $705) are much lower than that presented for the base case in Table 6.3 ($2,842 - $16,738). Thus, it is much more affordable to reduce emissions with the inexpensive, but energy-intensive drone, compared to the base case. This highlights the importance of drone technology, drone operations and electricity generation.

Table 6.4 Pareto efficient solutions for the inexpensive but energy-intensive drone case

u(DO)	u(TD)	Emissions	Cost	Marginal Emission Reduction Cost
(%)	(%)	(kg CO2e)	($)	($/tCO2e)
0.8	99.2	2,335	5,637	
7.0	93.0	2,447	5,558	705
7.6	92.4	2,464	5,552	353
11.6	88.4	2,617	5,509	281
15.6	84.4	2,813	5,471	194
20.7	79.3	3,112	5,428	144
26.5	73.5	3,513	5,385	107
33.1	66.9	4,032	5,344	79
41.0	59.0	4,744	5,303	58
51.8	48.2	5,863	5,262	37
79.2	20.8	9,280	5,222	12
0.0	100.0	2,336	5,646	
0.0	0.0	3,132	6,718	

The shape of the Pareto frontier in Fig. 6.6 is very different than that for the base case in Fig. 6.3, although both appear to be convex. Moving from right to left, Fig. 6.6 starts much flatter than Fig. 6.3 but then gets steep when approaching the left end. This shows how drone operating cost and energy consumption per mile can change the shape of the Pareto frontier and the underlying cost and emissions tradeoff.

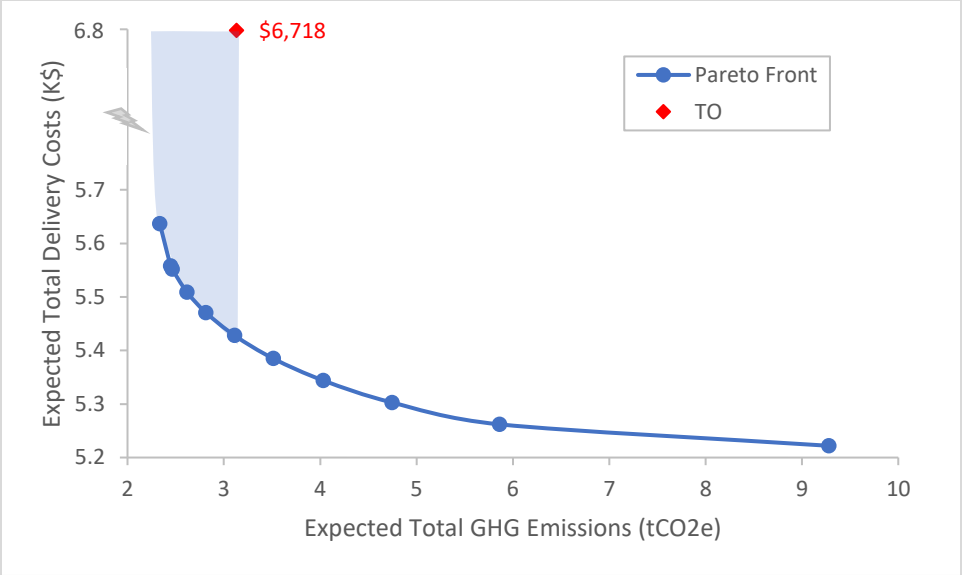

Figure 6.6 An illustration of the Pareto frontier for an inexpensive but energy-intensive drone (i.e., c_d = \$0.02/mile, Epm_d =180 Wh/mile)

Figure 6.6 also shows baseline solution of 100% truck-only delivery with the red diamond. The shaded blue area indicates the Pareto superior improvements available to the baseline solution when moving toward the Pareto frontier. Contrary to the base case observation in Fig. 6.3, Fig. 6.6 has the emissions-minimizing solution under the blue shaded area which indicates it is a Pareto superior improvement for truck-only delivery, whereas the cost-minimizing solution is not Pareto superior to truck-only delivery as it involves much greater emissions. The maximum emissions reduction compared to truck-

only delivery is about 797 kg CO2e (a 25% reduction) which can be achieved by reducing delivery costs simultaneously by $1,065 (or 16%). The maximum amount of cost reduction from 100% truck-only with no increase in GHG emissions is $1,496 (a 22% reduction). A tradeoff of costs and emissions is required when shifting from the 100% truck-only delivery system to a Pareto efficient solution outside the shaded area. For example, moving to the cost-minimizing solution from truck-only delivery reduces the delivery costs by $1,496 (or 29%) at the expense of increasing GHG emissions by 6,148 kg CO2e (or 196%).

Figure 6.7 shows the utilization of drone-only and truck-drone for the Pareto efficient solutions in Figure 6.6. The secondary vertical axis shows the utilization of drone-only delivery and truck-drone delivery as percentages of the total deliveries. The green shaded area represents the percent utilization of drone-only, and the orange striped area represents the percent utilization of truck-drone. As the Pareto efficient solution moves from left to right (i.e., from the emission-minimizing solution to the cost-minimizing solution), the utilization of drone-only delivery increases from 0.8% to 79.2%, whereas the utilization of truck-drone delivery decreases from 99.2% to 20.8%.

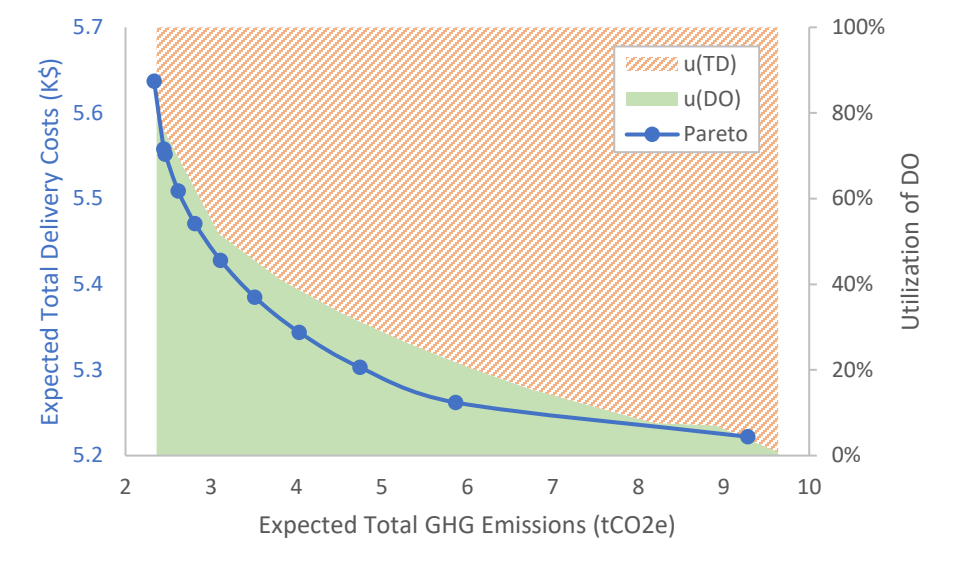

Figure 6.7 The Pareto frontier with the utilization of truck-drone and drone-only for an inexpensive, but energy-intensive drone (i.e., c_d = \$0.02/mile, Epm_d =180 Wh/mile)

6.3.3 The Impact of Drone Operating Cost and Energy Consumption Rates

This section examines the impact of the drone operating cost and energy consumption rate on the cost, emissions and delivery services used. The cost and emissions savings relative to truck-only delivery and the Pareto frontier strongly depend on the drone operating cost per mile (c_d) and the drone energy consumption per mile (Epm_d). Both c_d and Epm_d are very uncertain, therefore, we fix the two levels of c_d discussed in previous subsections (i.e., c_d = \$0.1/mile and c_d = \$0.02/mile) and vary Epm_d from 9 to 360 Wh/mile. We also fix the two levels of Epm_d discussed in previous subsections (i.e., Epm_d = 18 Wh/mile and Epm_d = 180 Wh/mile) and vary c_d from \$0.01/mile to \$0.5/mile.

Figures 6.8(a) and (b) show the Pareto frontiers associated with the different levels of Epm_d for c_d = \$0.1/mile and c_d = \$0.02/mile, respectively. Each Pareto efficient

solution reflects a certain utilization of drone-only delivery and truck-drone delivery. The lines with squares, circles, triangles, diamonds, and multiplication signs represent the Pareto frontiers for Epm_d =9, 18, 60, 180, and 360 Wh/mile, respectively. The darker the color, the greater the Epm_d value. Figures 6.8(c) and (d) show the Pareto frontiers associated with the different levels of c_d for $Epm_d = 18$ Wh/mile and $Epm_d = 180$ Wh/mile, respectively. The lines with squares, circles, triangles, diamonds, and multiplication signs represent the Pareto frontiers for $c_d = 0.5$, 0.1, 0.05, 0.02, and 0.01 $/mile, respectively. The lighter the color, the greater the c_d value. The red diamond represents the delivery system that uses 100% truck-only delivery. Please note that the vertical and horizontal scales of Figures 6.8(a)-(d) can be very different.

Figures 6.8(a)-(d) reveal very interesting phenomena about the impacts of c_d and Epm_d on the Pareto frontier and the cost and emissions savings relative to truck-only delivery. We first present an overview of the results and then elaborate with more detail for each graph. Figures 6.8(a)-(d) indicate that a relatively high c_d with a relatively high Epm_d or a relatively low c_d with a relatively low Epm_d can generate solutions that provide both cost and emissions savings relative to truck-only delivery (e.g., the Pareto efficient solutions below and to the left of the red diamond and red dashed line in Fig. 6.8(a) and (b), respectively). However, a relatively high c_d with a relatively low Epm_d or a relatively low c_d with a relatively high Epm_d can generate solutions that involve a tradeoff between cost and emissions (e.g., the Pareto efficient solutions above or to the right of the red dashed line in Fig. 6.8(a) and (b), respectively). For a relatively high c_d and low Epm_d (see Fig. 6.8(a) and Fig. 6.8(c), emissions can be reduced to a certain extent but at a considerable expense from increasing delivery costs relative to truck-only delivery. For a

relatively low c_d and high Epm_d (see Fig. 6.8(b) and Fig. 6.8(d)), emissions can be reduced only modestly but with a cost savings!

The Pareto frontiers are narrower (or involve smaller cost and emissions tradeoffs) for relatively high c_d and high Epm_d, or relatively low c_d and low Epm_d, compared with those for relatively high c_d and low Epm_d or relatively low c_d and high Epm_d. For example, in Fig. 6.8(a) the line with diamonds, i.e., the Pareto frontier for $Epm_d = 180$ Wh/mile, appears to be just one point, whereas the line with squares, i.e., the Pareto frontier for $Epm_d = 9$ Wh/mile, is a much longer line. Furthermore, the higher the c_d and Epm_d, the closer the Pareto frontier moves toward a 100% TO delivery system (the red diamond), indicating smaller (or even negative) cost and emission savings relative to truck-only delivery. The lower the c_d and Epm_d, the farther the Pareto frontier moves away from the baseline operation of TO, indicating greater cost and emission savings relative to truck-only delivery.

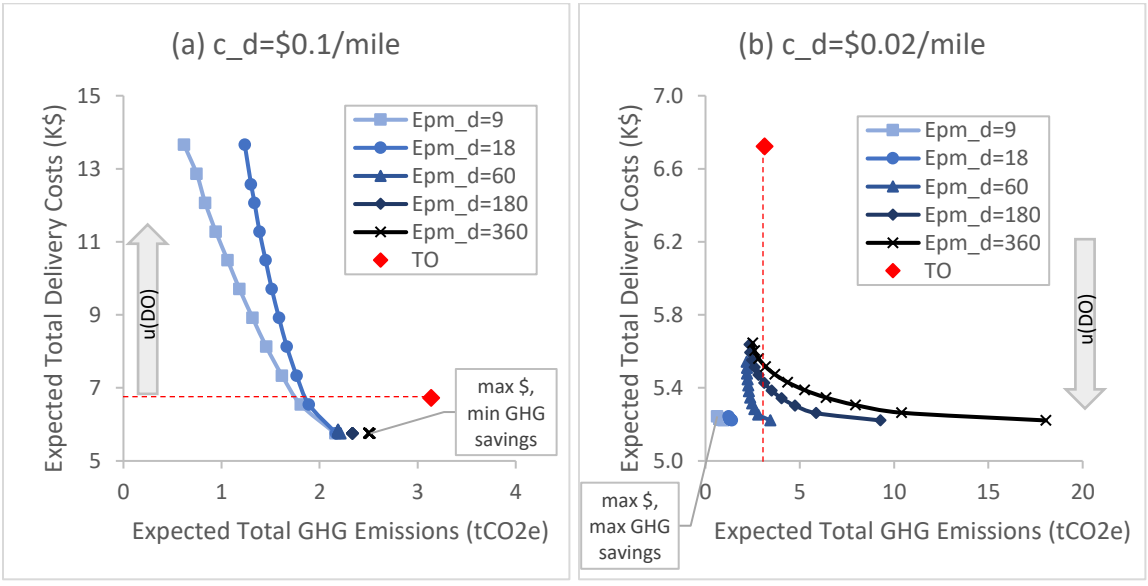

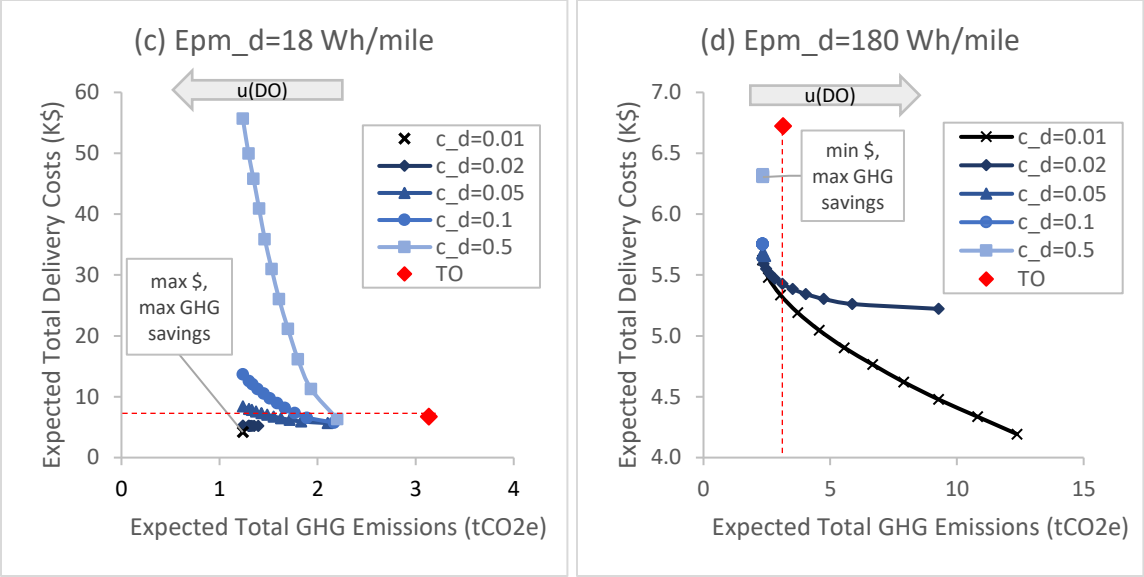

Figure 6.8: The impact of c_d and Epm_d on the cost and emissions tradeoff and savings relative to truck-only delivery

Figure 6.8 (a) shows that when drone operating cost per mile (c_d) is relatively high, the Pareto frontiers are to the left of the baseline operation of TO and that these involve only drone-only delivery (DO) and truck-drone delivery (TD) for the plausible range of Epm_d (9-360 Wh/mile). This indicates that drone delivery can reduce GHG emissions compared with truck-only delivery (TO) but the emission reduction might be achieved by increasing or decreasing delivery costs depending on Epm_d and the utilization of DO and TD. The emission reduction relative to truck-only increases as Epm_d decreases for the same use of services (i.e., moving horizontally to the left across different Pareto frontiers in Fig. 6.8(a)) or as the utilization of DO increases for the same Epm_d (i.e., moving along the same Pareto frontier to the left in Fig. 6.8(a)), whereas the associated cost reduction relative to truck-only is non-increasing (negative cost reduction indicates cost increase). The minimum emission reduction is about 617 kg CO2e (or 20%) with the maximum cost reduction of \$969 (or 14%) relative to truck-only at $Epm_d = 360$ Wh/mile where TD

serves 98.6% of the deliveries. For relatively high Epm_d values ($\geq$ 60 Wh/mile) or for relatively low Epm_d values with high utilizations of TD delivery ($\geq$72%), the Pareto efficient solutions are below the red dashed line in Fig. 6.8(a) which indicates they provide both cost and emission reductions relative to truck-only delivery. The maximum cost reduction relative to truck-only is about $969 (or 14%) regardless of Epm_d, as we have observed for the base case. This is because the same utilization of services are used to minimize delivery costs regardless of Epm_d. The maximum emission reduction with no increase in delivery costs is about 1,376 kg CO2e (or 44%) relative to truck-only delivery with $Epm_d = 9$ Wh/mile.

However, there is a tradeoff of cost and emission when moving from truck-only delivery towards the Pareto efficient solutions above the red dashed line, which correspond to relatively low Epm_d values with high utilizations of DO delivery. Interestingly, the maximum increase in delivery costs relative to truck-only delivery is about $6,930 (or 103%) for both $Epm_d = 9$ and 18 Wh/mile where DO is 100% used. This indicates emissions can be further reduced without increasing delivery costs when the utilization of services that minimize emissions does not change as Epm_d decreases.

Figure 6.8(b) shows that when drone operating cost per mile is relatively low (i.e., $c_d = \$0.02$/mile), the Pareto frontiers are below the current operation and again these solutions involve only DO and TD for the plausible range of Epm_d (9-360 Wh/mile). This indicates that drone delivery can reduce delivery costs compared with truck-only delivery, and that the cost reduction might be achieved by increasing or decreasing GHG emissions depending on Epm_d and the utilization of DO and TD. The cost reduction relative to truck-only delivery stays almost the same as Epm_d decreases for the same use of services (i.e.,

moving horizontally to the left across different Pareto frontiers in Fig. 6.8(b)) or increases as the utilization of DO increases for the same Epm_d (i.e., moving along the same Pareto frontier to the right in Fig. 6.8(b)), whereas the associated emission reduction relative to truck-only delivery increases as Epm_d decreases for the same use of services, or decreases as the utilization of DO increases for the same Epm_d (negative reduction indicates an emissions increase). The maximum cost reduction is about $1,501 (or 22%) relative to truck-only regardless of Epm_d. This is because the same utilization of services are used to minimize delivery costs regardless of Epm_d. The minimum cost reduction to reach a Pareto frontier is about $1,077 (or 16%) with the associate emissions reduction of 631 kg CO2e (or 20%) relative to truck-only delivery with $Epm_d = 360$ Wh/mile where TD delivery serves 99.8% of the deliveries. For relatively low Epm_d values (< 60 Wh/mile) or relatively high Epm_d values with modest to high utilizations of TD delivery ($\geq$32%), the Pareto efficient solutions are to the left of the red dashed line in Fig. 6.8(b) which indicate that both cost and emission reductions relative to truck-only delivery can be achieved. The emissions reduction relative to truck-only delivery increases as Epm_d decreases. The maximum emission reduction is about 2,518 kg CO2e (or 80%) with the associated near-maximum cost reduction of $1,479 (or 22%) relative to truck-only delivery with $Epm_d = 9$ Wh/mile. However, There is a tradeoff of cost and emission when moving from truck-only delivery towards the lowest cost Pareto efficient solutions to the right of the red dashed line that are generated from relatively high Epm_d values with high utilizations of DO delivery (and large emissions).

Similar to Fig. 6.8(a), Figure 6.8(c) shows that when drone energy consumption per mile (Epm_d) is relatively low, the Pareto frontiers are to the left of truck-drone delivery

and again involve only DO and TD for the plausible range of c_d ($0.01 - $0.5/mile), indicating that drone delivery can reduce GHG emissions compared with truck-only delivery, but the emissions reduction might be achieved by increasing or decreasing delivery costs depending on c_d and the utilization of DO and TD. The emissions reduction relative to truck-only delivery stays almost the same as c_d decreases for the same use of services (i.e., moving vertically down across different Pareto frontiers in Fig.6.8(c)) or increases as the utilization of DO increases for the same c_d (i.e., moving along the same Pareto frontier up and to the left in Fig. 6.8(c)), whereas the associated cost reduction relative to truck-only delivery increases as c_d decreases for the same use of services or decreases as the utilization of DO increases for the same c_d (negative reduction indicates cost increase). The maximum emissions reduction is about 1,899 kg CO2e (or 61%) relative to truck-only regardless of c_d. This is because the same utilization of services is employed to minimize emissions regardless of c_d. The minimum emissions reduction is about 934 kg CO2e (or 30%) with the associate cost reduction of $419 (or 6%) relative to truck-only delivery with $c_d = $0.5/mile. For relatively low c_d values ($< $0.05/mile) or relatively high c_d values with modest to high utilizations of TD delivery ($\geq$41%), the Pareto efficient solutions are below the red dashed line in Fig. 6.8(c) which indicates that both cost and emissions savings relative to truck-only delivery can be achieved. The cost reduction relative to truck-only delivery increases as c_d decreases. The maximum cost reduction of $2,530 (or 38%) with the maximum emission reduction of 1,899 kg CO2e (or 61%) relative to truck-only deliver is achieved simultaneously with $c_d = $0.01/mile. Again, there is a tradeoff of cost and emissions when moving from truck-only delivery

toward the Pareto efficient solutions above the red dashed line that are generated from relatively high c_d values with modest to high utilizations of DO delivery.

Figure 6.8(d) shows that when drone energy consumption per mile (Epm_d) is relatively high (180 Wh/mile), the Pareto frontiers are below the current operation and involve only DO and TD for the plausible range of c_d ($0.01 - $0.5/mile), indicating that drone delivery can reduce the delivery costs compared with truck-only delivery but the cost reduction might be achieved by increasing or decreasing GHG emissions depending on c_d and the utilization of DO and TD. The cost reduction relative to truck-only delivery increases as c_d decreases for the same use of services (i.e., moving vertically down across different Pareto frontiers in Fig.6.8(d)) or as the utilization of DO increases for the same c_d (i.e., moving down and to the right along the same Pareto frontier in Fig. 6.8(d)), whereas the associated emissions reduction relative to truck-only delivery is non-increasing (negative reduction indicates cost increase). The maximum emissions that can be reduced is about 800 kg CO2e (or 26%) relative to truck-only delivery regardless of c_d. This is because the same utilization of services are used to minimize emissions regardless of c_d. For relatively high c_d values ($\geq$ $0.05/mile) or relatively low c_d values with high utilizations of TD delivery ($\geq$79%), the Pareto efficient solutions are to the left of the red dashed line in Fig. 6.8(d) which indicates that both cost and emissions savings relative to truck-only delivery can be achieved. The minimum cost reduction of $419 (or 6%) with the maximum emission reduction of 793 kg CO2e (or 25%) relative to truck-only delivery is achieved at $c_d = $0.5/mile. The maximum cost reduction with no increase in GHG emissions is about $1,408 (or 21%) relative to truck-only delivery with $c_d = $0.01/mile where TD serves 79% of the deliveries. Once again, there is a tradeoff of cost and emissions

when moving from truck-only delivery towards the Pareto efficient solutions to the right of the red dashed line that are generated from relatively low c_d values with modest to high utilizations of DO delivery.

Table 6.5 summarizes the cost and emission savings relative to truck-only delivery for $c_d =$ \$0.1/mile and \$0.01/mile with Epm_d varying from 9 to 360 Wh/mile. Table 6.6 summarizes the cost and emission savings relative to truck-only delivery for $Epm_d = 18$ Wh/mile and 180 Wh/mile with c_d varying from \$0.01/mile to \$1.0/mile. Row 1 of Tables 6.5 and 6.6 shows Epm_d and c_d, respectively. Row 2 shows the ratio of the operating cost per mile to the operating emissions per mile for drone (i.e., $\frac{c_d}{e_d}$) in \$/kg CO2e. The reason for showing this ratio is that we observe that there is no tradeoff between cost and emission when the cost rate to emissions rate ratio for drone ($\frac{c_d}{e_d}$) is close to that for truck ($\frac{c_t}{e_t}$, which is 1.14 for the base case). Rows 3 and 4 show the maximum absolute and percentage emissions reductions relative to truck-only delivery, respectively. Rows 5 and 6 show the absolute and percentage cost reductions relative to truck-only delivery that are associated with the solutions in rows 3 and 4, respectively. Rows 7 and 8 show the maximum absolute and percentage cost reductions relative to truck-only delivery, respectively. Rows 9 and 10 show the absolute and percentage emission reductions relative to truck-only delivery that are associated with the solutions in rows 7 and 8, respectively. Rows 11-19 correspond to rows 2-10.

Table 6.5 shows that the maximum emission reduction relative to truck-only delivery decreases as Epm_d increases, whereas the maximum cost reduction relative to truck-only delivery does not change. The cost reduction associated with the maximum

emissions reduction is maximized when $\frac{c_d}{e_d} = \frac{c_t}{e_t} = 1.14$. Table 6.6 shows that the maximum emissions reduction relative to truck-only delivery stays almost the same as c_d increases, whereas the maximum cost reduction relative to truck-only delivery decreases. The emissions reduction associated with the maximum cost reduction is maximized when the cost rate to emissions are ratio for drone and truck are equal, i.e., $\frac{c_d}{e_d} = \frac{c_t}{e_t}$. When $\frac{c_d}{e_d}$ is considerably smaller than $\frac{c_t}{e_t}$, minimizing delivery costs will result in huge tradeoffs between cost and emissions. When $\frac{c_d}{e_d}$ is considerably greater than $\frac{c_t}{e_t}$, minimizing GHG emissions will result in huge tradeoffs between cost and emissions. This indicates that whenever there is a considerable asymmetry between $\frac{c_d}{e_d}$ and $\frac{c_t}{e_t}$, very different utilizations of services are used to minimize delivery costs and GHG emissions, which results in large cost and emission tradeoffs.

Table 6.5 The cost and emission savings relative to truck-only delivery for c_d = \$0.1/mile and \$0.02/mile with Epm_d varying from 9 to 360 Wh/mile.

	Epm_d	(Wh/mile)	9	18	26.8	30	36	45	60	90	134	180	360
c_d =\$0.1/mile	c_d/e_d	(\$/kg CO2e)	16.99	8.49	5.71	5.10	4.25	3.40	2.55	1.70	**1.14**	0.85	0.42
	Max Emission Reduction	(kg CO2e)	2,518	1,899	1,314	1,195	1,081	1,004	949	897	**848**	803	636
		(%)	80.3	60.5	41.9	38.1	34.5	32.0	30.3	28.6	**27.0**	25.6	20.3
	Associate Cost Reduction	(\$)	-6,930	-6,930	-4,453	-1,994	-189	569	870	960	**969***	967	963
		(%)	-103.1	-103.1	-66.2	-29.7	-2.8	8.5	12.9	14.3	**14.4**	14.4	14.3
	Max Cost Reduction	(\$)	969	969	969	969	969	969	969	969	**969**	969	969
		(%)	14.4	14.4	14.4	14.4	14.4	14.4	14.4	14.4	**14.4**	14.4	14.4
	Associate Emission Reduction	(kg CO2e)	976	967	958	954	948	939	924	893	**848**	801	617
		(%)	31.1	30.8	30.5	30.4	30.2	29.9	29.5	28.5	**27.0**	25.5	19.7
c_d =\$0.02/mile	c_d/e_d	(\$/kg CO2e)	3.40	1.70	**1.14**	1.02	0.85	0.68	0.51	0.34	0.23	0.17	0.08
	Max Emission Reduction	(kg CO2e)	2,518	1,899	**1,314**	1,196	1,081	1,005	949	897	847	801	631
		(%)	80.3	60.5	**41.9**	38.1	34.5	32.0	30.3	28.6	27.0	25.5	20.1
	Associate Cost Reduction	(\$)	1,479	1,479	**1,501***	1,467	1,369	1,266	1,180	1,119	1,095	1,086	1,077
		(%)	22.0	22.0	**22.3**	21.8	20.4	18.8	17.6	16.6	16.3	16.1	16.0
	Max Cost Reduction	(\$)	1,501	1,501	**1,501**	1,501	1,501	1,501	1,501	1,501	1,501	1,501	1,501
		(%)	22.3	22.3	**22.3**	22.3	22.3	22.3	22.3	22.3	22.3	22.3	22.3
	Associate Emission Reduction	(kg CO2e)	2,180	1,742	**1,314**	1,158	866	428	-302	-1,763	-3,900	-6,144	-14,906
		(%)	69.5	55.5	**41.9**	36.9	27.6	13.6	-9.6	-56.2	-124.3	-195.9	-475.3

Table 6.6 The cost and emission savings relative to truck-only delivery for $Epm_d = 18$ Wh/mile and 180 Wh/mile with c_d varying from \$0.01/mile to \$1.0/mile.

	c_d	**(\$/mile)**	**0.01**	**0.013**	**0.02**	**0.03**	**0.04**	**0.05**	**0.1**	**0.13**	**0.5**	**0.8**	**1.0**
$Epm_d = 18$ Wh/mile	c_d/e_d	(\$/kg CO2e)	0.85	**1.14**	1.70	2.55	3.40	4.25	8.49	11.38	42.47	67.96	84.95
	Max Emission Reduction	(kg CO2e)	1,899	**1,899***	1,899	1,899	1,899	1,899	1,899	1,899	1,899	1,899	1,899
		(%)	60.5	**60.5**	60.5	60.5	60.5	60.5	60.5	60.5	60.5	60.5	60.5
	Associate Cost Reduction	(\$)	2,530	**2,173**	1,479	428	-623	-1,675	-6,930	-10,504	-48,975	-80,508	-101,530
		(%)	37.6	**32.3**	22.0	6.4	-9.3	-24.9	-103.1	-156.2	-728.5	-1197.6	-1510.3
	Max Cost Reduction	(\$)	2,530	**2,173**	1,501	1,185	1,105	1,066	969	978	418	77	0
		(%)	37.6	**32.3**	22.3	17.6	16.4	15.9	14.4	13.7	6.2	1.2	0.0
	Associate Emission Reduction	(kg CO2e)	1,899	**1,899***	1,742	1,223	1,086	1,032	967	957	934	608	0
		(%)	60.5	**60.5**	55.5	39.0	34.6	32.9	30.8	30.5	29.8	19.4	0.0
$Epm_d = 180$ Wh/mile	c_d/e_d	(\$/kg CO2e)	0.08	0.11	0.17	0.25	0.34	0.42	0.85	**1.14**	4.25	6.80	8.49
	Max Emission Reduction	(kg CO2e)	801	801	801	802	802	802	803	**803***	796	788	784
		(%)	25.5	25.5	25.5	25.6	25.6	25.6	25.6	**25.6**	25.4	25.1	25.0
	Associate Cost Reduction	(\$)	1,101	1,096	1,086	1,071	1,056	1,041	967	**918**	397	-19	-295
		(%)	16.4	16.3	16.1	15.9	15.7	15.5	14.4	**13.7**	5.9	-0.3	-4.4
	Max Cost Reduction	(\$)	2,530	2,215	1,501	1,185	1,105	1,066	969	**918**	418	77	0
		(%)	37.6	32.9	22.3	17.6	16.4	15.9	14.4	**13.7**	6.2	1.2	0.0
	Associate Emission Reduction	(kg CO2e)	-9,238	-9,238	-6,144	-129	549	706	801	**803***	793	525	0
		(%)	-294.5	-294.5	-195.9	-4.1	17.5	22.5	25.5	**25.6**	25.3	16.7	0.0

Similar to Cachon (2014) that characterizes the cost and emission tradeoff between the cost and the emission minimizing solutions, we define the cost penalty for minimizing emissions as $\frac{z_c(s_e^*)-z_c^*}{z_c^*}$. The denominator is the optimal delivery costs and the numerator is the maximum cost reduction gap between the emissions and the cost minimizing solutions. This term can be interpreted as the percentage increase in delivery costs that a delivery system incurs when the emissions minimizing design is chosen. This provides a measure of the explicit cost to adopt an objective that minimizes emissions relative to the cost minimizing objective. Similarly, the emission penalty for minimizing costs is defined as $\frac{z_e(s_c^*)-z_e^*}{z_e^*}$. The denominator is the optimal emissions and the numerator is the maximum emission reduction gap between the cost and the emission minimizing solutions.

Table 6.7 summarizes the cost and emission reduction gaps and penalties for $c_d =$ \$0.1/mile and \$0.01/mile with Epm_d varying from 9 to 360 Wh/mile. Table 6.8 summarizes the cost and emission reduction gaps and penalties for $Epm_d = 18$ Wh/mile and 180 Wh/mile with c_d varying from \$0.01/mile to \$1.0/mile. Row 1 of Tables 6.7 and 6.8 shows Epm_d and c_d, respectively. Row 2 shows the ratio of the operating cost per mile to the emissions rate per mile for drone (i.e., $\frac{c_d}{e_d}$) in \$/kg CO2e. Rows 3-4 show the maximum emissions and cost reduction gaps between the cost and the emissions minimizing solutions, respectively. Row 5 shows the emissions penalty for minimizing delivery costs, and row 6 shows the cost penalty for minimizing emissions. Rows 7-11 correspond to rows 2-6.

Table 6.7 shows that the maximum emission and cost reduction gaps, the emissions penalty for minimizing costs, and the cost penalty for minimizing emissions all decrease

to zero as Epm_d increases to the critical Epm_d value where $\frac{c_d}{e_d} = \frac{c_t}{e_t} = 1.14$, and then these performance measures increase as Epm_d increases further above the critical Epm_d value. Interestingly, the cost penalty increases more dramatically than the emissions penalty for c_d =\$0.1/mile as Epm_d decreases to 18 Wh/mile. When Epm_d further decreases below 18 Wh/mile, the emissions penalty continues to increase, whereas the cost penalty stays the same. Both the emissions and cost penalties can be high for c_d =\$0.1/mile with low Epm_d, which indicates a clear tension between environmental and financial performance. However, the emissions penalty increases much more dramatically than the cost penalty for c_d =\$0.02/mile as Epm_d increases. The maximum cost penalty seems to be around just 8%, whereas the emissions penalty can be as high as 620%.

Similarly, Table 6.8 shows that the maximum emissions reduction gap, the maximum cost reduction gap, the emissions penalty for minimizing costs, and the cost penalty for minimizing emissions all decrease to zero as c_d increases to the critical c_d value where $\frac{c_d}{e_d} = \frac{c_t}{e_t} = 1.14$, and then these performance measures increase as c_d increases further above the critical c_d value. However, there is an exception for $Epm_d = 18$ Wh/mile at the critical c_d =\$0.013/mile that there is no cost and emissions tradeoff even as c_d further decreases. This is because drone-only delivery minimizes both cost and emissions when c_d and Epm_d are both low. While both emissions and cost penalties can be high for Epm_d =18 Wh/mile with high c_d, the cost penalty increases much more dramatically than the emissions penalty as c_d increases. The emission penalty increases more dramatically than the cost penalty for $Epm_d = 180$ Wh/mile as c_d dramatically deviates from the critical value.

Table 6.7 The cost and emissions reduction gaps and penalties between the cost and the emissions minimizing solutions for $c_d =$ \$0.1/mile and \$0.01/mile with Epm_d varying from 9 to 360 Wh/mile.

	Epm_d	**(Wh/mile)**	**9**	**18**	**26.8***	**30**	**36**	**45**	**60**	**90**	**134***	**180**	**360**
c_d =\$0.1/mile	c_d/e_d	(\$/kg CO2e)	16.99	8.49	5.71	5.10	4.25	3.40	2.55	1.70	**1.14**	0.85	0.42
	Max Emission Reduction Gap	(kg CO2e)	1,542	932	356	241	133	65	25	4	**0**	2	19
	Max Cost Reduction Gap	(\$)	7,899	7,899	5,422	2,962	1,158	400	98	9	**0**	1	5
	Emission Penalty for Minimizing Cost	(%)	249.2	75.3	19.5	12.4	6.5	3.1	1.1	0.2	**0.0**	0.1	0.7
	Cost Penalty for Minimizing Emission	(%)	137.3	137.3	94.2	51.5	20.1	6.9	1.7	0.2	**0.0**	0.0	0.1
c_d =\$0.02/mile	c_d/e_d	(\$/kg CO2e)	3.40	1.70	**1.14**	1.02	0.85	0.68	0.51	0.34	0.23	0.17	0.08
	Max Emission Reduction Gap	(kg CO2e)	337	157	**0**	38	216	577	1,252	2,660	4,747	6,945	15,536
	Max Cost Reduction Gap	(\$)	22	22	**0**	34	132	235	321	382	406	415	424
	Emission Penalty for Minimizing Cost	(%)	54.5	12.7	**0.0**	1.9	10.5	27.1	57.2	118.8	207.4	297.4	620.0
	Cost Penalty for Minimizing Emission	(%)	0.4	0.4	**0.0**	0.6	2.5	4.5	6.1	7.3	7.8	8.0	8.1

Table 6.8. The cost and emissions reduction gaps and penalties between the cost and the emissions minimizing solutions for $Epm_d = 18$ Wh/mile and 180 Wh/mile with c_d varying from \$0.01/mile to \$1.0/mile.

	c_d	**(\$/mile)**	**0.01**	**0.013**	**0.02**	**0.03**	**0.04**	**0.05**	**0.1**	**0.13**	**0.5**	**0.8[1]**	**1.0[2]**
$Epm_d = 18$ Wh/mile	c_d/e_d	(\$/kg CO2e)	0.85	**1.14**	1.70	2.55	3.40	4.25	8.49	11.38	42.47	67.96	84.95
	Max Emission Reduction Gap	(kg CO2e)	0	**0**	157	676	813	866	932	942	965	1,291	1,899
	Max Cost Reduction Gap	(\$)	0	**0**	22	758	1,729	2,741	7,899	11,422	49,393	80,586	101,530
	Emission Penalty for Minimizing Cost	(%)	0.0	**0.0**	12.7	54.6	65.7	70.0	75.3	76.1	78.0	104.4	153.5
	Cost Penalty for Minimizing Emission	(%)	0.0	**0.0**	0.4	13.7	30.8	48.5	137.3	196.8	783.5	1212.7	1510.3
$Epm_d = 180$ Wh/mile	c_d/e_d	(\$/kg CO2e)	0.08	0.11	0.17	0.25	0.34	0.42	0.85	**1.14**	4.25	6.80	8.49
	Max Emission Reduction Gap	(kg CO2e)	10,038	10,038	6,945	931	253	96	2	**0**	3	264	784
	Max Cost Reduction Gap	(\$)	1,429	1,119	415	115	49	25	1	**0**	21	97	295
	Emission Penalty for Minimizing Cost	(%)	429.8	429.8	297.4	39.9	10.8	4.1	0.1	**0.0**	0.1	11.2	33.3
	Cost Penalty for Minimizing Emission	(%)	34.1	24.8	8.0	2.1	0.9	0.4	0.0	**0.0**	0.3	1.5	4.4

[1]Truck-only and truck-drone are used to minimize delivery cost. [2]Truck-only is used exclusively to minimize delivery costs.

Given the tradeoff between financial and environmental performance, one approach to combine them is to associate a cost rate with emissions, and add emissions into the financial objective function. With an explicit price for carbon, a "carbon price", the negative externalities and the regulation risks associated with GHG emissions can be appropriately accounted for in the delivery system design that minimizes total delivery plus emissions costs. Estimates of carbon prices vary considerably, but generally fall in the range between $20 and $1,000 per metric ton of CO2e (Cachon, 2014) with low carbon prices being more common in practice (e.g., the United Nations Global Compact calls for $100/tCO2e). Therefore, we choose three levels of carbon prices, i.e., $50/tCO2e, $100/tCO2e, and $200/tCO2e, to show how the optimal delivery system design depends on carbon prices. This is shown for the base case scenario in Figure 6.9(a) and for the inexpensive, but energy intensive drone scenario in Figure 6.9(b). We also plot the carbon price of zero to reflect the delivery system that merely minimizes delivery costs and ignores the cost of emissions.

In Figure 6.9, the horizontal axis is the utilization of drone-only delivery (DO) because DO and TD are the only two services used, thus we could use DO utilization to represent the system design. The vertical axis is the expected total costs (in thousands of dollars) which includes the delivery costs and the cost of emissions by multiplying the carbon price by the quantity of the emissions. The lines with circles, triangles, squares, and diamonds represent the carbon prices of 0, $50/tCO2e, $100/tCO2e, and $200/tCO2e, respectively. The darker the line color, the greater the carbon price. Figure 6.9(a) shows that the carbon price has very little impact on the total delivery costs and the delivery system design in the base case. Even with a carbon price of $200/tCO2e, the incentive is

not sufficient enough for a delivery system to significantly reduce emissions. However, Figure 6.9(b) shows that for the inexpensive energy intensive drone, with a carbon price of $50/tCO2e, there is a significant change in the utilization of DO compared with no carbon price. For example, DO is reduced from about 80% to 41% when the carbon price increases from zero to $50/tCO2e. The GHG emissions is reduced by 4,536 kg CO2e (or 49%). This indicates that a relatively small carbon price would induce a significant shift in the delivery system and allow a large portion of the potential emissions reduction to be achieved. Higher carbon prices encourage a greater shift to TD delivery and at a $200/tCO2e carbon price, TD is used for 84% of the deliveries (DO is used for 16%). Results show the impact of carbon price is marginally diminishing. For example, the emission reduction is 49%, 62%, and 70% for carbon prices of $50/tCO2e, $100/tCO2e, and $200/tCO2e relative to carbon price of zero, respectively.

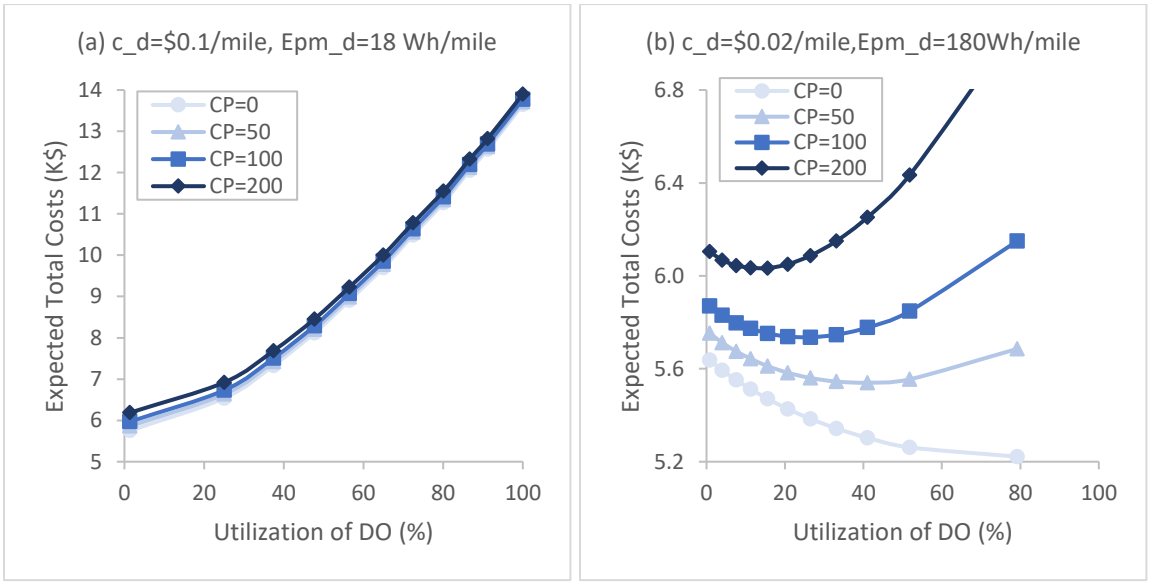

Figure 6.9 the impact of carbon price on total costs and DO utilization for (a) the base case c_d = $0.1/mile and Epm_d = 18 Wh/mile and (b) c_d = $0.02/mile and Epm_d = 180 Wh/mile

Appendix 6.A demonstrates more discussions on the impacts of carbon prices on the optimal delivery system designs with drone operating cost rate, drone energy consumption rate, and/or delivery density varying.

6.3.4 The Impact of Delivery Density (δ)

In Chapters 4 and 5 we observed that the cost and emission savings depend on delivery density. The delivery costs and the GHG emissions per delivery for truck-only delivery (TO) and truck-drone delivery (TD) decrease as delivery density increases, as the deliveries become closer together. However, delivery density does not affect drone-only delivery (DO). This is because the expected distance per delivery for multi-stop routes (i.e., TO and TD) decreases as deliveries get close to each other, whereas it is the same for the point-to-point delivery (i.e., DO). To assess the impact of delivery density on the cost and emissions tradeoff, we consider two other levels of delivery density in addition to the base case density of $\delta = 25$ deliveries per square mile: a relatively higher density of $\delta = 125$ deliveries per square mile , and a relatively lower delivery density of $\delta = 5$ deliveries per square mile. Those densities might represent different geographic locations (e.g., suburban, rural) or different times of the year (e.g., holiday season, off-season).

We explore four type of drones as shown in Figures 6.10(a)-(d): (a) a "current" drone with an operating cost per mile $c_d = \$0.1$/mile and energy consumption per mile of $Epm_d = 180$ Wh/mile; (b) a more energy-efficient drone with $c_d = \$0.1$/mile and $Epm_d = 18$ Wh/mile; (c) a more cost efficient drone with $c_d = \$0.02$/mile and $Epm_d = 180$ Wh/mile; and (d) a both cost and energy efficient drone with $c_d = \$0.02$/mile and $Epm_d = 18$ Wh/mile. In Figures 6.10(a)-(d), the lines with squares, circles, and triangles

represent the Pareto frontiers for delivery densities of 5, 25, and 125 deliveries per square mile, respectively. The darker the color, the greater the delivery density.

Overall, Figure 6.10 reveals that (i) the impact of delivery density on the cost and emissions tradeoff depends on the characteristics of the drone; (ii) for drones with relatively high c_d and Epm_d (Fig. 6.10(a)) or relatively low c_d and Epm_d (Fig. 6.10(d)), delivery density in the range between 5-125 has very little impact on the cost and emissions tradeoff; (iii) the Pareto frontier moves down and to the left as delivery density increases; (iv) the utilization of TD increases as delivery density increases, and the Pareto frontiers for different density levels become farther apart as TD utilization increases (this is because the cost and emission per delivery of TD decreases as density increases), whereas they are close to each other as DO utilization increases (this is because density has no impact on the cost and emission per delivery of DO).

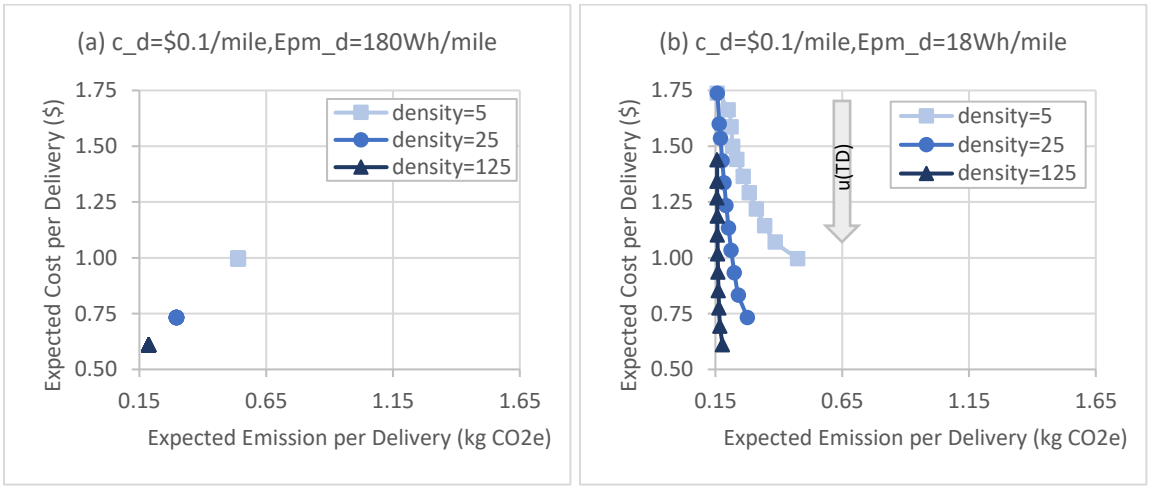

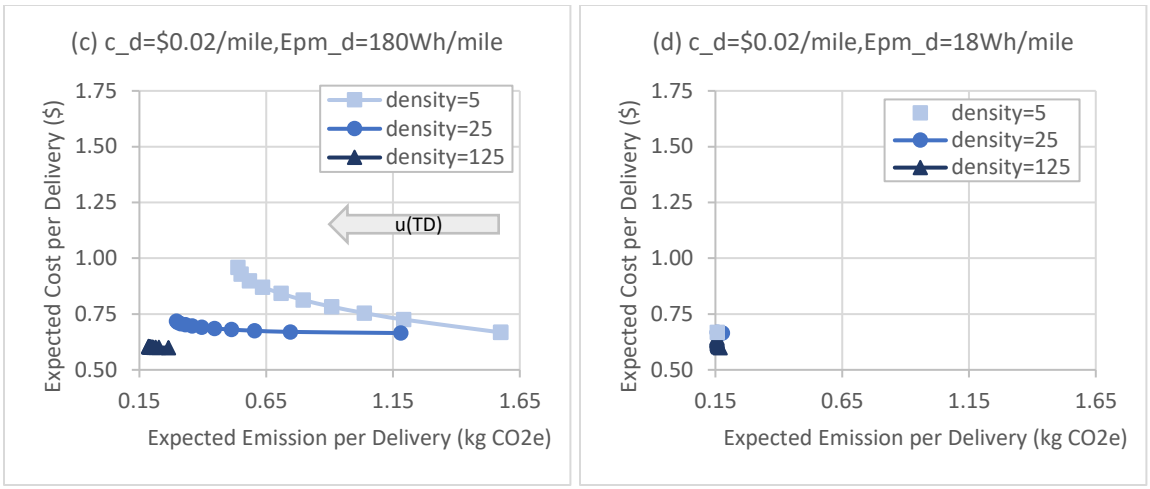

Figure 6.10 The impact of delivery density on cost and emission tradeoffs for different drone operations

Figure 6.10(a) shows that the Pareto frontier is reduced to nearly a single point (indicating no tradeoff between costs and emissions) for all three levels of delivery density. The higher the delivery density, the lower the cost and the emissions per delivery. This is because TD is largely used to minimize both cost and emissions when c_d and Epm_d are both high, and both the cost and emissions per delivery of TD decrease as the delivery density increases. Although a low delivery density makes DO relatively more competitive compared with TD (and TO), $\delta = 5$ is not low enough to significantly change the utilization of DO and TD. Interestingly, we observe a similar "little cost and emission tradeoff" phenomenon in Figure 6.10(d) when c_d and Epm_d are both low. Although TD is heavily used (serving 84% of the deliveries) to minimize delivery costs for $\delta = 125$, the cost and emissions per delivery do not differ significantly (<10%) from those for $\delta = 5$ and 25 where DO is heavily used (for $\geq$ 79% of the deliveries). This indicates that for relatively low c_d and Epm_d, DO is at least as good as TD even for a relatively high density $\delta = 125$.

Figure 6.10(b) shows that as delivery density increases, the Pareto frontiers appear to be steeper, and the maximum emissions reduction gap per delivery decreases, which indicates that with higher delivery density there is only very small room for improvement in emissions per delivery, and lower density has large potential improvements in emissions per delivery. For example, the maximum emissions reduction gaps per delivery are 0.317, 0.119, and 0.022 kg CO2e/delivery for $\delta = 5$, 25, 125, respectively. Although the emissions reduction gap for $\delta = 5$ is about 2.7 times greater than that for $\delta = 25$, the number of deliveries for $\delta = 5$ is only 1/5 of that for $\delta = 25$, thus, the total potential emission reduction is greater for density $\delta = 25$ versus $\delta = 5$. This highlights the difference between a "per delivery" view and a "total" view. Unlike the maximum emissions reduction gap, the maximum cost reduction gap per delivery for different density levels does not seem to dramatically differ from each other. It is only about 26% and 18% less for $\delta = 5$ and 125, relative to that for $\delta = 25$, respectively. The marginal emissions reduction cost (MERC) in Figure 6.10 (b) is lower for $\delta = 5$ than for $\delta = 25$ and 125, but it is well above \$800/tCO2e. This indicates that the carbon price needs to very high to effectively incentivize a delivery system when $c_d = \$0.02$/mile and $Epm_d = 180$ Wh/mile to reduce emissions, which we have discussed in previous subsection (e.g., Figure 6.9(a)).

Unlike Figure 6.10(b), Figure 6.10(c) shows as delivery density increases, the Pareto frontiers become flatter, which suggests a large emission reduction is possible at relatively little cost. However, the maximum cost and emission reduction gaps per delivery both decrease as delivery density increases, indicating that higher delivery densities have smaller cost and emission tradeoffs than lower densities. For example, the maximum cost reduction gaps are \$0.291, \$0.053, and \$0.005 per delivery for $\delta = 5, 25, 125$, respectively.

The maximum emission reduction gaps are 1.036, 0.884, 0.078 kg CO2e/delivery for $\delta =$ 5, 25, 125, respectively. Although it still requires a very high carbon price ($1148/tCO2e) to induce the emissions minimizing delivery system design even for a relatively high density $\delta = 125$, a carbon price of $100/tCO2e can induce a delivery system design that reduces emissions by about 85% for $\delta = 25$ and 125 but 0% for $\delta =5$. It would require a carbon price of about $350/tCO2e to achieve the same emission reduction of 85% for $\delta =5$.

Figures 6.11(a)-(d) adds the performance for truck-only delivery to Figures 6.10(a)-(d) to show the impacts of delivery density on the cost and emissions savings (and tradeoffs) of drone delivery relative to truck-only delivery. To be consistent, the square, the circle, and the triangle points represent truck-only delivery for a delivery density of 5, 25, and 125 deliveries per square mile, respectively. The darker the color, the greater the delivery density. For each delivery density level, the observations in Fig. 6.11 are consistent with what we have observed in Fig. 6.8 and Tables 6.5 and 6.6: (i) drone delivery provides both cost and emission savings (with very little tradeoff) relative to truck-only delivery when c_d and Epm_d are both relatively high or both relatively low (see Figures 6.11(a) and 6.11(d)); (ii) some emissions savings can be achieved with a concurrent reduction in cost when c_d is relatively high and Epm_d is low (Figure 11(b)), but greater reductions in emissions require an increase in costs; (iii) some cost savings can be achieved with a concurrent reduction in emissions when c_d is relatively low and Epm_d is high (Figure 11(c)), but greater reductions in costs require an increase in emissions.

In Figures 6.11(a)-(d), the cost and the emission per delivery for truck-only delivery decreases with delivery density as indicated by the nearly linear dashed line fitting the points of truck-only delivery for the three levels of density. As density increases, both cost

and emission per delivery of truck-only delivery decrease, but at a marginally diminishing rate as evidenced by the decreasing distance between two adjacent truck-only delivery points. The impacts of delivery density on the cost and emissions savings relative to truck-only delivery are: (i) the maximum cost and emission savings per delivery increase as delivery density decreases, but the total maximum cost and emission savings increase as delivery density increases because the decrease in savings per delivery is much slower than the increase in the number of deliveries as delivery density increases. For example, in Fig. 6.11(a), the maximum cost savings per delivery are \$0.55, \$0.24, and \$0.1, whereas the total maximum cost savings are \$340, \$969, and \$3,362 for $\delta = 5, 25, 125$, respectively. This again shows the need to consider both a "per delivery" view and a "total" view.

In Figure 6.11(b), as delivery density increases the maximum percentage emissions savings relative to TO decrease, whereas the associated percentage increase in delivery costs increases. The maximum cost savings and the associated emissions savings relative to TO decrease as delivery density increases. There is a clear tradeoff between cost and emission when the emissions minimizing objective is chosen. In Figure 6.11(c), the maximum percentage emission savings relative to TO increases, whereas the associated percentage cost savings relative to TO decreases as delivery density increases. The maximum percentage cost savings relative to TO decrease as delivery density decreases, and the associated percentage increase in emission is the greatest for $\delta = 25$. There is a clear tradeoff between cost and emissions when the cost minimizing objective is chosen for relatively medium to low density $\delta <125$. For example, the maximum percentage cost savings are 45%, 22%, and 14%, whereas the associated percentage increase in emissions are 121%, 196%, and 2% for $\delta = 5, 25, 125$, respectively.

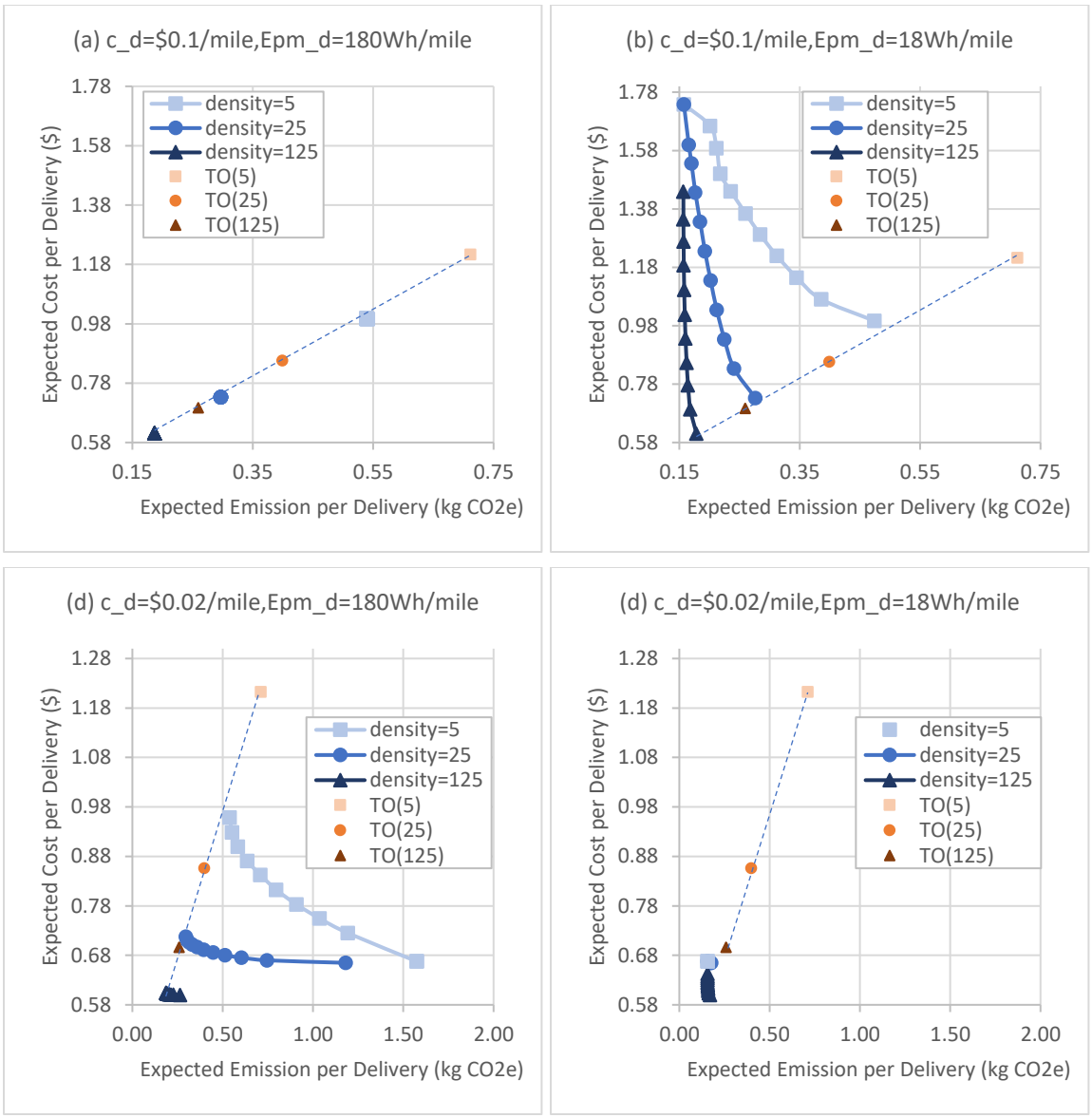

Figure 6.11 The impact of delivery density on cost and emissions savings and tradeoffs relatively to truck-only delivery

6.3.5 The Impact of Truck Capacity for Truck-drone Delivery (m_{td})

The truck capacity for truck-drone delivery also has an impact on the utilization of services and the cost and emissions savings based on the findings in Chapters 4 and 5. In addition to the base case truck capacity level (i.e., m_{td} =150 deliveries per truck), we

examine a relatively lower capacity level (i.e., $m_{td} = 75$ deliveries per truck) and a relatively higher capacity level (i.e., $m_{td} = 300$ deliveries per truck). All those deliveries can be done within the 8-hour work limit (see Chapters 4 and 5 for more detail on the route time for truck-drone delivery with a high capacity level).

Once again, we explore four type of drones as discussed in the previous subsection: (a) a drone with relatively high operating cost per mile of c_d = \$0.1/mile and energy consumption per mile of Epm_d = 180 Wh/mile; (b) a more energy-efficient drone with c_d = \$0.1/mile and Epm_d = 18 Wh/mile; (c) a more cost efficient drone with c_d = \$0.02/mile and Epm_d = 180 Wh/mile; and (d) a both more cost and energy efficient drone with c_d = \$0.02/mile and Epm_d = 18 Wh/mile. In Figures 6.12(a)-(d), the lines with squares, circles, and triangles represent the Pareto frontiers for truck-drone capacity m_{td} = 75, 150, and 300, respectively. The darker the color, the greater the truck capacity for truck-drone delivery. The orange dot represents truck-only delivery with a capacity of 150 deliveries.

The shapes of the Pareto frontiers in Figures 6.12(a)-(d) are very similar to those in Figures 6.11(a)-(d) correspondingly. This might indicate that the truck capacity for truck-drone delivery has the similar impact on the cost and emissions tradeoff as the delivery density does. Overall, Figure 6.12 reveals that (i) the impact of truck capacity for truck-drone delivery on the cost and emissions tradeoff depends on the characteristics of the drone; (ii) for drones with relatively high c_d and Epm_d (Fig. 6.12(a)) or relatively low c_d and Epm_d (Fig. 6.12(d)), truck capacity for truck-drone delivery ranging between 75-300 has limited impact on the cost and emissions tradeoff; (iii) the Pareto frontier moves down and to the left as truck capacity for truck-drone delivery increases; (iv) the utilization of

TD increases as the truck capacity for truck-drone delivery increases, and the Pareto frontiers for different capacity levels become farther apart as TD utilization increases, whereas they are close to each other as DO utilization increases (this is because truck-drone capacity has no impact on the cost and emission of DO).

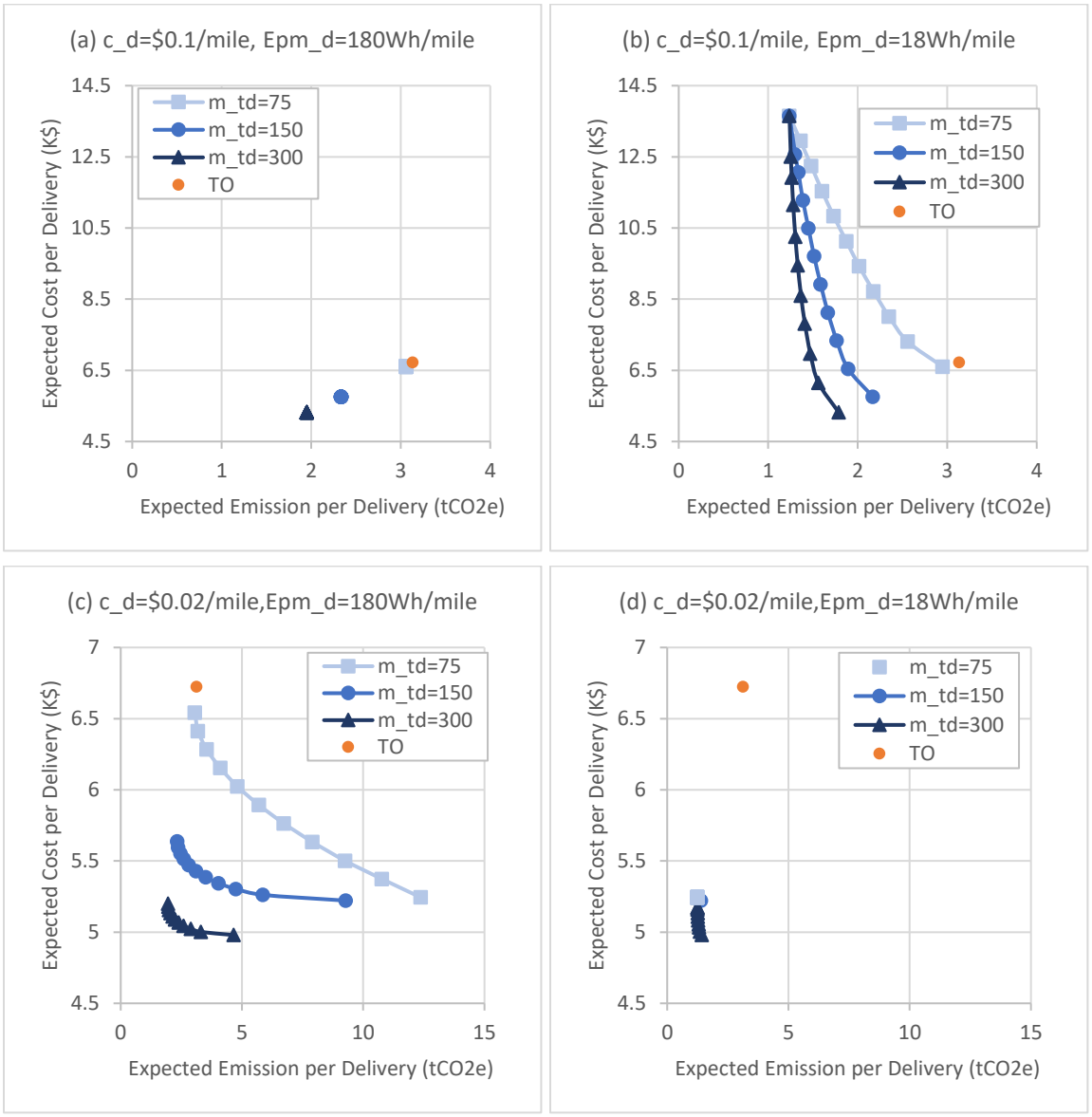

Figure 6.12 The impact of truck-drone capacity on the cost and emission savings and tradeoffs for different drone operations

Compared with truck-only delivery, we again see behaviors in Figure 6.12 that are consistent with what we observed in Figure 6.8 and Tables 6.5 and 6.6: (i) drone delivery provides both cost and emissions savings (with very little tradeoff) relative to truck-only delivery when c_d and Epm_d are both relatively high or both relatively low; (ii) the emissions savings are achieved by increasing or decreasing delivery costs when c_d is relatively high and Epm_d is relatively low; (iii) the cost savings are achieved by increasing or decreasing GHG emissions when c_d is relatively low and Epm_d is relatively high. However, we do see that the cost and emissions savings per delivery decrease as the truck capacity for truck-drone delivery decreases as the Pareto frontiers move closer to the orange dot.

In Figure 6.13, we show how minimizing cost and minimizing emissions affect the utilization of drone-only delivery (DO), truck-drone delivery (TD), and truck-only delivery (TO) with the four types of drones and the three levels of truck capacity for truck-drone delivery. In all 12 panels of Figure 6.13, the vertical axis is the utilization of DO, TD, and TO in percentages. Each bar represents a Pareto efficient solution with the left most bar being the cost-minimizing solution and the right most bar being the emissions-minimizing solution. The colors blue, orange, and gray represent DO, TD, and TO, respectively (see the electronic version for a better visualization). Each row of Figure 6.13 has four sub-figures representing the four types of drones with the same level of truck capacity for truck-drone. Each column Figure 6.13 has three sub-figures representing the three levels of truck capacity for truck-drone delivery for the same type of drone.

Moving down the columns of Figure 6.13, we observe that the utilization of TD increases as truck capacity for truck-drone delivery increases. For the relatively low truck-

drone capacity of 75, TO serves for up to about 50% of the deliveries when c_d and Epm_d are relatively high (top left panel of Fig. 6.13). When c_d and Epm_d are both high (column 1 of Fig. 6.13) or both low (column 4 of Fig. 6.13), then one of the three services dominates the other two (except for the low truck capacity for truck-drone delivery where TO and TD are used about half-and-half), and this is explains why we observe little cost and emission tradeoff in the corresponding Figures 6.12(a) and (d). Columns 2 and 3 of Figure 6.13 correspond to Figures 6.12(b) and (c), and they explain why we observe considerable cost and emissions tradeoffs in Figures 6.12(b) and (c), because the utilization of delivery services that minimize cost and minimizes emissions are very different. Note that the two center panels in the top row include solutions that utilize all three delivery services.

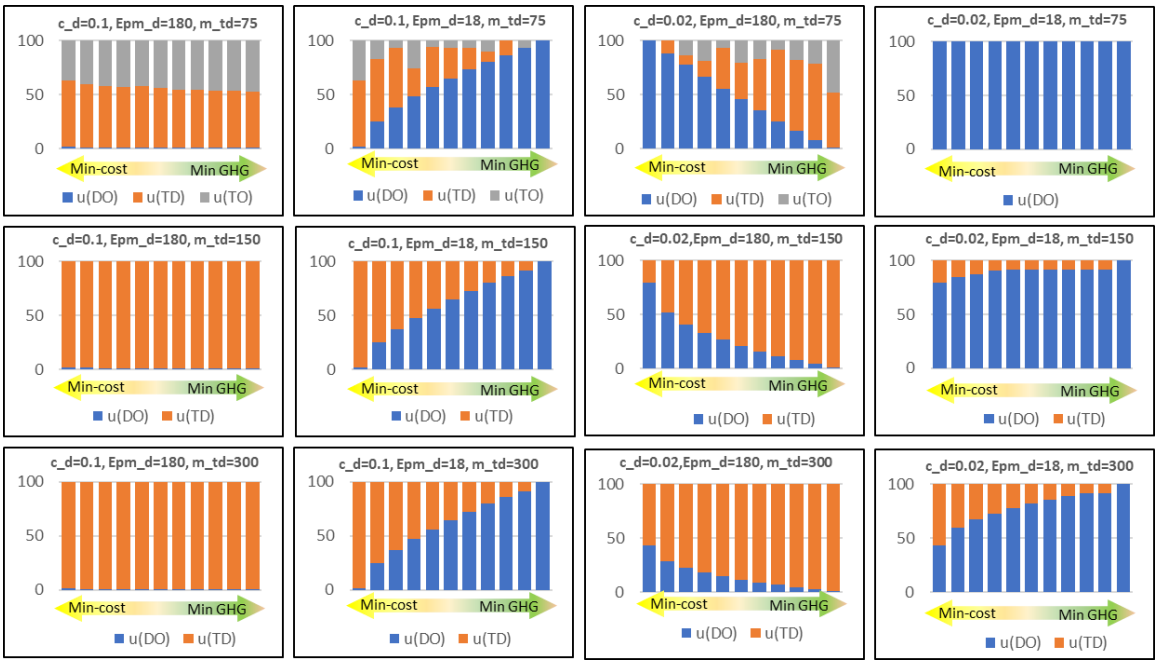

Figure 6.13 The utilization of DO, TD, and TO for different drone operations and system objectives

6.4 Conclusions

This chapter examines the tradeoff of cost and emissions for drone delivery, including drone-only delivery (DO), truck-drone delivery (TD), and truck-only delivery (TO). A delivery system design problem (DSDP) IP model was formulated to partition the delivery region and assign delivery services to subregions, based on minimizing the delivery costs, minimizing the GHG emissions or finding Pareto efficient solutions. The DSDP model developed in this chapter allows an assessment of the potential tradeoffs between the delivery costs and the GHG emissions and the magnitude of the potential cost and emission savings relative to the truck-only delivery when different system designs are chosen.

The magnitude of the cost and emissions tradeoff depend strongly on the drone operating cost per mile and the drone operating emissions per mile (including the drone energy consumption rate and the carbon intensity of the electricity). The truck capacity for truck-drone delivery and the delivery density have very similar, but more limited impacts on the magnitude of the cost and emissions tradeoff. The cost and emissions savings relative to truck-only depend strongly on drone operating cost per mile, drone operating emissions per mile, truck-drone capacity, and delivery density.

There are cases in which there is a very small, or no, cost and emissions tradeoff (i.e., the delivery system design is the same for minimizing delivery costs and minimizing GHG emissions). For example, this very small tradeoff occurs when the drone operating cost per mile and the drone operating emissions per mile are both low or both high. In each case, this result occurs because similar utilizations of delivery services minimize both delivery costs and minimize GHG emissions. If drone operating cost and emissions are

both low, then drone-only delivery is extensively used for both objectives. If drone operating cost and emissions are both high (but still much lower than those for truck-only delivery), then truck-drone delivery is extensively used for both objectives. We identify that when the ratio of drone operating cost to drone emissions rate is close to the ratio for trucks ($1.14/kg CO2e), then the magnitude of the cost and emissions tradeoff is small.

There are cases, however, when the ratio of drone operating cost to drone emissions rate differs from the ratio for trucks. For example, if the drone operates very cost efficiently, but is energy intensive (e.g., from a particular drone design or from operating at very high speed, as for the case described in subsection 6.3.2), then its cost to emissions ratio can be much smaller than that for a truck. In this case, the delivery system that minimizes delivery costs largely uses drone-only delivery to exploit the low operating cost of drones through high drone utilization, whereas the delivery system that minimizes emissions largely uses truck-drone delivery to exploit the cost (and distance) efficient way of using drones relative to drone-only. Results for this setting showed that minimizing emissions increases delivery costs by only 8%, whereas minimizing delivery costs increases emissions by 297%. Further, the results showed that a carbon price of $100/tCO2e may be effective to induce a delivery system design that considerably reduces emissions (by about 85%).

However, if the cost rate to emissions rate ratio for drones is much greater than that for trucks, we observe a considerable cost and emission tradeoff but in the opposite order to that above. The cost minimizing delivery system largely uses truck-drone delivery, whereas the emission minimizing delivery system largely uses drone-only delivery. Results showed that minimizing emissions increases delivery costs by about 137%, and minimizing delivery costs increases emissions by 75%. In this situation, a carbon price of

$1,000/tCO2e is still too low to incentivize a delivery system to reduce emissions. This indicates that the projection for the operating cost and emissions properties of drones is very important for determining how drones would be used in light of different carbon prices.

The magnitude of cost and emissions savings relative to truck-only delivery depend strongly on the drone operating cost per mile, the drone operating emission per mile, the truck-drone capacity, and the delivery density. As drone operating cost per mile and drone operating emissions per mile both decrease, the cost and emissions savings relative to truck-only both increase. For the most cost- and emissions-efficient drone considered (i.e., $c_d =$ \$0.02/mile and $Epm_d =$ 18 Wh/mile) where truck-drone delivery makes 150 deliveries per route, the cost and the emissions savings relative to truck-only delivery are 22% (or \$0.19/delivery) and 61% (or 0.24 kg CO2e/delivery), respectively. These savings would increase as truck-drone capacity increases or the delivery density decreases. To put the numbers in perspective, it would represent for UPS about \$1.1 billion and 1.4 million metric tonnes of CO2e savings per year in the U.S. (assuming the daily package volume is 16 million (Holland et al., 2017) for 365 days in a year). A 1.4 million metric tonnes CO2e reduction is equivalent to removing more than 300,000 cars (or 0.1% of U.S. registered cars) from the road for one year (Bureau of Transportation Statistics, 2021), or switching more than 800,000 cars (or 0.3% of U.S. registered cars) from 20 mpg to 25 mpg, or removing 2% of Missouri's coal fired electricity plants which generated about 75 million tonnes of CO2 in 2010 (Schneider et al., 2013). For the least cost- and emissions-efficient drone considered (i.e., $c_d =$ \$0.1/mile and $Epm_d =$ 180 Wh/mile) where truck-drone delivery makes 75 deliveries per route, the cost and the emissions savings relative to truck-only delivery are much smaller, at only 2% (or \$0.01/delivery and 0.015 kg CO2e/delivery,

respectively). Based on the same assumptions above, this would represent for UPS about $58 million and 87,600 metric tonnes CO2e savings per year in the U.S.

Drones have great potential to reduce GHG emissions and delivery costs if they are used appropriately. The delivery system design that minimizes cost can be very different from the design that minimizes emissions, or very similar, depending on the drone characteristics and operating environment, which might result in a very small or a very considerable cost and emissions tradeoff. Truck-drone capacity tends to be a very important factor in providing savings relative to conventional truck-only delivery when the drones are not considerably more cost and emissions efficient than trucks. In addition to further improvements in drone technology, improvements in drone operations might also be fruitful to: (i) increase truck-drone capacity; (ii) increase the number of drones operated per truck; (iii) reduce drone-only travel distances by building more drone centers; and (iv) allow drones to make multiple deliveries.

Chapter 7: Conclusions and Future Research

This dissertation examines the economic and the environmental impacts of using drones for home delivery. Three delivery services are modeled: (i) drone-only delivery (DO) where the drone departs from and returns to a depot after each delivery, (ii) hybrid truck-drone delivery (TD) where the drone departs from and returns to a delivery truck, and the drone and the truck make deliveries in parallel, and (iii) conventional truck-only delivery (TO) where a truck departs from and returns to a depot after making a number of deliveries. Consistent with the findings in the literature, this research suggests that drones have great potential to reduce greenhouse gas (GHG) emissions and delivery costs if they are used appropriately. In addition, this research also identifies that the delivery system design that minimizes cost can be very different from the design that minimizes emissions, or very similar, depending on the drone characteristics (e.g., drone energy consumption rate, drone operating cost rate, marginal drone stop cost) and operating environment (e.g., the carbon intensity of electricity, the delivery density, the size of the delivery region), which might result in a very small or a very considerable cost and emissions tradeoff. Truck-drone capacity tends to be a very important factor in providing savings relative to conventional truck-only delivery when the drones are not considerably more cost and emissions efficient than trucks.

7.1 Conclusions

Energy consumption is a critical constraint for drone delivery operations to achieve their full potential of reducing cost, cutting emissions, and providing fast delivery. An accurate estimation of drone energy consumption ensures feasible as well as efficient operating decisions. In **Chapter 3**, we classify and evaluate five fundamental energy

consumption models for drone delivery using a uniform framework. We discuss and highlight key similarities and differences in drone energy models. We also provide an understanding of why the energy consumption models differ from each other, and identify important parameters that contribute to these differences. Our results document a wide variability in the published academic literature on drone energy consumption rates, due to different drone types, operating conditions and fundamental assumptions of drone energy consumption models. The selection of the lift-to-drag ratio and the power transfer efficiency, both of which are difficult to assess without taking measurements in flight, can be crucial in accurately estimating energy consumption for drones. The energy consumption differences we document have strong implications for accurately modeling the energy and environmental implications of all drone operations, including delivery. Given that the models in the literature can provide drone energy consumption rates that differ by a factor of 3-5 (or more), great care must be taken in translating results from transportation modeling (e.g., drone route modeling and optimization) to estimates and policy recommendations involving energy and emissions. Any of the five fundamental drone energy consumption models could be used, but whatever model is adopted needs to be calibrated appropriately to accurately reflect drone operations and performance in the setting of interest.

Incorporating drones into a conventional truck delivery system offers more delivery options as deliveries can be made by drone-only service, truck-only service, truck-drone service, or a combination of the three services. However, incorporating drones also complicates the optimal design of the delivery system. **Chapter 4** lays the theoretical foundation for modeling the expected delivery costs and GHG emissions that facilitates a

strategic analysis of the design of truck and drone delivery systems. Continuous approximation models are derived for estimating the expected delivery costs for DO, TD, and TO delivery services. The delivery region is then partitioned based on the best use of different delivery services (i.e., DO, TD, and TO) that minimize delivery costs. Both theoretical analyses and numerical scenarios are provided to illustrate the circumstances in which drone delivery (i.e., DO and TD) provides large and small cost savings relative to truck-only delivery and to quantify the scale of the savings. Results suggest that the potential cost savings from DO and TD can be huge, but depend strongly on the drone operating parameters (i.e., drone operating cost rate, marginal drone stop cost, and truck drone capacity) and the operating environment (i.e., the delivery region size and the delivery density). In most cases, truck-drone delivery is the dominant delivery service, whereas drone-only delivery serves very small percentages of customers who are located close to the depot. However, drone-only delivery tends to be used more intensively when the drone operating cost is very inexpensive and/or the delivery density is very low. Only when drone operating cost is very high, drone stop cost is high, and/or truck-drone capacity is low will truck-only delivery be used to some extent.

In **Chapter 5**, we extend the continuous approximation models and analyses for expected GHG emissions for estimating DO, TD and TO delivery services. We conduct a similar analysis to Chapter 4 to examine the emissions savings relative to truck-only delivery. Results suggest that the percentage emissions savings of the emission-minimizing delivery system relative to truck-only delivery can be much more substantial than the percentage cost savings of the cost-minimizing delivery system with the base case setting. However, high percentage emissions savings might be achieved by considerably increasing

or decreasing the delivery costs, depending on the drone energy consumption rate, the carbon intensity of electricity, the drone operating cost rate, the delivery density, and the delivery region size. Furthermore, the partitioning of the delivery region that minimizes GHG emissions is very different from that which minimizes delivery costs. Drone-only delivery is often the dominant delivery service, whereas truck-drone delivery serves small percentages of customers who are located far from the depot. But truck-drone delivery can be used extensively when the drone energy consumption rate is relatively high, the delivery density is very high, and/or the size of the delivery region is large.

For both cost-minimizing and emissions-minimizing delivery systems, a signal for very large savings is when DO can be used extensively, whereas a signal for very small savings is when TO is used. Even if drone delivery provides a small percentage cost and/or emissions savings relative to truck-only delivery, where the delivery density is high, then using drones can substantially reduce truck travel distances, driver work hours, and the number of trucks required and, thus, improve the delivery service level. In most cases, truck-drone delivery is a very important delivery approach that can provide both cost and emissions savings.

Based on the models in Chapters 4 and 5, **Chapter 6** examines the potential tradeoffs between cost and emissions for the drone-based delivery systems that include DO, TD and TO delivery services. A delivery system design problem (DSDP) IP model is formulated to partition the delivery region and assign delivery services to subregions, based on minimizing the delivery costs, minimizing the GHG emissions or finding Pareto efficient solutions. Analysis of the Pareto frontier is presented for several scenarios. Results suggest that the magnitude of the cost and emissions tradeoffs depends strongly on the

drone operating cost rate and the drone operating emissions rate (including the drone energy consumption rate and the carbon intensity of the electricity). The truck capacity for truck-drone delivery and the delivery density have very similar, but more limited impacts on the magnitude of the cost and emissions tradeoff.

When the ratio of drone operating cost rate to drone emissions rate differs from the ratio for trucks (e.g., in the base case setting), there are considerable tradeoffs between the delivery costs and emissions savings because very different delivery services are used to minimize delivery costs or GHG emissions. However, when the ratio of drone operating cost rate to drone emissions rate is close to the ratio for trucks, there are small tradeoffs between the delivery costs and emissions savings because the same delivery system nearly minimizes both delivery costs and emissions. Therefore, the projections for the operating cost and emissions properties of drones are very important for determining how drones might be used in light of different carbon prices (and regulations). If the cost rate to emissions rate ratio for drones is much smaller than that for trucks, a carbon price of $100/tCO2e may be effective to induce a delivery system design that considerably reduces emissions. However, if the cost rate to emissions rate ratio for drones is much larger than that for trucks, a carbon price of $1,000/tCO2e may still be too low to incentivize a delivery system to just slightly reduce emissions.

7.2 Future Research

Drone delivery is an exciting new transportation option and it provides great potential for improved delivery service levels with reduced costs, energy consumption and GHG emissions. This dissertation suggests a number of important areas for future research. Clearly, a better understanding of the accuracy of drone energy models is needed through

comparing results to empirical data derived from comprehensive drone delivery field tests. These empirical tests might best be undertaken in a partnership between government agencies (e.g., the U.S. Department of Energy or EPA), academic institutions, and private sector firms. The importance of avionics and wind conditions on drone energy consumption is an area especially needing more attention, with particular care to the numbers, sizes and types of drones deployed. Future research can also help identify which type of model (complex or simple) is best in different settings, and whether or when more parsimonious models are "accurate enough" to use.

In addition to further improvements in drone technology and related regulation, improvements in drone operations might also be fruitful to:

- Explore drone use in high service level circumstances (e.g., one-hour delivery, two-hour delivery), as higher service levels involves higher truck operating costs per mile and lower capacities.
- Model alternate utilization of drones in truck-drone delivery (TD): (i) relax the assumption that the truck and the drone make alternate deliveries; (ii) extend the model to allow multiple drones to be launched from the truck; (iii) design new delivery swaths where the truck makes deliveries in the middle part of the swath (to further reduce truck travel distances) and the drones make the more distant deliveries; (iv) allow drones to make more than one delivery per flight; (v) explicitly model truck drone synchronization and waiting time.
- Model alternate utilization of drones in drone-only delivery (DO): (i) allow drones to make multiple deliveries per flight; (ii) model multiple drone operational locations at which drones can be launched and recovered, (iii) include explicit fixed

and variable costs for drone centers to determine the optimal number of drone centers and examine the tradeoff between reduced transportation costs and increased facility costs and the costs for operating the drone centers.

- Other model extensions could: (i) allow drones to "ride" with public transit or shared vehicles (e.g., Uber); (ii) model queueing aspects of operations at takeoff/landing locations when using multiple drones; or (iii) model the need for drone air traffic control systems if drone delivery is used at scale.
- Compare different technologies (e.g., drones, autonomous ground vehicles, alternative-fuel vehicles) that can reduce cost and/or emissions in transportation, and design delivery systems that best utilize those emerging technologies.
- Develop more accurate data on drone operating cost and energy consumption, including impacts of different drone delivery methods (e.g., parachuting, landing on ground, tethering) to help develop better delivery system designs.

References

Abbasi, M. and Nilsson, F., 2016. Developing environmentally sustainable logistics: Exploring themes and challenges from a logistics service providers' perspective. *Transportation Research Part D: Transport and Environment*, *46*, pp.273-283.

Adams E., 2016. DHL's Tilt-Rotor 'Parcelcopter' is both awesome and actually useful. *WIRED*. Retrieved January 23rd, 2020 from: https://www.wired.com/2016/05/dhls-new-drone-can-ship-packages-around-alps/.

Agatz, N., Bouman, P. and Schmidt, M., 2018. Optimization approaches for the traveling salesman problem with drone. *Transportation Science*, *52*(4), pp.965-981.

Ai S., 2019. Personal communication, December 1st, 2019.

Ansari, S., Başdere, M., Li, X., Ouyang, Y. and Smilowitz, K., 2018. Advancements in continuous approximation models for logistics and transportation systems: 1996–2016. *Transportation Research Part B: Methodological*, *107*, pp.229-252.

Apex Insight, 2020, Retrieved February 28th, 2021 from: https://apex-insight.com/product/global-parcel-delivery-market/.

Barth, M., Younglove, T. and Scora, G., 2005. Development of a heavy-duty diesel modal emissions and fuel consumption model. UC Berkeley Research Reports. Permalink https://escholarship.org/uc/item/67f0v3zf.

Beardwood, J., Halton, J. H. and Hammersley, J. M., 1959. The shortest path through many points. In *Mathematical Proceedings of the Cambridge Philosophical Society* (Vol. 55, No. 4, pp. 299-327). Cambridge University Press.

Bektaş, T. and Laporte, G., 2011. The pollution-routing problem. *Transportation Research Part B: Methodological*, *45*(8), pp.1232-1250.

BloombergNEF, 2020. Electric Vehicle Outlook 2020. Retrieved February 5th, 2021 from: https://about.bnef.com/electric-vehicle-outlook/.

Bouman, N., Agatz, N., and Schmidt, M., 2018. Dynamic programming approaches for the traveling salesman problem with drone. *Networks*, 72(4), 528–542.

Braekers, K., Ramaekers, K. and Van Nieuwenhuyse, I., 2016. The vehicle routing problem: State of the art classification and review. *Computers & Industrial Engineering*, *99*, pp.300-313.

Brander, M., 2012. Greenhouse gases, CO2, CO2e, and carbon: What do all these terms mean? *Ecometrica, Bethesda, MD. https://ecometrica. com/assets/GHGs-CO2-CO2e-and-Carbon-What-Do-These-Mean-v2*, *1*.

Bureau of Transportation Statistics, 2021. Number of U.S. Aircraft, Vehicles, Vessels, and Other Conveyances. Retrieved February 5th, 2021 from: https://www.bts.gov/content/number-us-aircraft-vehicles-vessels-and-other-conveyances.

CA.GOV, 2020. Governor Newsom Announces California Will Phase Out Gasoline-Powered Cars & Drastically Reduce Demand for Fossil Fuel in California's Fight Against Climate Change. Retrieved February 5th, 2021 from: https://www.gov.ca.gov/2020/09/23/ .

Campbell, J.F., 1993. One-to-many distribution with transshipments: An analytic model. *Transportation Science*, *27*(4), pp.330-340.

Campbell, J. F., Sweeney, D. and Zhang, J., 2017. Strategic design for delivery with trucks and drones. *Supply Chain Analytics Report SCMA (04 2017)*.

Capgemini Research Institute, 2019. The last-mile delivery challenge. Retrieved December 12th, 2020 from: https://www.capgemini.com/wp-content/uploads/2019/01/.

Chauhan, D., Unnikrishnan, A. and Figliozzi, M., 2019. Maximum coverage capacitated facility location problem with range constrained drones. *Transportation Research Part C: Emerging Technologies*, *99*, pp.1-18.

Cheng, C., Adulyasak, Y. and Rousseau, L.M., 2020. Drone routing with energy function: Formulation and exact algorithm. *Transportation Research Part B: Methodological*, *139*, pp.364-387.

Chiang, W. C., Li, Y., Shang, J. and Urban, T. L., 2019. Impact of drone delivery on sustainability and cost: Realizing the UAV potential through vehicle routing optimization. *Applied energy*, *242*, pp.1164-1175.

Choudhury, S., Solovey, K., Kochenderfer, M.J. and Pavone, M., 2019. Efficient large-scale multi-drone delivery using transit networks, arXiv preprint arXiv:1909.11840.

Chung, S.H., Sah, B. and Lee, J., 2020. Optimization for drone and drone-truck combined operations: A Review of the State of the Art and Future Directions, *Computers and Operations Research*, doi: https://doi.org/10.1016/j.cor.2020.105004.

Coelho, B.N., Coelho, V.N., Coelho, I.M., Ochi, L.S., Haghnazar, R., Zuidema, D., Lima, M.S. and da Costa, A.R., 2017. A multi-objective green UAV routing problem. *Computers & Operations Research*, *88*, pp.306-315.

Cohen, J. K., 2019. WakeMed Health & Hospitals joins forces with UPS, FAA for drone pilot. *Modern Healthcare*. Retrieved January 23rd, 2020 from: https://www.modernhealthcare.com/care-delivery/wakemed-health-hospitals-joins-forces-ups-faa-drone-pilot.

Cordeau, J. F., Laporte, G., Savelsbergh, M. W. and Vigo, D., 2007. Vehicle routing. *Handbooks in operations research and management science*, *14*, pp.367-428.

Costello, B. and Karickhoff A., 2019. Truck driver shortage analysis 2019. *Arlington, VA: The American Trucking Associations*.

Daganzo, C. F., 1984. The length of tours in zones of different shapes. *Transportation Research Part B: Methodological*, *18*(2), pp.135-145.

Daganzo, C. F., 1984. The distance traveled to visit N points with a maximum of C stops per vehicle: An analytic model and an application. *Transportation science*, *18*(4), pp.331-350.

Daganzo, C. F., 2005. Logistics systems analysis. *Springer Science & Business Media*.

Daganzo, C.F. and Newell, G.F., 1986. Configuration of physical distribution networks. *Networks*, *16*(2), pp.113-132.

Dantzig, G. B. and Ramser, J. H., 1959. The truck dispatching problem. *Management science*, *6*(1), pp.80-91.

D'Andrea, R., 2014. Guest editorial can drones deliver?. *IEEE Transactions on Automation Science and Engineering*, *11*(3), pp.647-648.

Dekker, R., Bloemhof, J. and Mallidis, I., 2012. Operations Research for green logistics–An overview of aspects, issues, contributions and challenges. *European journal of operational research*, *219*(3), pp.671-679.

Demir, E., Bektaş, T. and Laporte, G., 2014. A review of recent research on green road freight transportation. *European Journal of Operational Research*, *237*(3), pp.775-793.

Di Franco, C. and Buttazzo, G., 2015. Energy aware coverage path planning of UAVs, 2015 IEEE International Conference on Autonomous Robot Systems and Competitions. https://ieeexplore.ieee.org/stamp/stamp.jsp?tp=&arnumber=7101619

DJI website, 2020. Phantom 4 specifications. Retrieved May 3rd, 2020 from: https://www.dji.com/phantom-4-pro-v2/specs retrieved May 3rd, 2020

Dorling, K., Heinrichs, J., Messier, G. G. and Magierowski, S., 2017. Vehicle routing problems for drone delivery. *IEEE Transactions on Systems, Man, and Cybernetics: Systems*, *47*(1), pp.70-85.

Drones in HealthCare. A role for drones in healthcare. Retrieved January 23rd, 2020 from: https://www.dronesinhealthcare.com/.

Edenhofer, A., 2018. DHL Parcelcopter. Retrieved March 15th, 2021 from: https://www.dpdhl.com/en/media-relations/specials/dhl-parcelcopter.html.

Eilon, S., Watson-Gandy, C. D. T. and Christofides, N., 1971. Expected distances in distribution problems. In: Distribution management: Mathematical Modeling and Practical Analysis. London: Griffin.

Ellegood, W.A., Campbell, J.F. and North, J., 2015. Continuous approximation models for mixed load school bus routing. *Transportation Research Part B: Methodological*, *77*, pp.182-198.

Ferrandez, S.M., Harbison, T., Weber, T., Sturges, R. and Rich, R., 2016. Optimization of a truck-drone in tandem delivery network using k-means and genetic algorithm. *Journal of Industrial Engineering and Management (JIEM)*, *9*(2), pp.374-388.Figliozzi, M.A., 2007. Analysis of the efficiency of urban commercial vehicle tours: Data collection, methodology, and policy implications. *Transportation Research Part B: Methodological*, *41*(9), pp.1014-1032.

Figliozzi, M.A., 2017. Lifecycle modeling and assessment of unmanned aerial vehicles (Drones) CO2e emissions. *Transportation Research Part D: Transport and Environment*, *57*, pp.251-261.

Filippone, A., 2006. Flight performance of fixed and rotary wing aircraft. Washington, DC, USA: AIAA, 2006.

Finnveden, G., Hauschild, M. Z., Ekvall, T., Guinée, J., Heijungs, R., Hellweg, S., ... and Suh, S., 2009. Recent developments in life cycle assessment. *Journal of environmental management*, *91*(1), pp.1-21.

Franceschetti, A., Jabali, O. and Laporte, G., 2017. Continuous approximation models in freight distribution management. *TOP*, *25*(3), pp.413-433.

Freightwaves, 2019. UPS Mandates Maximum 70 Hours in 8 Days for Package Drivers. Retrieved February 5th, 2021 from: https://www.freightwaves.com/news/ups-mandates-longer-workweeks.

Goodchild, A. and Toy, J., 2018. Delivery by drone: An evaluation of unmanned aerial vehicle technology in reducing CO_2 emissions in the delivery service industry. *Transportation Research Part D: Transport and Environment*, *61*, pp.58-67.

Guinée, J. B., De Haes, H. U. and Huppes, G., 1993. Quantitative life cycle assessment of products: 1: Goal definition and inventory. *Journal of Cleaner Production*, *1*(1), pp.3-13.

Guinee, J.B., Heijungs, R., Huppes, G., Zamagni, A., Masoni, P., Buonamici, R., Ekvall, T. and Rydberg, T., 2011. Life cycle assessment: past, present, and future.

Gulden, T. R., 2017. The energy implications of drones for package delivery. RAND Corporation, Santa Monica, CA.

Ha, Q. M., Deville, Y., Pham, Q. D. and Hà, M. H., 2018. On the min-cost traveling salesman problem with drone. *Transportation Research Part C: Emerging Technologies*, *86*, pp.597-621.

Heath N., 2018. Project Wing: A cheat sheet on Alphabet's drone delivery project. Retrieved January 23rd, 2020 from: https://www.techrepublic.com/article/project-wing-a-cheat-sheet/.

Ho, H.W. and Wong, S.C., 2006. Two-dimensional continuum modeling approach to transportation problems. *Journal of Transportation Systems Engineering and Information Technology*, *6*(6), pp.53-68.

Hoffmann, G., Huang, H., Waslander, S. and Tomlin, C., 2007. Quadrotor helicopter flight dynamics and control: Theory and experiment. In *AIAA Guidance, Navigation and Control Conference and Exhibit* (p. 6461).

Hong, I., Kuby, M. and Murray, A.T., 2018. A range-restricted recharging station coverage model for drone delivery service planning. *Transportation Research Part C: Emerging Technologies*, *90*, pp.198-212.

Horvath, A., 2006. Environmental Assessment of Freight Transportation in the US (11 pp). *The International Journal of Life Cycle Assessment*, *11*(4), pp.229-239.

Huang, H., Savkin, A.V. and Huang, C., 2020a. Reliable Path Planning for Drone Delivery using a Stochastic Time-Dependent Public Transportation Network. *IEEE Transactions on Intelligent Transportation Systems*.

Huang, H., Savkin, A.V. and Huang, C., 2020b. A new parcel delivery system with drones and a public train. *J Intell Robot Syst.* https://doi.org/10.1007/s10846-020-01223-yJeong, H. Y., Song, B. D., and Lee, S., 2019. Truck-drone hybrid delivery routing: Payload-energy

dependency and No-Fly zones, *International Journal of Production Economics* 214 (2019) 220–233.

Intergovernmental Panel on Climate Change (IPCC), 2018. IPCC Special Report on Global Warming of 1.5^{o}C. https://report.ipcc.ch/sr15/pdf/sr15_spm_final.pdf.

ISO, 2006a. ISO 14040: environmental management–lifecycle assessment–principles and framework. International Organization for Standardization, Geneva.

Josephs L., 2019. UPS wins first broad FAA approval for drone delivery. *CNBC*. Retrieved January 23rd, 2020 from: https://www.cnbc.com/2019/10/01/ups-wins-faa-approval-for-drone-delivery-airline.html.

Kellermann, R., Biehle, T. and Fischer, L., 2020. Drones for parcel and passenger transportation: A literature review. *Transportation Research Interdisciplinary Perspectives*, *4*, 100088.

Keeney, T., 2015. Amazon Drones Could Deliver a Package in Under Thirty Minutes for One Dollar. Retrieved June 30th, 2016 from: https://ark-invest.com/research/amazon-drone-delivery#fn-5091-4.

Keeney, T., 2020. Parcel Drone Delivery Should Supercharge Ecommerce. Retrieved March 3rd, 2021 from: https://ark-invest.com/articles/analyst-research/parcel-drone-delivery/.

Keyes, D., 2020. Target's digital sales grew 282% annually in April. Business Insider. Retrieved February 28th, 2021 from: https://www.businessinsider.com/target-digital-sales-skyrocketed-during-pandemic-2020-5.

Khoufi, I., Laouiti, A. and Adjih, C., 2019. A survey of recent extended variants of the traveling salesman and vehicle routing problems for unmanned aerial vehicles. *Drones*, *3*(3), pp.66.

Kirchstein, T., 2020. Comparison of energy demands of drone-based and ground-based parcel delivery services. *Transportation Research Part D: Transport and Environment* 78, 1-18. https://doi.org/10.1016/j.trd.2019.102209

Kithacharoenchai, P., Min, B-C. and Lee, S., 2020. Two echelon vehicle routing problem with drones in last mile delivery. *International journal of Production Economics* 225, 107598.

Koiwanit, J., 2018. Contributions from the Drone Delivery System in Thailand to Environmental Pollution. In *Journal of Physics: Conference Series* (Vol. 1026, No. 1, p. 012020). IOP Publishing.

Lammert, M., 2009. *Twelve-month evaluation of UPS diesel hybrid electric delivery vans* (No. NREL/TP-540-44134). National Renewable Energy Lab.(NREL), Golden, CO (United States).

Langelaan, J.W., Schmitz, S., Palacios, J. and Lorenz, R.D., 2017. Energetics of rotary-wing exploration of titan. In: Aerospace Conference, 2017 IEEE, pages 1–11. IEEE.

Langevin, A., Mbaraga, P. and Campbell, J. F., 1996. Continuous approximation models in freight distribution: An overview. *Transportation Research Part B: Methodological*, *30*(3), pp.163-188.

Laporte, G., 2007. What you should know about the vehicle routing problem. *Naval Research Logistics (NRL)*, *54*(8), pp.811-819.

Laporte, G., 2009. Fifty years of vehicle routing. *Transportation Science*, *43*(4), pp.408-416.

Lee, D., 2019. Amazon to deliver by drone 'within months'. Retrieved July 12th, 2019 from: https://www.bbc.com/news/technology-48536319.

Lee, D. Y., Thomas, V. M. and Brown, M. A., 2013. Electric urban delivery trucks: Energy use, greenhouse gas emissions, and cost-effectiveness. *Environmental science & technology*, *47*(14), pp.8022-8030.

Leishman, J. G., 2002. Principles of helicopter aerodynamics (Vol. 12). Cambridge University Press.

Li, X., Ma, J., Cui, J., Ghiasi, A. and Zhou, F., 2016. Design framework of large-scale one-way electric vehicle sharing systems: A continuum approximation model. *Transportation Research Part B: Methodological*, *88*, pp.21-45.

Lin, C., Choy, K. L., Ho, G. T., Chung, S. H. and Lam, H. Y., 2014. Survey of green vehicle routing problem: past and future trends. *Expert systems with applications*, *41*(4), pp.1118-1138.

Lin, J., Zhou, W. and Du, L., 2018. Is on-demand same day package delivery service green? *Transportation Research Part D: Transport and Environment*, *61*, pp.118-139.

Liu, Y., 2019. An optimization-driven dynamic vehicle routing algorithm for on-demand meal delivery using drones. *Computers & Operations Research*, *111*, pp.1-20.

Liu, Z., Sengupta, R. and Kurzhanskiy, A., 2017. A power consumption model for multi-rotor small unmanned aircraft systems. In *2017 International Conference on Unmanned Aircraft Systems (ICUAS)* (pp. 310-315). IEEE.

Lohn, A. J., 2017. What's the buzz? The city-scale impacts of drone delivery (No. RR-1718-RC).

Macrina, G., Pugliese, L. D. P., Guerriero, F. and Laporte, G., 2020. Drone-aided routing: A literature review. *Transportation Research Part C: Emerging Technologies*, *120*, 102762.

Moore, A.M., 2019. Innovative scenarios for modeling intra-city freight delivery. Moore *Transportation Research Interdisciplinary Perspectives* 3, doi: http://dx.doi.org/10.1016/j.trip.2019.100024.

Murray, C. C. and Chu, A. G., 2015. The flying sidekick traveling salesman problem: Optimization of drone-assisted parcel delivery. *Transportation Research Part C: Emerging Technologies*, *54*, pp.86-109.

Murray, C. C. and Raj, R., 2020. The multiple flying sidekicks traveling salesman problem: Parcel delivery with multiple drones. *Transportation Research Part C: Emerging Technologies*, *110*, pp.368-398.

Novaes, A.G., de Cursi, J.E.S. and Graciolli, O.D., 2000. A continuous approach to the design of physical distribution systems. *Computers & Operations Research*, *27*(9), pp.877-893.

Otto, A., Agatz, N., Campbell, J., Golden, B. and Pesch, E., 2018. Optimization approaches for civil applications of unmanned aerial vehicles (UAVs) or aerial drones: A survey. *Networks*, *72*(4), pp.411-458.

Ouyang, Y., Nourbakhsh, S.M. and Cassidy, M.J., 2014. Continuum approximation approach to bus network design under spatially heterogeneous demand. *Transportation Research Part B: Methodological*, *68*, pp.333-344.

Palmer, A., 2020. Amazon wins FAA approval for Prime Air drone delivery fleet. *CNBC*. Retrieved February 27th, 2021 from: https://www.cnbc.com/2020/08/31/amazon-prime-now-drone-delivery-fleet-gets-faa-approval.html.

Park, J., Kim, S., and Suh, K., 2018. A comparative analysis of the environmental benefits of drone-based delivery services in urban and rural areas. *Sustainability*, *10*(3), 888.

Plumer B., 2018. New U.N. Climate Report Says Put a High Price on Carbon. Retrieved on February 7th, 2021 from: https://www.nytimes.com/2018/10/08/ .

Poikonen, S. and Golden, B., 2020. Multi-visit drone routing problem. *Computers & Operations Research*, *113*, pp.104-802.Quora, 2020. How many stops does a UPS driver do. Retrieved February 5th, 2021 from: https://www.quora.com/How-many-stops-does-a-UPS-driver-do.

Rehkopf, T., 2019. DHL launches its first regular fully-automated and intelligent urban drone delivery service. Retrieved March 15th, 2021 from: https://www.dpdhl.com/en/media-relations/press-releases/2019/dhl-launches-its-first-regular-fully-automated-and-intelligent-urban-drone-delivery-service.html.

Rojas Viloria, D., Solano-Charris, E. L., Muñoz-Villamizar, A. and Montoya-Torres, J. R., 2020. Unmanned aerial vehicles/drones in vehicle routing problems: a literature review. *International Transactions in Operational Research*.

Rotaru, C. and Todorov, M., 2017. Helicopter flight physics, DOI: 10.5772/intechopen.71516, https://www.intechopen.com/books/flight-physics-models-techniques-and-technologies/helicopter-flight-physics.

Schermer, D., Moeini, M. and Wendt, O., 2019. A hybrid VNS/Tabu search algorithm for solving the vehicle routing problem with drones and en route operations. *Computers & Operations Research*, *109*, pp.134-158.

Schneider, J., Madsen, T. and Boggs, J., 2013. America's dirtiest power plants: Their oversized contribution to global warming and what we can do about it. *Environment American Research and Policy Center*.

Shavarani, S.M., Nejad, M.G., Rismanchian, F. and Izbirak, G., 2018. Application of hierarchical facility location problem for optimization of a drone delivery system: a case

study of Amazon prime air in the city of San Francisco. *The International Journal of Advanced Manufacturing Technology*, *95*(9-12), pp.3141-3153.

Sheffi, Y., 2020. *The New (Ab) Normal: Reshaping Business and Supply Chain Strategy Beyond Covid-19*. MIT CTL Media.

Smilowitz, K.R. and Daganzo, C.F., 2007. Continuum approximation techniques for the design of integrated package distribution systems. *Networks: An International Journal*, *50*(3), pp.183-196.

Stolaroff, J. K., Samaras, C., O'Neill, E. R., Lubers, A., Mitchell, A. S. and Ceperley, D., 2018. Energy use and life cycle greenhouse gas emissions of drones for commercial package delivery. *Nature communications*, *9*(1), 409.

Swoop Aero, 2019. Drones for medical deliveries: the value of using technology for good. Retrieved January 23rd, 2020 from: https://swoop.aero/2019/10/21/drones-technology-for-good/.

Szplett, D.B., 1984. Approximate procedures for planning public transit systems: a review and some examples. *Journal of Advanced Transportation*, *18*(3), pp.245-257.

The World Bank, 2020, What is carbon pricing? Retrieved February 5th, 2021 from: https://carbonpricingdashboard.worldbank.org/what-carbon-pricing.

The World Health Organization, 2018. Climate change and health. Retrieved July 12th, 2019 from: https://www.who.int/news-room/fact-sheets/detail/climate-change-and-health.

Troudi, A., Addouche, S. A., Dellagi, S. and Mhamedi, A., 2018. Sizing of the drone delivery fleet considering energy autonomy. *Sustainability*, *10*(9), 3344.

Tseng, C-M., Chau, C-K., Elbassioni, K. and Khonji, M., 2017a. Flight Tour Planning with recharging optimization for battery-operated autonomous drones, 29 March 2017, https://pdfs.semanticscholar.org/76d2/307395999118ca3fb406c1d95e337bf3953b.pdf

Tseng, C-M., Chau, C-K., Elbassioni, K. and Khonji, M., 2017b. Autonomous recharging and flight mission planning for battery-operated autonomous drones, 12 September 2017, https://arxiv.org/pdf/1703.10049.pdf

Tseng, C-M., 2020. Personal communication , January 22 and 25, 2020.

U.S. Department of Energy, 2019. FY2018 Energy Efficient Mobility Systems Annual Progress Report. United States Department of Energy, Office of Energy Efficiency and Renewable Energy, Vehicle Technologies Office, doi:10.2172/1525359.

U.S. Department of Energy, 2020. FY2019 Energy Efficient Mobility Systems Annual Progress Report. United States Department of Energy, Office of Energy Efficiency and Renewable Energy, Vehicle Technologies Office, doi:10.2172/1525359.

U.S. Environmental Protection Agency, 2020. Greenhouse gas emissions of typical passenger vehicle. Retrieved February 5th, 2021 from: https://www.epa.gov/greenvehicles/greenhouse-gas-emissions-typical-passenger-vehicle.

U.S. Environmental Protection Agency, 2020. Greenhouse Gas Emissions from a Typical Passenger Vehicle. Retrieved February 5th, 2021 from: https://www.epa.gov/greenvehicles/greenhouse-gas-emissions-typical-passenger-vehicle.

U.S. Global Change Research Program, 2018. The Fourth National Climate Assessment. Retrieved July 12th, 2019 from: https://nca2018.globalchange.gov/downloads/NCA4_2018_FullReport.pdf.

Vaughan, R., 1984. Approximate formulas for average distances associated with zones. *Transportation science, 18(3)*, pp.231-244.

Williams, N. and Murray, D., 2020. An Analysis of the Operational Costs of Trucking: 2020 Update.

Wu, F., Yang, D., Xiao, L. and Cuthbert, L., 2019. Energy consumption and completion time tradeoff in rotary-wing UAV enabled WPCN, IEEE Access 7, 79617-79635,10.1109/ACCESS.2019.2922651

Xu, J., 2017. Design perspectives on delivery drones. RAND.

Yurek, E. E., and Ozmutlu, H. C., 2018. A decomposition-based iterative optimization algorithm for traveling salesman problem with drone. *Transportation Research Part C: Emerging Technologies*, *91*, pp.249-262.

Zeng, Y. and Zhang, R., 2017. Energy-efficient UAV communication with trajectory optimization. *IEEE Transactions on Wireless Communications*, *16*(6), pp.3747-3760.

Zeng, Y., Xu, J. and Zhang, R., 2019. Energy minimization for wireless communication with rotary-wing UAV. *IEEE Transactions on Wireless Communications*, *18*(4), pp.3747-3760.

Zhang, J., Campbell, J. F., Sweeney II, D. C. and Hupman, A. C., 2021. Energy consumption models for delivery drones: A comparison and assessment. *Transportation Research Part D: Transport and Environment*, *90*, p.102668.

Zhang, J., Zhao, Y., Xue, W. and Li, J., 2015. Vehicle routing problem with fuel consumption and carbon emission. *International Journal of Production Economics*, *170*, pp.234-242.

Appendix

Appendix 3.A

This appendix provides a derivation of the energy consumption for a battery powered aircraft in steady level flight (i.e. at a constant altitude and constant speed), as in D'Andrea (2014), based on fundamental principles of flight. Four fundamental forces acting on an aircraft in steady flight are thrust to move forward, weight from gravity acting on the aircraft mass, lift in the direction opposing gravity, and drag in the direction opposing travel (from aerodynamic effects of the shape of the aircraft, such as friction with air). The amount of energy in joules needed to fly a distance d (measured in meters) at constant altitude can be modeled as

$$E_{fly} = T \times d \, , \tag{3.A1}$$

where T is the thrust force measured in Newtons (kg-m/sec^2). Note that this does not account for the energy involved with the vertical travel components to lift the aircraft from the ground to a cruising altitude and to lower it back to the ground. For drone delivery, this may occur twice each trip, once at takeoff/landing and once for the delivery; however, drone deliveries may not require landing, as the package may be lowed via a tether or dropped via parachute.

An important factor for aircraft performance is the lift-to-drag ratio r, a unitless parameter which captures the efficiency of the aircraft design in keeping the aircraft airborne. Values of the lift-to-drag ratio range widely from about 10-20 for commercial passenger aircraft to about 4 for helicopters in cruising flight, to typically smaller values for UAV rotocopters. The lift-to-drag ratio varies with aircraft speed due to drag and the

aerodynamic affects from lifting surfaces, but is constant in steady flight. To keep the aircraft in steady flight, lift is equal to weight and thrust is equal to drag, so

$$T = drag = \frac{lift}{r} = \frac{weight}{r} = \frac{mass \times g}{r}, \tag{3.A2}$$

where g is the acceleration due to gravity (9.8 m/sec^2) and $mass$ is the total weight of the aircraft (body, battery and payload) in kg. Combining (3.A1) and (3.A2) gives

$$E_{fly} = \frac{(m_1+m_2+m_3)\times g}{r} \times d, \tag{3.A3}$$

where $m_1$is the mass of the aircraft structure, m_2 is the mass of the aircraft battery and m_3 is the mass of the payload.

An important parameter for battery powered drones is the efficiency for converting battery power to "flight" power delivered by the rotors, denoted η (unitless), where $\eta < 1$. Thus, the energy required from the battery for steady flight is

$$E_{fly} = \frac{(m_1+m_2+m_3)\times g}{\eta r} \times d. \tag{3.A4}$$

Additional energy is consumed by the drone avionics required for safe flight, including communications, sensing, computation, etc. Let P_{avio} be the power required for the aircraft (drone) avionics in joules per second of flight. The energy for avionics (in joules) for a flight of distance d is then

$$E_{avio} = P_{avio} \times \frac{d}{v}. \tag{3.A5}$$

The total energy expended by the aircraft battery (in joules) on a flight of distance d is from equations (3.A4) and (3.A5):

$$E_{tot} = \frac{(m_1+m_2+m_3)g}{r\eta} d + P_{avio} \times \frac{d}{v}. \tag{3.A6}$$

The total energy expended per meter of flight Epm is then

$$Epm = \frac{(m_1+m_2+m_3)g}{r\eta} + \frac{P_{avio}}{v}. \tag{3.A7}$$

This is equivalent to the formula presented in D'Andrea (2014) for power

$$\frac{(m_1+m_2+m_3)v}{370\, r\eta} + P_{avio}$$

because power equals $Epm \times v$, and the constant 370 in the denominator of the first term results from substituting in 9.81 for g and measuring speed in km/hr rather than m/sec (3600/9.81 = 367).

Appendix 3.B

The model in Kirschstein (2020) for steady flight is based on the power model in Langelaan et al. (2017) where the power for constant speed flight includes four components for: induced power for lift, power to overcome parasite drag, profile power, and ascending/descending power (based on flight angle θ). This is expressed as a function of the mass and flight angle:

$$P(m_k, v_a, \gamma) = \kappa w T + \frac{1}{2}\rho\left(\sum_{k=1}^{3} C_{D_k} A_k\right) {v_a}^3 + \frac{\rho\sqrt{\varsigma/\pi} n N c c_d}{8} {v_T}^3 \left(1 + 3\left(\frac{v_a}{v_T}\right)^2\right) + (g \sum_{k=1}^{3} m_k) v_a \sin\theta \quad \text{(3.B1)}$$

where $v_T = \sqrt{\frac{6}{nNcc_l\rho\sqrt{\varsigma/\pi}}}\sqrt{g\sum_{k=1}^{3} m_k}$ is the blade tip speed. The parameter w, like the induced velocity in Stolaroff et al. (2018), is found by solving the following equation

$$w = \frac{T}{2n\rho\varsigma\sqrt{(v_a cos\alpha)^2 + (v_a sin\alpha + w)^2}}, \quad \text{(3.B2)}$$

where T is from equation (20) and α is from equation (15) in chapter 3.

The energy per meter for steady level flight ($\theta = 0$) for a total drone mass of m (including battery and payload if any) with avionics power P_{avio} is

$$Epm = \frac{P(m, v_a, 0)}{\eta v_a} + \frac{P_{avio}}{\eta_c v_a}. \quad \text{(3.B3)}$$

Kirschstein (2020) uses a total energy efficiency η for drone flight power that includes the motor, transmission and battery charging efficiency, but only the charging efficiency η_c for the avionics.

For a delivery by a drone moving at speed v_a with no wind to a distance d from the depot, the total energy including take-off and ascent at 45° to an altitude of alt, level flight, hovering for time t_{hover}, and then landing, is

$$Epm = \frac{1}{v_a}\left[\frac{P(m,v_a,0)}{\eta} + \frac{P_{avio}}{\eta_c}\right] + \frac{1}{v_a}\frac{alt}{d}\frac{1}{\eta}[P(m,v_a,45°) + P(m,v_a,-45°) - 2P(m,v_a,0)]$$

$$+ \frac{t_{hover}}{d}\left[\frac{P(m,0,0)}{\eta} + \frac{P_{avio}}{\eta_c}\right]. \qquad (3.B4)$$

The return trip would be the same, but without the payload ($m = m_1 + m_2$). The first term in (3.B4) is for the level flight, which will usually be the majority of the trip (unless the delivery is for a very short distance), the second term is for the ascending and descending, and the last term is for hovering.

Appendix 3.C

Zeng and Zhang (2017) formulate the power for a fixed wing drone in steady flight to overcome the induced drag and parasitic drag based on Filippone (2006) as

$$P = \frac{1}{2}\rho \sum_{k=1}^{3} C_{D_k} A_k \, {v_a}^3 + \frac{2(\sum_{k=1}^{3} m_k)^2 g^2}{(\pi e_o A_R)\rho S v_a}, \tag{3.C1}$$

where e_o is the Oswald (wing span) efficiency, and A_R is the aspect ratio of the wing. For this model

$$Epm = \frac{1}{2}\rho \sum_{k=1}^{3} C_{D_k} A_k \, {v_a}^2 + \frac{2(\sum_{k=1}^{3} m_k)^2 g^2}{(\pi e_o A_R)\rho S {v_a}^2}. \tag{3.C2}$$

In a related article, Zeng et al. (2019) formulate the power for a rotorcopter drone in steady flight. Similar to Liu et al. (2017) power is modeled to overcome induced drag, parasite drag and the blade profile drag. The authors provide a general formula, then simplify it (see equation (13) in Zeng et al. (2019)) to

$$P = \frac{W^{3/2}}{\sqrt{2n\rho\varsigma}}\left[\frac{1.1\sqrt{W}}{v_a\sqrt{2n\rho\varsigma}}\right] + \sum_{k=1}^{3}\frac{1}{2}\rho {v_a}^3 C_{D_k} A_k + P_0\left(1 + \frac{3{v_a}^2}{{U_{tip}}^2}\right), \tag{3.C3}$$

where U_{tip} is the tip speed of the rotor blade and P_0 depends on the air density and details of the rotors (similar to the parameter c_2 in Liu et al (2017)). The situation being modeled is essentially the same as in Liu et al. (2017) and so the models are quite similar (compare equation (20) vs. equation (17)). Wu et al (2019) use this same drone energy consumption formula to model the use of a drone to wirelessly recharge ground stations via radio frequency energy sent from the drone.

Appendix 4.A

Suppose we have an odd number of deliveries in a truck-drone route that n cycles contain both a truck and a drone delivery and the $(n+1)th$ cycle contain only a truck delivery. The distance per delivery is given by

$$VMT_{td} = \frac{w}{6} + \frac{1}{\delta w} + \sqrt{\left(\frac{w}{3}\right)^2 + \left(\frac{1}{\delta w}\right)^2} + \frac{1}{2n+1}\left(\frac{w}{3} - \sqrt{\left(\frac{w}{3}\right)^2 + \left(\frac{1}{\delta w}\right)^2}\right) \quad (4.A1)$$

As long as $n \gg 1$, eq.(1.A) is approximately equivalent to eq.(10).

Appendix 4.B: Optimal Swath Width for Truck-drone Delivery

A nonnegative linear combination of a set of convex functions is a convex function (Boyd and Vandenberghe (2004)). Suppose both $f(x)$ and $g(x)$ are convex functions, then $h(x) = f(x) + g(x)$ is a convex function, which has a global minimum. Suppose $f(x)$ is minimized at x_1, $g(x)$ is minimized at x_2, and $x_1 < x_2$.

$$h'(x_1) = f'(x_1) + g'(x_1) = g'(x_1) < 0$$

$$h'(x_2) = f'(x_2) + g'(x_2) = f'(x_2) > 0$$

Thus, the x that minimizes $h(x)$ should be $x_1 < x < x_2$. Thus, the minimum of the sum of two convex functions is between the two minimums of the component convex functions.

As described in Section 4.3.3, the expected cost of serving a customer at distance d for truck-drone delivery is given by

$$C_{td} = \frac{2c_t d}{m_{td}} + c_t\left(\frac{w}{6} + \frac{1}{\delta w}\right) + c_d\sqrt{\left(\frac{w}{3}\right)^2 + \left(\frac{1}{\delta w}\right)^2} + s_t + \frac{1}{2}s_d. \quad (4.B1)$$

Let

$$f(w) = c_t\left(\frac{w}{6} + \frac{1}{\delta w}\right), \tag{4.B2}$$

$f(w)$ is a convex function and is minimized at $w_{td}^{t*} = \sqrt{\frac{6}{\delta}} = \sqrt{2}w_{to}^*$, and $f(w_{td}^{t*}) = c_t\frac{\sqrt{2}}{\sqrt{3\delta}}$.

Let

$$g(w) = c_d\sqrt{\left(\frac{w}{3}\right)^2 + \left(\frac{1}{\delta w}\right)^2}, \tag{4.B3}$$

$g(w)$ is a convex function and is minimized at $w_{td}^{d*} = w_{to}^* = \sqrt{\frac{3}{\delta}}$, and $g\left(w_{td}^{d*}\right) = c_d\frac{\sqrt{2}}{\sqrt{3\delta}}$.

Suppose that $h(w) = f(w) + g(w)$, so

$$h(w) = c_t\left(\frac{w}{6} + \frac{1}{\delta w}\right) + c_d\sqrt{\left(\frac{w}{3}\right)^2 + \left(\frac{1}{\delta w}\right)^2}, \tag{4.B4}$$

and $h(w)$ is also a convex function and is minimized at w_{td}^* where $w_{to}^* < w_{td}^* < \sqrt{2}w_{to}^*$.

To simplify $h(w_{td}^*)$, we assume $w_{td}^* = kw_{to}^*$ where $1 < k < \sqrt{2}$, and $\alpha = \frac{c_d}{c_t}$, then we have

$$h(k) = \frac{c_t}{\sqrt{3\delta}}\left(\frac{k}{2} + \frac{1}{k} + \alpha\sqrt{k^2 + \frac{1}{k^2}}\right), \tag{4.B5}$$

and k is solved by taking the first derivative of $h(k)$ and setting it equal to zero, which is shown as follows:

$$h'(k) = \frac{c_t}{\sqrt{3\delta}}\left(\frac{1}{2} - \frac{1}{k^2} + \frac{1}{2}\alpha\left(k^2 + \frac{1}{k^2}\right)^{-1/2}\left(2k - \frac{2}{k^3}\right)\right) = 0\,,$$

$$(k^2 - 2)\sqrt{k^2 + \frac{1}{k^2}} + 2\alpha\left(k^3 - \frac{1}{k}\right) = 0\,,$$

$$\alpha = \frac{(2-(k^*)^2)\sqrt{(k^*)^4+1}}{2((k^*)^4-1)} \quad . \tag{4.B6}$$

There is not simple closed form solution for k^* though it is a function of only α (the ratio of drone and truck operating costs) Equation (4.B6) solves for α as a function of k^*. The optimal value k^* is a decreasing function of α which can be found numerically and is shown in Figure 4.B1.

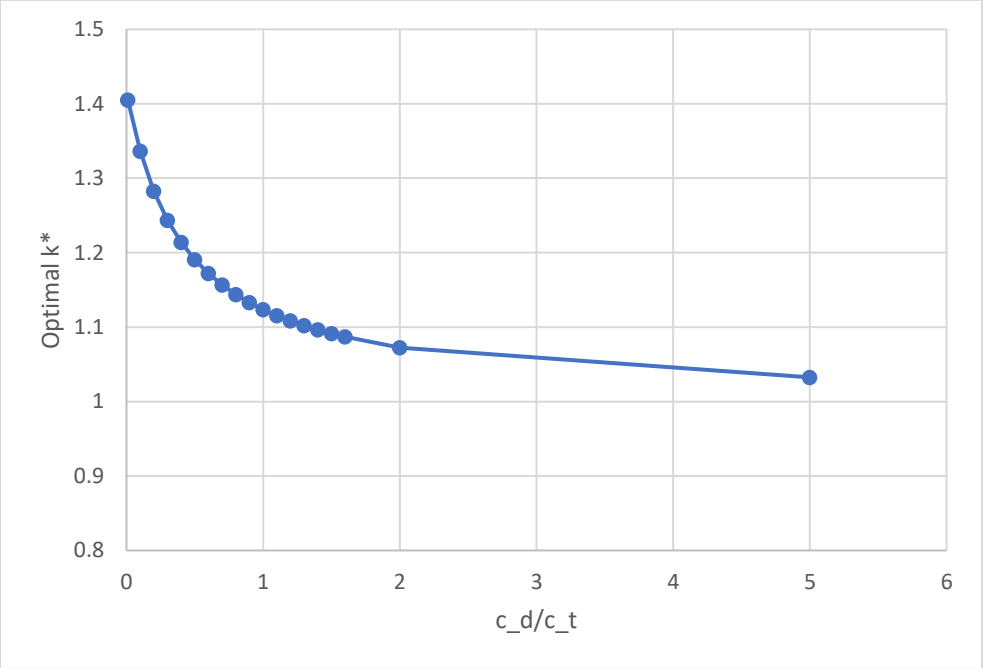

Figure 4.B1. Optimal k^* versus the ratio of drone to truck operating cost rate $\frac{c_d}{c_t}$

It can be proved mathematically that k^* is a monotonically decreasing function of α so there is a unique k^* for each α.

We rewrite equation (4.B6) in order to use properties of monotonicity of function

$$\alpha \frac{2(k^4-1)}{(2-k^2)} = \sqrt{k^4+1} \quad . \tag{4.B7}$$

Suppose that

$$f(k) = \frac{2(k^4-1)\alpha}{(2-k^2)}, \tag{4.B8}$$

$$g(k) = \sqrt{k^4+1}\ , \tag{4.B9}$$

$1 < k_1 < k_2 < \sqrt{2}$, then we have the following:

$$\frac{f(k_2)}{f(k_1)} = \frac{2(k_2^4-1)\alpha}{(2-k_2^2)} \frac{(2-k_1^2)}{2(k_1^4-1)\alpha} = \frac{(k_2^4-1)}{(k_1^4-1)} \frac{(2-k_1^2)}{(2-k_2^2)} > 1 \tag{4.B10}$$

Thus, $f(k_1) < f(k_2)$, $f(k)$ is monotonically increasing in $k \in (1, \sqrt{2})$.

Similarly,

$$\frac{g(k_2)}{g(k_1)} = \frac{\sqrt{k_2^4+1}}{\sqrt{k_1^4+1}} > 1. \tag{4.B11}$$

Thus, $g(k_1) < g(k_2)$, $g(k)$ is also monotonically increasing in $k \in (1, \sqrt{2})$.

For $f(k) = g(k)$, there is only one k for any given α.

Substituting the expression in (4.B6) for α into $h(k)$, we obtain the optimal local transportation cost per delivery

$$h(k^*) = \frac{c_t}{\sqrt{3\delta}} \frac{2(k^*)^3-k^*}{(k^*)^4-1}, \tag{4.B12}$$

$h(k)$ is a monotonically decreasing function on $k \in (1, \sqrt{2})$. For each given α, we can calculate the optimal cost per delivery C_{td}^* as given by

$$C_{td}^* = \frac{2c_t d}{m_{td}} + \frac{c_t}{\sqrt{3\delta}} \frac{2(k^*)^3-k^*}{(k^*)^4-1} + s_t + \frac{1}{2} s_d\ , \tag{4.B13}$$

(4.B13) provides the benchmark for us to check how good are any approximations for k^*, which will be shown in appendix 4.C.

Appendix 4.C: Approximation for the Optimal Truck-drone Swath Width

The optimal swath width (determined by k^* in Appendix 4.B) does not lend itself (nor does the optimal truck-drone delivery cost C_{td}^*) to a closed form solution, thus, we approximate the optimal cost (C_{td}^*) to facilitate the analyses.

Based on equations (4.B1), (4.B2) and (4.B3), the cost function can be written as

$$C_{td} = \frac{2c_t d}{m_{td}} + f(w) + g(w) + s_t + \frac{1}{2}s_d > \frac{2c_t d}{m_{td}} + f(w_{td}^{t*}) + g\left(w_{td}^{d*}\right) + s_t + \frac{1}{2}s_d,$$

Substituting $f(w_{td}^{t*}) = c_t \frac{\sqrt{2}}{\sqrt{3\delta}}$ and $g\left(w_{td}^{d*}\right) = c_d \frac{\sqrt{2}}{\sqrt{3\delta}}$, we have

$$C_{td}^* > \frac{2c_t d}{m_{td}} + c_t \frac{\sqrt{2}}{\sqrt{3\delta}} + c_d \frac{\sqrt{2}}{\sqrt{3\delta}} + s_t + \frac{1}{2}s_d = \frac{2c_t d}{m_{td}} + c_t(1+\alpha)\frac{\sqrt{2}}{\sqrt{3\delta}} + s_t + \frac{1}{2}s_d. \quad (4.C1)$$

The inequality always holds true because functions $f(w)$ and $g(w)$ cannot reach their minimums simultaneously. We approximate C_{td}^* by this lower bound

$$\tilde{C}_{td}^* = \frac{2c_t d}{m_{td}} + c_t(1+\alpha)\frac{\sqrt{2}}{\sqrt{3\delta}} + s_t + \frac{1}{2}s_d. \quad (4.C2)$$

Note that the approximation in (4.C2) essentially replaces the exact optimal local delivery cost $\frac{c_t}{\sqrt{3\delta}}\frac{2(k^*)^3 - k^*}{(k^*)^4 - 1}$ in (4.B13) by an approximation $\frac{c_t}{\sqrt{3\delta}}(1+\alpha)\sqrt{2}$ in (4.C7), which makes the model more elegant and easier for further analyses. Figure 4.C1 shows the very close agreement between the two coefficients of $\frac{c_t}{\sqrt{3\delta}}$ in the exact optimal $\left(\frac{2(k^*)^3 - k^*}{(k^*)^4 - 1}\right)$ and approximated $\left((1+\alpha)\sqrt{2}\right)$local delivery cost.

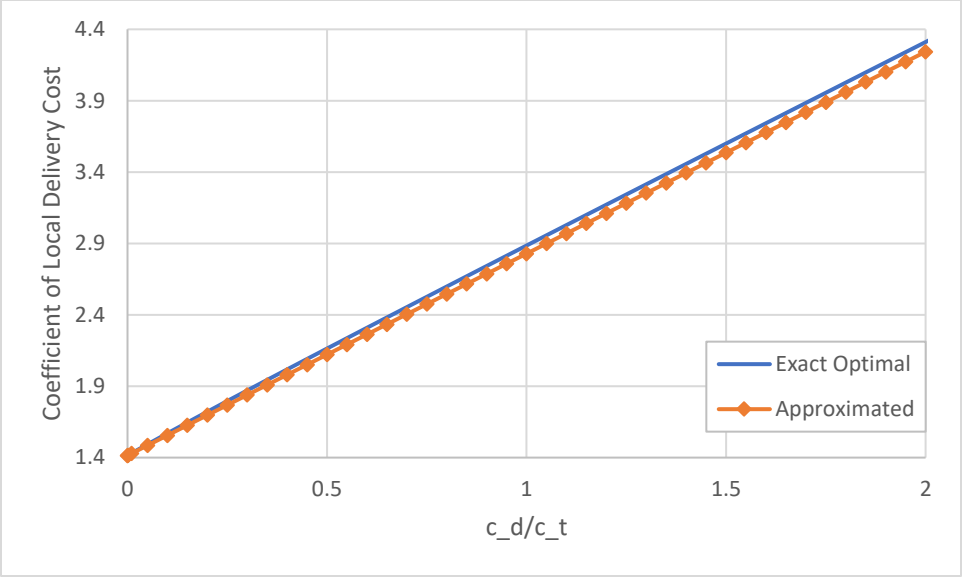

Figure 4.C1. The approximated versus the optimal coefficients of the local delivery cost as a function of $\frac{c_d}{c_t}$

Appendix 6.A: The Impact of Carbon Prices on Optimal Delivery System Designs

This appendix considers the impact of carbon prices on the total cost and the optimal delivery system design. The base case drone has an operating cost of $0.1/mile and an energy consumption of 18 Wh/mile. This appendix considers situations where: (1) drone operating cost per mile is fixed at $0.1/mile and drone energy consumption per mile has six levels (i.e., 9, 18, 36, 60, 90, and 180 Wh/mile); (2) drone energy consumption per mile is fixed at 18 Wh/mile and drone operating cost per mile has six levels (i.e., $0.01/mile, $0.02/mile, $0.03/mile, $0.05/mile, $0.1/mile, and $0.5/mile), and (3) drone energy consumption per mile is fixed at 180 Wh/mile and drone operating cost per mile has six levels (i.e., $0.01/mile, $0.02/mile, $0.03/mile, $0.05/mile, $0.1/mile, and $0.5/mile). For each situation, I consider four levels of carbon prices (i.e., 0, $50/tCO2e, $100/tCO2e, and $200/tCO2e) to show how the optimal delivery system design depends on carbon prices.

For each figure, the horizontal axis is the utilization of drone-only delivery (DO) because DO and TD are the only two services used, thus we could use DO utilization to represent the system design. The vertical axis is the expected total costs (in thousands of dollars) which includes the delivery costs and the cost of emissions by multiplying the carbon price by the quantity of the emissions. The solid, round dot, short dashed, and long dashed lines represent the carbon prices of 0, $50/tCO2e, $100/tCO2e, and $200/tCO2e, respectively. The darker the line color, the greater the carbon price. The round dot indicates the optimal utilization of DO that minimizes total costs.

Figure 6A.1 consists of a panel of six sub-figures (a)-(f), with each associated with a different drone energy consumption rate to show the total cost-service utilization

relationship under varying carbon prices (i.e., the impact of carbon price on the optimal delivery system design). An overview of Figure 6A.1 shows that the total cost – service utilization relationship is not very sensitive to drone energy consumption rates when the drone operating cost is not very low. Figures 6A.1(a)-(f) show that the carbon price has very little impact on the delivery system design. This is because the delivery costs account for a large portion of the total costs due to a relatively high drone operating cost per mile. Even with a carbon price of $200/tCO2e, the incentive is not sufficient enough for a delivery system to significantly reduce emissions. In other words, emissions is a small part of total costs, so the optimal utilization of DO is the same for the range of carbon prices considered (0-200 $/tCO2e).

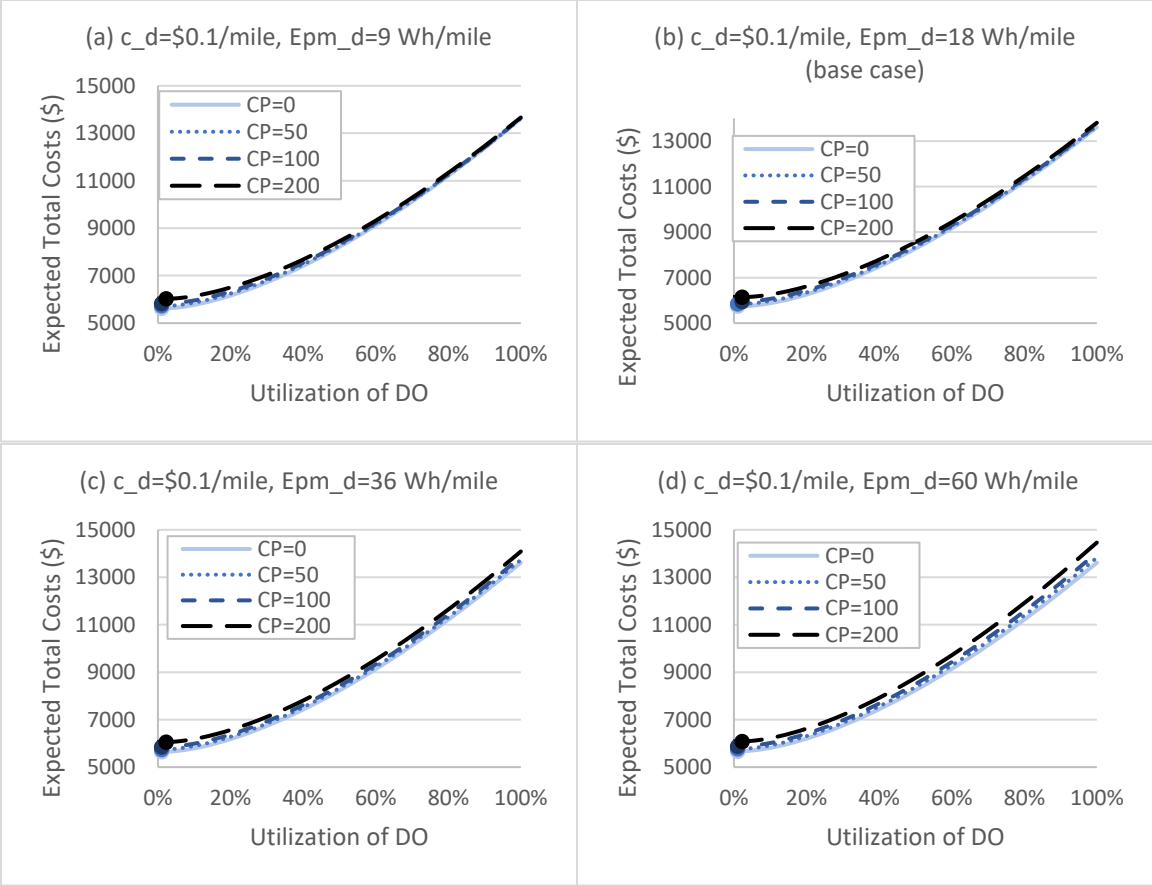

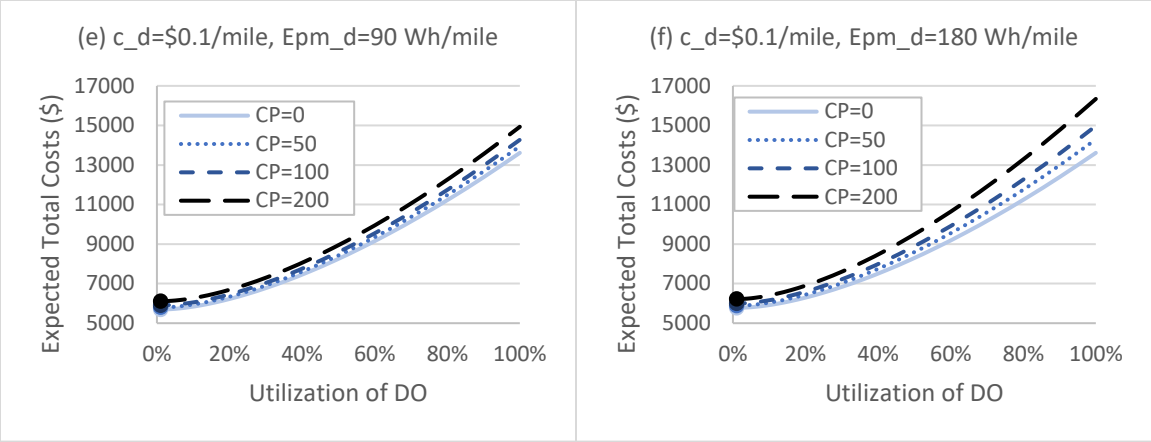

Figure 6A.1. The impact of carbon price on the optimal delivery system design with drone energy consumption per mile varying

Figure 6A.2 also consists of a panel of six sub-figures (a)-(f), with each associated with a different drone operating cost rate to show the total cost-service utilization relationship under varying carbon prices (i.e., the impact of carbon price on the optimal delivery system design). An overview of Figure 6A.2 shows that the total cost-service utilization relationship is significantly impacted by different levels of drone operating cost rate, as the shape of the total cost curves dramatically change with respect to drone operating cost rates. Figures 6A.2(a)-(f) also show little impact of the carbon price on the optimal delivery system design (i.e., the position of the round dots do not change much for each figure). This is because drone-only is 100% used to minimize greenhouse gas (GHG) emissions with this very energy efficient drone. When drone operating cost per mile is low, drone-only is also the service that minimizes delivery costs, thus, the carbon price provides no incentive to change the delivery services. However, when drone operating cost per mile is just greater than $0.03/mile, drone-only delivery service becomes very expensive to operate, thus, it requires a very high carbon price to incentivize an emissions-minimizing

delivery system design. A carbon price of $200/tCO2e is not sufficient enough to cause that change.

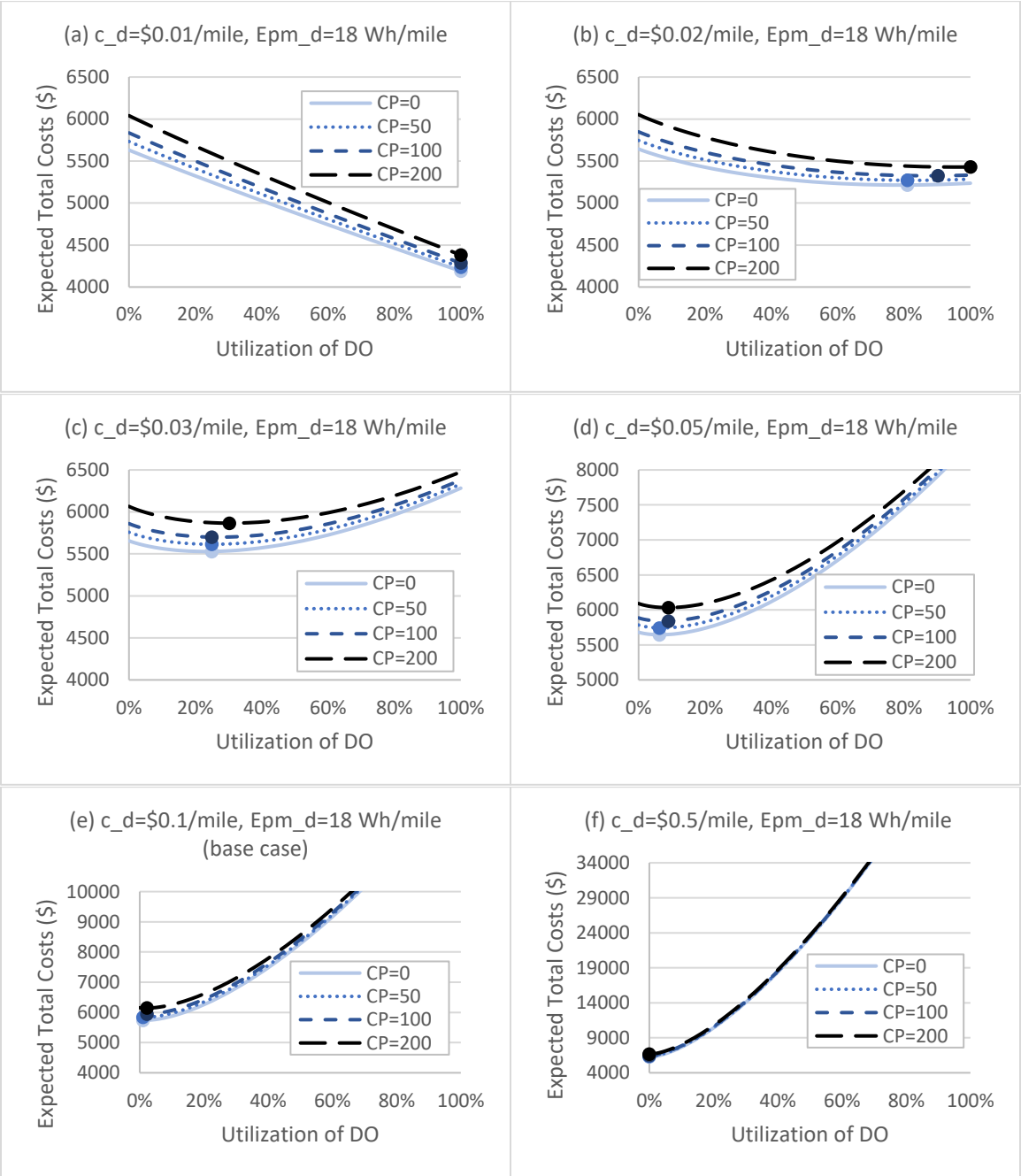

Figure 6A.2. The impact of carbon price on the optimal delivery system design with drone energy consumption per mile varying

Figure 6A.3 demonstrates situation (3) where drone energy consumption per mile is fixed at 180 Wh/mile and drone operating cost per mile has six levels (i.e., \$0.01/mile, \$0.02/mile, \$0.03/mile, \$0.05/mile, \$0.1/mile, and \$0.5/mile). Everything else stays the same. It consists of a panel of six sub-figures (a)-(f), with each associated with a different drone operating cost rate to show the total cost-service utilization relationship under varying carbon prices. Figure 6A.3 shows that the total cost-service utilization relationship is significantly impacted by different level of drone operating cost rate, as the shape of the total cost curves dramatically change with respect to different drone operating cost rates. For this relatively energy inefficient drone, we see that the impact of carbon price (on the optimal delivery system design) and how it depends on the drone operating cost per mile. When drone operating cost per mile is very low, the carbon price needs to be relatively high to incentivize an emissions-minimizing delivery system design (e.g., Figure 6A.3(a)). Figure 6A.3(b) shows that for a very inexpensive but energy intensive drone, there is a significant change in the utilization of DO with a carbon price of \$50/tCO2e compared to no carbon price. When drone operating cost continues to increase, the carbon price has little impact on the optimal delivery system design.

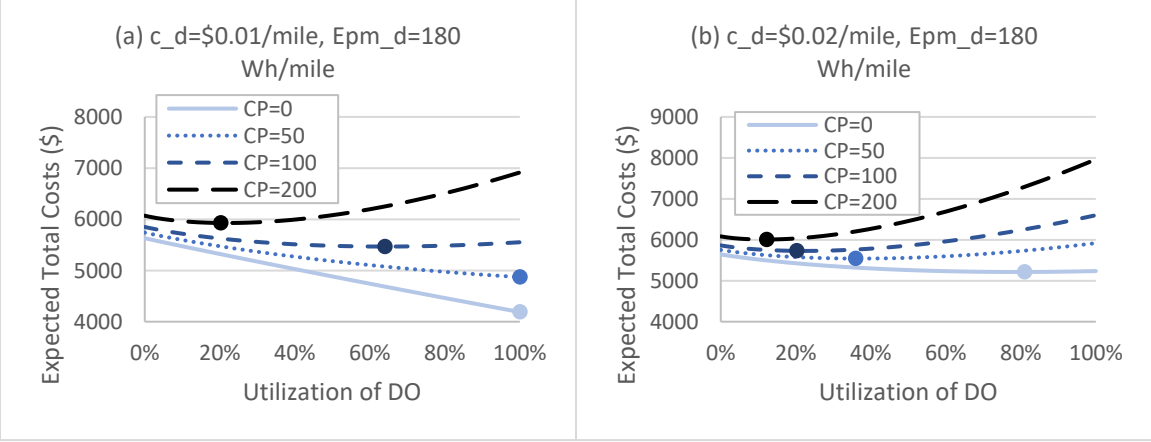

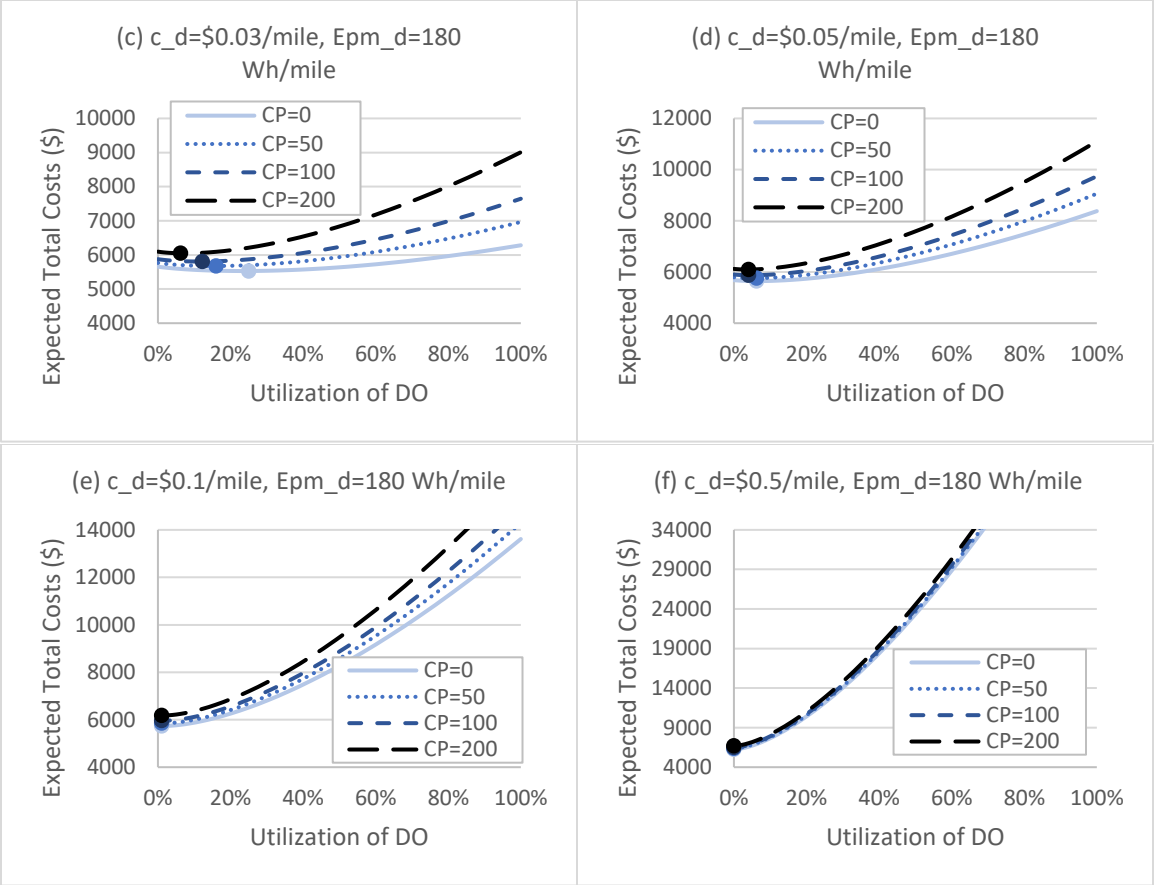

Figure 6A.3. The impact of carbon price on the optimal delivery system design with drone operating cost per mile varying

To assess the impact of delivery density (indicated as number of deliveries per square mile), I considered five density levels:1, 5, 25, 125 and 625 deliveries per square mile for both the base case drone as described in Figure 6A.1(e) (i.e., drone operating cost of $0.1/mile and drone energy consumption of 18 Wh/mile), and the very inexpensive but energy inefficient drone as described in Figure 6A.3(b) (i.e., drone operating cost of $0.02/mile and drone energy consumption of 180 Wh/mile). As delivery density increases, the number of deliveries increases, therefore the expected total costs increase. Figure 6A.4 consists of five sub-figures, with each associated with a different delivery density to show

the impact of delivery density on the optimal system design with carbon price varying for the base case drone. It shows that delivery density has very little impact on the optimal delivery system design except with low delivery density. The impact of carbon price on the optimal delivery system design is very little except with low delivery density as well.

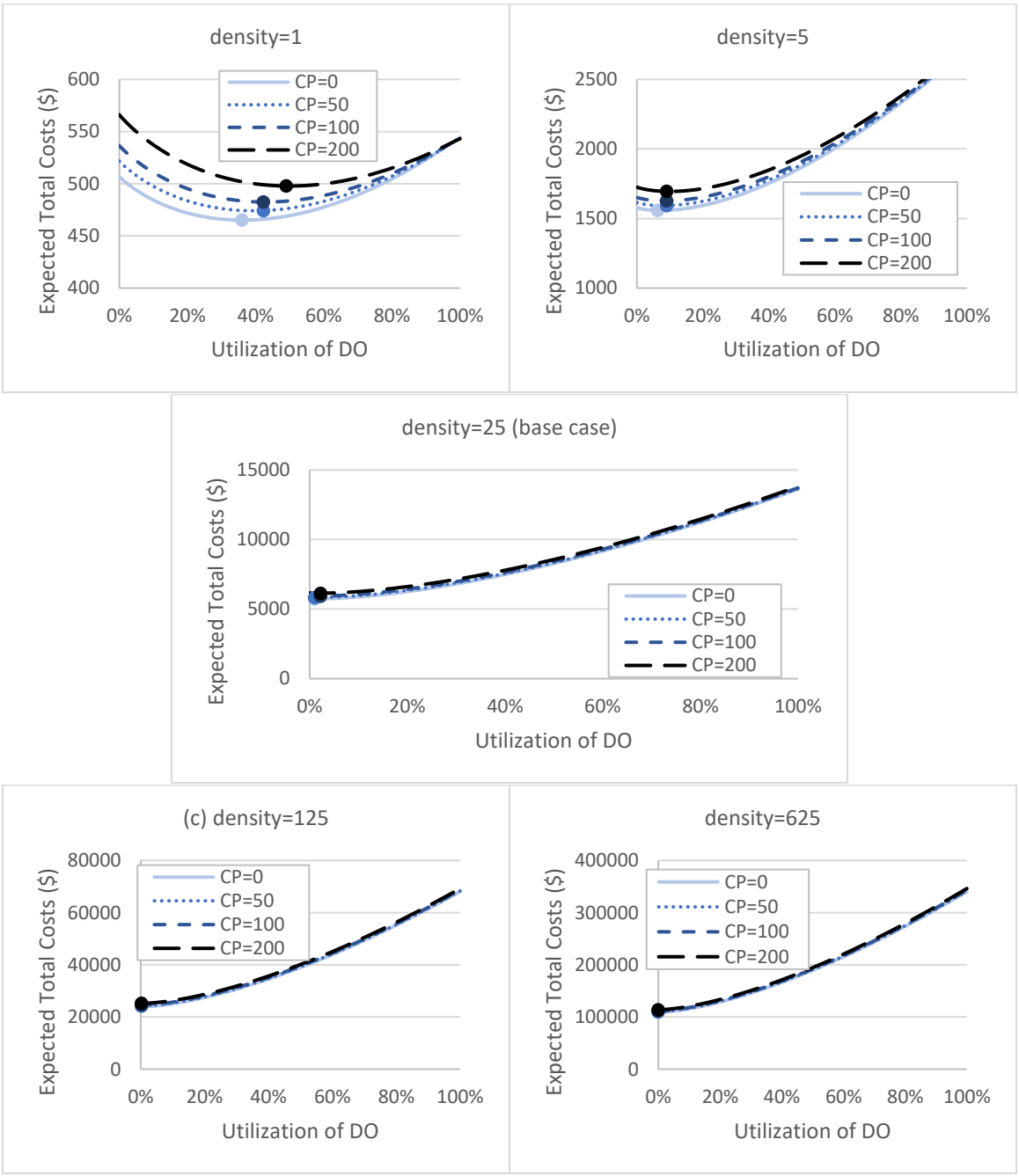

Figure 6A.4. The impact of carbon price on the optimal delivery system design with delivery density varying.

Similarly, Figure 6A.5 consists of five sub-figures, with each associated with a different delivery density to show the impact of delivery density on the optimal delivery system design with carbon price varying for the very cost efficient, but energy inefficient drone. When the drone is very cost efficient but energy inefficient, DO is very inexpensive to operate but is relatively environmentally unfriendly. When delivery density is low (i.e., 5 deliveries per square mile), the optimal delivery system design changes only when carbon price is as high as $200/tCO2e. Carbon price has the most impact on the optimal delivery system design when delivery density is moderate (e.g., between 5-125), whereas its impact is very little for both very low and very high delivery density.

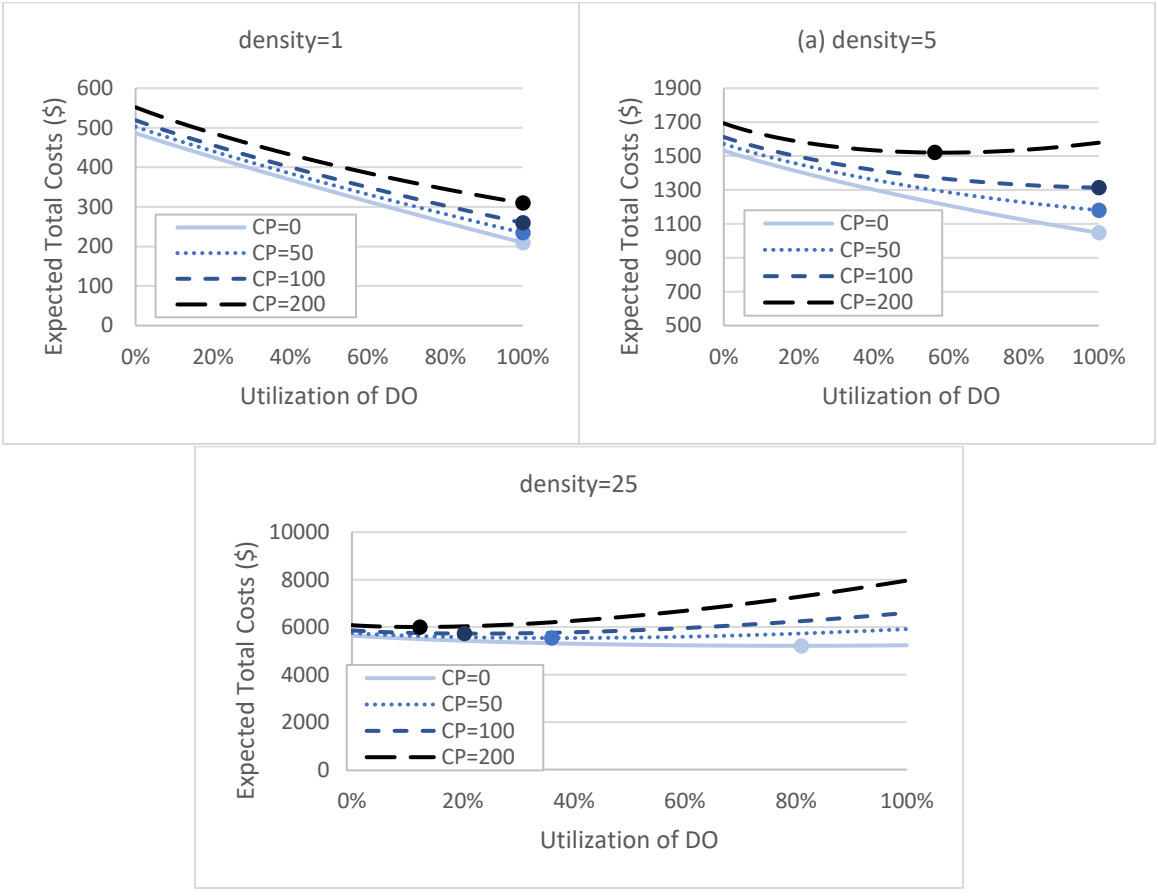

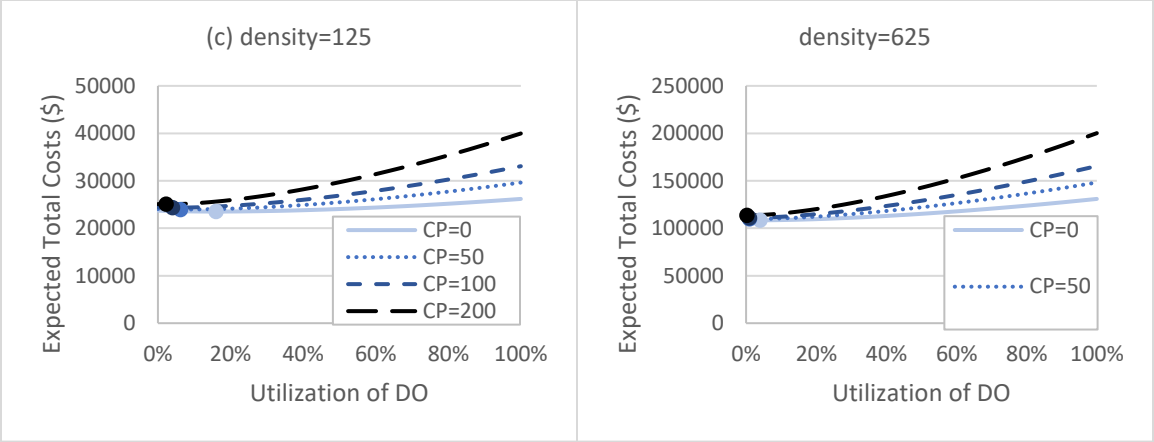

Figure 6A.5. The impact of carbon price on the optimal delivery system design with delivery density varying.

Based on Figures 6A.4-5, the impact of delivery density (and carbon price) on the optimal delivery system design also depends on drone operating cost per mile and drone energy consumption per mile.